THE UNIVERSITY OF ARIZONA
Wyant College of Optical Sciences

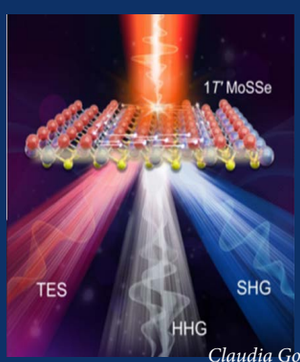

Claudia Gollner

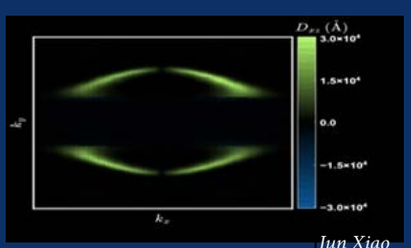

Jun Xiao

Abstract Proceedings

ULTRAFAST DYNAMICS & METASTABILITY

ULTRAFAST BANDGAP PHOTONICS

2024

XII Conference

Professor Michael K.Rafailov

University of Alberta

Professor Rolf Binder

University of Arizona Tucson

Abstract Proceedings comprising summaries of research papers prepared for two closely related Conferences dedicated to studies of nonequilibrium states in condenced matter– Ultrafast Bandgap Photonics and Ultrafast Dynamics and Metastability which forming the Conference. The Conference builds a bridge between cutting edge modern physics and emerging applications which are desperately in need. Conference is vertically integrated, covering the area of interaction of high intensity and low energy pulses with condensed matter, from fundamental physics to practically applicable energy sources, devices and technologies.

This Conference is the 12th in a series of International symposia, conferences and workshops on Ultrafast Dynamics and closely related and application technology driven by Ultrafast Bandgap Photonics which we are running from 2013. University of Arizona Wyant College of Optical Sciences is hosting the 12th Conference in Tucson Arizona-the 1st time for the event to be held in Arizona, which is a home for one the most advanced physics and electro-optics centers of the country.

Conference is organized by sections that are focused either on research field or on phenomena. The division is pretty much conditional, while providing direct access to general topics of interest for the research community and applications as well. Phenomenology topics, like ultrafast dynamic in heterostructures and spin-and orbital ultrafast phenomena may overlap areas of studies like noneqilibrium high temperature superconductivity and ultrafast magnetism, creating multiple entries into the Conference sessions and respectfully to the Proceedings.General reviews of Ultrafast Dynamics and Ultrafast Bandgap Photnics progresss as well as the most interesting recent discoveries are presented here as the Plenary and Keynote papers. Proceedings is oranized in alphabetic order while index section provides easy search for specific researchers who authored the papers. Keynote papers, where results and considerations of most common interest topics are presented, while the Astract Proceedings is compiled based alphabetic list of the speakers in Program -as it was presented at the Symposium. Plus to Table of Contents the Abstract Prosceeding has list of authors where the authors of submitted papers are listed with their papers associated page numbers.

The Abstract Proceeding is actually a snapshot of most interesting and noticeable research results in Ultrafast Dynamics and Ultrafast Bandgap Photonics which one can get in 2024. a snapshot of up to date research results and progress in Ultrafast Dynamics and Metastability and the applications in Ultrafast Bandgap Photonics. It is an Encyclopedia of Ultrafast Dynamics, Metastability and Ultrafast Bandgap Photonics that presents the status quo in the disciplines ranging from theoretical physics to photovoltaics for energy generation and covering practically many phenomena of interests in interaction of low energy-high intensity pulses with complexly organized condensed matter in form of low dimentional structures of different origins as well as bulk materials in different ambient contitions including temperature, static pressure, electric and magnetic potentials, biased irradience as well as different types of excitation energy- from photonic to electrical pulses and so on.

In Loving Memory of Elena

Content

Terahertz nonlinear and parametric spectroscopy of quasiparticles and Condensates in quantum materials

R.D. Averitt
University of California San Diego, La Jolla, CA 92093

Coherent terahertz pulses are a powerful probe of low-energy electrodynamics in quantum materials. This includes materials such as superconductors and charge density wave materials since ~0.1-10 THz is the appropriate energy scale to access electrodynamic signatures associated with condensate responses [1-4]. Advances in terahertz techniques including broadband and high-field generation enable dynamic measurements that provide new insights into these materials. For example, terahertz drive can induce nonlinear optical responses arising from coherent order parameter dynamics. This, in turn, provides a route to identify subtle effects not available from linear response measurements. More generally, THz light-matter interactions is one of many complementary ultrafast optical techniques that, in addition to providing insights into ground state properties, will enable on-demand control of quantum materials [5-7]. In this contribution, we focus on coherent condensate responses in the superconducting cuprate $La_{1.85}Sr_{0.15}CuO_4$ (LSCO) and the excitonic insulator Ta_2NiSe, (TNS) [8, 9]. The data in Fig. 1(a) from LSCO show the terahertz reflectivity of a c-axis oriented crystal with the terahertz electric field polarized perpendicular to the copper oxygen planes.The low frequency response corresponds to c-axis tunneling of Cooper pairs and is a well-defined signature of superconductivity (i.e., appearing below the superconducting transition temperature). This feature is fairly insensitive to the incident field strength, though the plasma edge (minimum in the reflectivity near 1.7 THz) does exhibit a slight redshift with increasing field. In contrast, the reflectivity above 1.7 THz dramatically increases with electric field strength and arises from third harmonic generation from the condensate [8]. Another example of a nonlinear many-body condensate response occurs in the putative excitonic insulator TNS. The data in Fig. 1(b) shows the reflectivity enhancement from 0.5 - 7.5 THz following excitation with 0.5 eV pulses. The broad reflectivity enhancement is punctuated by peaks corresponding to infrared active phonons in TNS, with the largest enhancement occurring at 4.7 THz. DFT calculations show strong electron phonon coupling for this mode. As shown in Ref. [9], this leads to phonon-squeezing, which serves as a coherent many-body response that drives stimulated parametric emission in the presence of a terahertz probe beam. The amplitude of this enhanced reflectivity (not shown) rapidly decreases with increasing temperature and serves as a reporter of a condensate-like behavior in TNS which is difficult to otherwise detect.

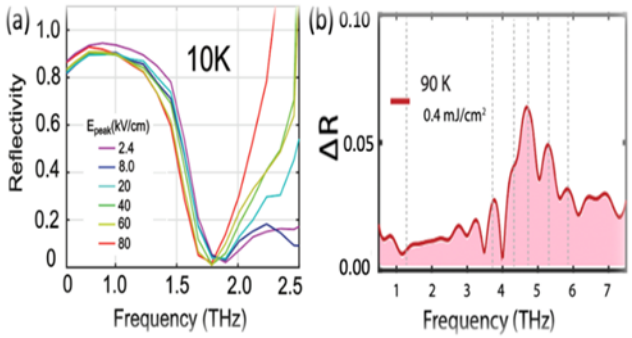

Fig. 1. Condensate response at THz: (a) *Nonlinear reflectivity from c-axis LSCO at 10K. Below 1.5 THz, the reflectivity corresponds to c-axis tunneling of Cooper pairs. The decrease in reflectivity at ~1.5 THz corresponds to the plasma edge. With increasing THz electric field (see inset), the reflectivity above 2.0 THz is enhanced. This response is from third harmonic generation arising from the superconducting condensate and vanishes above the superconducting transition temperature (not shown).* ***(b)*** *Pump-induced reflectivity enhancement in the quasi-1D excitonic insulator TNS. The enhanced reflectivity arises from parametric stimulated emission associated with the exciton condensate. The peaks correspond to phonon enhancement of the emission arising from phonon squeezing.*

These results highlight that nonlinear terahertz techniques enable characterization of subtle interactions in quantum materials. In particular, condensates exhibit strong nonlinear and parametric light-matter interactions that encode information about these contemporary materials.

References

[1] R. Matsunaga, N. Tsuji, H. Fujita, A. Sugioka, K. Makise. Y. Uzawa, H. Terai, Z. Wang, H. Aoki, R. Shimano, *Science* **345**, 1145 (2014).
[2] M.Porer, U.Leierseder, J.-M.Ménard, H.Dachraoui. L.Mouchliadis, I.Perakis, U. Heinzmann, J. Demsar, K. Rossnagel, R. Huber, *Nature Materials* **13**, 857 (2014)
[3] S. Rajasekaran, J. Okamoto, L. Mathey, M. Fechner, V. Thampy, G. D. Gu, A. Cavalleri, *Science* **359**, 575 (2018).
[4] L. Luo, M. Mootz, J. H. Kang, C. Huang, K. Eom, J. W. Lee, C. Vaswani, Y. G. Collantes, E. E. Hellstrom, I. E. Perakis, C. B. Eom, J. Wang, Nature Physics **19** 201 (2023).
[5] A. de la Torre, D. M. Kennes, M. Claassen, S. Gerber, J. W. Mclver, M. A. Sentef, *Reviews of Modern. Physics* **93**, 041002 (2021).
[6] M.Borsch, M. Meierhofer, R. Huber, M. Kira, *Nature Reviews Materials* **8**, 668 (2023).
[7] D. N. Basov, R. D. Averitt, D. Hsieh, *Nature Materials* **16,** 1077 (2017).
[8] K. Kaj, K. A. Cremin, I. Hammock, J. Schalch, D. N. Basov, R. D. Averitt, *Physical Review* B **107**, L140504 (2023).
[9] S. R. UI Haque, M. H. Michael, J. Zhu, Y. Zhang, L. Windgätter, S. Latini, J. P. Wakefield, G.-F. Zhang, J. Zhang, A. Rubio, J. G. Checkelsky, E. Demler, R. D. Averitt, *Nature Materials* **23**, (2024).

***** Acknowledgement: I would like to thank the many collaborators who have contributed to this work and, in particular, the co-authors of Refs. [8,9]. Research supported by DARPA "Driven Nonequilibrium Quantum Systems" (DRINQS) program under award number D18AC00014 and U.S. National Science Foundation DMR-1810310.

Designing and probing exciton quantum phase transitions in 2D Semiconductor heterostructures

Y. Bai[1], Z. Sun[1], Y. Liu[2], X. Y. Zhu[2]
[1]*Brown University, Providence, RI 02912, USA*
[2]*Columbia University, New York, NY 10027, USA*

Designing and harnessing quantum phases of matter is a central goal in modern physical sciences and information technologies. These quantum phases are predominantly characterized as interacting many-body systems, where quantum phase transitions occur due to the competition between many-body Coulomb potentials and the particles' kinetic energy. In this context, interlayer excitons in 2D transition metal dichalcogenides (TMDC) with type-II-aligned heterostructures offer a versatile bosonic system for realizing quantum phases of matter, given by their large out-of-plane dipole moments that enable long-range Coulomb interactions. By constructing a symmetric $WSe_2/MoSe_2/WSe_2$ heterotrilayer, we have realized ordered phases of interlayer excitons [1,2]. This ordered phase is characterized by sharp photoluminescence persisting at an exciton density of ~10^{12} cm^{-2}, an electric -field-driven exciton Mott transition, and negligible exciton mobility. More recently, we have further regulated the competition between exciton many-body Coulomb potentials and kinetic energy by constructing a $WS_2/WS_2/WSe_2/WSe_2$ hetero-twisted double homobilayer [3]. This system hosts emergent heavy excitons with distinct photoluminescence compared to that observed in regular heterobilayers, originating from the Coulomb binding of highly hybridized electrons and holes residing in each twisted homobilayer.

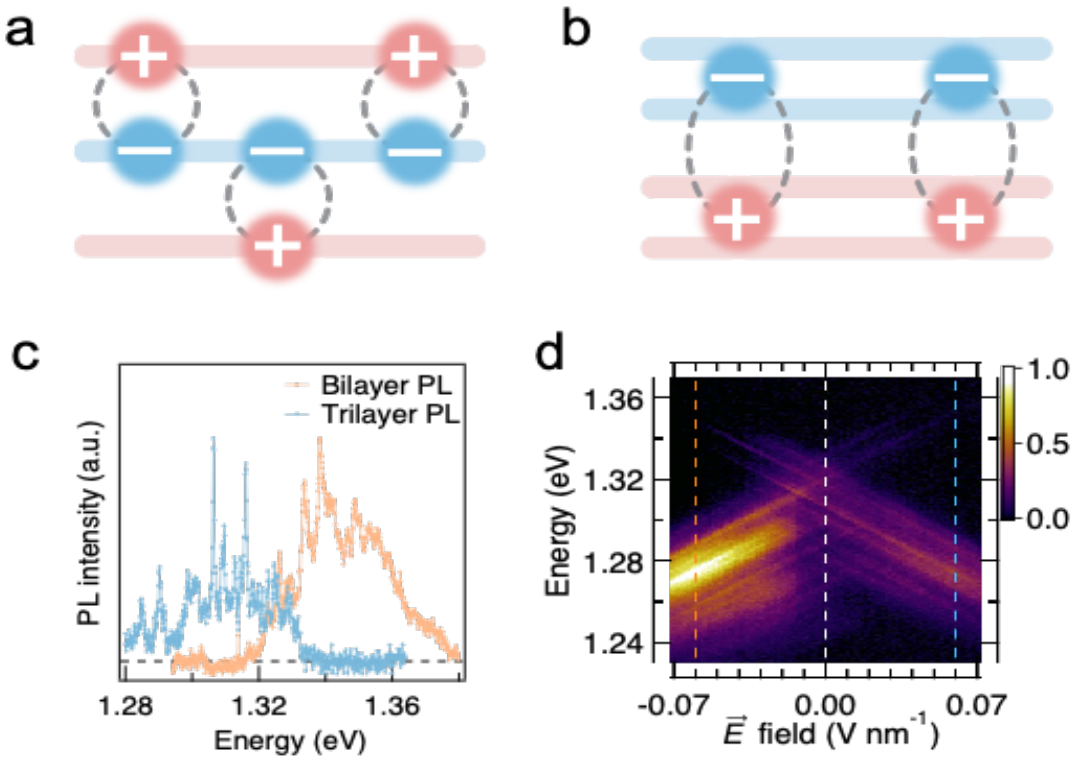

***Fig. 1. (a) Schematic of staggered excitons in a TMDC heterotrilayer**, and **(b)** excitons composed of hybridized electrons and holes in a TMDC hetero four layer. **(c)** Photoluminescence spectra of interlayer excitons in bilayer and trilayer. **(d)** Electric-field-dependent photoluminescence spectra revealing field-drive exciton Mott transitions.*

Our experimental observations underscore that multilayer interlayer excitons can be explored as a capable model bosonic system for programming a range of quantum phases of matter.

References

[1] Y. Bai, Y. L. Li, S. Liu, Y. J. Guo, J. Pack, J. Wang, C. R. Dean, J. Hone, X. Y. Zhu, *Nano Letters* **23**, 11621 (2023).
[2] Y. Slobodkin, Y. Mazuz-Harpaz, S. Refaely-Abramson, S. Gazit, H. Steinberg, R. Rapaport, *Physical Review Letters* **125**, 255301 (2020).
[3] Z. Sun, H. Sun, Y. Bai, *in preparation* (2024).

Ultrafast structural relaxation and coherent excitation of triplet pairs

D. Bain, A. Musser
Cornell University, Ithaca, NY 14850, USA

In organic electronics, excited state phenomena are regularly complicated by the presence of dark states. Dark states can lead to unwanted loss pathways or occasionally be used to steer photochemical reactions towards a desired result. A unique dark state that exists as a distinct intermediate during singlet fission (or triplet-triplet annihilation) is the multiexciton triplet pair state (^{1}TT). Traditionally, ^{1}TT cannot be directly populated from the ground state or emit a photon based on symmetry selection rules, however, there are growing reports of ^{1}TT emission in increasingly diverse systems [1]. For the first time, we demonstrate that ^{1}TT can be directly photoexcited in a range of pentacene derivatives [2]. This effect is generalized to a wide range of aggregation types with varying degrees of coupling strength and is further generalized from intermolecular to intramolecular singlet fission. We are additionally able to enhance the brightness of ^{1}TT through specifically tunned aggregation. By utilizing singlet fission and pentacene as a model system, we provide insight not only into the ^{1}TT formation mechanism relevant to singlet fission applications (light harvesting, quantum information science), but more broadly provide fundamental photophysical insight into how dark states can be populated in organic materials.

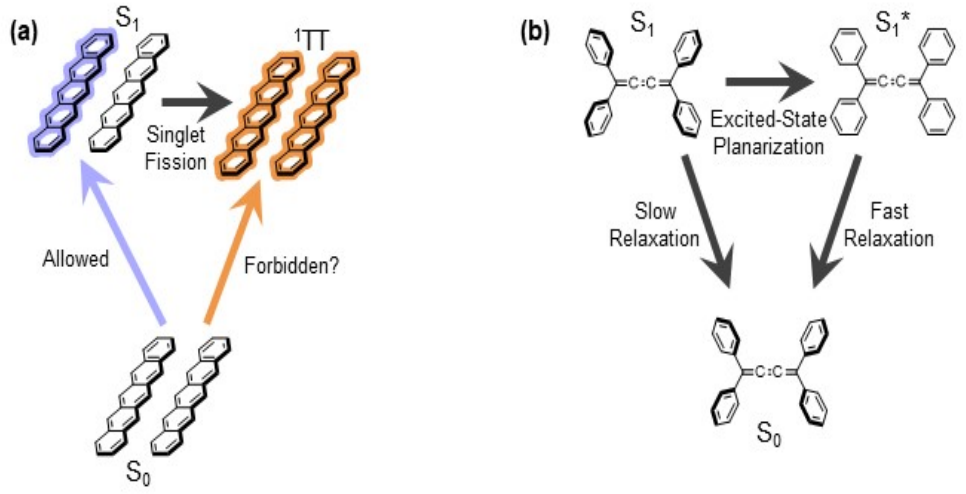

Fig. 1. (a) Direct excitation of ^{1}TT in pentacene-based systems. *Direct photoexcitation of ^{1}TT relies on coherent mixing of both ^{1}TT and S_1 with a charge resonance state.* ***(b) Excited state quenching of [3]-cumulenes through ultrafast structural relaxation.*** *The excited state of cumulenes are typically short lived but can be enhanced only through specific types of rigidification eventually useful for singlet fission applications.*

Despite pentacenes' abundant use as a model system in the singlet fission field, they suffer from poor stability, weak absorption, and too low triplet energies. To expand the scope of materials useful for singlet fission and direct ^{1}TT excitation which address these issues, we targeted a unique yet understudied class of molecules. Cumulenes are molecules consisting of cumulative double bonds and have predicted biradical character in the ground state as well as reasonable triplet energies – qualities that make them attractive for singlet fission [3]. Unfortunately, the excited state lifetimes of cumulenes are typically short and time resolved spectroscopic measurements remain scarce. We are able to elucidate the excited state relaxation pathway in [3]-cumulenes through detailed transient absorption spectroscopy and ultimately enhance their lifetime which will pave the way for subsequent applications related to singlet fission [4].

References

[1] C. K.Yong, A. J. Musser, S.L Bayliss, S. Lukman, H.Tamura, O. Bubnova, R. K. Hallani, A. Meneau, R. Resel, M. Maruyama, S. Hotta, L. M. Herz D. Beljonne, J. E. Anthony, J. Clark, H. Sirringhaus, *Nature Communications* **8**, 15953 (2017).
[2] J. Kim, D. C. Bain, V. Ding, K. Maiumder, D. Windemuller, J. Feng, J. Wu, S. Patil, J. Anthony, W. Kim. A. J. Musser, *Nature Chemistry* **16,** (2024)
[3] J. Messelberger, A. Grünwald, P Pinter, M. M Hansmann, D. Munz, *Chemical Science* **9**, 6107 (2018).
[4] D. Bain, J. Chang, Y. Lai, T. Khazanov, P. J. Milner, A. Musser, *Photochem* 4, 138 (2023).
* Acknowledgements: Supported by the U.S. Department of Energy, Office of Science, Basic Energy Sciences, CPIMS Program under Early Career Research Program (Award No. DE-SC0021941).

Giant dynamical magnetoelectric coupling in a van der Waals multiferroic

F. Y. Gao[1], X. Peng[1], X. Cheng[2], E.V. Böstrom[3], D.Kim[1], R.K. Jain[4], D.Vishnu[5], K.Raju[4], R. Sankar[4]
S.-F. Lee[4], M. A. Sentef[6], T. Kurumaji[7], X. Li[1], P. Tang[2], A. Rubio[2], E.Baldini[1]
[1] *The University of Texas at Austin, Austin, TX 78712, USA*
[2] *Max Planck Institute for the Structure and Dynamics of Matter, 22761 Hamburg, Germany*
[3] *Universidad del País Vasco, 48940 Leioa, Spain*
[4] *Institute of Physics, Taipei 115201, Taiwan*
[5] *National Tsing Hua University, Hsinchu300044, Taiwan*
[6] *University of Bremen, 28359 Bremen, Germany*
[7] *California Institute of Technology, Pasadena, CA 91125, USA*

Helical spin structures are expressions of magnetically induced chirality, entangling the dipolar and magnetic orders in materials [1-4]. The recent discovery of helical van der Waals multiferroics down to the ultrathin limit raises prospects of large chiral magnetoelectric correlations in two dimensions [5,6]. However, the exact nature and magnitude of these couplings have remained unknown so far. Here we perform a precision measurement of the dynamical magnetoelectric coupling for an enantiopure domain in an exfoliated flake of the van der Waals multiferroic NiI_2 (Fig. 1a) [7]. We evaluate this interaction in resonance with a collective electromagnon mode, capturing the impact of its oscillations on the dipolar and magnetic orders of the material with a suite of ultrafast optical probes (Fig. 1b).

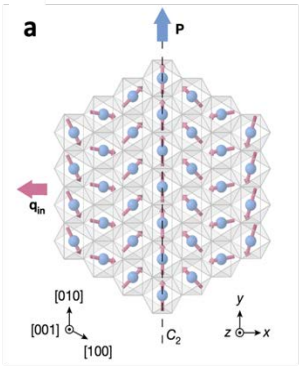

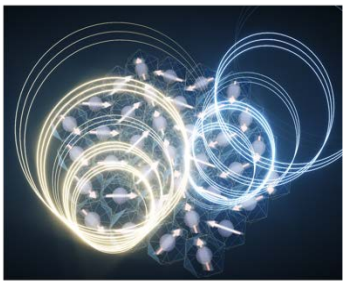

***Fig. 1. a-The spin-spiral order of NiI_2** depicted on the (001) plane with the in-plane component of the propagation vector q_{in} and electric polarization P along y. Also shown is the x, y, z coordinate system, where y ∥ [010] and z ∥ [001]. Figure adapted from Ref. [7]. **b**-Pictorial representation of chiral electromagnon oscillations in NiI_2. Credits: E. Baldini and Ella Maru Studio.*

.

Our data show a giant natural optical activity at terahertz frequencies, characterized by quadrature modulations between the electric polarization and magnetization components. First-principles calculations further show that these chiral couplings originate from the synergy between the non-collinear spin texture and relativistic spin–orbit interactions, resulting in substantial enhancements over lattice-mediated effects. Our findings highlight the potential for intertwined orders to enable unique functionalities in the 2D limit and pave the way for the development of van der Waals magnetoelectric devices operating at terahertz speeds.

References

[1] D. Khomskii, *Physics* **2**, 20 (2009).
[2] Y. Tokura, S. Seki, N. Nagaosa, *Reports on Progress in Physics* **77**, 076501 (2014).
[3] M. Fiebig, T. Lottermoser, D. Meier, M. Trassin, *Nature Reviews Materials* **1**, 16046 (2016).
[4] N. A. Spaldin, R. Ramesh, *Nature Materials* **18**, 203 (2019).
[5] H. Ju, Y. Lee, K.-T. Kim, I. H. Choi, C. J. Roh, S. Son, P. Park, J. H. Kim, T. S. Jung, J. H. Kim, K. H. Kim, J.-G. Park, J. S. Lee, *Nano Letters* **21**, 5126–(2021).
[6] Q. Song, C. A. Occhialini, E. Ergeçen, B. Ilyas, D. Amoroso, P. Barone, J. Kapeghian, K. Watanabe, T. Taniguchi, A. S. Botana, S. Picozzi, N. Gedik R. Comin, *Nature* **602**, 601 (2022).
[7] F. Y. Gao†, X. Peng†, X. Cheng, E. Viñas Böstrom, D. Kim, R. K. Jain, D. Vishnu, K. Raju, R. Sankar, S.-F. Lee, M. A. Sentef, T. Kurumaji, X, Li P. Tang, A. Rubio, E. Baldini, *Nature* **632**, 273 (2024).

* Acknowledgements: Work in the Baldini group at University of Texas at Austin was primarily supported by the Robert A. Welch Foundation under grant F- 2092 -20220331 (to F.Y.G. for data taking and analysis), the National Science Foundation under grant DMR - 2308817 (to X.P. for data taking and analysis), and the Air Force Office of Scientific Research under Young Investigator Program award FA9550-24-1-0097 (to E.B. for data interpretation manuscript writing and supervision). E.V.B. acknowledges funding from the Horizon Europe research and innovation program of the European Union under the Marie Skłodowska – Curie grant agreement no. 101106809. A.R. and E.V.B. acknowledge support from the Cluster of Excellence 'CUI: Advanced Imaging of Matter'—EXC 2056—project ID 390715994, and Grupos Consolidados (IT1453-22). A.R. and E.V.B. also acknowledge support from the Max Planck– New York City Center for Non-Equilibrium Quantum Phenomena. The Flatiron Institute is a division of the Simons Foundation. R.S. acknowledges financial support provided by the Ministry of Science and Technology in Taiwan under project nos. NSTC 111-2124-M-001-009, 110-2112-M-001-065-MY3 and Academia Sinica, project no. AS - iMATE - 111-12. D.S.K. and X.L. acknowledge support from NSF DMR-1720595, DMR-2308817 for spectroscopy studies and the Air Force Office of Scientific Research under award number FA2386 - 21-1-4067 for bulk crystals, and the Welch Foundation Chair F - 0014 for sample preparation. Part of the experiments were performed at the user facility supported by the National Science Foundation through the Center for Dynamics and Control of Material under cooperative agreement no. DMR-2308817 and the Major Research Instrumentation (MRI) program DMR-2019130. Open access funding is provided by the University of Texas at Austin and the Max Planck Society.

Magnetic manipulation of electronic topology with chiral phonons

A. Baydin
Rice University, Houston TX 77025, USA

Chiral phonons arise in crystals with broken mirror symmetries. In a magnetic field, the circular motion of lattice ions in a chiral phonon leads to a finite magnetic moment, even when the host material is purely nonmagnetic. Further, via electron-lattice and spin-orbit interactions, chiral phonons are predicted to induce novel topological phases of matter. To explore such hitherto unobserved phenomena, we studied $Pb_{1-x}Sn_xTe$, which is a narrow-bandgap semiconductor that exhibits a topological phase transition as a function of Sn composition, x – from a trivial insulator ($x < 0.32$) to a topological crystalline insulator ($x > 0.32$). In addition, this material system possesses soft optical phonons (in the terahertz frequency range) and exhibits ferroelectric instabilities. First, I will describe our observations of novel magnetic phenomena associated with chiral phonons in PbTe [1]: magnetic circular dichroism, a Zeeman splitting, and a diamagnetic shift. I will show that these observations result from magnetic field-induced morphic changes in the crystal symmetries through the Lorentz force exerted on the lattice ions. Fig. 1 (Left) depicts the schematic of the PbTe lattice with and without a magnetic field. When the magnetic field is applied, the motion of ions becomes circular. Second, we observed phonon magnetic moment values larger by two orders of magnitude for films in the topological crystalline insulator phase than those in topologically trivial films [2]. Furthermore, the sign of the effective phonon g-factor was opposite in the two phases.

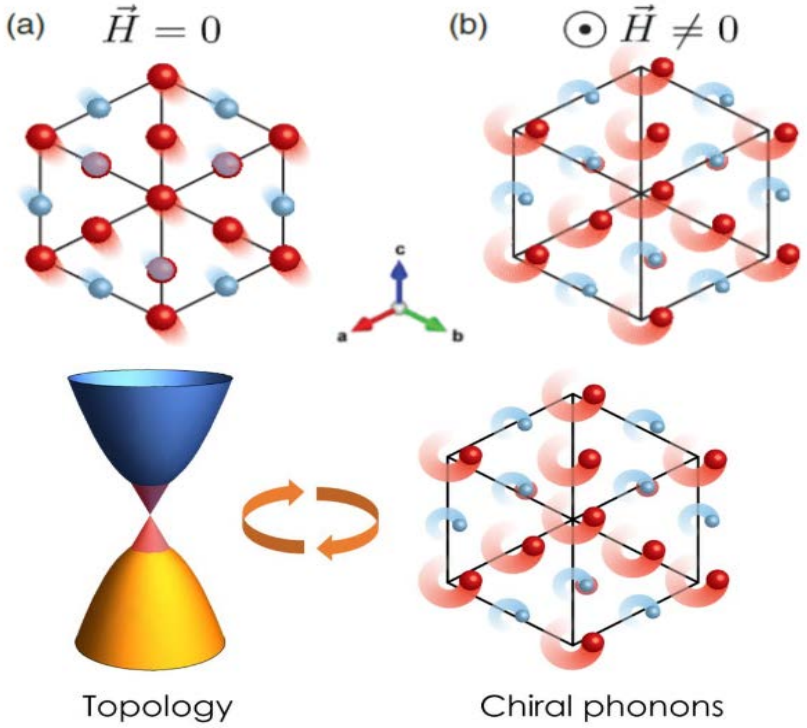

***Fig. 1. Top**: **Schematic of the PbTe crystal structure** with real space lattice displacements (**a**) without and (**b**) with a magnetic field applied perpendicular to the lattice plane. Blue **(red)** spheres represent Te (Pb) ions [1].*
***Below**: Schematic diagram illustrating the connection between the topology of the electronic band structure and chiral phonons in $Pb_{1-x}Sn_xTe$ [2].*

As illustrated in Fig. 1 (Right), these results strongly hint at the interplay between the magnetic properties of chiral phonons and the topology of the electronic band structure.

References

[1] A. Baydin, F. G. G. Hernandez, M. Rodriguez-Vega, A. K. Okazaki, F. Tay, G. T. Noe II, I. Katayama, J. Takeda, H. Nojiri, P. H. O. Rappl, E. Abramof G. A. Fiete, J. Kono, *Physical Review Letters* **128**, 075901 (2022).
[2] F. G. G. Hernandez, A. Baydin, S.Chaudhary, F. Tay, I. Katayama, J. Takeda, H. Nojiri, A. K.Okazaki, P. H. O. Rappl, E. Abramof, M. Rodriguez-Vega G. A. Fiete, J. Kono, *Science Advances* **9**, eadj4074 (2023).

Inverse chirality induced spin selectivity with Terahertz emission spectroscopy

Y.Dong[1], A. McConnell[2], D. Sun[2], M.C. Beard[1]
[1]*National Renewable Energy Laboratory; Golden, CO, 80401, USA*
[2]*North Carolina State University; Raleigh, NC, 27695, USA*

Chirality induced spin selectivity (CISS) represents a charge-to-spin conversion, whereby a charge current induces a spin polarization. Most demonstrations and measurements of CISS involve incorporating chiral molecules, semiconductors, or metals into ferromagnetic heterostructures and then measuring the magnetoresistance (MR). Large spin polarized currents are measured using a magnetic conductive AFM probe (mCP-AFM) [1], however macroscopic MR measurements yield small MR response [2]. We have also demonstrated CISS where the polarization of light is measured as a reporter of the spin-injection from a chiral perovskite semiconductor into a non-chiral III-V light emitter structure [3]. A non-contact method of evaluation CISS is desired. Here, we utlize THz emission spectroscopy (TES) to measure the inverse CISS (ICISS) effect. ICISS is a spin-to-current process.

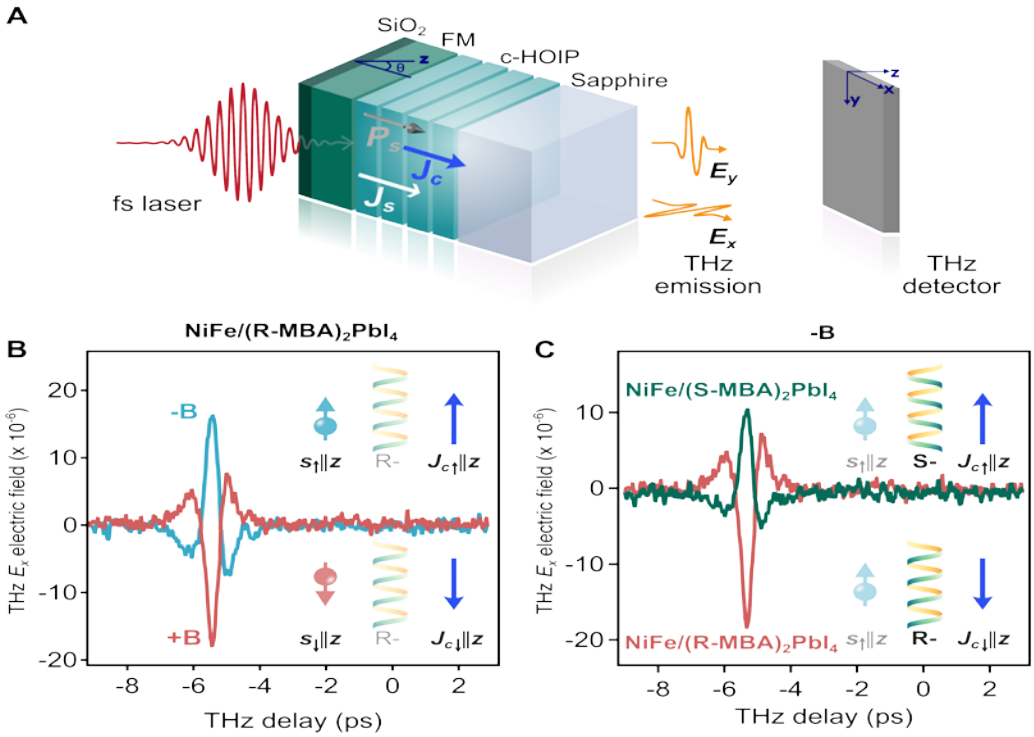

Fig. 1. **A magnetic field is applied out-of-plane** and spin-current is generated in a FM in contact with the chiral perovskite (c-HOIP labeled here).

A magnetic field is applied out-of-plane and spin-current is generated in a FM in contact with the chiral perovskite (c-HOIP labeled here). The THz field generated is measured as a function of out-of-plane angle rotation. When the field (B) or the chirality(C) is reversed the THz field is also reversed. That is we find that ICISS produces a THz waveform for both up and down spins but the phase is 180° different when either the chirality or the spin polarization changes. We describe our results in terms of a chiral spin-splitting of the bands and discuss implications for CISS. We also distinguish between THz emission due to ICISS and the inverse Rashba-Edelstein effect (IREE).

References

[1] H. Lu, C. Xiao, C. Xiao, T. Li, A. E. Maughan, A. Levin, R. Brunecky, J. J. Berry, D.B. Mitzi,V. Blum, M.C. Beard, *Journal of the American Chemical Society* **142**. 13030 (2020).
[2] H Lu, J Wang, C Xiao, X Pan, X Chen, R Brunecky, JJ Berry, K Zhu, MC Beard, ZV Vardeny, *Science Advances* **5,** (2019).
[3] M P. Hautzinger, X. Pan, S. C. Hayden, J. Y. Ye, Q. Jiang, M. J. Wilson, A. J. Phillips, Y. Dong, E. K. Raulerson, I. A. Leahy, C.- S. Jiang J. L. Blackburn, J.M. Luther, Y.Lu, K.Jungjohann, Z. V.Vardeny, J. J. Berry, K. Alberi, M. C. Beard, *Nature* **631**, 307(2024).

Hybrid timescale pump-probe spectroscopy for Floquet engineering

C. A. Belvin
California Institute of Technology, Pasadena, CA 91125 USA

The time periodic electric field of light can coherently modify the Hamiltonian of a material, known as Floquet engineering, potentially creating novel out-of-equilibrium many-body phases [1-3]. Recent progress has been made experimentally in the coherent engineering of the electronic band structure in a variety of solids [4-7]. However, it has been proposed theoretically that Floquet engineering can also lead to collective reorganization of microscopic degrees of freedom, which has yet to be observed experimentally. One example of particular interest is the ability to engineer spin interactions and realize exotic magnetic phases [8-10]. In order to achieve this, the duration of the periodic Floquet drive must be long enough for the spins to collectively reorganize, typically on the picosecond timescale, which is in contrast to typical ultrafast spectroscopy Floquet experiments that rely on intense femtosecond laser pulses. In this talk, I will describe our efforts to develop new experimental hybrid timescale techniques that employ long pulse Floquet driving while simultaneously probing the response of the system on ultrafast timescales. I will also discuss preliminary data on van der Waals magnets using this technique.

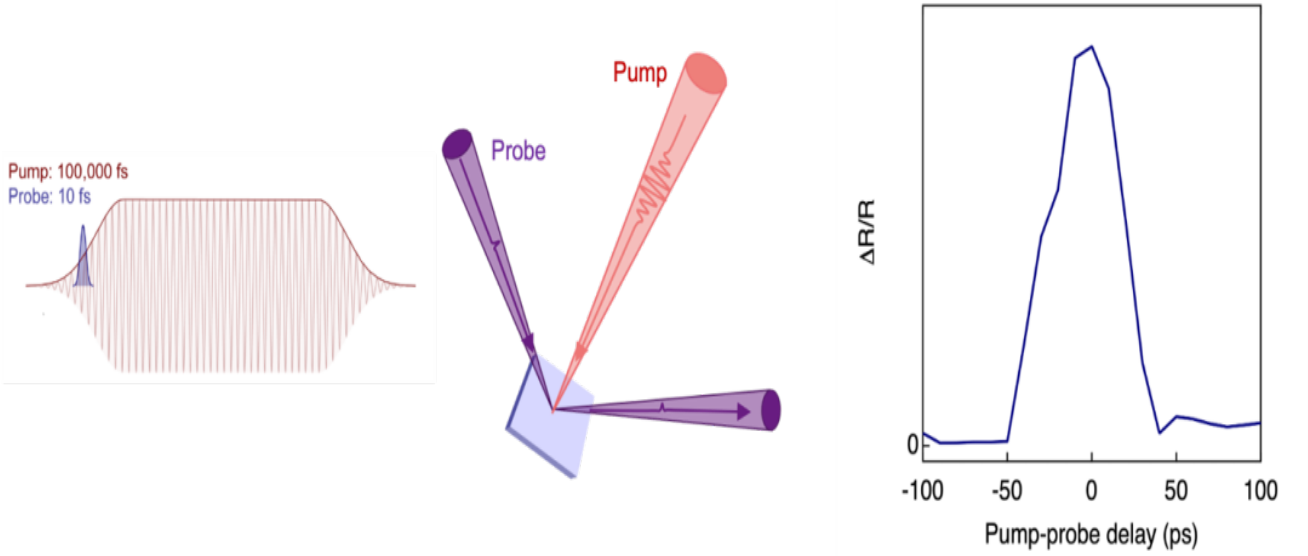

***Fig. 1. Left** : Schematic of our hybrid timescale experimental approach involving long pulse (100 ps) driving and short pulse (100 fs) probing. **Right**: Example transient reflectivity scan taken using this hybrid timescale technique.*

In this talk, I will describe our efforts to develop new experimental hybrid timescale techniques that employ long pulse Floquet driving while simultaneously probing the response of the system on ultrafast timescales. I will also discuss preliminary data on van der Waals magnets using this technique.

References

[1] A. de la Torre, D. M. Kennes, M. Claassen, S. Gerber, J. W. McIver, M. A. Sentef, *Reviews of Modern Physics* **93**, 041002 (2021).
[2] C. Bao, P. Tang, D. Sun, S. Zhou, *Nature Reviews Physics* **4**, 33 (2022).
[3] T. Oka, S. Kitamura, *Annual Review of Condensed Matter Physics* **10**, 387 (2019).
[4] F. Mahmood, C.-K. Chan, Z. Alpichshev, D. Gardner, Y. Lee, P. A. Lee, N. Gedik, *Nature Physics* **12**, 306 (2016).
[5] J. W. McIver, B. Schulte, F.-U. Stein, T. Matsuyama, G. Jotzu, G. Meier, A. Cavalleri, *Nature Physics* **16**, 38 (2020).
[6] S. Zhou, C. Bao, B. Fan, H. Zhou, Q. Gao, H. Zhong, T. Lin, H. Liu, P. Yu, P. Tang, S. Meng, W. Duan, S. Zhou, *Nature* **614**, 75 (2023).
[7] J.-Y. Shan, M. Ye, H. Chu, S. Lee, J.-G. Park, L. Balents, D. Hsieh, *Nature* **600**, 235 (2021).
[8] J. H. Mentink, K. Balzer, M. Eckstein, *Nature Communications* **6**, 6708 (2015).
[9] M. Claassen, H.-C. Jiang, B. Moritz, T. P. Devereaux, *Nature Communications* **8**, 1192 (2017).
[10] S. Chaudhary, D. Hsieh, G. Refael, *Physical Review B* **100**, 220403(R) (2019).

* We acknowledge support from the Brown Science Foundation and the Gordon and Betty Moore Foundation.

Polaritons in plasmonic and laser heterostructures

R. Binder[1], N.H. Kwong[1], M. Spotnitz[2], J. R. Schaibley[1]
[1]*University of Arizona, Tucson, AZ 85721, USA*
[2]*Sandia National Laboratories, Albuquerque, NM 87123, USA*

Semiconductor structures, including bulk, quantum wells, two-dimensional (2D) layers, and microcavities, support formation of exciton-polaritons, i.e., eigenmodes or quasi-particles composed of excitons and light. Exciton polaritons can exist in 2D layers or semiconductor quantum wells (often called quantum well polaritons or 2D-layer polaritons), at surfaces or interfaces (for example surface-plasmon polaritons in the case of a planar interface between a metal and a dielectric), at surfaces with adjacent 2D layers (for example exciton-surface-plasmon polaritons), and in microcavities (microcavity polaritons). The fact that excitons in 2D semiconductors, such as various monolayer transition-metal dichalcogenides (TMDs), e.g., $MoSe_2$ or WS_2, have very strong binding energies (on the order of 500 meV, as opposed to about 5 meV in bulk GaAs) makes them ideal candidates for strong light-matter coupling and thus strong polaritonic effects, including, for example, a modification of the group velocity or large changes in the effective mass. Exciton-polaritons ("polaritons" for short) can also provide optical nonlinearities that may be exploited in communication network devices. Polaritons are always open-pumped-dissipative systems, which means that non-trivial non-Hermitian effects can be possible. The open-pumped-dissipative character also affects possible condensation phenomena, such as formation of a Bose-Einstein condensate or a polaritonic Bardeen-Cooper-Schrieffer (BCS) state. While exciton-polaritons can often be viewed as hybridized states combining two particles (exciton and photon), with the exciton behaving like a point Boson (at least at low excitation densities), interesting physical effects can also result from the fact that the exciton itself is a composite particle (comprising an electron and a hole). This may not only lead to deviations from the bosonic nature but can enable non-trivial effects like valley-dependent electron-hole (e-h) exchange interactions, which can affect optical nonlinearities. In this talk, we review our recent research activities on the linear and nonlinear optical properties of 2D semiconductors and semiconductor quantum wells in two geometries: plasmonic heterostructure (i.e., monolayer in proximity to metal surface), and microcavities containing GaAs quantum wells. The specific heterostructure design has a substantial influence on the exciton-polariton characteristics, and enables design of specific target properties, such as strong ultrafast optical nonlinearity [1] and strong reduction of group velocity [2], or strong modification (even qualitative modification) of the polaritons' effective mass and related transport effects [3,4]. While part of the talk will be on plasmonic devices that allow for ultrafast (sub-picosecond) modulations, we also discuss recently obtained insights into the lasing properties of microcavity lasers, in particular GaAs quantum well microcavity lasers [5-9].In this talk, we present a microscopic many-particle theory of polariton lasers in the BCS regime with special emphasis on fluctuation modes. Their complex landscape includes Goldstone modes, spectral continua, and quasi-Higgs modes (possibly at exceptional points) [6]. Experimental demonstration of a polariton laser operating in the BCS regime has been achieved [5] in the group of Hui Deng, University of Michigan. For theoretical analysis of those experiments, we used a microscopic many-particle theory to compute experimental observables such as emission frequency. We have also studied linear response and fluctuation modes of the polariton laser, i.e. a driven-dissipative quantum many-particle system prepared in a spontaneous broken-symmetry steady state, using optical frequencies (interband transitions) [6] and terahertz frequencies (intraband transitions) [7,8].In the talk, we focus mainly on the collective fluctuation modes (as opposed to the spectral continua), which emerge as discrete eigenvalues from the diagonalization of the microscopic fluctuation matrix. An important task is the classification of the collective modes. This turns out to be more complicated than the well-known textbook classifications of Goldstone modes (phase modes) and Higgs mode (amplitude modes). The reason is because (1) the electron-hole pairs, that take the role of Cooper pairs in superconductivity, are not point bosons, but composite particles with an internal motion (or internal degree of freedom), (2) the order-parameter consists not only of the electron-hole pairs but also the cavity light field, and (3) the linear response/fluctuations involves not only the order parameter but also the charge carrier distribution and density. The internal motion can be described by the electronic wave vector $\mathbf{k}$, and for each wave vector the interband polarization $P(\mathbf{k})$ is part of the complex-valued order parameter. The linear response of each $P(\mathbf{k})$ and the laser field E can then be classified in terms phase and amplitude perturbations. We define a mode to be an amplitude (phase) mode if all $P(\mathbf{k})$ and the laser field E are amplitude (phase) modes. Additionally, we allow for fluctuations of the carrier distribution function $f(\mathbf{k})$ and the carrier density. Fig. 1 shows a schematic overview of this scenario.

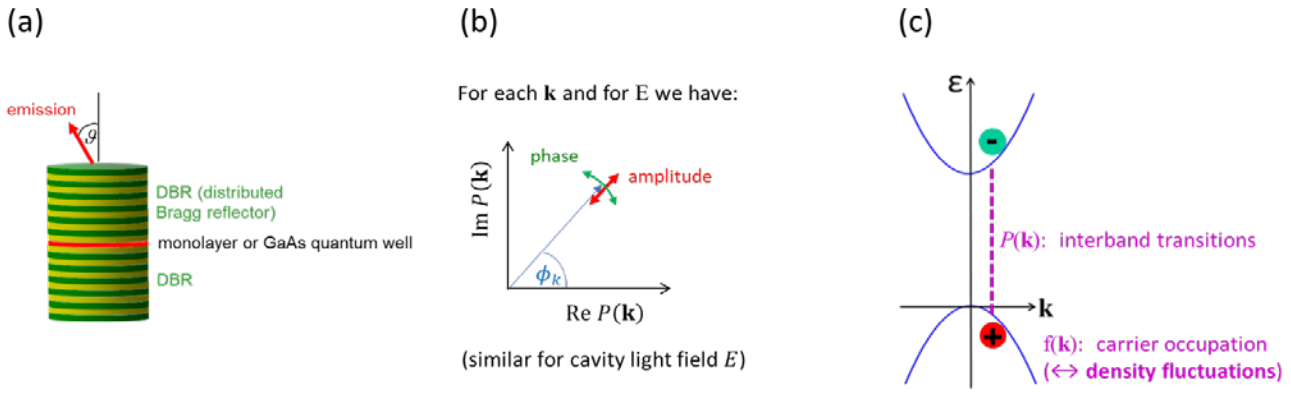

Fig. 1 Schematic overview of fluctuations in a semiconductor laser. ***(a)*** *Sketch of a microcavity laser,* ***(b)*** *sketch of phase and amplitude fluctuations for each interband polarization,* ***(c)*** *sketch of electronic band structure with interband polarization and carrier distribution (occupation).*

In this work, we diagonalize the microscopic fluctuation matrix, which is obtained from linear perturbations of the laser in steady-state. Discrete energy eigenstates of the fluctuation matrix correspond to collective modes, and are analyzed in terms of their phase, amplitude and density fluctuation characteristics. In Fig. 2 we show the results (here as means of the electronic wave vector) for the right (R) and left (L) eigenvectors of the fluctuation matrix for 3 collective modes (Goldstone mode G_0, Mollow-like mode M, and the mode T_0, which is a collective mode resulting from a THz source). In the ratio x/R , the size of the amplitude response is denoted by R, the size of the phase response (arc length) by α, and the size of the density response by f.

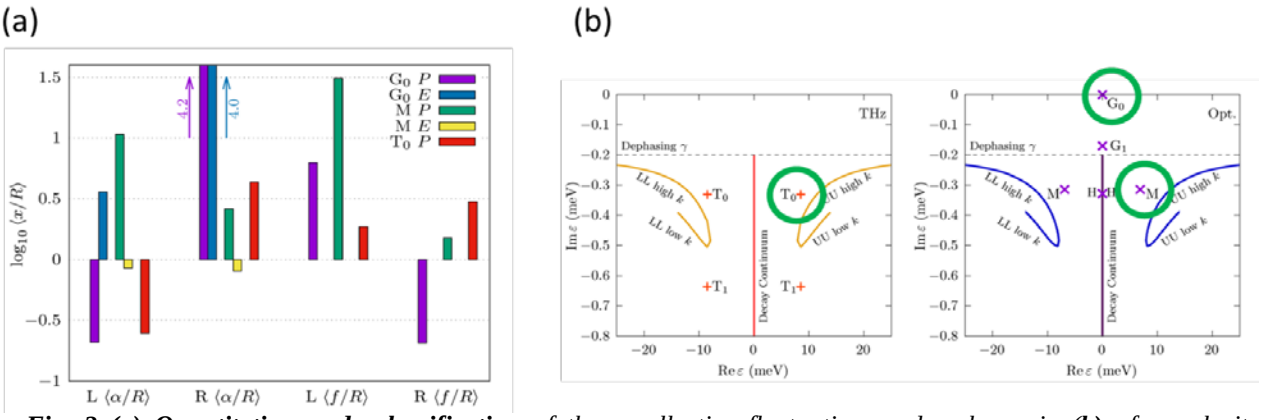

Fig. 2 (a) Quantitative mode classification *of three collective fluctuation modes shown in* ***(b)*** *of a polariton microcavity laser. In* ***(b)****, the fluctuation spectra (complex energy eigenvalues) are shown for the case of a THz probe (****left****) and an optical probe with frequency similar to the lasing frequency (****right****). In* ***(a)*** *the ratios of the mean (i.e., average taken over the electronic wave vector) phase, amplitude and density responses are plotted for the three modes highlighted with green circles in* ***(b)****. After [8].*

Only in the case of G_0 do we find one of those components to be dominant (namely the phase response), while in the other modes the phase, amplitude and density responses are of comparable magnitude, hence ruling out pure Higgs modes. More details can be found in Ref. [8].

References

[1] M. Klein, B. H. Badada, R. Binder, A. Alfrey, M. McKie, M. R. Koehler, D. G. Mandrus, T. Taniguchi, K. Watanabe, B. J. LeRoy, J. Schaibley, *Nature Communications* **10**, 3264 (2019).
[2] M. Klein, R. Binder, M.R. Koehler, D.G. Mandrus, T. Taniguchi, K. Watanabe, J.R. Schaibley, *Nature Communications* **13**, 6216 (2022).
[3] R. Binder, J. R. Schaibley, N. H. Kwong, *Physical Review* B **109**, 125301 (2024).
[4] N. H. Kwong, J.R. Schaibley, R. Binder, *Physical Review* B **104**, 245434 (2021).
[5] J. Hu, Zh. Wang, S. Kim, H. Deng, S. Brodbeck, Ch. Schneider, S. Hoefling, N.H. Kwong, R. Binder, Physical Review. X **11**, 011018 (2021).
[6] R. Binder, N.H. Kwong, *Physical Review* B **103**, 085304 (2021).
[7] M. Spotnitz, N.H. Kwong, R. Binder, *Physical Review* B **104**, 115305 (2021).
[8] M. Em. Spotnitz, N. H. Kwong, R. Binder, Physical Review B **107**, 125309 (2023).
[9] N. H. Kwong, M. Em. Spotnitz, R. Binder, Physical Review B **109**, 045306 (2024).
* Acknowledgements: R.B. gratefully acknowledges financial support from NSF under grant number DMR 1839570, and CPU time at HPC, University of Arizona. J.R.S. acknowledges funding from AFOSR Grant number: FA9550-20-1-0217.

A lightwave-electronics toolbox for quantum

M. Borsch[1], Z. Mi[1], R. Huber[2], M. Kira[1]
[1] *University of Michigan, Ann Arbor, MI 48109, USA.*
[2] *University of Regensburg, 93040 Regensburg, Germany.*

Lightwave electronics utilizes optical-carrier waves of light as fast biasing fields to drive electronic states and quantum coherences on femtosecond timescales and up to petahertz clock rates. We have previously demonstrated a set of tools based on lightwave-electronic principles to reconstruct the band structure of quantum materials [1], quantify dynamic many-body correlations with attosecond precision [2], and switch the pseudospin of coherent excitations in valleytronic materials within a few femtoseconds [3]. Here, we propose a new technique that adds the capability to probe the temporal shape of lightwaves to the lightwave-electronics toolbox. Using the quantum-dynamic cluster expansion [4], we quantitatively predict the lightwave-driven many-body dynamics of realistic quantum materials to optimize the lightwave switching of valleytronic states. Under optimized conditions, we find an intriguing frequency-comb-like emission regime when the valleytronic state is continually switched back and forth. In this regime, the emitted light is highly sensitive to the driving field (Fig. 1 c and d) and precisely probes the lightwave itself.

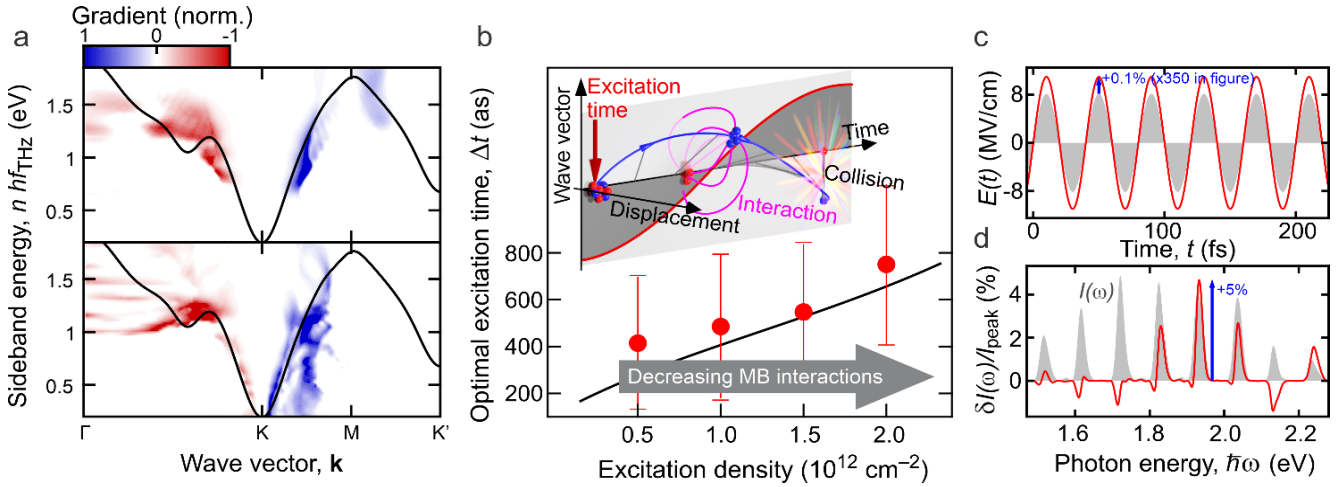

Fig. 1. Capabilities of the lightwave-electronics toolbox. a *Reconstruction of the band structure of WSe_2 monolayer based on harmonic-sideband intensities mapped as function of the field strength and frequency of the generating lightwave. The reconstruction based on odd (top) and even (bottom) sideband orders is shown.* ***b.****Direct measurement of the excitonic interaction strength [2] in a WSe_2 monolayer using the quasiparticle-collider approach (inset, see Ref. [5] with attosecond resolution. A comparison between measured (dots) and computed (black line) optimal excitation time Δt (relative to the lightwave) that maximizes HSB emission. The optimal excitation time increases with the excitation density, consistent with longer excitation-collision trajectories caused by weakened Coulombic interaction at increased excitation.* ***c, d*** *Sensitivity of valleytronic combs to fluctuations of the lightwave. A continuous back-and-forth switching of the valleytronic state using a sinusoidal lightwave (Panel c, shaded area) generates emission of equidistant frequency lines in the spectral domain (Panel d, shaded area). A small change of 0.1% in the amplitude of the lightwave (Panel c, red line) leads to changes of up to 5% in the spectral domain (Panel d, red line), demonstrating the high sensitivity of valleytronic combs to electric-field fluctuations.*

This sensitivity allows for the detection of time-dependent fluctuations of the electric field with high accuracy, extending all the way to quantum tomography of lightwaves.We will present how this new approach of quantum tomography can be applied to lightwaves in the THz-to-NIR domain and discuss the new capabilities it adds to our lightwave-electronics toolbox.

References

[1] M.Borsch, C. P. Schmid, L. Weigl, S. Schlauderer, N. Hofmann, C. Lange, J. T. Steiner, S. W. Koch, R. Huber, M. Kira, *Science* **370**, 1204 (2020)
[2] J. Freudenstein, M. Borsch, M. Meierhofer, D. Afanasiev, C. P. Schmid, F. Sandner, M. Liebich, A. Girnghuber, M. Knorr, M. Kira, R. Huber *Nature* **610**, 290 (2022).
[3] F. Langer, C. Schmid, S. Schlauderer, M. Gmitra, J. Fabian, P. Nagler, C. Schüller, T. Korn, P. G. Hawkins, J.T. Steiner, U. Huttner, S. W. Koch M Kira, R. Huber, *Nature* **557**, 76 (2018).
[4] M. Kira and S. W. Koch, Semiconductor Quantum Optics, *Cambridge University. Press* (2012).
[5] F. Langer, M. Hohenleutner, C. Schmid, C. Poellmann, P. Nagler, T. Korn, C. Schüller, M. S. Sherwin, U. Huttner, J. T. Steiner, S. W. Koch, M. Kira R. Huber, *Nature* **533**, 225 (2016).
* Acknowledgement(s): M.B. and M.K. acknowledge support from ARO through Award W911NF1810299.

Time-resolved ARPES at the Advanced Laser Light Source (ALLS) user facility: New insights into the ultrafast quenching of superconductivity in Bi-based cuprates

D. Armanno, J. M. Parent, F. Goto, A. Longa, G. Jargot, F. Légaré, N. Gauthier, F. Boschini
Institut National de la Recherche Scientifique, Varennes QC J3X 1S2, Canada

Time- and angle-resolved photoemission spectroscopy (TR-ARPES) is a powerful technique that provides direct access to the light-induced ultrafast dynamics of the electronic band structure of quantum materials with both momentum and energy resolutions [1]. When probing the transient response of long-range condensates (e.g., superconductors), TR-ARPES studies have conventionally employed near-infrared light excitation to drive ultrafast quenching of macroscopic condensates [1].
The TR-ARPES endstation at the Advanced Laser Light Source (ALLS) user facility provides mid-infrared optical excitation capabilities (0.15-0.8 eV range) along with a 6 eV probe (soon to be upgraded to >10 eV extreme ultraviolet via high harmonic generation) [2]. Furthermore, the ALLS TR-ARPES endstation, although relying on low photon energy probe pulses, can map a large area in momentum space by taking advantage of a new state-of-the-art hemispherical analyzer (ASTRAIOS 190, SPECS) with single octupole deflector technology and sample bias [3].
Fig. 1a demonstrates the momentum mapping capabilities of our TR-ARPES system by showing the Fermi surface mapping of optimally doped $Bi_2Sr_2CaCu_2O_{8+\delta}$ (Bi2212), a prototypical high-Tc cuprate superconductor, where we prove the ability to reach up to ~85% of the antinodal $(0,\pi)$ distance. Figure 1(b) shows that 300 meV pump excitation induces ultrafast filling of the superconducting gap, similar to what has been reported for near-infrared excitation [4].

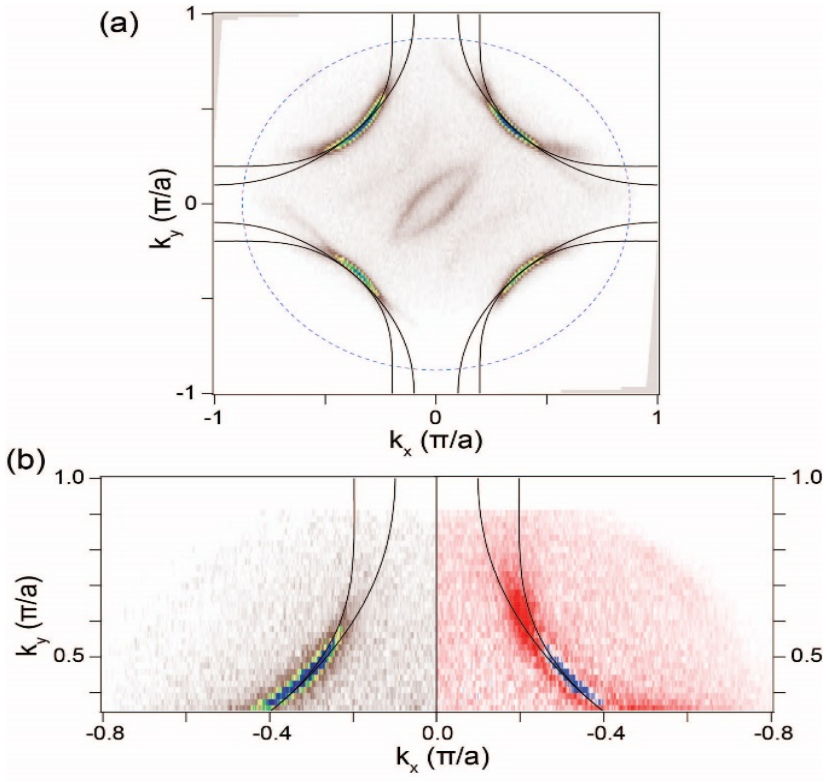

Fig. 1. (a) *Fermi surface mapping of optimally-doped Tc~91 K Bi2212. The solid lines show the bonding and antibonding bands. The dashed blue circle shows the momentum space that can be accessed using 6 eV photons.*
(b) *Photoexcited Fermi surface (**left**) and differential Fermi surface (**right**) at zero pump-probe delay upon 300 meV excitation.*

I will discuss how mid-infrared light, with photon energy well below the charge transfer gap of Bi2212, quenches the superconducting condensate over a wide momentum range. In addition, I will present preliminary data on the normal state that lies beneath the superconducting dome when superconductivity is quenched in an ultrafast fashion.

References

[1] F. Boschini. M. Zonno. A. Damascelli. *Review of Modern Phvsics.* **96.** 015003 (2024)
[2] A Longa, J. M. Parent, B.K. Frimpong, D. Armanno, N. Gauthier, F. Légaré, F. Boschini, G. Jargot, *Optics Express* **32,** 29549 (2024).
[3] N. Gauthier , J.A. Sobota, H. Pfau, A. Gauthier, H. Soifer, M. D. Bachmann, I. R. Fisher, Z.-X. Shen, P. S. Kirchmann, *Review of Scientific Instruments* **92**, 123907 (2021).
[4] F. Boschini, E. H. da Silva Neto, E. Razzoli, M. Zonno, S. Peli, R. P. Day, M. Michiardi, M. Schneider, B. Zwartsenberg, P. Nigge, R. D. Zhong J. Schneeloch, G. D. Gu, S. Zhdanovich,A. K. Mills, G. Levy,D. J. Jones,C. Giannetti,A. Damascelli, *Nature Materials* **17**, 416 (2018).

Metastable dynamics and transport in type-II InAs/AlAsSb Quantum wells

H. P. Piyathilaka[1], R. Sooriyagoda[1], V. R. Whiteside[2], T. D. Mishima[2], M. B. Santos[2]
I. R. Sellers,[3] A. D. Bristow[1]
[1] *West Virginia University, Morgantown, WV 26506. USA*
[2]*University of Oklahoma, Norman, OK 73019, USA*
[3] *SUNY Buffalo, Buffalo, NY 14260, USA*

Control of electronic, optical and thermal properties in semiconductor nanostructures allows for a wide range of device design. This is particularly true for devices that require prolonged lifetimes of hot photocarriers to allow for higher charge separation and extraction yields. A type-II InAs/InAsSb multiple quantum wells (MQWs) is explored for its potential as a prototype hot-carrier device [1] using temperature dependent transient absorption and AC photoconductivity in a single setup with a terahertz (THz) probe pulse. The setup allows for non-destructive measurements of electronic and electron-lattice properties. The tunable optical pump can excite photocarriers at and above the bandgap of the MQW system. At ≈100 meV above the bandgap, transient absorption reveals a metastable excited state with a lifetime of several picoseconds [2]. At low temperature and high excitation density, the dynamics in the metastable state results in strong Auger scattering. At lower excitation densities or higher lattice temperature, the dynamics are dominated by radiative recombination. To suppress Auger scattering at higher temperatures the band structure of the system transitions from Type-I-like to type-II-like, with complicated dynamics in intermediate temperatures that are defined by the filling of defect states at the interfaces of the wells. This result is confirmed by measurements of the photocarrier mobility as a function of temperature [3]. At higher temperatures, increases diffusion that will reduces the carrier density to values required for Auger scattering. These result of the transient absorption and AC photoconductivity are summarized in Fig. 1.

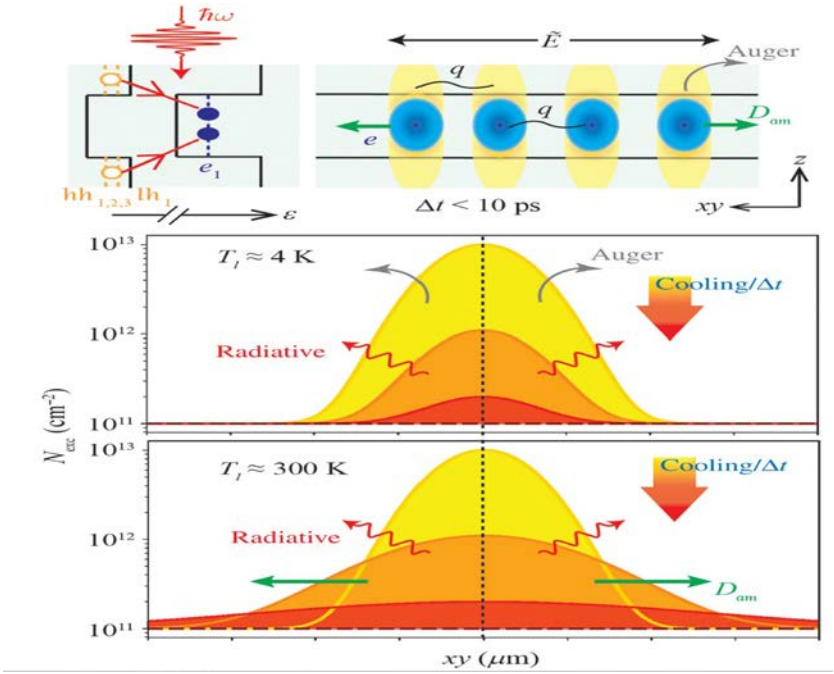

Fig. 1 Schematic diagram of the type-II band aligned MQW system *with the excitation (ħω) from the heavy hole to electron bands. Also shown is the spatial arrangement of the photocarriers. The spatial distributions of photocarriers under different lateral decay after the initial excitation during cooling. This is shown for low and ambient lattice temperatures indicating a difference in diffusion (D_{am}).*

These results illustrate that complete carrier dynamics and transport measurements are required to separate the contributions to the cooling, recombination, and diffusion of carriers that can occur in specific device geometry.

References

[1] H. Esmaielpour, V. R. Whiteside, H. P. Piyathilaka, S. Vijeyaragunathan, B. Wang, E. Adcock-Smith, K. P. Roberts, T. D. Mishima, M. B. Santos A. D. Bristow, I. R. Sellers, *Scientific Reports* **8**, 12473 (2018).
[2] H. P. Piyathilaka, R. Sooriyagoda, H. Esmaielpour, V. R. Whiteside, T. D. Mishima, M. B. Santos, I. R. Sellers, A. D. Bristow, *Scientific Reports* **11** 10483 (2021).
[3] H. P. Piyathilaka, R.Sooriyagoda, V. R.Whiteside, T. D.Mishima, M. B.Santos, I. R. Sellers, A. D. Bristow, *Physical Review Applied* **18**, 014001 (2022)

Indirect excitons in heterostructures

L.V. Butov
University of California San Diego, La Jolla, CA 92093

A spatially indirect exciton (IX), also known as an interlayer exciton, is a bound pair of an electron and a hole confined in separated layers in a semiconductor heterostructure (HS). Due to their long lifetimes, orders of magnitude longer than lifetimes of spatially direct excitons (DXs), IXs can thermalize below the temperature of quantum degeneracy that gives an opportunity to create quantum excitonic states. We present recent results in quantum IX systems: the Fermi-edge singularity due to the Cooper-pair-like excitons [1] and the excitonic Bose polarons [2] in GaAs/AlGaAs HS and the long-range IX transport [3] and the IX mediated long-range spin transport in $MoSe_2/WSe_2$ HS [4].

The Fermi-edge singularity due to the Cooper-pair-like excitons [1]. In neutral dense electron-hole systems at low temperatures, theory predicted Cooper-pair-like excitons at the Fermi energy. Optical excitations create electron-hole systems with the density controlled via the excitation power. The separation of electron and hole layers enables the realization of a dense and cold electron-hole system. We found a strong enhancement of photoluminescence intensity at the Fermi edge energy of the neutral dense ultracold electron-hole system that demonstrates the emergence of an excitonic Fermi edge singularity due to the formation of Cooper-pair-like excitons at the Fermi edge. Our measurements also show a crossover from the hydrogen-like excitons to the Cooper-pair-like excitons with increasing density, consistent with the theoretical prediction of a smooth transition.

The excitonic Bose-polarons [2]. Bose polarons are mobile impurities dressed by excitations of a surrounding degenerate Bose gas. These many-body objects have been realized in ultracold atomic gasses and become a subject of intensive studies. We found that Bose polarons are formed by DXs immersed in degenerate Bose gases of IXs in electron-hole bilayers. We detected both attractive and repulsive Bose polarons by measuring photoluminescence excitation spectra. We controlled the density of IX Bose gas by optical excitation and observed an enhancement of the energy splitting between attractive and repulsive Bose polarons with increasing IX density, in agreement with our theoretical calculations.

The long-range IX transport in TMD HS [3]. Long lifetimes of IXs allow implementing long-range exciton transport. The van der Waals HS composed of atomically thin layers of transition-metal dichalcogenides (TMD) offer the opportunity to explore IXs in moiré superlattices. IX transport in TMD HS was intensively studied and diffusive IX transport with 1/e decay distances up to ~ 4 μm was realized in earlier studies. We found the IX long-range transport with 1/e decay distances reaching and exceeding 100 μm in a $MoSe_2/WSe_2$ HS. The IX long-range transport vanishes at temperatures above ~10 K. With increasing IX density, IX localization followed by IX long-range transport and IX re-entrant localization are observed. The non-monotonic dependence of IX transport on density is in qualitative agreement with the Bose-Hubbard theory prediction for superfluid and insulating phases in periodic potentials of moiré superlattices.

The IX mediated long-range spin transport in TMD HS [4]. The spin relaxation caused by scattering of the particles carrying the spin, limits the spin transport. We explored IXs in van der Waals TMD HS as spin carries. Due to the coupling of the spin and valley indices in TMD HS, the spin transport is coupled to the valley transport, therefore, for simplicity, we use the term 'spin' also for 'spin-valley'. We observed the IX mediated long-distance spin transport with the decay distances reaching and exceeding 100 μm. The emergence of long-distance spin transport is observed at the densities and temperatures where the IX transport decay distances and, in turn, scattering times are strongly enhanced. The suppression of IX scattering suppresses the spin relaxation and enables the long-distance spin transport. This mechanism of protection against the spin relaxation makes IXs a platform for the realization of long-distance decay-less spin transport.

References

[1] D. J. Choksy, E.A. Szwed, L.V. Butov, K.W. Baldwin, L. N. Pfeiffer, *Nature Physics* **19**, 1275 (2023).
[2] E. A. Szwed, B.Vermilyea, D.J. Choksy, Z. Zhou, M. M. Fogler, L.V. Butov, D. K.Efimkin, K.W. Baldwin, L.N. Pfeiffer *arXiv:2406.15660*(2024)
[3] L. H. Fowler-Gerace, Zhiwen Zhou, E.A. Szwed, D.J. Choksy, L.V. Butov, *Nature Photonics* **18**, 823 (2024).
[4] Z. Zhou, E.A. Szwed, D.J. Choksy, L.H. Fowler-Gerace, L.V. Butov, *arXiv:2406.04440* (2024).

* Acknowledgement(s): The studies were supported by DOE Award DE-FG02-07ER46449, NSF Grant 1905478, Gordon and Betty Moore Foundation Grant GBMF9615 and NSF grant DMR 2011750.

Optical control of superconductivity in high-T_C cuprates

M. Buzzi
Max Planck Institute for the Structure and Dynamics of Matter, 22761 Hamburg, Germany

Tailored optical excitation in certain high-T_c cuprates has been shown to induce superconducting-like interlayer coherence at temperatures far above T_c, as evidenced by the terahertz-frequency optical properties in the nonequilibrium state [1,2]. In this talk I will discuss our latest experiments in the field of optical control of superconductivity in $YBa_2Cu_3O_{6+x}$, which have led to considerable advances both in optimizing the nonequilibrium state and understanding its nature. In the first part of the talk, I will discuss how the enhancement of the "superfluid density" $\omega\sigma_2$, and the dissipative response of quasiparticles, σ_1, can be optimized by systematically tuning the duration and energy of the mid-infrared excitation pulse while keeping the peak field fixed [3]. We found that the photoinduced $\omega\sigma_2$ saturates to the zero-temperature equilibrium value for pulses made longer than the phonon dephasing time, while the dissipative component continues to grow with increasing pulse duration. This finding suggests that superfluid and dissipation remain uncoupled as long as the drive is on, enabling the identification of an optimal regime of pump pulse durations for which the superconducting-like response is maximum and dissipation is minimized.I will then discuss whether these out-of-equilibrium superconducting-like states also show a dynamical diamagnetic response, beyond the documented transient optical conductivities. To this end, we have developed a novel, ultrafast optical magnetometry technique to measure changes in the magnetic field in the vicinity of a $YBa_2Cu_3O_{6.48}$ sample with $\sim 1\ \mu T$ sensitivity and sub-picosecond time resolution (Fig. 1).

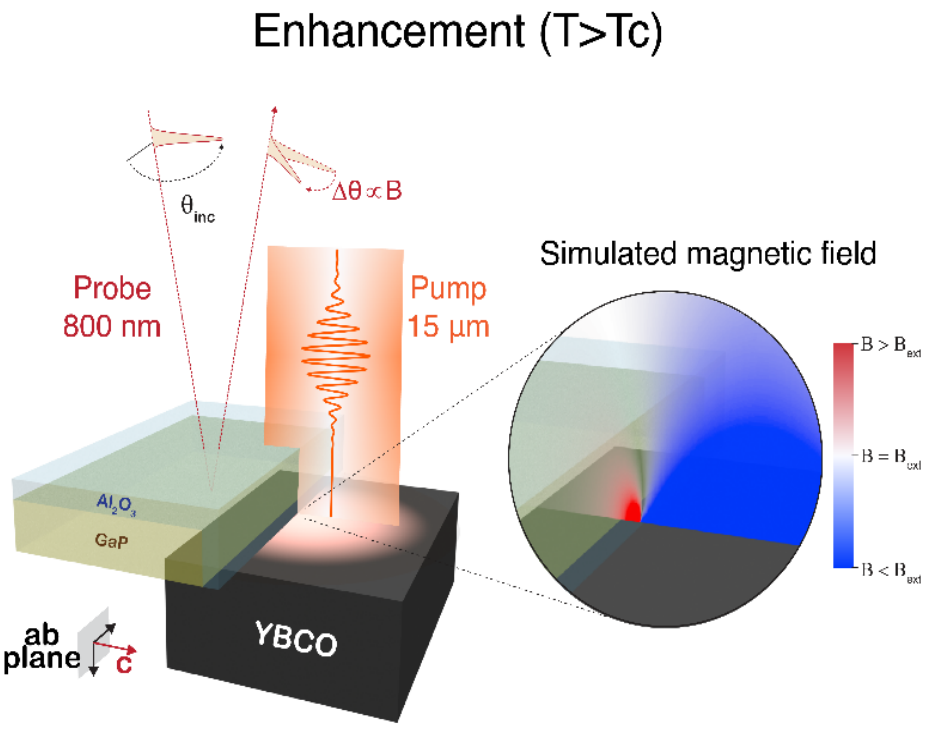

Fig. 1. Magnetic field expulsion after phonon excitation in $YBa_2Cu_3O_{6.48}$. Schematic of the experiment. *A thin Al_2O_3 crystal is placed on top and next to the exposed side of the GaP (100) detection crystal to completely reflect the 15 μm pump and prevent it from generating a spurious non-linear optical response in the GaP (100) crystal. The thin Al_2O_3 crystal also creates a well-defined edge in the mid infrared pump beam, shaping the photo-excited region into a half disc of ~ 375 μm diameter. The expected changes due to magnetic field expulsion upon photo-excitation are shown in the magnified area on the right. The time dependent magnetic field is sampled positioning the probe beam in the vicinity of the edge of the photo-excited region.*

We provide evidence that, under the same excitation conditions that generate a transient superconducting-like state in this material, a prompt expulsion of a statically applied magnetic field ensues, a response indicative of the appearance of an ultrafast Meissner effect [4].

References

[1] W. Hu, S. Kaiser, D. Nicoletti, C. R. Hunt, I. Gierz, M. C. Hoffmann, M. Le Tacon, T. Loew, B. Keimer, A. Cavalleri, *Nature Materials* **13**, 705 (2014)
[2] B. Liu, M. Först, M. Fechner, D. Nicoletti, J. Porras, B. Keimer, A. Cavalleri, *Physical Review* X **10**, 011053, (2020).
[3] A. Ribak, M. Buzzi, D. Nicoletti, R. Singla, Y. Liu, S. Nakata, B. Keimer, A. Cavalleri, Physical Review B 107, 104508, (2023).
[4] S. Fava, G. De Vecchi, G. Jotzu, M. Buzzi, T. Gebert, Y. Liu, B. Keimer, A. Cavalleri, *Nature* **632**, 75 (2024).

Efficient high-order harmonic generation from novel van der Waals crystals and heterostructures

A.Mushtaq[1], T. D. Journigan[1], V.Turkowski[1], R. Siebenaller[2], D. A. Jeff[1], T.-C. Truong[1], M.Y.Noor[2]
D. Khatri[1], C. Lantigua[1], K. Harrison[1], S. I. Khondaker[1], E. Rowe[3], J. T. Goldstein[3], M. A. Susner[2]
E.Chowdhury[2], M.Chini[2]
[1] *University of Central Florida, Orlando, FL 32816 USA*
[2] *The Ohio State University, Columbus, OH 43210 USA*
[3] *Air Force Research Laboratory, Wright-Patterson Air Force Base, OH 45433 USA*

Recent research into two-dimensional (2D) van der Waals materials has provided a novel platform to realize size reduction, enhanced efficiency, and new capabilities in next-generation nonlinear optic and optoelectronic devices. Metal thio- and seleno-phosphates (MXPs) are a class of 2D materials that possess outstanding magnetic, ferroelectric, and nonlinear optical properties suited for new device architectures [1]. Copper indium thiophosphate (CIPS, $CuInP_2S_6$) is one exemplary material that belongs to the MXPs family. CIPS, when synthesized with Cu deficiencies (i.e. $Cu_{1-x}In_{1+x/3}P_2S_6$) segregates into self-assembled heterostructures of CIPS and IPS ($In_{4/3}P_2S_6$) within the same crystal. CIPS and Cu-deficient CIPS have previously been reported to have extraordinary second- and third-order nonlinear optical properties [2]. Exfoliated CIPS crystals under the influence of strain has been found to exhibit a ~160-fold increase in the efficiency of second harmonic generation (SHG) compared to an unstrained sample [3].Here, we investigate high-order harmonic generation (HHG) from bulk and exfoliated MXP crystals (CIPS, IPS, and Cu-deficient CIPS, Fig. 1a) using femtosecond mid-infrared laser pulses and infer that their extraordinary nonlinear properties carry over also to the high-order nonlinear response. We observe high conversion efficiency in the HHG emission from Cu-deficient CIPS in comparison to both pure CIPS and IPS, with higher conversion efficiency from the exfoliated samples in comparison to bulk crystals. Interestingly, we observe perturbative scaling of the HHG in all samples (Fig. 1b), suggesting that the efficient harmonic generation originates from the extraordinary nonlinear optical properties of the crystal, rather than nonperturbative strong-field physics.

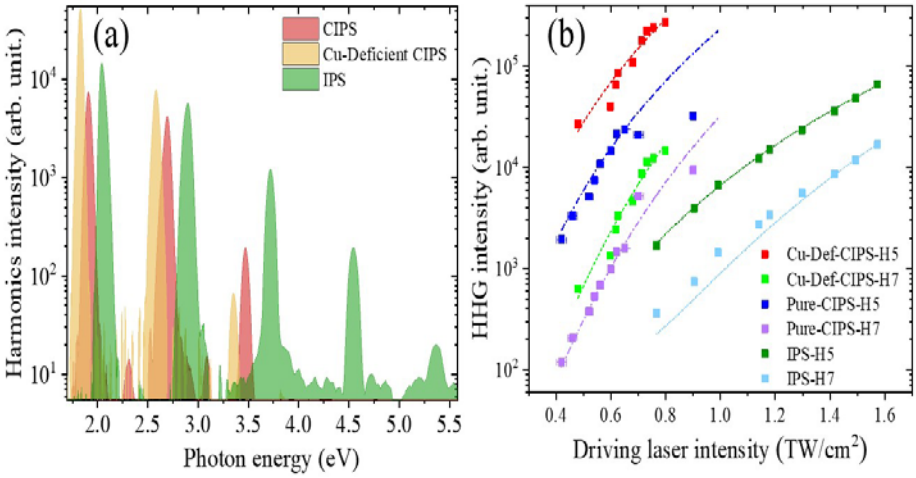

Fig. 1. **(a) HHG spectrum** recorded for exfoliated CIPS (180 nm thick flake), Cu-deficient-CIPS (70 nm thick flake) and IPS (<100 nm thick flake) following 3.2, 3.4 and 3.1 μm excitations. **(b)** Integrated HHG intensity plotted as a function of input driving laser intensity. Fits are made using power law, $I_q \propto I_0^q$ where I_0 and I_q are the intensities of the driving laser and harmonic fields, respectively, and q is the harmonic order.

In addition to the above experimental studies, we perform first-principles studies of HHG to uncover the origins of the extraordinary high-order nonlinear optical response from CIPS and Cu-deficient CIPS using time-dependent density functional theory and dynamical mean-field theory. Our calculations suggest that both electron-electron correlations and strain in the CIPS/IPS heterostructures of Cu-deficient CIPS play important roles.

References

[1] M.A. Susner, M. Chyasnavichyus, M.A. McGuire, P. Ganesh, P. Maksymovych, *Advanced Materials* **29**, 1602852 (2017).
[2] A. Mushtaq, L. Clink, M.Y. Noor, C.Kuz,E. DeAngelis, R.Siebenaller, A. Fisher, D.Verma, R.C. Myers, B.S. Conner, M.A., Susner, E. Chowdhury *Journal of Physical Chemistry Letters* **13**, 10513 (2022).
[3] S. Rahman, T. Yildirim, M. Tebyetekerwa, A.R. Khan, Y. Lu, *ACS Nano* **16**, 13959 (2022).

* Acknowledgements: This research was primarily supported by the Air Force Office of Scientific Research (AFOSR) under award no. FA9550-20-1-0284. Work performed at The Ohio State University was supported by the AFOSR Grant LRIR 23RXCOR003, AOARD - MOST Grant F4GGA21207H002, and AFOSR award no. FA9550-20-1- 0278. We also acknowledge support from the National Research Council's Senior NRC Associateship program sponsored by the National Academies of Sciences, Engineering, and Medicine. KH, SIK and MC acknowledge support from DMR 2121953 from NSF Partnerships for Research and Education in Materials (PREM). Also, we would like to thank Prof. Roberto C. Myers from The Ohio State University for measurements of the room temperature PL spectrum.

Ultrafast and cavity electrodynamical control of Optical nonlinearities in quantum materials

M. Claassen
University of Pennsylvania, Philadelphia, PA 19104, USA

Quantum control, the on-demand coherent manipulation of a macroscopic quantum system, is one of the defining challenges of modern physics. In solid-state settings, ultrafast pump-probe experiments have enabled the selective manipulation of quantum states in quantum materials, while recent advances in cavity quantum electrodynamics promise to extend quantum-optical protocols to correlated electron systems. In this talk, I will discuss how classical and quantum optical nonlinearities can provide a particularly useful window into the nature of quantum states in materials which are far from thermal equilibrium and strongly dressed by light. First, I will describe recent experimental and theoretical work showing that driving the one-dimensional Mott insulator Sr_2CuO_3 with a MIR pump can transiently Floquet engineer the wave functions of Mott-Hubbard excitons, leading to an ultrafast and controllable renormalization of the third-order nonlinear optical response [1]. The effect is rooted in a near-degeneracy between parity-even and parity-odd holon-doublon excitonic bound states, which are coupled via the pump field to realize quantum control of the final states for third-harmonic generation. I will then describe how ultrafast light pulses can tip the balance between different pairing symmetries in conventional s-wave superconductors with closely competing odd-parity spin-triplet pairing instabilities [2]. Such systems can host a Bardasis-Schrieffer mode associated with odd-parity order parameter oscillations, which upon strong excitation with light can trap the system in a metastable triplet superconducting state. The coupling of photons to odd-parity pairing fluctuations is a purely quantum-geometric quantity of the Fermi surface, serving as a guiding principle for ultrafast control.

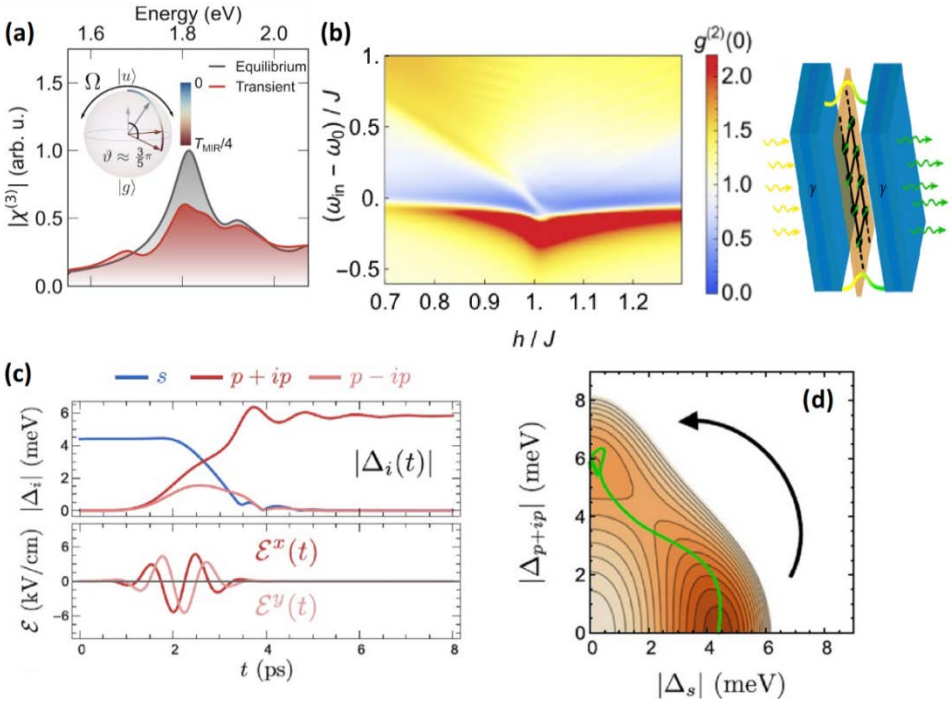

Fig. 1. (a) Ultrafast suppression of third-harmonic generation (THG) *in a one-dimensional Mott insulator, depicted via the third-order susceptibility in (gray) and out-of-equilibrium (red). Inset depicts the ultrafast dressing of even/odd Mott exciton wave functions via a MIR pulse.* ***(b)*** *Second-order photon coherence* $g^{(2)}(\tau = 0)$ *for transmission through a single-mode cavity strongly coupled to an Ising quantum magnet, tuned across its quantum critical point via a transverse field* h*, and depicted as a function of detuning of the driving field from the bare cavity resonance.* ***(c)*** *Ultrafast excitation with light of a Bardasis-Schrieffer mode in a conventional s-wave superconductor hosting a competing spin-triplet pairing instability can* ***(d)*** *realize a metastable p+ip superconducting state.*

Finally, I will discuss how the strong light-matter coupling regime of quantum materials placed inside optical cavities can be interrogated via second-order photon coherence measurements of light transmitted through the cavity [3]. I will describe how coupling a Mott insulator to cavity photons can manipulate magnetic exchange interactions to realize a photon blockade regime for transmitted light, if the magnetic state in the material is near a quantum critical point. Here, measurements of $g^{(2)}$ are predicted to exhibit strong antibunching for transmitted photons, constituting a key signature of cavity quantum-electrodynamical control of the magnetic phase.

References

[1] D. Baykusheva, D.Carmichael, C.Weber, I-Te Lu, C.Homes, I.Zaliznyak, G.Gu, M.P.Dean, A.Rubio, D. Kennes, M. Claassen, M. Mitrano, *to be submitted* (2024)
[2] S. Gassner, C. S. Weber, M. Claassen, *Nature Communications* **15**, *1776 (2024).*
[3] B. Kass, S. Talkington, A. Srivastava, M. Claassen, *to be submitted (2024).*
* Acknowledgement(s): M.C. acknowledges support from the DoE, Basic Energy Sciences (Award No. DE- SC0024494), and the NSF (Award No. DMR-2132591)

Control of electron-phonon coupling in perovskite nanocrystals

L. Dai[2], N.C. Greenham[1]
[1] *Cavendish Laboratory, University of Cambridge*
[2] *Massachusetts Institute of Technology*

Understanding and control of ultrafast non-equilibrium processes in semiconductors is crucial for making use of quantum states, opening opportunities to surpass traditional limits in optoelectronic devices for energy harvesting, light emission, and quantum technologies. In this paper, we first demonstrate our work in slowing down hot carrier relaxation through strategies involving electronic structure management, phonon structure management, and decoupling carriers from defects. These approaches effectively engineer carrier-phonon, phonon-phonon, and carrier-carrier (defect) interactions. Subsequently, we demonstrate the alignment of the transition dipole moment in self-assembled nanoplatelets, resulting in polarised electroluminescence with a high degree of polarization comparable to single nanocrystals. First of all, we introduce new perovskite nanocrystals, formamidinium tin iodide nanocrystals (FASnI3 NCs), where quantum confinement significantly influences the electronic structure. The evolution in electronic structure from a continuous band structure to separate energy states is directly observed with decreasing nanocrystal size. The appearance of separate energy levels slows down the cooling of hot carriers by two orders of magnitude at low injected carrier densities. We attribute the slowed carrier cooling to a phonon bottleneck effect, where the discrete energy level structure effectively suppresses carrier cooling by optical phonon emission, leading to significant enhancement in cooling time. Importantly, this slow cooling is observed in the limit of low-intensity illumination, making it practically relevant. In addition to manipulating the electronic band structure, we demonstrate the management of the phonon band structure by introducing tin into lead halide perovskites. Increasing the tin content leads to screened Fröhlich interaction, suppressed Klemens decay, and reduced thermal conductivity (acoustic phonon transport), contributing to slowed relaxation mediated by the hot phonon bottleneck effect. To further control ultrafast non-equilibrium processes on a timescale of tens to hundreds of femtoseconds, we decouple hot carriers from sub-bandgap defects via sodium doping, resulting in a decreased energy loss rate during the thermalisation process. The control over non-equilibrium electron dynamics we achieved offers new insights into the intrinsic photophysics of perovskite nanocrystals, with direct implications for hot carrier solar cells. In addition to adjusting the electronic and phonon structures, we also achieve the modulation of exciton fine structure, along with the precise alignment of the transition dipole moment in self-assembled nanoplatelets. This results in a substantial number of excitons recombining at a specific energy level within the triplet manifold with minimal relaxation to other triplet states, leading to polarised electroluminescence with a high degree of polarisation approaching that of single nanocrystals. Our approach addresses the critical challenge of translating the high degree of polarisation found in photo-excited individual nanocrystals to an electrically driven film level, opening up a new frontier for enabling spin-related technologies through precise control of dynamics at the fine-structure level.

References

[1] L. Dai, Z.Deng, F. Auras, H. Goodwin, Z. Zhang, J. C. Walmsley, P. D. Bristowe, F. Deschler, N. C. Greenham, *Nature Photonics* **15,** 696 (2021)
[2] L. Dai, J. Ye, N.C. Greenham, *Light: Science & Applications* **12**, 208 (2023).
[3] J. Ye, A.Ren, L. Dai, T. K.Baikie, R. Guo, D. Pal, S. Gorgon, J.E. Heger, J. Huang, Y. Sun, R. Arul, G. Grimaldi, K. Zhang, J. Shamsi, Y.Huang H. Wang, J. Wu, A. F.Koenderink, L.T. Murciano, M. Schwartzkoph, S.V. Roth, P. Müller-Buschbaum, J. J. Baumberg, S. D. Stranks, N. C. Greenham L. Polavarapu, W. Zhang, A. Rao, R. L. Z Hoye. *Nature Photonics* **18**, 586 (2024).

Ultrafast imaging of polariton propagation and nonlinear optics in Semiconductor microcavities

D. Xu, A. Mandal, D. Basov, J. Schuck, D. Reichman, M. Delor
Columbia University, New York. NY 1002, USA

When excitonic systems such as van der Waals semiconductors are embedded in photonic cavities, excitons and photons can hybridize to form part-light part-matter eigenstates known as exciton-polaritons. Polaritons are in the vanguard of current interest as observations indicate their propensity for dramatically enhancing energy harvesting, nonlinear optical interactions, and even chemical selectivity by combining strong matter-like interactions with light-like long-range delocalization. We have developed unique ultrafast optical imaging approaches to track polariton transport with femtosecond and few-nanometer spatiotemporal resolution and with momentum selectivity (Fig. 1a). First, I will describe how we have leveraged this approach to provide detailed microscopic insight on polariton transport in the presence of finite disorder (Fig. 1b). Specifically, we have shown that polaritons can undergo a coherent to incoherent crossover, resulting in a switch from ballistic to diffusive transport [1]. The degree of polariton coherence depends sensitively on the strength of underlying exciton-phonon interactions. These results reveal that polaritons do not necessarily propagate at the group velocity inferred by their dispersion, due to finite exciton-mediated interactions with the material lattice. Polaritons thus act as sensitive reporters of underlying disorder, and tuning the latter allows controlling polariton properties towards specific applications. Second, I will show striking data directly visualizing light propagation and harmonic conversion within waveguides of the highly nonlinear material 3*R*-MoS_2 (Fig. 1c) [2]. This approach allows us to directly extract the phase-matching angle, waveguide mode profile and losses without any *a priori* knowledge of material properties.

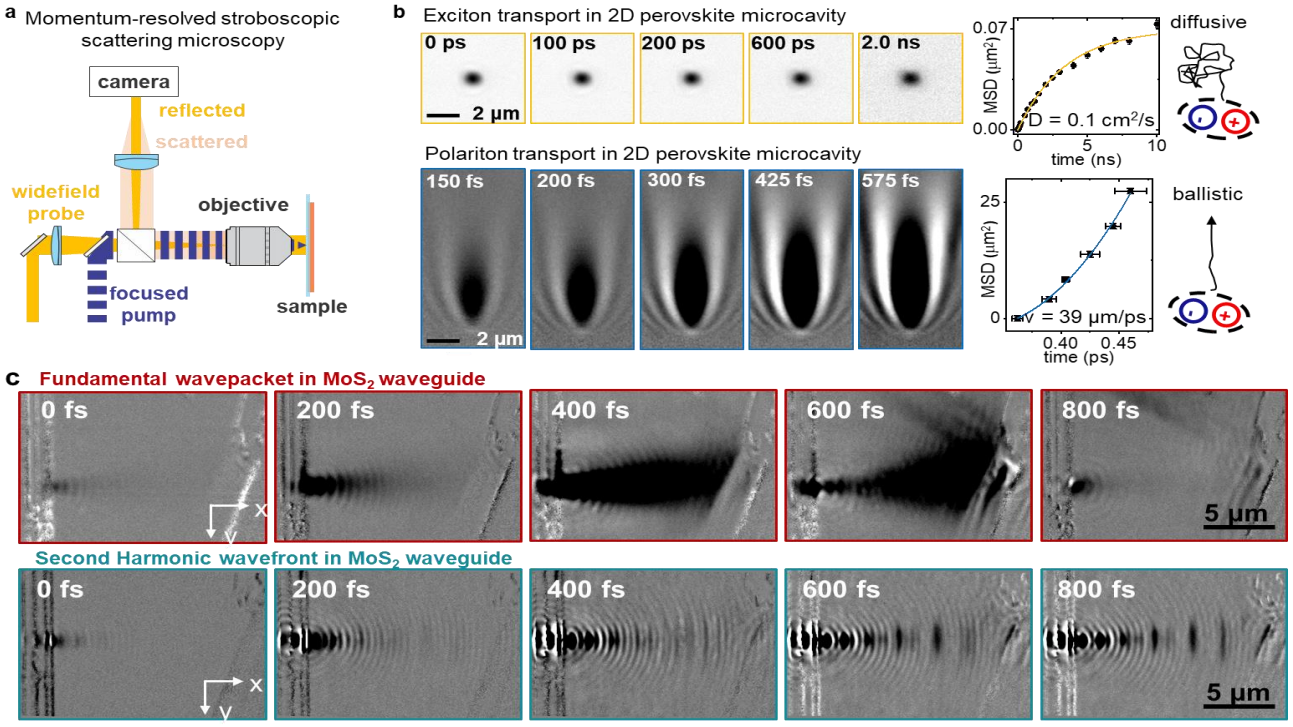

Fig. 1. ***(a)*** *Schematic for momentum-resolved ultrafast scattering microscopy.* ***(b)*** *Imaging exciton and exciton-polariton transport in semiconductor microcavities.* ***(c)*** *Imaging fundamental and second harmonic waves in semiconductor waveguides.*

We use this approach to achieve birefringent phase-matched second harmonic generation in multimode waveguides, and polariton-assisted modal phase-matching in single-mode waveguides of 3R-MoS_2 for highly efficient nonlinear optical conversion.

References

[1] D. Xu, A. Mandal, J.M. Baxter, S.-W. Cheng, I. Lee, H.Su, S.Liu, D.R. Reichman, M. Delor, *Nature Communications* **14**, 3881 (2023).
[2] D. Xu, Z. Peng, C. Trovatello, S. Cheng, X. Xu, A. Sternbach, D. Basov, J. Schuck, M. Delor, *(submitted)*, (2024).

Extreme nonlinear opto-magnonic effects in a layered Magnetic semiconductor

G. M. Diederich[1], M. Nguyen[2], J. Cenker[2], J. Fonseca[2], S. Pumulo[2], Y. J. Bae[3], D. G. Chica[4], X. Roy[4], X. Zhu[4]
D. Xiao[2], Y. Ren[5], X. Xu[2]

[1] *University of Maryland Baltimore, Baltimore, MD 21250, USA*
[2] *University of Washington, Seattle, WA 98195, USA*
[3] *Cornell University, Ithaca, NY 14853, USA*
[4] *Columbia University, New York, NY 1002, USA*
[5] *University of Delaware, Newark, DE 19716, USA*

The nonlinear dynamics of collective excitations offer both intriguing fundamental phenomena and significant practical applications. A prime illustration is the field of nonlinear optics, where diverse frequency mixing processes are central to advancing photonic technology [2]. Demonstration of these frequency mixing processes in magnons holds considerable potential for practical applications in magnonics [3], an emerging frontier of spintronics and an important platform for developing quantum transducers [4] and wave-based computing [5] beyond traditional paradigms. While perturbative nonlinear interactions in magnons have been shown [6,7], the non-perturbative regime of magnon nonlinearity has only been accessed under very specifically engineered circumstances [8]. Further, coupling of these nonlinear magnons to a semiconductor exciton, which would greatly extend the feasibility of nonlinear magnonics in hybrid quantum systems [9], has never been demonstrated to our knowledge.

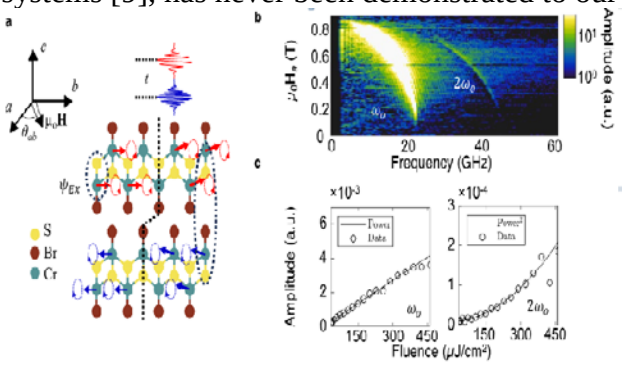

***Fig. 1. Coupling of excitons and nonlinear magnons in CrSBr**. [1]: **a-** Crystal structure of CrSBr with two distinct spin orientations corresponding to distinct phases in the optical magnon precession. θ_{ab} denotes the angle between the in-plane magnetic field and the intermediate magnetic axis a. Black dashed ovals illustrate the delocalization of the exciton wavefunction, ψ_{Ex}, at two different points in the spin wave where pump and probe pulses excite and measure the system at some delay, t. **b-** Fourier transform of the transient optical reflectivity from thin CrSBr at $\mu_o \boldsymbol{H} \approx 0.45$ T. **c-** Power dependence of the amplitudes of the fundamental (ω_o) and second harmonic ($2\omega_o$) magnon modes measured at $\mu_o \boldsymbol{H} \approx 0.35$ T. The magnetic field is applied along the a crystal axis for the data in (**b-c**).*

In this talk, I will present an extension to our previous works [10-11] on the van der Waals semiconducting magnet CrSBr that extends the exciton-magnon coupling into the nonlinear magnon regime. I will show how we can employ transient optical reflectivity to probe the exciton resonance and its magnon-modulated frequency shift (Fig. 1a), providing access to magnon sidebands in the frequency domain. In the resulting magnon spectra, we see replicas of the fundamental magnon sideband at integer multiples of the magnon frequency (Fig 1b,c) produced by nonlinear magnons. I will then show how we can leverage a symmetry-breaking magnetic field to couple the two distinct magnon modes, inducing the appearance of sum- and difference-frequency generation (SFG & DFG) of the magnon modes in our spectra. Further, by selecting a field orientation that brings the DFG mode into resonance with one of the fundamental modes, I will show how we can induce parametric magnon amplification. Finally, I will demonstrate that we can enter the non-perturbative nonlinear magnon regime by presenting results that show high harmonic magnon generation spanning over 20 harmonic orders of exciton-coupled magnons.These results show that CrSBr is an excellent candidate system for exploring the fundamental nonlinear physics of magnons. Further, they provide a path forward to implementing nonlinear magnonics into hybrid quantum systems by leveraging the coupling between magnons and excitons in CrSBr.

References

[1] G. Diederich M. Nguyen, J.Cenker,J. Fonseca, S. Pumulo, Y.Bae, D. Chica, X. Roy, X. Zhu, D. Xiao, Y. Ren, X Xu, *Nature Nanotechnology*, (2024)
[2] R. W. Boyd, *Nonlinear Optics*, Springer, 2008.
[3] S. Zheng, Z. Wang, Y. Wang, F. Sun, Q. He, P. Yan, H. Yuan, *Journal of Applied Physics* **134**, 151101 (2023).
[4] N. Crescini, C. Braggio, G. Carugno, R. Di Vora, A. Ortolan, G. Ruoso, *Communications Physics* **3**, 164 (2020).
[5] K. Baumgaertl, D. Grundler, *Nature Communications* **14**, 1490 (2023).
[6] C. Huang, L. Luo, M. Mootz, J. Shang, P. Man, L. Su, I. Perkins, Y. Yao, A. Wu, J. Wang, *Nature Communications* **15**, 3214 (2024).
[7] Z. Zhang, F. Gao, J.Curtis, Z.Liu, A.von Hoegen, M.Wong, T. Kurihara, T. Suemoto, P. Narang, E.Baldini, K.Nelson, *Nature Physics* **126** 801 (2024)
[8] H. Fu, K. Huang, K. Watanabe, T. Taniguchi, J. Zhu, *Physical Review* X **11**, 021012 (2021).
[9] D. Lachance-Quirion, Y. Tabuchi, A. Gloppe, K. Usami, Y. Nakamura, *Applied Physics Express* **12**, 070101 (2019).
[10] Y. Bae, J.Wang, A.Scheie, J.Xu, D.Chica, G.Diederich, J. Cenker, M.Ziebel, Y.Bai,H.Ren, C.Dean,M.Delor, X.Xu, X.Roy,A.Kent,X. Zhu, *Nature* **609** 282 (2022)
[11] G. Diederich, J. Cenker, Y. Ren, J. Fonseca, D. Chica, Y. Bae, X. Zhu, X. Roy, T. Cao, D. Xiao, X. Xu, *Nature Nanotechnology* **18**, 23(2023)

* The authors thank L. Fu, M.Rudner, and G, Rafael for helpful discussions. This work was mainly supported by the DoE, (DE - SC0012509). Sample Fabrication and measurements are supported by AFOSR FA9550 - 19 - 1 -0390 and FA9550-21-1-0460. Synthesis of the CrSBr crystals is supported by the NSF MRSEC (DMR - 2011738) and Programmable Quantum Materials, an Energy Frontier Research Center funded by the DOE, under award DE- SC0019443.X.X.acknowledges support from the State of Washington funded Clean Energy Institute and from the Boeing Distinguished Professorship in Physics.

How nonlinearity distorts the evidence for Photoinduced superconductivity

J. S. Dodge, L. Lopez, D.G. Sahota
Simon Fraser University, Burnaby, BC V5A 1S6, Canada

We recently identified a large systematic error that corrupts the evidence for photoinduced superconductivity in K_3C_{60} [1]. Most of this evidence has come from time-resolved terahertz (TR-THz) spectroscopy, which is sensitive to the nonequilibrium electrodynamic response of materials at the relevant frequencies and timescales [2-5]. However, TR-THz directly measures the complex reflection amplitude $r(\omega)$, not the local nonequilibrium complex conductivity $\sigma(\omega)$, and to relate them one needs to specify the complex photoconductivity depth profile $\Delta\sigma(\omega; z)$, which typically is not known independently. We showed that at the high excitation densities employed in these experiments, the photoconductivity depth profile must be distorted from the profile originally used to interpret the experiments. When we correct for this distortion, we obtain nonequilibrium conductivity spectra that are qualitatively different from those originally reported.

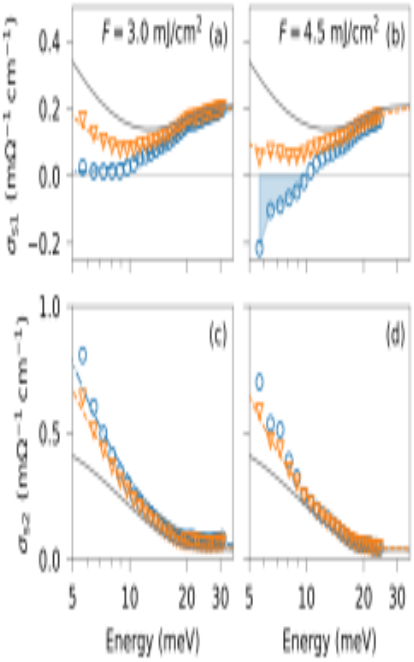

Fig. 1. Real (a,b) and imaginary (c,d) parts of the complex surface conductivity σ_{surf} *for F=3.0 mJ/cm² **(a,c)** and for F=4.5 mJ/cm² **(b,d)** with different profile assumptions. The spectra* $\sigma_{surf}(\omega; P_{exp})$ *reported by Budden et al. [4] and by Buzzi et al. [5] are shown as open circles in panels **(a,c)** and **(b,d)**, respectively. The corrected spectra* $\sigma_{surf}(\omega; P_{sat})$ *are shown as open triangles. Lines show Drude-Lorentz fits to* $\sigma_{surf}(\omega; P_{sat})$ ***(dashed)*** *and the equilibrium conductivity,* $\bar{\sigma}(\omega)$ ***(solid)***. *For the shaded region in (b) Buzzi et al. [5] reported negative real surface conductivity, which they interpreted as evidence for Higgs-mediated optical parametric amplification of terahertz radiation. This effect disappears when we account for the depth profile distortion that we derive from the observed sublinear fluence dependence.*

The corrected results are consistent with a model in which photoexcitation enhances the carrier mobility but does not produce superconductivity. We have evidence that this effect compromises all previous TR-THz evidence for photoinduced superconductivity, not just in K_3C_{60}. More recent results provide additional support for our The corrected results are consistent with a model in which photoexcitation enhances the carrier mobility but does not produce superconductivity. We have evidence that this effect compromises all previous TR-THz evidence for photoinduced superconductivity, not just in K_3C_{60}. More recent results provide additional support for our reinterpretation [6-8].

References

[1] J. S. Dodge, L. Lopez, D. G. Sahota, *Physical Review Letters* **130**, 146002 (2023).
[2] A. Cavalleri, *Contemporary Physics*. **59**, 31 (2018).
[3] M. Mitrano A. Cantaluppi, D. Nicoletti, S. Kaiser, A. Perucchi, S. Lupi, P. Di Pietro, D. Pontiroli, M. Riccò, A. Subedi, S. R. Clark, D. Jaksch, A. Cavalleri, *Nature*. **530**, 461 (2016).
[4] M. Budden, T. Gebert , M. Buzzi, G. Jotzu, E. Wang, T. Matsuyama, G. Meier, Y. Laplace, D. Pontiroli , M. Riccò, F. Schlawin, D. Jaksch, A. Cavalleri, *Nature Physics* **17**, 611 (2021).
[5] M. Buzzi,G. Jotzu, A. Cavalleri , J. I.Cirac,E.A. Demler,B.I. Halperin, M.D.Lukin, T.Shi, Y.Wang, D. Podolsky, *Physical Review* X, **11**, 011055 (2021).
[6] E. Rowe, B. Yuan, M. Buzzi, G. Jotzu, Y. Zhu, M. Fechner , M. Först, B. Liu, D. Pontiroli , M. Riccò, A. Cavalleri *Nature Physics*, 1(2023).
[7] E. Wang, J. D. Adelinia, M. Chavez-Cervantes, T. Matsuyama , M. Fechner , M. Buzzi, G. Meier, A. Cavalleri, *Nature Communications* **14**,7233 (2023).
[8] M. Buzzi, D. Nicoletti, E. Rowe, E. Wang, A. Cavalleri, *arXiv.2303.10169*, (2023).

Nanoscale confinement of dynamical spin textures

H. A. Dürr
Uppsala University, 75 120 Uppsala, Sweden

Light-matter interaction at the nanoscale in magnetic alloys and heterostructures is a topic of intense research in view of potential applications in high-density magnetic recording. Future magnetic data storage media will require magnetic nanoparticles with stable ferromagnetic order at diameters of only 10 nm and smaller [1]. In this respect, granular thin films of the $L1_0$-ordered phase of FePt displaying perpendicular magnetic anisotropy are one of the most suitable storage media. The FePt nanoparticles composing such granular materials remain ferromagnetic resulting from the strong magneto-crystalline anisotropy needed to overcome the superparamagnetic limit. However, an unwanted byproduct is the large magnetic field required to reverse the nanoparticle magnetization. Applications strive to reduce the magnetic switching field by locally heating the nanoparticles above their Curie temperature with a laser to thermally assist the switching, a technique known as heat-assisted magnetic recording. Nanoparticle assemblies also provide a unique platform for understanding light-matter interactions at nanoscale dimensions. For instance, the well-established magnetoresistance in FePt leads to a strongly anisotropic lattice expansion on the few-ps timescale [2]. The complex dielectric response of nanoparticle assemblies to optical laser illumination can lead cause certain nanoparticles to be in the "shadow" of their neighbors, i.e. they behave as if optical excitation is practically nonexistent [3]. Here we show that quenching of the FePt ferromagnetic order following fs laser excitation leads to the formation of magnetic spin textures close to their ultimate size limit given by the magnetic exchange length [4]. The situation resembles the generation of magnetic spin-wave solitons using the current-driven spin torque generated by magnetic nanocontacts [5]. Time-resolved x-ray scattering provides access to the characteristic frequency content of spin-wave solitons perimeter shown in Fig. 1, presence of a chiral exchange interaction.

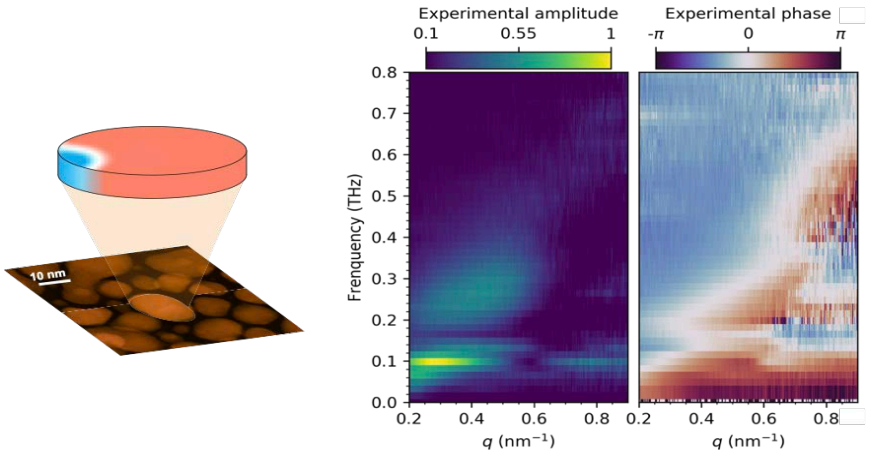

***Fig. 1. Left**: Schematic of a dynamic spin-wave soliton (blue magnetization) within a cylindric nanoparticle (red magnetization) superimposed onto a TEM image of an FePt nanoparticle array (brown) in an amorphous carbon matrix (black) [4]. **Middle** and **right**: Wavevector, q, dependence of amplitude and phase, respectively, of the Fourier transform of measured time-domain pump-probe diffraction date from the samples shown on the left [4].*

Varying the FePt nanoparticle size allows us to separate the scattering from the solitons and the nanoparticles. The spin-wave soliton generation process at the perimeter of FePt nanoparticles offers the exciting prospect for the formation of topologically protected spin textures as so far only observed in the presence of a chiral exchange interaction.

References

[1] A. Moser, K.Takano, D.T. Margulies, M. Albrecht, Y. Sonobe, Y. Ikeda, S. Sun. E.E Fullerton, *Journal of Physics D: Applied Physics* **35,** R157 (2002)
[2] A. Reid, X. Shen, P. Maldonado, T. Chase, E. Jal, P. W. Granitzka, K. Carva, R. K. Li, J. Li, L. Wu, T. Vecchione, T. Liu, Z. Chen, D. J. Higley N. Hartmann, R. Coffee, J. Wu, G. L. Dakovski, W. F. Schlotter, H. Ohldag, Y. K. Takahashi, V. Mehta, O. Hellwig, A. Fry, H. A. Dürr, *Nature Communications* **9**, 388 (2018).
[3] P. W. Granitzka, E.Jal, L.Le Guyader, M. Savoini, D.J. Higley, T.Liu, Z.Chen, T. Chase, H.Ohldag, G.L. Dakovski, W. Schlotter, S.Carron, M.Hoffman P. Shafer, E. Arenholz, O. Hellwig, V. Mehta, Y. K. Takahashi, J. Wang, E.E. Fullerton, J. Stöhr, A. H. Reid, H.A. Dürr, *Nano Letters* **17**, 2426 (2017)
[4] D. Turenne, A. Yaroslavtsev, X.Wang, V.Unikandanuni, I.Vaskivskyi, M.Schneider, E. Jal, R. Carley, G. Mercurio, R. Gort, N. Agarwal, B. van Kuiken L. Mercadier, J. Schlappa, L. LeGuyader, N. Gerasimova, M. Teichmann, D. Lomidze, A. Castoldi, D. Potorochin, D. Mukkattukavil, J. Brock N. Z. Hagström, A. H. Reid, X. Shen, X. J. Wang, P Maldonado, Y. Kvashnin, K. Carva, J. Wang, Y. K. Takahashi, E. E. Fullerton, S. Eisebitt P. M. Oppeneer, S. Molodtsov, A. Scherz, S. Bonetti, E. Iacocca, H.A. Dürr, *Science Advances* **8**, eabn0523 (2022).
[5] D. Backes, F. Macià, S. Bonetti, R. Kukreja, H. Ohldag, A. D. Kent, *Physical Review Letters* **115**, 127205 (2015).
[6] F. Büttner, B. Pfau, M. Böttcher, M. Schneider, G.Mercurio, C.M. Günther, P. Hessing, C. Klose, A. Wittmann, K. Gerlinger, L.-M. Kern, C. Strüber C. von Korff Schmising, J. Fuchs, D. Engel, A. Churikova, S. Huang, D. Suzuki, I. Lemesh, M. Huang, L. Caretta, D. Weder, J. H. Gaida, M. Möller T. R. Harvey, S. Zayko,, K.Bagschik, R.Carley, L.Mercadier, J. Schlappa, A.Yaroslavtsev, L. Le Guyarder, N. Gerasimova, A.Scherz, C.Deiter, R. Gort D. Hickin, J. Zhu, M. Turcato, D. Lomidze, F.Erdinger, A. Castoldi, S.Maffessanti, M. Porro, A.Samartsev, J. Sinova, C.Ropers, J. H. Mentink, B.Dupé G. S. D. Beach,S. Eisebitt, *Nature Materials* **20**, 30 (2021).

Transient chirality induced by nonlinear phononics

Z. Zeng[1], M. Först[1], M. Buzzi[1], E. Amuah[1], C. Putzke[1], P.J.W. Moll[1]
D. Prabhakaran[2], P.G. Radaelli[2], A. Cavalleri[2]
[1]*Max Planck Institute for the Structure and Dynamics of Matter, 22761 Hamburg, Germany*
[2]*University of Oxford, Oxford OX1 3PU, United Kingdom*

Optically induced functional phenomena in condensed matter are rare, as they require that spatial or temporal symmetries are lowered through interaction with an oscillatory dipolar field. Especially challenging is the search for optically induced chirality in a non-chiral material, because it requires that all mirrors and all roto-inversions be simultaneously broken. On the other hand, chirality is also a pervasive form of symmetry that is intimately connected to the physical properties of solids as well as to chemical and biological activity, making it an attractive target. Here, we use nonlinear phononics to show that chirality of either handedness can be induced in the non-chiral piezoelectric material BPO_4. At equilibrium, two compensated sub-structures of opposite handedness coexist within the unit cell. By resonantly driving either one of two orthogonal, doubly degenerate infrared-active phonon modes with intense mid-infrared light pulses, we displace a second lattice distortion with a positive or negative amplitude, uncompensating the staggered chirality and creating a picosecond-lived structure with either handedness.

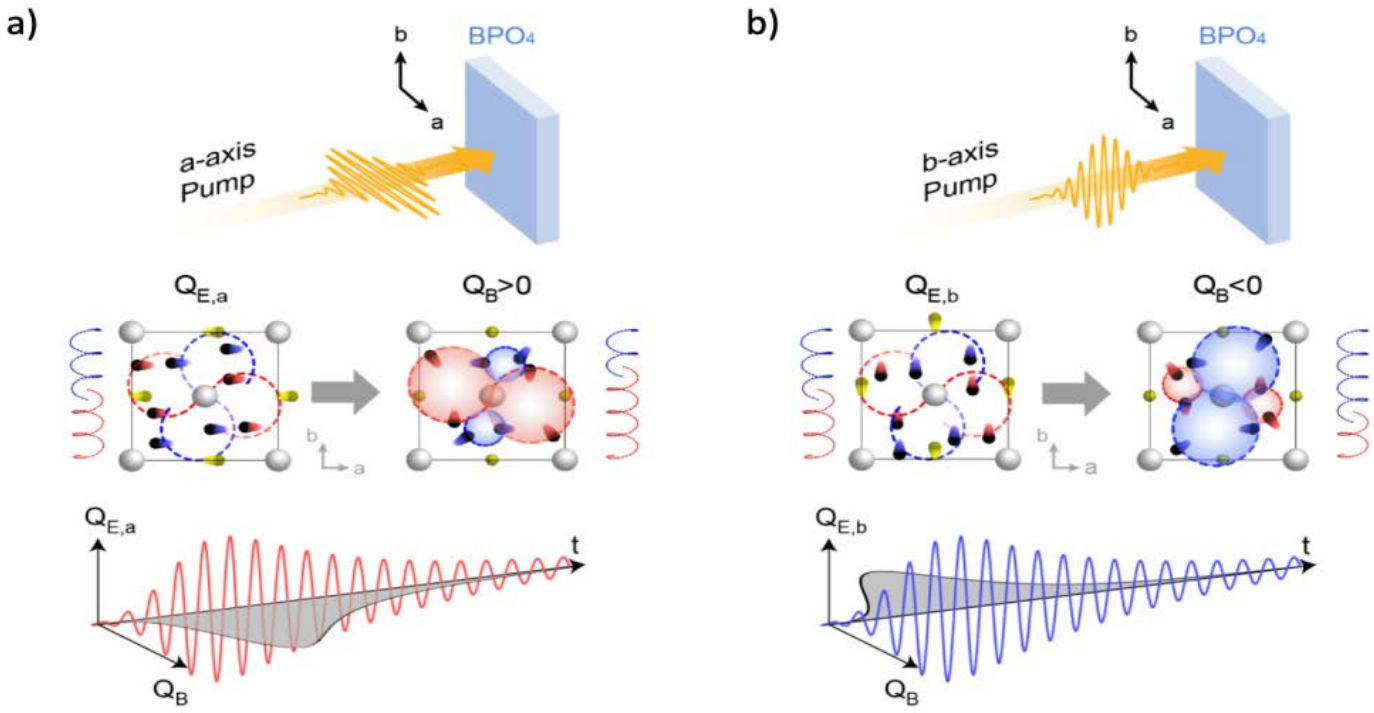

Fig. 1: Sketch of the nonlinear phononic interaction used to induce the chiral state. ***(a)*** *A mid-infrared pump electric field polarized along the a axis induces coherent oscillations of the mode $Q_{E,a}$ about its equilibrium position. A positive transient displacement along the coordinates Q_B of a B-symmetry mode is induced via anharmonic phonon coupling, driving the system into the non-equilibrium chiral state with left handedness.* ***(b)*** *Exciting the doubly generate E-symmetry phonon along the b axis induces coherent oscillations of the $Q_{E,a}$ mode about its equilibrium position. In this case, a negative transient displacement is induced along the Q_B mode coordinates, driving the system into a chiral state with right handedness.*

The rotary power of the transient photo-induced chiral phases found experimentally is comparable to the static value of prototypical chiral α-quartz, limited by the strength of the strength of the mid-infrared excitation pulse.

Reference

Z. Zeng, M. Först, M. Fechner, M. Buzzi, E. Amuah, C. Putzke, P.J.W. Moll, D. Prabhakaran, P. Radaelli, A. Cavalleri *arXiv:2407.08491*(2024).

Nonequilibrium dynamics of an interacting binary disordered alloy after Interaction quench

H. F. Fotso
SUNY at Buffalo, Buffalo, New York 14260, USA

We use our recently introduced nonequilibrium DMFT+CPA [1, 2] to investigate the nonequilibrium dynamics of a binary disordered alloy featuring a strong interaction, when the system is subjected to an interaction quench. The method combines the capacities of DMFT (dynamical mean field theory) to treat strongly correlated systems [3,4] and the capacity of the CPA (coherent potential approximation) to treat disordered systems [5,6], to effectively address the interplay of disorder and interaction for the nonequilibrium system. In the present studies, the system is described by the Anderson-Hubbard model describing itinerant electrons on a lattice with finite hopping between nearest neighboring sites, with a Coulomb interaction U between electrons of opposite spins occupying the same site, and a random site-dependent energy V_i. This random onsite energy is characterized by a disorder strength W defined by the distribution of V_i Values. In earlier work, we examined the so-called "box" disorder where V_i's follow a uniform distribution between $-W$ and $+W$. Here, we focus on the case of a disordered binary alloy where V_i's can take, with an equal probability, two possible values, $-W$ and $+W$. We first apply our time domain approach to the equilibrium problem, evaluating the density of states as a function of interaction and disorder strengths. Unlike the uniform disorder where as expected from CPA, increased disorder merely results in the broadening of the density of states, we show that for binary disorder, increased disorder leads to a gaped density of states. This transition with disorder strength is pushed to stronger disorder when the interaction is increased. Similarly, the Mott insulator transition is pushed to stronger interaction strength by increased disorder. Next, we analyze the nonequilibrium dynamics via the relaxation of the kinetic, potential and total energy of the isolated system as a function of time, when the interaction strength is abruptly changed at a given time, from $U_1=0$ to a finite constant value $U_2= U> 0$. For weak interaction and disorder, the nonequilibrium dynamics shows an evolution with similarities with that of the "box" disorder. However, clear differences emerge when the disorder strength approaches the threshold of the disorder gap. Altogether, the results illustrate the nontrivial interplay between disorder and interaction for a binary alloy. Fig. 1 illustrates the equilibrium problem, and Fig. 2 presents some results obtained from our nonequilibrium DMFT+CPA solution.

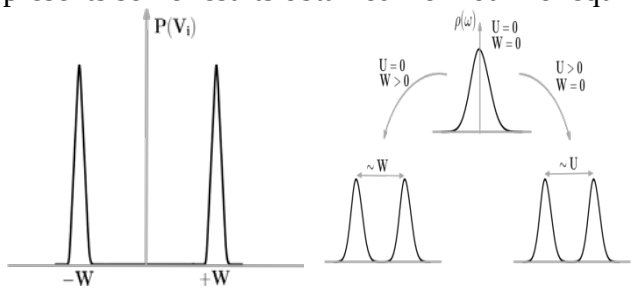

Fig. 1. *Schematic illustration of the equilibrium problem.* ***Left*** *: Binary disorder distribution.* ***Right****: Density of states of the Anderson-Hubbard model for different limits. For a noninteracting clean system, the density of state is gapless with a width that is defined by the the hopping amplitude. For a disordered noninteracting system, a disorder gap appears at a critical disorder strength. For an interacting clean system, a Mott insulator gap appears at a critical interaction value.*

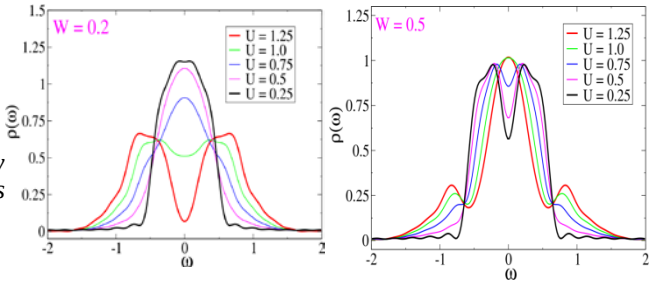

Fig. 2. *Density of state for the Anderson-Hubbard model with finite disorder and interaction.* ***Left*** *: Disorder strength W = 0.2.* ***Right****: Disorder strength W = 0.5. These results show that the Mott transition is pushed to stronger interactions strength by the increase in disorder strength [7].*

Altogether, the results illustrate the nontrivial interplay between disorder and interaction for a binary alloy.

References

[1] E. Dohner, H. Terletska, K.-M. Tam, J. Moreno, H. F. Fotso, *Physical Review* B **106** 195156 (2022).
[2] E. Dohner, H. Terletska, H. F. Fotso, *Physical Review* B **108**, 144202 (2023),
[3] J. K. Freericks, Physical Review B **77**, 075109 (2008).
[4] H. F. Fotso, J. K. Freericks, *Frontiers in Physics* **8**, 324 (2020).
[5] Y. Zhu, L. Liu, H. Guo, Physical Review B **88**, 205415 (2013).
[6] A. V. Kalitsov, M. G. Chshiev, J. P. Velev, Physical Review B **85**, 235111 (2012).
[7] E. Dohner, K.-M. Tam, H. Terletska, H. F. Fotso, (in preparation), (2024).

* We acknowledge support from the Department of Energy under grant number DE-SC0024139.

Near perfect conductor dynamics near the transition from single to double well potentials in electron-phonon driven Charge-density-wave materials driven by femtosecond pumps

J.K. Freericks[1], M. Petrovic[1], M. Weber[2]
[1]*Georgetown University, Washington, DC 20057 USA*
[2] *Max Planck Institute for the Physics of Complex Systems, 01187 Dresden, Germany*

We explore a transient decoupling between electrons and phonons in a one-dimensional charge-density-wave system modeled with the Holstein or Su-Schrieffer-Heeger model. In a standard pump-probe setting, the pump pulse can be fine-tuned to excite the model system so that the electron-phonon interaction briefly disappears. Switching off the electron-phonon coupling can drastically change the conducting properties of a material: an insulator can be transiently turned into a perfect conductor for a brief time. The defining characteristics of the decoupling is the dynamical slowdown, where the closer the pump gets to the critical decoupling fluence, the longer the system stays in the transient conducting state. Passing through the critical fluence is accompanied by the doubling of the phonon oscillation frequency which can be observed in the time-resolved photoemission spectrum. A schematic of the systems and the different regimes we study is given in Fig. 1.

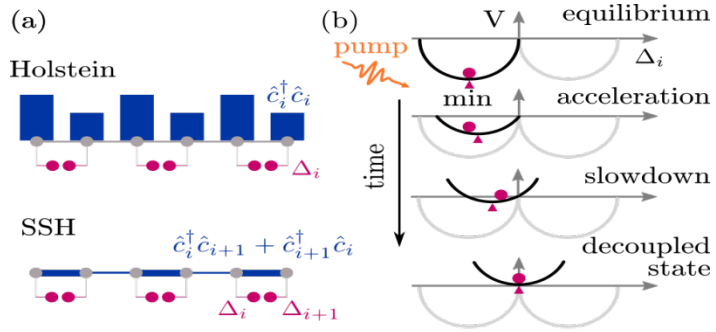

Fig. 1. Schematic of the two studied models: the Holstein and the SSH model. *The blue bars in the upper panel in (a) represent an onsite charge density, which is coupled to a local phonon coordinate Δi (dark red dots). In the SSH model, the local bond length $\Delta_{i+1} - \Delta_i$ is coupled to the local bond current (blue stripes in the lower panel in **(a)**). **(b)** Dynamical slowdown in the Holstein model explained in terms of a single phonon coordinate (**dark red dots**) moving in a local parabolic potential energy (**black curve**). The dark red triangles show the local potential minimum at a given time moment, while the gray parabolas show the two possible equilibrium potential profiles.*

We model the electron-phonon coupling in the Holstein model as a local charge coupling, while in the Su-Schrieffer-Heeger model it is a modulation of the hopping on the lattice. In both cases, when the phonon coordinate vanishes, the electron-phonon coupling goes to zero, and the system can be described by a perfect conductor (lattice electrons with no scattering). Eventually, the metastable phase is destroyed and the system relaxes to a case where the phonons oscillate with time and conventional electron-phonon coupling returns. One needs to have fine tuning of the pump fluence to achieve this state, because it arises when the system has a transition from the phonon oscillating in one well, to oscillating in two wells. Because we model this system with semiclassical phonons, the new phase is easiest to create at T=0. But, even at nonzero T, we find the behavior remains.As an example of how the phonon coordinate is pinned to a plateau value and how the conductivity is enhanced in this region,see Fig. 2.

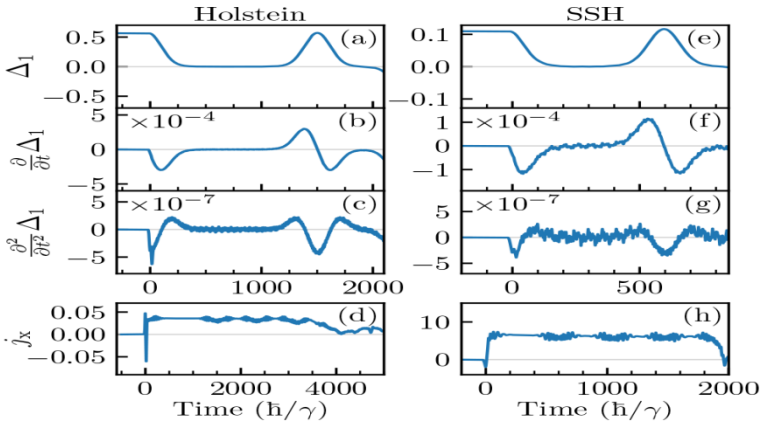

Fig. 2. Time evolution of the first phonon coordinate in the Holstein model (a)*, its speed **(b)**, the force acting on it **(c)**, and the current along the x direction. Panels **(e)–(h)** show the corresponding data forthe SSH model. There are L = 110 sites in thesystem, Ω = 0.02 γ/ħ, ω_p = 0.01 γ/ħ, and σ_p =10ħ/γ. The critical field in the Holstein model is E_0 = 0.4276130143995 and for the SSH model E_0 = 0.07022968248795.The coupling constants are the same λ = λ′ = 0.6..*

This work is being prepared for publication. The theory for this work is in [1], while an application to impulse phonons is in [2].

References

[1] M. Weber, J. K. Freericks, *Physical Review* E **105**, 025301 (2022).
[2] M. Petrovic, M. Weber,J. K. Freericks, *Physical Review* X, *in print* (2024).

* Acknowledgement(s): This work was supported by the U.S. DOE - BES) under Award DE-FG02-08ER46542. J.K.F. was also supported by the McDevitt bequest at Georgetown University. This research used resources of t he National Energy Research Scientific Computing Center (NERSC), a U.S. DOE Office of Science User Facility operated under Contract no. DE- AC02-05CH11231.

Structural dynamics driven by ultrafast Laser-induced demagnetization

S. K.K. Patel[1], O. Y. Gorobtsov[2], D. Cela[1], S.B. Hrkac[1], N. Hua[1], R. Medapalli[1], A. G. Shabalin[1], J.Wingert[1]
J. M. Glownia[3], D. Zhu[3], M.Chollet[3], O. G. Shpyrko[1], A.Singer[2], E.E. Fullerton[1]
[1]*University of California San Diego, La Jolla, CA 92093, USA*
[2]*Cornell University, Ithaca, NY 14853, USA*
[3]*SLAC National Accelerator Laboratory, Menlo Park, CA 94025, USA*

Strongly correlated materials exhibiting coupling between degrees of freedom such as charge, spin, and lattice, are the focus of materials research. Understanding the mechanisms underlying these emergent phenomena is critical to manipulating material properties for development of new technologies. Antiferromagnetic materials are of particular interest in spintronics, given their terahertz characteristic switching frequency. The possibilities of optically manipulating magnetization without applied magnetic fields have attracted growing attention over the last twenty years. There are further opportunities for ultrafast control in strongly correlated systems where the coupling between spin, charge, and lattice degrees of freedom results in the emergence of complex order such as antiferromagnetism and density wave systems.Chromium is one example of a strongly correlated material with coupling of spin, charge, and lattice. It is an incommensurate spin density wave (SDW) antiferromagnet that exhibits a charge density wave (CDW) and periodic lattice distortion (PLD) as a second harmonic of its spin density wave (SDW) below its Néel temperature of 311 K [1]. In this talk I will describe recent experiments probing the ultrafast coupling and control of the SDW and CDW dynamics in response to photoexcitation pumps probed by an X-ray free-electron laser (XFEL) [2-7]. We find that ultrafast suppression of the SDW order converts the static CDW into a dynamic coherent phonon where the amplitude can be further controlled by secondary optical pulses. We show critical slowing of the recovery of the ordering near phase transition temperatures of the SDW/CDW order. These results suggest new avenues for manipulating and researching the behavior of photoexcited states in charge and spin order systems out of equilibrium. A thin film of Cr was deposited by magnetron sputtering on to a single-crystal MgO (001) substrate. X-ray diffraction and x-ray reflectivity measurements confirm (001) growth out-of-plane and a film thickness of about 28-nm. X-ray diffraction made at the Advanced Photon Source show Laue fringes around the (002) Bragg peak, with CDW satellite peaks aligned to specific fringes, indicating a half-integer number of CDW/PLD periods between the film interfaces (Fig. 1). As the film is cooled below the Néel temperature of around ~300 K, the satellite peaks appear on the seventh fringe, indicating 7.5 CDW periods in the film. There is a hysteretic region between 210 K and 245 K in which, as the film cools, the satellite peak disappears from the seventh fringe and appears on the eighth fringe, indicating a transition in which spins and charge reorient such that there are 8.5 CDW periods in the film. Time-resolved measurements diffraction measurements were conducted at the XPP instrument at the Linac Coherent Light Source x-ray free-electron laser at SLAC National Laboratory. The film was excited by 800 nm optical pulses of duration 45 fs at three fluences at initial sample temperatures ranging from 130 K to 300 K. X-ray pulses of energy 8.9 keV and duration 15 fs were used to measure the time-resolved x-ray diffraction response of some of the Laue fringes to a maximum time delay of 400 ns to track the position and intensity of the satellite peak as shown in Fig. 1. Initial results demonstrate that moderate ultrafast photoexcitation can transiently enhance the CDW amplitude by up to 30% above its equilibrium value, while strong excitations lead to an oscillating, large-amplitude CDW state that persists above the equilibrium transition temperature. Both effects result from dynamic electron-phonon interactions, providing an efficient mechanism to selectively transform a broad excitation of the electronic order into a well-defined, long-lived coherent lattice vibration. This mechanism may be exploited to transiently enhance order parameters in other systems with coupled degrees of freedom. We extended this results to combine double photoexcitation with XFEL probe to control and detect the lifetime and magnitude of the intermediate vibrational state near the critical point of the SDW in chromium. We apply Landau theory to identify the mechanism of control as a repeated partial quench and sub picosecond recovery of the SDW. Our results showcase the capabilities to influence and monitor quantum states by combining multiple optical photoexcitation with an XFEL probe. Finally, we explored the long-time recovery. At temperatures far below the hysteretic phase transition, the recovery of both fringe intensities proceeds as expected based on thermal recovery on the order of 10 ns and the expected temperature dependence of the ordering parameter.

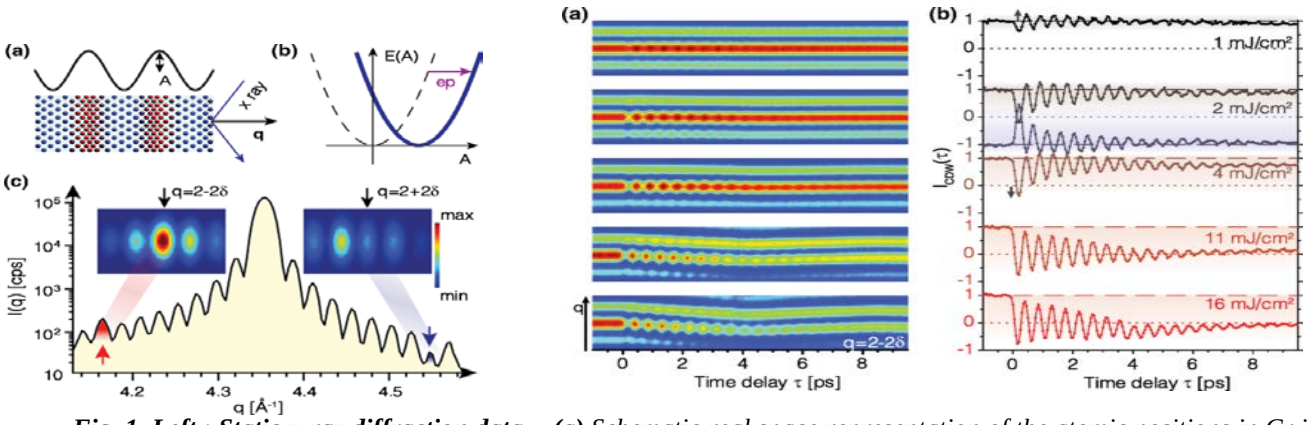

Fig. 1. Left : Static x-ray diffraction data. ***(a)*** *Schematic real space representation of the atomic positions in Cr in the presence of a CDW. The corresponding charge density modulation with the CDW amplitude A and the scattering geometry are also shown.* ***(b)*** *The potential energy surface for the CDW amplitude A. In the low-temperature ground state, the potential energy surface is shifted towards a nonvanishing value due to the electron-phonon (ep) coupling.* ***(c)*** *X-ray diffraction from a Cr thin film recorded with synchrotron radiation around the (002) Bragg peak (in photons per second) measured at a film temperature of 115 K. The intensity is increased (reduced) at the positions of the CDW satellites for low (high) q values (indicated by arrows). Insets: Diffraction patterns (linear scale) collected with the x-ray free-electron laser at two different momentum transfers q=2−2δ and q=2+2δ in the ground state, corresponding to different incident angles of x rays..* ***Right****: Time resolved x-ray diffraction data.* ***(a)*** *Time dependence of the intensity in the vicinity of the CDW satellite at q=2−2δ (see* ***Left****) for a series of pump fluences (incident, p polarization).* ***(b)*** *The black and red lines show the normalized transient intensity differences. From Ref. 3.*

As the ground state temperature approaches the phase transitions, however, the time scales of recovery significantly lengthen, such that the ground state is not reached even at the maximum delay time of 400 ns as shown in Fig. 2. Similar results were found for different laser fluences, where the intensities of the fringes changed but the time scales for recovery depend solely on the ground state temperature. We extend the existing formalism for Landau modeling of SDW/CDW systems to include the boundary conditions imposed by the thin film geometry. The resulting model of the free energy surface is shown in Fig. 2. We reproduce the temperature dependence of the energy barrier shown in Fig. 2(left) with the solid lines.

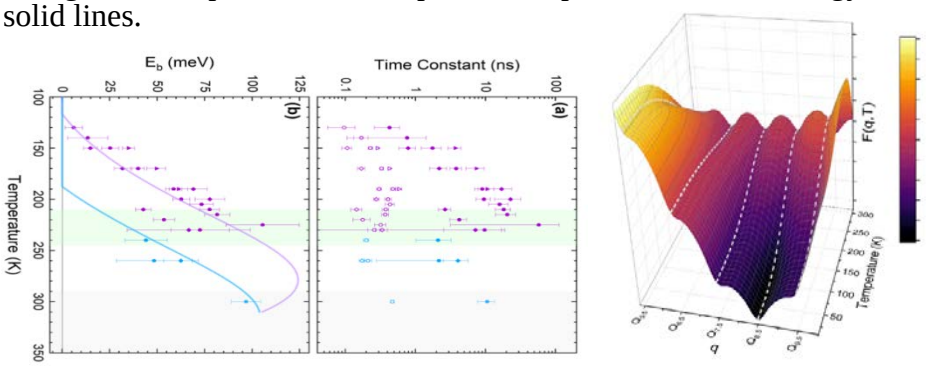

Fig. 2. Left : (a) Time constants *τ_slow (solid data points) and τ_fast (open data points) for the recovery of CDW order to its initial state from a double exponential fit. Fits were made to the time-dependent CDW amplitude on fringe 8 below the transition* ***(blue). (b)*** *Energy barrier calculated from τ_slow for the transition from NCDW = 7.5 to 8.5* ***(purple data points)*** *or from from NCDW = 6.5 to 7.5 CDW* ***(blue data points).*** *The* ***solid lines*** *are the energy barriers calculated for both transitions from the Landau free energy model with added boundary pinning terms. Fitting constants and energy barriers are includedfor data at laser fluences 4.2 mJ/cm2 (****diamonds****), 7.4 mJ/cm2 (****circles****), and 9.2 mJ/cm2 (****triangles****).* ***Right*** *: Landau free-energy F(q,T) model of the CDW wavevector for a Cr film. Dashed lines show the potential for the wavevectors corresponding to 9.5, 8.5, 7.5, and 6.5 CDW periods in the film. From Ref. 7*

Thus, we have assessed the energy of the system through the time domain.

References

[1] E. Fawcett, *Review of Modern Physics* **60**, 209 (1988).
[2] A. Singer, S. K. K. Patel, V. Uhlíř, R. Kukreja, A. Ulvestad, E. M. Dufresne, A. R. Sandy, E. E. Fullerton, O. G. Shpyrko, *Physical Review* B **94** 174110 (2016).
[3] A. Singer, S. K. K. Patel, R. Kukreja, V. Uhlíř, J. Wingert, S. Festersen, D. Zhu, J. M. Glownia, H. T. Lemke, S. Nelson, M. Kozina, K. Rossnagel M.Bauer, B. M. Murphy, O. M. Magnussen, E. E. Fullerton, O. G. Shpyrko. *Physical Review Letters* **117**, 056401 (2016).
[4] J. Wingert, A. Singer, S. K. K. Patel, R. Kukreja,M. J. Verstraete, A.H. Romero,V. Uhlíˇr , S. Festersen, D. Zhu, J. M. Glownia,H. T. Lemke, S. Nelson M. Kozina,K. Rossnagel , B. M. Murphy , O. M. Magnussen,E. E. Fullerton,O. G. Shpyrko, *Physical Review* B **102**, 041101 (2020).
[5] O. Y. Gorobtsov, L. Ponet, S. K. K. Patel, N. Hua, A. G. Shabalin, S. Hrkac, J. Wingert, D. Cela, J. M. Glownia, D. Zhu, R. Medapalli, M. Chollet E. E. Fullerton, S. Artyukhin, O. G. Shpyrko, A. Singer, *Nature Communications* **12**, 2865 (2021).
[6] J. Li, O.Y. Gorobtsov, S.K. K. Patel, N.Hua, B.Gregory, A.G. Shabalin, S.Hrkac, J.Wingert, D.Cela, J. M. Glownia, M. Chollet, D. Zhu, R. Medapalli E. E. Fullerton, O. G. Shpyrko, A.Singer, *Communications Physic*s 5, 125 (2022).
[7] S. K. K. Patel, O. Y. Gorobtsov, D. Cela, S.B. Hrkac, N. Hua, R. Medapalli, A.G. Shabalin, J. Wingert, J. M. Glownia, D.Zhu, M.Chollet, O.G. Shpyrko A. Singer, E. E. Fullerton, *APL Materials* **12**, 061111 (2024).

Probing charge carrier dynamics in 2D transition metal dichalcogenides with Terahertz emission spectroscopy

C. Gollner[1], C. Xia[2], M. Taghinejad[2], Z. Zhang[2], F. Liu[2], M. L. Brongersma[2], T. Heinz[2], A. Lindenberg[2]
[1]*SLAC National Accelerator Laboratory, Menlo Park, CA 94025, USA*
[2]*Stanford University, Stanford, CA 94305, USA*

The discovery of monolayer (ML) group-VI transition metal dichalcogenide (TMD) semiconductors in 2010 [1,2] sparked a rapidly growing field for engineered photonic materials. This class of low-dimensional materials are an ideal platform for multiple applications in electronics, optoelectronics, and valleytronics [3, 4], as well as for field-effect-transistor based systems [5] or quantum emitters [6]. The most outstanding features of 2D TMDs are the sizeable band gap, large exciton binding energy, and controllable interlayer coupling in heterostructure devices, which can be adjusted through doping, strain, external fields or by the stacking formations of van der Waals (vdW) materials. Yet, potential applications require a detailed comprehension for the temporal evolution of exciton formation and dissociation, interfacial charge transfer, and nonlinear polarization in symmetry-broken materials. This is particularly true for electronic and optoelectronic devices such as transistors, photodetectors, or solar cells, wherein charge carrier dynamics at the metal-semiconductor interface largely determine the functionality of the device. Most commonly, time-resolved exciton dynamics are studied with transient absorption measurements [7] or second harmonic (SH) generation spectroscopy [8], requiring detailed spectroscopic signatures of the involved material and elaborate interpretation of possible relaxation channels. In contrast, time-domain terahertz (THz) emission spectroscopy (TES) provides a direct method to probe a transient photo-current by recording the emitted THz radiation following ultrafast laser excitation. A schematic THz emission spectroscopy setup and recorded THz waveform is shown in Fig. 1a for charge transfer from a TMD monolayer (ML) to a metallic bulk material. Sampling the time variation and polarization of the radiated electric field provide a contact free, quantitative method for determining the magnitude, directionality, and temporal variation of the transient current density, which permits to directly study charge carrier dynamics, nonlinear susceptibility, structure symmetry, carrier diffusion, surface depletion, and many more.

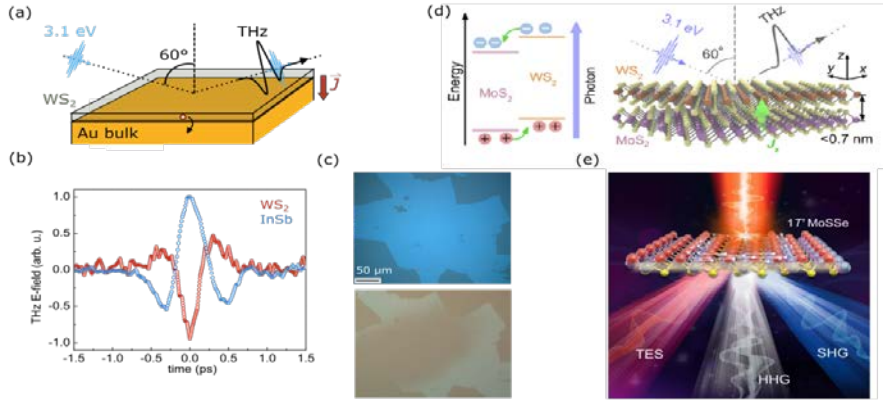

Fig.1 (a) Schematic of THz emission *from a TMD-bulk interface following excitation with a 400 nm femtosecond pulse.* ***(b)*** *Emitted THz waveform (red) exhibiting opposite polarity compared to THz emission from InSb (blue), suggesting hole transfer from WS_2 to Au.* ***(c)*** *WS_2 monolayers on a fused silica substrate before and after excitation with a 400 nm pulse under ambient conditions.* ***(d)*** *Illustration of THz emission from a TMD heterostructure due to interfacial charge transfer between the constituent monolayers [9].* ***(e)*** *Frequency down- and up-conversion in a TMD Janus material caused by the broken spatial symmetry [10].*

In this talk, I want to review recent efforts of our group on THz emission spectroscopy on 2D materials by recording interfacial currents in TMD heterostructures [9], attributed to a transient current flow due to charge carrier separation between the constituent monolayers (see Fig. 1d), and THz emission due to optical rectification as a result of a large second-order optical nonlinearity enabled by strong inversion symmetry breaking in the Janus topological semiconductor *1T'* MoSSe [10] (Fig. 1e), respectively. Finally, I will present our recent results on probing photo-induced degradation in WS_2 monolayers by THz emission spectroscopy. Because many 2D materials with atomic-scale thickness suffer from oxidation and degradation effects under ambient conditions, which hampers their practical applications, it is necessary to further investigate potential protection strategies for large scale 2D materials. Instead of encapsulating WS_2 MLs with a preservative hBN coating, which is limited in its scalability, in this work, we exploit Au substrates to prevent photo-induced degradation in the 2D TMD material and probe the surface properties as well as charge carrier dynamics with THz emission spectroscopy. In the case of WS_2 MLs on a fused silica substrate, THz emission can be attributed to resonant optical rectification when the sample is excited above the electronic band gap with a 400 nm (3.09 eV) wavelength laser pulse. However, while the emitted THz field is stable under a dry nitrogen environment, the THz signal vanishes under ambient conditions within minutes and obvious optical damage of the sample is visible under the microscope (see Fig. 1c). In contrast, in the case of WS_2 on a gold substrate, the THz signal remains stable under ambient conditions, and no optical damage can be observed. Moreover, pump polarization studies indicate that THz radiation is due to interfacial charge

transfer from the TMD monolayer to the metallic substrate. Comparing the polarity of the generated THz pulse from the semiconductor-metal interface with a reference InSb sample (see Fig. 1b), for which the THz signal is ascribed to the Photo-Dember effect, we conclude that the interfacial current flow is dominated by hole transfer from the WS_2 ML to the Au substrate. We hypothesize that the enhanced stability of WS_2 monolayer on the gold substrate is due to quenching of the photoexcited carriers through nonradiative recombination in the gold substrate and thus, the number of excited carriers available for chemical reaction at the surface is greatly reduced. The ongoing studies demonstrate the capability of THz emission spectroscopy to unravel ultrafast processes and suggest an effective strategy to enhance the durability of TMD-based devices by using metallic substrates.

References

[1] K. F. Mak, C. Lee, J.Hone, J.Shan, T.F. Heinz, *Physical Review Letters* **105**, 136805 (2010).
[2] A. Splendiani, L. Sun, Y.Zhang, T.Li, J.Kim, C.Y. Chim, G.Galli, F. Wang, *Nano Letters* **10**, 1271 (2010).
[3] Q. H. Wang, K. Kalantar-Zadeh, A. Kis, J.N. Coleman, M.S. Strano, *Nature Nanotechnology* **7**, 699 (2012).
[4] X. Xu, W. Yao, D. Xiao, T.F. Heinz, *Nature Physics* **10**, 343 (2014).
[5] X. Yin, C.S. Tang, Y. Zheng, J. Gao, J. Wu, H. Zhang, M.Chhowalla, W.Chen, A.T.S. Wee, *Chemical. Society Reviews* **50**, 10087 (2021).
[6] X. Liu, M.C. Hersam. *Nature Reviews Materials* **4**. 669 (2019).
[7] H. Zhu, J. Wang, Z. Gong, Y.D. Kim, J.Hone, X.Y. Zhu, *Nano Letters* **17** , 3591 (2017).
[8] J. E. Zimmermann , M. Axt, F. Mooshammer, P. Nagler, C. Schüller, T. Korn, U. Höfer, G. Mette, *ACS Nano* **15**, 14725. (2021).
[9] E. Y. Ma,B. Guzelturk, G. Li, L. Cao, Z.X. Shen, A.M. Lindenberg, T.F. Heinz, *Science Advances* **5**, eaau0073 (2019).
[10] J. Shi, H.Xu, C.Heide, C.H.Fu, C.Xia, F.de Quesada, H.Shen, T.Zhang, L.Yu, A.Johnson, F.Liu, E.Shi, L.Jiao, T.Heinz, S.Ghimire, J.Li, J.Kong Y. Guo A. M. Lindenberg, *Nature Communications* **14**, 4953 (2023).

Memory and transient states in Relaxation pathways of a Mott insulator far from equilibrium

O. Yu. Gorobtsov[1], Y. Kalcheim[3], Z. Shao[1], A. Shabalin[2], N. Hua[2], D. Weinstock[1], R. Bouck[1], M. Seaberg[4]
D. Zhu[4], O. Shpyrko[2], I. Schuller[2], A. Singer[1]

[1] *Cornell University, Ithaca, NY 14853, USA*
[2] *University of California San Diego, La Jolla, CA 92093, United States*
[3] *Technion-Israel Institute of Technology, Haifa 32000, Israel*
[4] *SLAC National Accelerator Laboratory, Menlo Park, CA 94025, USA*

Control over the structure and function of quantum materials remains among the ultimate challenges of modern science and technology [1]. Memory and structural effects during metal-insulator transitions in quantum materials can illuminate hidden physics and lead to novel electronic technologies [2] [3] [4]. Nonetheless, an understanding of the memory effects and nonlinearities influencing the transition pathways far from equilibrium across timescales varying by multiple orders of magnitude remains elusive. We employed x-ray Bragg diffraction covering timescales from femtoseconds to microseconds to trace the pathways of far-from-equilibrium photoexcited transitions in V_2O_3 epitaxial films. We uncovered changes in transition timescale up to 5 orders in magnitude, where the memory of initial conditions induces, unusually, a stretched exponential relaxation over multiple microseconds.

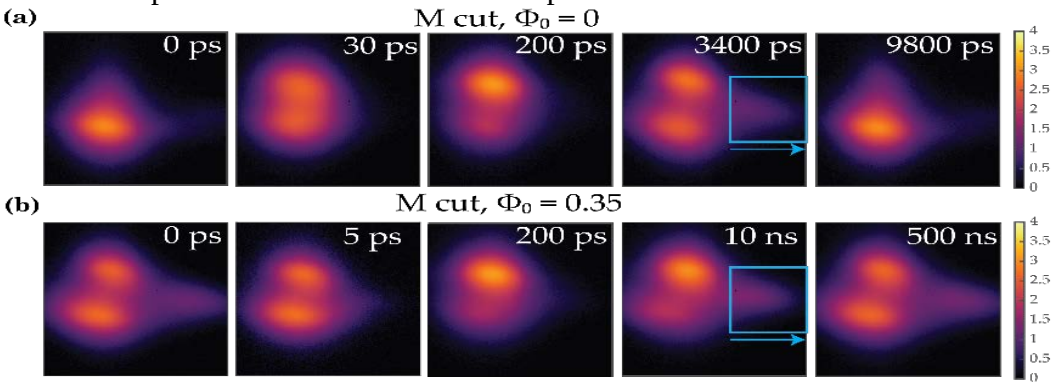

Fig. 1: Evolution of diffraction peak structure in V_2O_3 after photoexcitation. *(a-b) Snapshots of a phase transition representing principal stages of the entire transition pathway for different starting phase ratios.*

Our results illuminate the critical role of memory in shaping the non-equilibrium evolution of the system post-photoexcitation, offering a promising framework for manipulating and accessing transient states with enhanced control and mimicking biological systems with varying excitation barrier height.

References

[1] D.N. Basov, R. D. Averitt, D. Hsieh, *Nature Materials* **16,** 1077 (2017).
[2] J. del Valle, P. Salev, F. Tesler, N. M. Vargas, Y. Kalcheim, P. Wang, J. Trastoy, M.- H. Lee, G. Kassabian, J.G. Ramírez, M. J. Rozenberg I. K. Schuller. *Nature* **569**. 388 (2019).
[3] Y. J Lee, Y. Kim, H. Gim, K. Hong, H.W. Jang, *Advanced Materials* **36,** 2305353 (2024).
[4] O. Yu. Gorobtsov, L. Miao, Z. Shao, Y. Tan, N. I. Schnitzer, B. H. Goodge, J. Ruf , D. Weinstock, M. Cherukara, M. V. Holt, H. Nair, L.-Q. Chen L. F. Kourkoutis, D. G. Schlom, K. M. Shen, A. Singer, *Advanced Materials* **36,** 2403873 (2024).

Driving optomagneto dynamics between correlated triplet pair states in Single-crystal singlet fission materials

G. Mayonado[1], W. Goldthwaite[1], F. Zhu[1], J. E. Anthony[2], O.Ostroverkhova[1]
M. W. Graham[1]
[1]*Oregon State University, Corvallis, OR USA 97331*
[2]*University of Kentucky, Lexington, KY USA 40506*

Tunable magnetic field (±7T) TA microscopy drives conversion between correlated triplet pair states in singlet fission semiconductors, to show ultrafast spin-conversion from S=0 (singlet) to S=1 (triplet) and S=2 quintet staites. Singlet fission (SF) is an efficient charge multiplication process in organic semiconductors that converts one singlet optical excitation to two triplet excitons ($2xT_1$) via a singlet S=0 correlated triplet pair ^{1}(TT) state to conserve spin.[1] Ultrafast triplet pair spin conversions to S>0 states, ^{1}(TT) $\rightarrow$ ^{m}(TT) are theoretically predicted when the intermolecular exchange energy vanishes ($J\rightarrow 0$) and the states are degenerate as shown in Fig. 1c. Of particular importance is ^{1}(TT)$\rightarrow$ ^{5}(TT) conversion to the S=2 quintet state which the overall SF efficiency is suspected to hinge critically upon.[1] Unfortunately, the small J value separating these states and their optically dark nature makes ultrafast spin conversion measurements difficult. To date, the critical role that S=1 (triplet) and S=2 (quintet) ^{m}(TT) states play in SF has only been observed in electron spin resonance (ESR) and photoluminescence which show sharp resonant signal dips at specific resonant B-field.[2] Using tunable B-fields (0-7 T), we induce strong-field Zeeman splitting on single-crystal semiconductors to uncover the ultrafast formation dynamics that drive both ^{m}(TT) spin-state conversions and triplet pair spatial separation to ^{1}(T…T). To isolate the dynamics of the different correlated triplet pair states, we apply B-field-dependent transient absorption (TA) microscopy to single-crystal organic semiconductors. Figure 1 shows the TA spectral dynamics for the exoergic SF system, TIPS-pentacene (TIPS-Pn), and highlights a competition between the $^1(TT)_A$ and $^1(TT)_B$ populations. A tunable B-field (±7T, OptiCool, Quantum Design) is applied perpendicular to the brickwork lattice plane (200 K). Pump excitation was resonant with the S_1 states (NOPA, ~40 fs), while the probe was either broadband whitelight or resonant with the ^{1}(TT) ESA peak near 1.28 eV (OPA, ~60 fs). The two beams are coupled collinearly into a microscope via 4f confocal scanning optics to illuminate a ~2 μm spot on the thin crystal regions depicted in Fig. 1a.

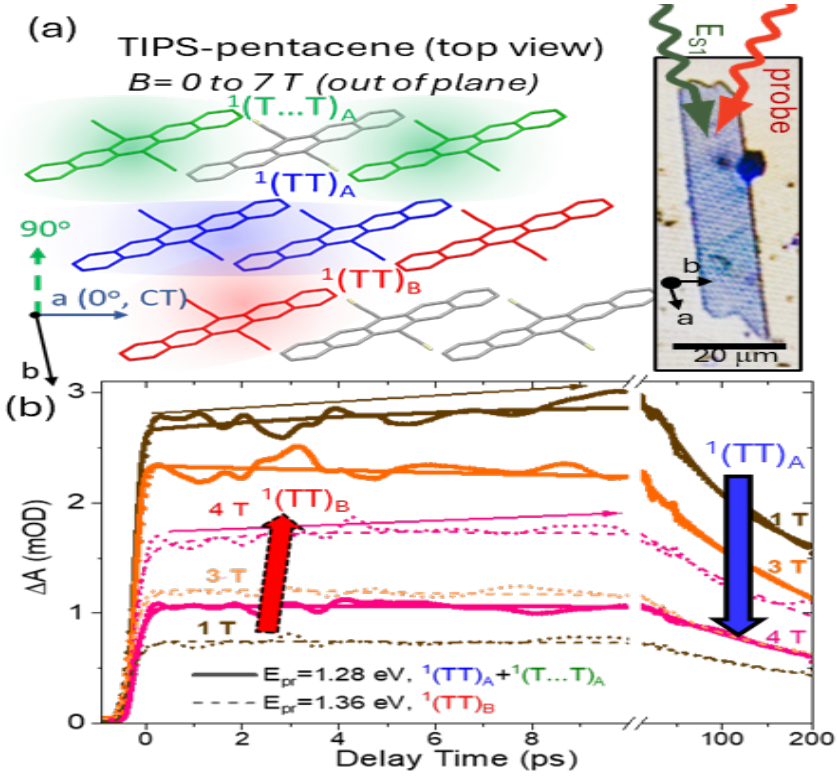

Fig. 1, Singlet Fissiont triplet pais TIPS-Pn): *B-field driven inter-triplet conversion dynamics.* ***(a)*** *Top view of the TIPS-Pn single crystal (left: structure, right: crystal photo) measured by TA microscopy. The eclipsed brickwork packing (right) motif supports correlated triplet-pair states that are predominately delocalized along the CT-axis.* ***(b)*** *With increasing magnetic field, the TA kinetics of the decreasing [$^1(TT)_A$+$^1(T...T)_A$] peak population peak probed at 1.30 eV decreases is anti-correlated with the increasing $^1(TT)_B$ population peak probed at 1.36 eV.*

The sharp population dips occurring at B=2.5 and 4 T in Fig. 2a can be understood using a spin Hamiltonian for four electrons, where the linear Zeeman state splitting term is $H_{TT}(\mathbf{B})=g\mu_B\mathbf{B}\cdot\mathbf{S}$ [1], plotted in Fig. 2b. Both TIPS-Pn and diF-antradithiophene (ADT) systems show similar 'resonant-dips' that we associate with ultrafast spin conversion to S=1 and S=2 triplet pair states when the Zeeman splitting causes a degeneracy at the S=0 state crossing circled in Fig. 2b.For B-fields beyond ~4 T, Fig. 1d shows the $^1(TT)_A$ population at 1.30 eV is gradually suppressed while a corresponding *blue*-shifted peak that we call $^1(TT)_B$ becomes the dominant peak centered at 1.36 eV. For B>~ 4T, the $2xT_1$ transition state plotted in Fig. 1e is lower than the singlet $^1(TT)_A$ state, suggesting states like $^1(TT)_B$ may become both stable and favorable owing to its different intermolecular coupling motif, where J<~0.

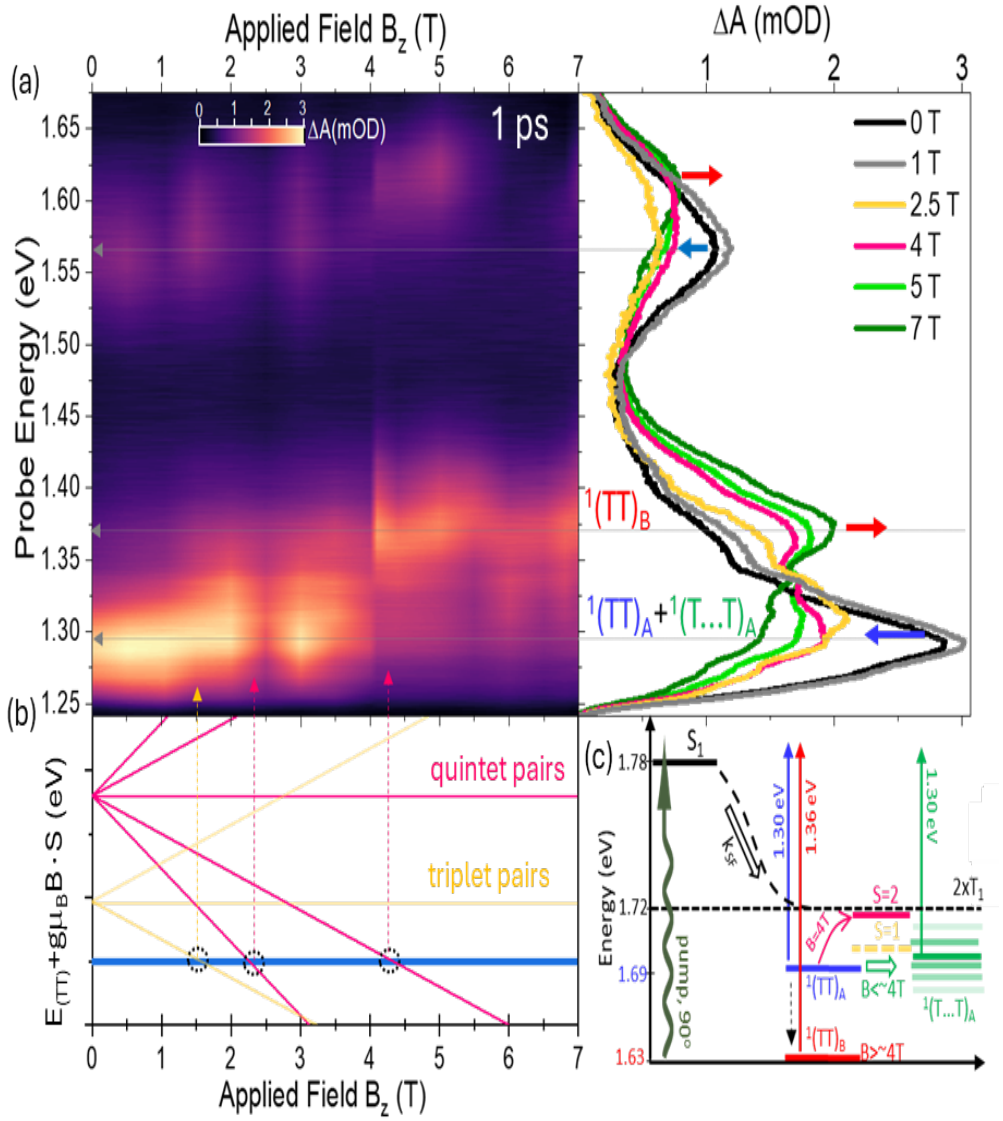

Fig. 2, B-field ultrafast spin-exchange resonances, (a) *Single-crystal TA spectra at 1 ps delay time plotted against the applied magnetic field (0 to 7 T). Sharp resonant decreases in all peaks occurs at the labeled B=2.2 and 4.2 T positions, consistent with ultrafast low-J coherent creation of triplet and quintet states when degeneracy with the populated S=0 states is achieved. The corresponding (on right) TA spectra show [$^1(TT)_A$+$^1(T...T)_A$] ESA peak probed E_{pr}=1.30 eV decreasing, with $(TT)_B$ at 1.36 eV increases correspondingly.* ***(b)*** *Prediction of expected Zeeman splitting of singlet (S=0, blue), triplet (S=1, yellow) and quintet TT-pair (S=2, pink) highlights the degeneracy with the populated singlet S=0 state at B=~1.5, 2.2 and 4 T.* ***(c)*** *Energy level diagram shows the relevant ESA transitions for TIPS-Pn. New conversion pathways for $^1(TT)_A$ occur resonantly to $^{m=3,5}(TT)_A$ states.*

In summary, both single-crystal SF systems studied show highly efficient ultrafast spin conversion to triplet and quintet states at roughly the same B-field resonances seen in prior steady-state studies. For B > ~ 4 T, the dominant $^1(T\ldots T)$ separated triplet pair state is greatly diminished, resulting in corresponding enhancements for $^1(TT)_B$ or S_1 state populations in TIPS-Pn and diF-ADT, respectively. Going forward, we show SF dynamics can be strongly modulated by applied B-fields, revealing the rich nature of correlated triplet-pair states and ultrafast spin conversion that underpin this efficient charge multiplying process.

References

[1] W. Kim, A.J. Musser, *Advances in Physics* X **6,** 1918022 (2021).
[2] J. Kim ,D.C. Bain,V. Ding,K.Majumder, D.Windemuller, J.Feng, J. Wu, S. Patil, J.Anthony, W. Kim, A. J. Musser, *Nature Chemistry*, doi: 10.1038/s41557-024-01556-3, (2024).
[3] G. Mayonado, K. V. Vogt, J. Van Schenck, L. Zhu, J. Anthony, O. Ostroverkhova, M. W. Graham, *Journal of Phyisical Chemistry* C **126**, 4433 (2022)

***** Acknowledgments: This material is based upon work supported by DoD award number FA9550-22-1-0276.

Low-dimensional magnetism at oxide interfaces and the possibility of Controlling it with ultrafast THz excitation

A. X. Gray
Temple University, Philadelphia, PA 19122, USA

Emergent magnetic phenomena at interfaces are at the forefront of materials science, crucial for advancing spintronics and magnetic storage technologies [1]. In particular, stabilizing and controlling low-dimensional interfacial ferromagnetic ground states in systems composed of two nonferromagnetic materials is of significant importance from both fundamental and technological perspectives [2,3]. Here, we explore low-dimensional interfacial ferromagnetism in $CaMnO_3/CaMnO_3/CaRuO_3$ and $LaNiO_3/CaMnO_3$ superlattices, utilizing advanced synchrotron-based X-ray spectroscopy, density functional calculations, and ultrafast THz-pump tr-MOKE spectroscopy [4,5]. We derive detailed magnetic profiles of the ferromagnetic layers at these interfaces and demonstrate that the magnetic moments can be tuned by adjusting thickness, layering, and introducing point defects. Additionally, we employ time-resolved magneto-optic Kerr effect, optical reflectivity, and transmissivity spectroscopies on variable-thickness $LaNiO_3/CaMnO_3$ superlattices to disentangle multiple interrelated electronic and magnetic processes driven by ultrafast high-field THz pulses.

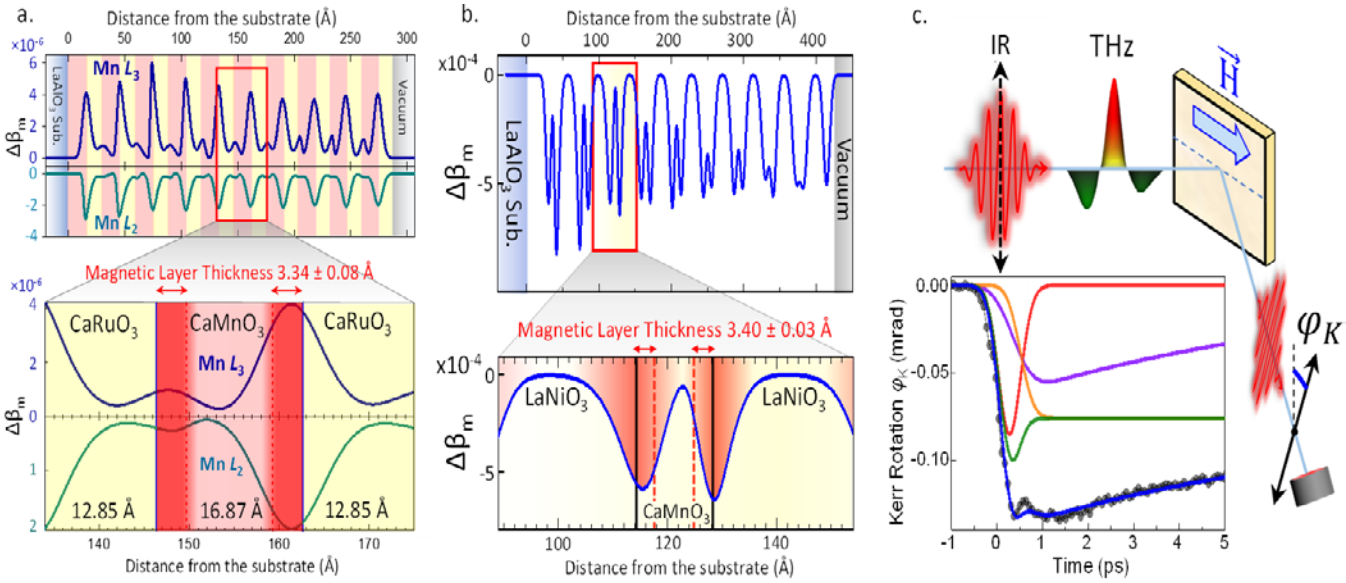

***Fig. 1. (a)**: **Depth-resolved magneto-optical profile** of a $CaMnO_3/CaRuO_3$ superlattice measured via momentum-resolved resonant magnetic X-ray reflectivity. The expanded region in the lower panel reveals an asymmetry in the magnetic moment at the top and bottom $CaMnO_3$ interfaces. **(b)**: A similar magneto-optic profile for a $LaNiO_3/CaMnO_3$ superlattice. **(c)**: Schematics and the delay trace of the THz-pump IR MOKE probe response of the $LaNiO_3/CaMnO_3$ magnetic interface decomposed into several electronic and magnetic dynamical components.*

By extending the scope of traditional magnetic interface studies and providing deeper insight into atomic-level interactions, this work paves the way for future innovations in magnetic storage and spintronics.

References

[1] F. Hellman, A.Hoffmann Materials, Y.Tserkovnyak, G. S. D. Beach, E.E. Fullerton, C.Leighton, A.H. MacDonald, D. C. Ralph, D.A. Arena, H.A. Dürr P. Fischer, J. Grollier, J. P. Heremans, T. Jungwirth, A. V. Kimel, I. N. Krivorotov, S. J. May, A. K. Petford-Long, J. M. Rondinelli, N. Samarth I. K. Schuller A. N. Slavin, M. D. Stiles, O. Tchernyshyov, A. Thiaville, B. L. Zink, *Review of Modern Physics* **89**, 025006 (2017).
[2] R.U. Chandrasena, C. L. Flint, W. Yang, A. Arab, S. Nemšák, M. Gehlmann, V. B. Özdöl, F. Bisti, K. D. Wijesekara, J. Meyer-Ilse, E. Gullikson E.Arenholz, J. Ciston, C. M. Schneider, V. N. Strocov, Y. Suzuki, A. X. Gray, *Physical Review* B **98**, 155103 (2018).
[3] J. R. Paudel, M. Terilli, T.-C. Wu, J. D. Grassi, A. M. Derrico, R. K. Sah, M. Kareev, C. Klewe, P. Shafer, A. Gloskovskii, C. Schlueter, V. N. Strocov J. Chakhalian, A. X. Gray, *Physical Review* B **108**, 054441 (2023).
[4] J. R. Paudel, A. Mansouri Tehrani, M. Terilli, M. Kareev, J. Grassi, R. K. Sah, L. Wu, V. N. Strocov, C. Klewe, P. Shafer, J. Chakhalian, N. A. Spaldin A.X. Gray, *arXiv:2405.01445* (2024).
[5] A. M. Derrico, M. Basini, V. Unikandanunni, J. R. Paudel, M. Kareev, M. Terilli, T.- C. Wu, A. Alostaz, C. Klewe, P. Shafer, A. Gloskovskii C.Schlueter, C. M. Schneider, J. Chakhalian, S. Bonetti, A. X. Gray, *arXiv:2402.04302* (2024).
* Acknowledgements: authors acknowledge support from the US Air Force Office of Scientific Research (AFOSR) under award number FA9550-23-1-0476; and from the U.S. Department of Energy, Office of Science, Office of Basic Energy Sciences, Materials Sciences and Engineering Division, under Award No. DE-SC0019297.

Quantum decoherence by magnetic fluctuations in a candidate Axion insulator from electric quadrupole second harmonic generation

R. Saatjian[1], S. Dovrén[1], K. Yamakawa[2], R. S. Russell[1], J. G. Analytis[2], J. W. Harter[1]
[1] *University of California, Santa Barbara, CA 93106, USA*
[2] *University of California, Berkeley, CA 94720, USA*

In magnetic topological insulators, spontaneous time-reversal symmetry breaking by intrinsic magnetic order can open an energy gap in the topological surface spectrum [1]. In the resulting state, exotic properties like axion electrodynamics, the quantum anomalous Hall effect, and other topological magnetoelectric responses are expected to emerge [2-5]. A detailed understanding of the magnetic order and its coupling to the topological surface states is essential to harness and tune these properties. In this presentation, we will describe recent experiments leveraging near-resonant electric quadrupole optical second harmonic generation to probe magnetic fluctuations in the candidate axion insulator $EuSn_2(As,P)_2$ across its antiferromagnetic phase boundary [6]. We observe a pronounced dimensional crossover in the quantum decoherence induced by magnetic fluctuations, where two-dimensional in-plane ferromagnetic correlations at high temperatures give way to three-dimensional long-range order at the Néel temperature. We also observe the breaking of rotational symmetry within the long-range-ordered antiferromagnetic state and map out the resulting spatial domain structure.

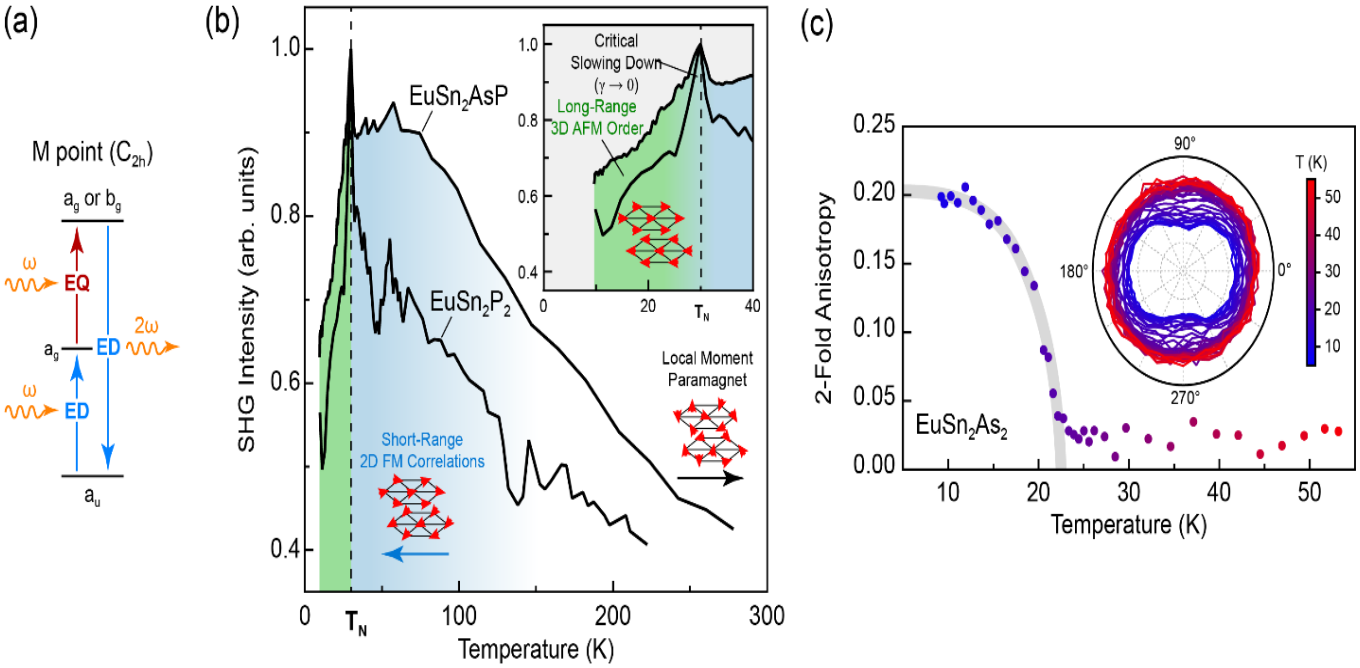

Fig. 1. Second harmonic generation in $EuSn_2(As,P)_2$. ***(a)*** *Energy level diagram showing resonant electric quadrupole second harmonic generation (SHG) between electronic states at the M point.* ***(b)*** *Temperature dependence of SHG. Upon cooling from room temperature, SHG increases dramatically, with a sharp peak at the Néel temperature.* ***(c)*** *Spontaneous rotational symmetry breaking in the antiferromagnetic phase from SHG rotational anisotropy measurements.*

More generally, we demonstrate the unique capabilities of nonlinear optical spectroscopy to study quantum coherence and fluctuations in magnetic quantum materials.

References

[1] Y. Tokura, K. Yasuda, A. Tsukazaki, *Nature Reviews Physics* **1**, 126 (2019).
[2] A. M. Essin, J. E. Moore, D. Vanderbilt, *Physical Review Letters* **102**, 146805 (2009).
[3] R. Li, J. Wang, X.-L. Qi, S.-C. Zhang, *Nature Physics* **6**, 284 (2010).
[4] R. S. K. Mong, A. M. Essin, J. E. Moore, *Physical Review* B **81**, 245209 (2010).
[5] R. Yu, W. Zhang, H.-J. Zhang, S.-C. Zhang, X. Dai, Z. Fang, *Science* **329**, 61 (2010).
[6] R. Saatjian, S. Dovrén, K. Yamakawa, R. S. Russell, J. G. Analytis, J. W. Harter, *to be submitted* (2024).

* Acknowledgements: This work was supported by the U.S. Air Force Office of Scientific Research (AFOSR) under Award No. FA9550-22-1-0270. The research reported here made use of the shared facilities of the Materials Research Science and Engineering Center (MRSEC) at UC Santa Barbara: NSF DMR–2308708. The UC Santa Barbara MRSEC is a member of the Materials Research Facilities Network (www.mrfn.org).

Attosecond quantum tunneling current switching in graphene

M. Th. Hassan.
University of Arizona, Tucson, AZ 85721, USA.

The electron motion dynamics of graphene open the door for developing ultrafast graphene-based optoelectronics [1]. In this work [2], we exploited a graphene-silicon-graphene (Gr-Si-Gr) phototransistor and demonstrated the generation of sub-microamperes light-induced current by few-cycle laser pulses. In our transistor, the current flows based on quantum tunnelling between the graphene sides through the silicon junction. Hence, the generated current is gated in time, which allows us to access and record the ultrafast instantaneous field-induced current. The field-induced current modulates periodically in real-time, following the waveform of the driver field, enabling a current switching between two states (ON and OFF) with a time speed of 630 attoseconds (1.6 petahertz) and > 95% switching contrast. Moreover, we demonstrate a control of the light-induced current amplitude by increasing the induction laser beam intensity and determining the consequent enhancement of our phototransistor photoconductivity. Finally, the flexibility of our transistor setup allowed us to combine a DC current (IV), generated by applying an external voltage, with the light-induced current to demonstrate several logic gates within our phototransistor. Notably, the presented experiments are performed under ambient standard temperature and pressure conditions, making this phototransistor at the technology readiness level for developing attosecond and lightwave quantum optoelectronics [3].

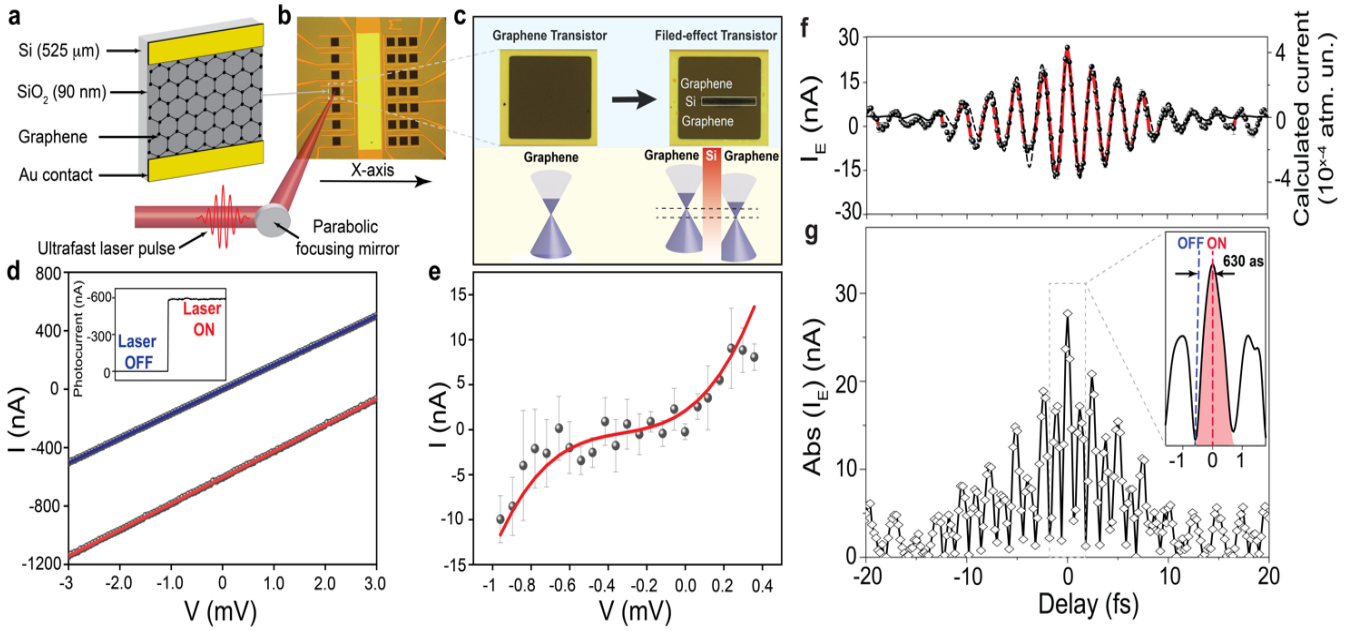

Fig. 1. (a) The graphene channel transistor composition. *(**b**) The setup of the graphene phototransistor. The laser beam is focused on the graphene channel by a parabolic mirror. (**c**), The normal graphene channel and the generated Gr-Si-Gr FET were obtained by focusing the laser in the medial of the channel and moving it in the x-axis by linear stage. The illustration in the bottom shows the difference in the band structure of graphene and Gr-Si-Gr transistors. (**d**), The measured IV curve in the case of laser ON (blue line) and laser OFF (red line). The inset shows the switching ON and OFF of the current signal by the laser beam. (**e**), The IV curve of the FET was obtained by subtracting the IV curves shown in **d**. (**f**)The instantaneous field-induced current (average of three measurements) is shown as the red line. The calculated intraband current is plotted in a dashed black line. (**g**), Absolute current measured signal. The inset shows the current switching ON and OFF with a periodicity of 630 as.*

Notably, the presented experiments are performed under ambient standard temperature and pressure conditions, making this phototransistor at the technology readiness level for developing attosecond and lightwave quantum optoelectronics [3].

References

[1] D. Hui, H. Alqattan, M. Sennary, N. V. Golubev, M. T. Hassan, *Science Advances* **10,** eadp5805 (2024).
[2] M. Sennary, J. Shah, M. Yuan, A. Mahjoub, V. Pervak, N. Golubev, M. Hassan, arXiv:2407:1680 (2024).
[3] M. T. Hassan, ACS Photonics **11**, 334 (2024).

* Acknowledgement(s): The author acknowledges support from the Gordon and Betty Moore Foundation (Grant GBMF 11476) and the Air Force Office of Scientific Research (award number FA9550-22-1-0494).

Lightwave electronics - from high harmonics spectroscopy to Floquet topological insulators

C.Heide
Stanford University, Stanford, CA 94305, USA

Tailored ultrashort light fields are crucial in observing and exploiting ever-faster physical phenomena. Precisely controlling the electromagnetic field of light allows the control of processes inside atoms, molecules, and solids on a sub-cycle timescale of the laser pulse, providing access to the femto-to-attosecond timescale. Such waveform control opens prospects for engineering and probing material properties on unprecedented timescales [1]. Beyond fundamental applications, it is also relevant for technology applications such as efficient charge transfer, signal processing, and computation at speeds that exceed the current gigahertz clock rates by orders of magnitudes [2]. First, I will present how the electric field of intense laser pulses can be controlled to generate and, most importantly, measure synthesized light waves. These fields are then applied to quantum materials such as graphene, where I demonstrate that on attosecond and femtosecond times scales, electrons inside of solids are steered by the lightfield, so fast that this occurs entirely coherently, which means that quantum mechanics governs their dynamics. Utilizing quantum interferences, we probe graphene's band structure and coherence [3-5]. Next, I demonstrate coherent control of photocurrents in light-dressed graphene. Here, we utilize circularly polarized laser pulses to dress the graphene band structure to obtain a Floquet Topological Insulator (FTI). Subsequently, we use phase-locked second harmonic pulses to drive electrons in the underlying FTI. This approach allows us to measure the resulting all-optical anomalous Hall photocurrents, FTI valley-polarized currents, and photocurrent circular dichroism, all phenomena that put FTIs on equal footing with equilibrium topological insulators [6].

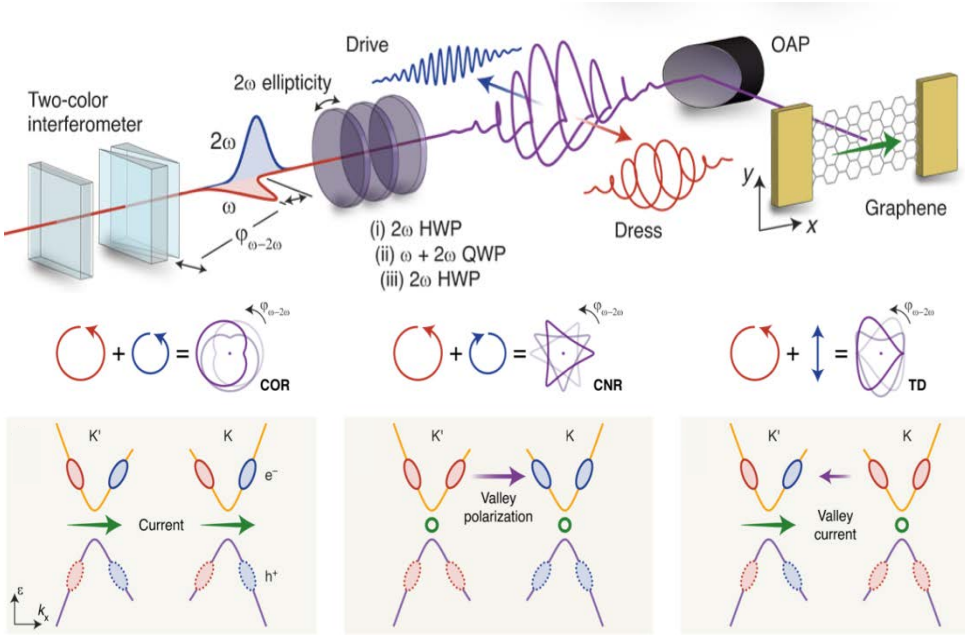

Fig. 1. Experimental schemes for generating photocurrent, valley current and polarization in graphene.

In the last part of my talk, I will demonstrate how electrons driven in a band structure generate extreme nonlinear light emission, known as high-harmonic generation (HHG). HHG can then be used to perform ultrafast spectroscopy [1]. Measuring and understanding this emission allows the mapping of various material properties, such as quantum phases and coherence, as well as its band structure and topology, which are often obscured in conventional measurement schemes [7-9].

References

[1] C. Heide, Y. Kobayashi, S.R.U. Haque, S. Ghimire, *Nature Physics, in print* (2024).
[2] C. Heide, D. Keathley, M. Kling, *Nature Review Physics, in print* (2024).
[3] T. Boolakee, C Heide, A.Garzón-Ramírez, H.B. Weber, I. Franco, P. Hommelhoff., *Nature* **605** , 251 (2022).
[4] C. Heide, T. Eckstein, T. Boolakee, C.Gerner, H.B. Weber, I. Franco, P. Hommelhoff, *Nano Letters* **21** , 9403 (2021).
[5] T. Weitz, C. Heide, P. Hommelhoff, *Physical Review Letters* **20**, 206901 (2024).
[6] T. Weitz, D. Lesko, S. Wittigschlager, W. Li, C. Heide, O. Neufeld, P. Hommelhoff, *arXiv:2407.17917* (2024).
[7] C. Heide, Y. Kobayashi , D. R. Baykusheva, D. Jain, J.A. Sobota, M. Hashimoto, P.S. Kirchmann, S. Oh, T. F. Heinz, D. A. Reis, S. Ghimire, *Nature Photonics* **16**, 620 (2022).
[8] C. Heide, Y. Kobayashi, A.C. Johnson, F. Liu, T.F. Heinz, D.A. Reis, S. Ghimire, *Optica* **9**, 512 (2022).
[9] C. Heide, Y. Kobayashi , A.C. Johnson, T.F. Heinz, D.A. Reis, F. Liu, S. Ghimire, *Nanophotonics* **12**, 255 (2023).

Generation of ultrashort optical pulses by a transient Plasmonic resonance

A. Husakou[1], I.Babushkin[1], Olga Fedotova[3], R.Rysetsky[3], T.Smirnova[4], O.Khasanov[3], A. Fedotov[4], U.Sapaev[5]
[1]*Max Born Institute, 12489 Berlin, Germany*
[2] *Leibnitz Hannover University, 30167 Hannover, Germany*
[3]*Scientific and Practical Materials Research Center, 220072 Minsk, Belarus*
[4]*Belarus State University, 220030 Minsk, Belarus*
[5]*Tashkent State Technical University, 100097 Tashkent, Uzbekistan*

Numerous fields of modern ultrafast optics, such as time-resolved spectroscopy [1], manufacturing and investigation of surfaces [2], molecular dynamics and reactions [3], material modification and so on, often require short, sub-10-fs intense pulses at high frequencies. Such pulses are typically obtained by a two-step approach which includes frequency conversion, for example by means of nonlinear crystals, and subsequent pulse shortening. Here we propose and theoretically investigate the generation of short sub-5-fs pulses in a composite of dielectric nanoparticles due to a transient plasmonic resonance which is excited dynamically for a short period of time during the pump pulse. The key idea is illustrated in Fig. 1.

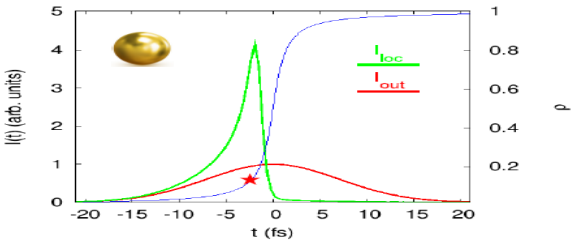

Fig. 1. The schematic representation of the key idea of the investigation. *In the composite with spherical inclusions, the intensity inside the nanoparticles I_{loc} **(green curve)** can be high compared to external intensity I_{out} **(red curve)** during the short time range as the pulse passes the plasmonic resonance. The resonance takes place when the relative plasma density **(blue curve)** crosses certain value **(indicated by a star)**.*

For a composite which consists of small spherical nanoparticles with dielectric function ε_i inside of the host medium with dielectric function of ε_h, the ratio x between the local field inside of the nanoparticle E_{loc} and the external field E_{out} is given by [4]

$$x = \frac{3\varepsilon_h}{2\varepsilon_h + \varepsilon_i - \delta\varepsilon_{pl}}, \tag{1}$$

where we have taken into account the modification $-\delta\varepsilon_{pl}$ of the dielectric function ε_i by the plasma, which occurs due to photoionization by a strong optical pulse. Here we assume that the host material has higher bandgap and therefore negligible ionization rate. Upon the pulse propagation through the nanostructure, the plasma density increases with time. At certain point in time the system can pass through a plasmonic resonance, with the position being determined by the zero of the denominator in Eq. (1). During the short time which the system spends near the resonance, the local field experiences strong enhancement. This leads to generation of a strong and short third harmonic pulse due to third-order susceptibility of the inclusions. Simulations of the pulse propagation were performed in the (1+1)D geometry using a unidirectional propagation equation without slowly-varying-envelope approximation [5]. The following effects were included into the simulation: group velocity dispersion, linear material loss, scattering loss, third-order nonlinearity of both host and inclusions, photoionization of inclusions, plasma dynamics and its influence on the dielectric function of the inclusions, as well as the temporal dependence of the factor x. For the sake of space we present here only a novel system of equations which describes the dynamics of the relative plasma density and the local field. This system constitutes the core of the model:

$$\left[\frac{\partial^2}{\partial t^2} + \nu\frac{\partial}{\partial t}\right] E_{loc}(t) = \kappa\rho(t)E_{loc}(t) + \frac{3\varepsilon_h}{2\varepsilon_h + \varepsilon_i}\left[\frac{\partial^2}{\partial t^2} + \nu\frac{\partial}{\partial t}\right] E_{out}(t), \tag{2}$$

$$\frac{\partial\rho(t)}{\partial t} = \Gamma(E_{loc}(t)). \tag{3}$$

Here ν is the electron velocity decay rate, $\kappa = Ne^2/(m_e\varepsilon_0)$, where N is the concentration of atoms or molecules, and $\Gamma(E)$ is the field-dependent ionization rate. The simulations were performed for a typical case of 55-fs, 800-nm pulses with intensity of 0.75 TW/cm^2 propagating through a composite made of fused silica and AlN spherical nanoparticles with a filling factor of 0.003. In Fig. 2 the results of the simulations are shown. One can see that at the time when the plasma density (blue) passes its resonance value (dashed), the local field becomes much higher than the incident field, forming a short peak. As soon as the plasma density increases further, the factor x and the local field drop. This leads to a formation of a short few-cycle third-harmonic pulse, as shown in the right panel. In the present simulation, the third harmonic pulse has a FWHM duration of 5 fs.

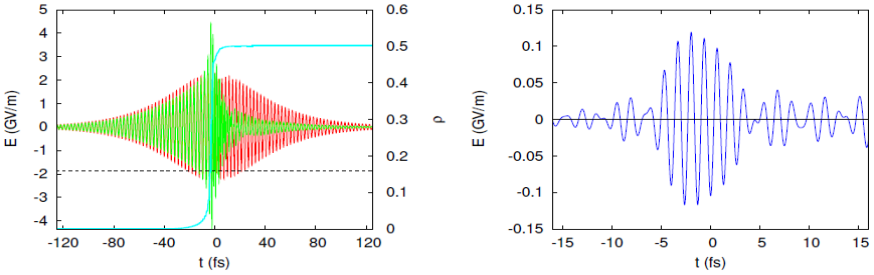

***Fig. 2. The results of simulations for the parameters given in text. Left**, the temporal dependence of the incident field (red), local field **(green)**, and relative plasma density **(blue)** is shown. By the horizontal dashed line, the relative plasma density which corresponds to the plasmonic resonance is indicated. **Right**, the generated third-harmonic pulse is illustrated by the blue curve.*

At higher intensities and with higher filling factor (not shown), we predict generation of even shorter pulses, with duration down to 0.8 fs, albeit with strong pedestal. The conversion efficiencies reach values of up to 1%. In the conclusion, we investigated the formation of short local-field bursts due to the fast transition of a nanocomposite through a plasmonic resonance. We also predict generation of third-harmonic pulses with femtosecond and even sub-femtosecond durations by this mechanism.

References

[1] F. Krausz, M. Ivanov, *Review of Modern Physics* **81**, 163(2009).
[2] P. Jürgens *et al*., Nature Physics **16**, 1035–1039 (2020).
[3] S. Baker, J. S. Robinson, C.A. Haworth, H. Teng, R.A. Smith, C.C. Chirila, M. Lein, J.W.G. Tisch, J. P. Marangos, Science **312**, 424 (2006).
[4] J. E. Sipe, R. W. Boyd, *Physical Review* A **46**, 1614 (1992).
[5] A. Husakou, J. Herrmann, *Optics Express* **17**, 12481 (2009).

* Acknowledgement(s): authors acknowledge support from Air Force Office of Scientific Research (FA8655-22-1-7175); European Research Executive Agency (H2020-MSCA-RISE-2018-823897); Cluster of Excellence Phoenix D (390833453); Bulgarian National Science Fund (KP-06-COST/7); World Bank Project (REP-04032022-206); Uzb-Ind (2021-96/83).

Resonant excitation of van der Waals antiferromagnets

J. A. Warshauer, H. Chen, D.A.B. Lopez, Q. Tan, J. Tang, X. Ling, W.Hu
Boston University, Boston, MA 02215, USA

Excitons are bound electron-hole pairs that broadly exist in weakly correlated semiconductors and semimetals. There has been a growing interest in experimental verification of unconventional excitons in strongly correlated materials, and studying the interplay between excitons and charge, spin and lattice degrees of freedom. However, the beauty of rich excitonic physics is limited by the exciton's lifetime before the electron-hole recombination. Long-lived excitons are appealing for the realization of exciton condensation and optoelectronic device applications, making materials with long-lived excitonic states highly sought after. Van der Waals magnets are an emerging material family for investigating light-matter interactions and spin correlated excitations. The discovery of an ultranarrow photoluminescence peak in the antiferromagnetic material $NiPS_3$, identified as a spin-correlated exciton state, opening up novel opportunities to study coherent many-body excitons [1-4]. Despite extensive interest in the ultra-narrow spin-correlated exciton, there are no studies on resonant driving at exciton levels in $NiPS_3$ or other van der Waals magnets in this family.

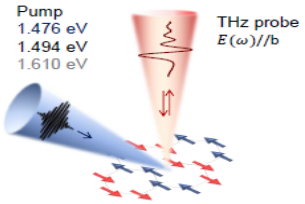

Fig. 1. A sketch of the optical pump THz probe experiment on $NiPS_3$ [5].

Here, we report the discovery of a long-lived photo-induced state with a negative photoconductivity in the van der Waals antiferromagnet $NiPS_3$, which appears exclusively with resonant pumping at the exciton level in the antiferromagnetic state. Our study provides new insights to understand the nature of the spin-orbit-entangled exciton, for which limited data and diverse interpretations exist.

References

[1] S. Kang, K. Kim, B. H. Kim, J. Kim, K. I. Sim, J.- U. Lee,S. Lee, K. Park, S. Yun, T. Kim, A. Nag, A. Walters, M. Garcia-Fernandez, J. Lim, L. Chapon K.-J. Zhou, Y.-W. Son, J. H. Kim, H. Cheong, J.-G. Park, *Nature* **583**, 785 (2020).
[2] F. Dirnberger, R. Bushati, B. Datta, A. Kumar, A. H. MacDonald, E. Baldini, V. M. Menon, *Nature Nanotechnology* **17**, 1060 (2022).
[3] D. Jana, P. Kapuscinski, I. Mohelsky, D. Vaclavkova, I. Breslavetz, M. Orlita, C. Faugeras, M. Potemski, *Physical Review* B **108** (2023).
[4] T. Klaproth, S. Aswartham, Y. Shemerliuk, S. Selter, O. Janson, J. van den Brink, B. B¨uchner, M. Knupfer, S. Pazek, D. Mikhailova, A. Efimenko R. Hayn, A. Savoyant, V. Gubanov, A. Koitzsch, *Physical Review Letters* **131,** 256504 (2023).
[5] J. A. Warshauer, H. Chen, D. A. B. Lopez, Q. Tan, J. Tang, X. Ling, W.Hu, *(submitted)*, (2024).

* Acknowledgement(s):This material is based upon work supported by the NSF under Grant No.1944957. H. C., D. A. B. L. and W. H. acknowledge support from the U.S. DOE, Office of Science, Office of Basic Energy Sciences Early Career Research Program under Award Number DE-SC-0021305. Work by Q. T., J. T. and X. L. were supported by the NSF under Grant No. (1945364) and the U.S. DOE, Office of Science, Basic Energy Sciences under Award DE-SC0021064, Q.T. acknowledges support of the Laursen Graduate Research Award.

Photophysics of photocatalytic and radical systems

V. M. Huxter
University of Arizona, Tucson, AZ 85721

Radicals and other open-shell molecules are central to chemical transformations and redox chemistry, with stable radical systems being of interest for applications in materials chemistry, catalysis, spintronics, and quantum information. Here, we investigate the ultrafast optical properties and spin-tunable behaviors of hexaethyl tripyrrin-1,14-dione (H3TD1) and its metal complexes, specifically focusing on copper(II) and palladium(II) systems (Cu-TD1 and Pd-TD1, respectfully). These neutral radical systems demonstrate exceptional stability and are promising for future applications in quantum materials and catalysis. Building on our understanding of these systems, we also use time-resolved nonlinear spectroscopy to determine the mechanisms of photoredox catalysis. Our work on Cu-TD1[1] reveals temperature-dependent spin-tunable properties driven by the presence of unpaired electrons on both the copper metal center and the tripyrrolic TD1 ligand. Using two-dimensional electronic spectroscopy (2DES) shown in Fig. 1, we characterized the spin dynamics of the system at room temperature and 77 K.

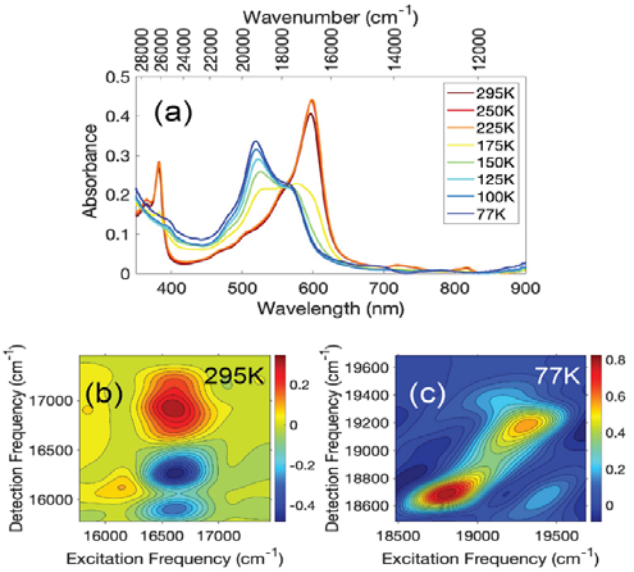

Fig. 1. Temperature-dependent antiferromagnetic coupling *of a Cu-tripyrrindione complex.* ***(a)*** *Temperature-dependent absorption traces of the complex in a toluene/methylcyclohexane solution.* ***(b)*** *2DES measurement of the complex at room temperature.* ***(c)*** *2DES measurement of the complex at 77 K. The off-diagonal peak arises because of the antiferromagnetic coupling. All measurements in a N_2 environment in a cryostat.*

At room temperature, the copper complex exists as monomers with short-lived excited states, decaying in picoseconds. However, at 77 K, the molecules dimerize in part through ferromagnetic and antiferromagnetic coupling, resulting in the formation of long-lived excitonic states. This transition from short-lived monomers to long-lived dimers highlights the potential of these systems for spin-based technologies. To further explore the properties of these metal neutral radical complexes, we compared the optical properties of Pd-TD1 and Cu-TD1[2], which display tunable spin states that result in triplet, doublet, or singlet configurations depending on the metal center and the redox state of the ligand. The Pd(II) and Cu(II) complexes have ligand-based radicals, which give rise to doublet and triplet states, respectively. Time-resolved spectroscopic techniques were used to investigate the optical properties and dynamics of these systems. We observed that the copper neutral radical and oxidized complexes, as well as the palladium neutral radical complex, exhibit rapid relaxation timescales, returning to their ground states within tens of picoseconds. In contrast, the oxidized palladium complex exhibits significantly longer relaxation dynamics. The ability to modulate spin states via stable open-shell configurations and reversible redox activity in these tripyrrolic systems offers opportunities for catalytic applications, as well as the exploration of magnetism and conductivity in novel materials. The optical properties and ultrafast dynamics of H3TD1 alone in solution are modulated by hydrogen-bonding interactions. Our work has shown how the solvent environment drives aggregation and mediates non-radiative relaxation pathways[3]. In solvents with low hydrogen-bonding affinity, H3TD1 tends to form hydrogen-bonded dimers, whereas in solvents capable of donating or accepting hydrogen bonds, H3TD1 remains a monomer. This monomer-dimer relationship has a significant impact on the ultrafast dynamics, with the dimer form exhibiting faster internal conversion compared to the monomer. The ultrafast relaxation dynamics of the monomer and dimer in solution were characterized using time-correlated single-photon

counting, fluorescence upconversion, and transient absorption (TA). Additionally, the time-resolved behavior of these species was modeled using a Pauli master equation treatment for a three-level system. Steady-state absorption and fluorescence measurements allowed us to determine the solvent-dependent optical properties, including quantum yields and extinction coefficients. These findings provide insight into how the molecular environment influences the excited state dynamics in H3TD1. In parallel, we explore the broader implications of our work on radicals in the context of photoredox catalysis[4]. Photoredox catalysis has revolutionized organic synthesis, providing sustainable methods to drive single-electron transfer reactions through light absorption. Historically, photoredox catalysis was dominated by transition metal catalysts such as ruthenium and iridium compounds. However, recent developments have shifted the focus towards organic photocatalysts, which are more sustainable, tunable, and cost-effective. Despite these advances, the mechanistic understanding of organic photoredox catalysis remains incomplete, as many of the underlying processes, including solvent effects, catalyst degradation, and non-productive reaction pathways, are not fully understood.
In photoredox catalysis, closed-shell organic catalysts absorb light to generate excited species that drive chemical reactions as shown in Fig. 2.

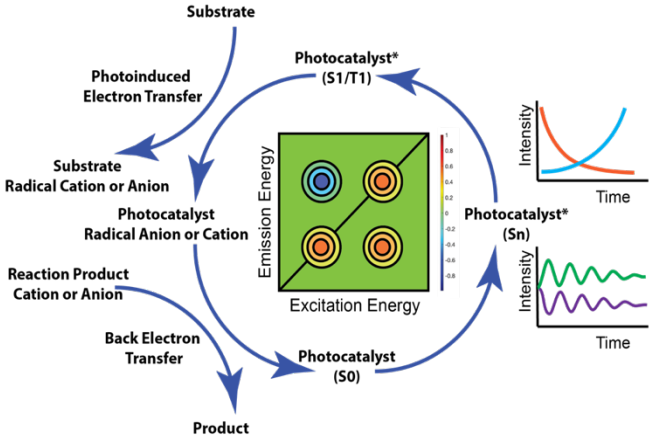

Fig. 2. Cartoon 2DES plot (center, green background) *with a generic photoredox catalysis cycle. In a 2DES measurement, excitation and emission energies correlate to each other, allowing individual signal contributions to be resolved and mapped. The traces on the right side represent the rise and decay of excited states (**top**) and the action of vibrational modes coupled to the electronic states **(bottom)**.*

However, the standard models describing these processes are generally oversimplified. A detailed understanding of the mechanisms of photoredox catalysis is necessary to improve the efficiency of photoredox catalysis. Time-resolved optical techniques, such as TA and 2DES, offer new insights into the excited-state dynamics of photoredox systems. TA measurements provide a broad overview of excited-state lifetimes and decay pathways, while 2DES offers enhanced resolution for separating overlapping signals and identifying transient intermediates. For example, in the case of the Cu-TD1 complex, 2DES was used to resolve intermediate species that were otherwise obscured in traditional TA measurements. This capability is particularly important in complex photocatalytic systems, where multiple reaction pathways may produce overlapping signals that complicate mechanistic analysis.
Further investigation into the roles of organic radicals, solvent dynamics, and spin states in photoredox catalysis are essential for advancing this field. Organic radicals typically exhibit short lifetimes, making them inefficient as primary catalytic agents. However, preaggregation or physical association of catalysts and reactants, as well as the involvement of longer-lived closed-shell species, may enhance reaction efficiency. Moreover, solvents play an important role in modulating charge transfer rates and stabilizing reaction intermediates[5]. Our time-resolved spectroscopic studies use advanced spectroscopic techniques to investigate both the ultrafast dynamics of metal-organic radical systems and the mechanistic intricacies of organic photoredox catalysis. By revealing the complex interactions between radicals, solvents, and catalytic intermediates, we provide new insights into the design of more efficient catalysts and the development of sustainable synthetic methodologies.

References

[1] A. Kumar, B. Thompson, R. Gautam, E. Tomat, V. Huxter, *The Journal of Physical Chemistry Letters* **14**, 11268 (2023).
[2] B. Cho, A. Swain, R. Gautam, E. Tomat, V. M. Huxter, *Physical Chemistry Chemical Physics* **24**, 15718 (2022).
[3] A. Swain, B. Cho, R. Gautam, C. J. Curtis, E. Tomat, V. M. Huxter, *The Journal of Physical Chemistry B* **123**, 5524(2019).
[4] V. M. Huxter, *The Journal of Physical Chemistry Letters* **15**, 7945(2024).
[5] B. J. Thompson, A. Kumar, V. M. Huxter, *Physical Chemistry Chemical Physics* **26**, 19900 (2024).
* Acknowledgements: V. M. H. gratefully acknowledges support from the donors of the American Chemical Society Petroleum Research Fund through Grant 65536-ND6 and support from the National Science Foundation through a CAREER Award (Grant 2236610).

Strong light-matter interactions and nonlinearities from first principles: from Exciton dynamics to giant exciton-driven Floquet effects

F. H. da Jornada
Stanford University, Stanford CA 94305, USA

Optical nonlinearities and ultrafast phenomena in materials enable one to design critical optoelectronic components, ranging from established gain media for lasing to promising all-light optical computers, and design novel forms of matter that are not accessible in the electronic ground state. One must often consider atomistic and many-electron interactions to unambiguously predict and interpret such photophysical processes. However, until recently, predictive methods, such as those based on many-body perturbation theory and interacting Green's function (e.g., the Bethe-Salpeter equation) were largely restricted in describing linear-response properties close to equilibrium. Here, we present results from recently developed formalisms for computing the interaction of excitons with other quasiparticles and collective excitations from first principles, including nonlinear optical properties of materials without adjustable parameters. We will first present a recently developed approach to compute exciton-phonon interactions and exciton linewidth on monolayer MoS_2. We show that coherent interactions between phonons and photons yield a factor of three increase of the exciton linewidth compared to the typically considered, first-order process[1-2]. We will also discuss our recent efforts to understand the spectroscopic signatures of excitons in low-dimensional and moiré materials [3-5], which can now be accessed with state-of-the-art momentum microscopes. We will discuss nonlinearities predicted in the optical properties of monolayer materials, and how we can understand them within the language of an exciton-driven Bloch-Floquet effect [6-7]. We will also discuss recent results from our group on the robustness of such effects with the coherence of the driving bosonic fields.

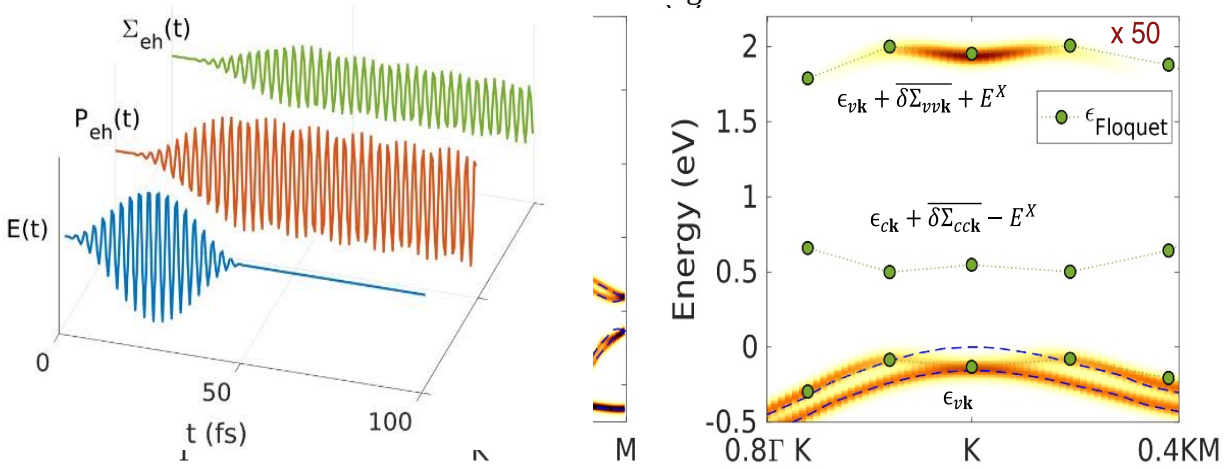

***Fig. 1. Left*: Simulated external electric field** *E(t), induced polarization $P_{eh}(t)$, and change in the self-energy matrix element $\Sigma_{eh}(t)$ obtained from a first-principles time-dependent adiabatic GW simulation on monolayer MoS_2 to simulated a pump-probe experiment including many-electron interactions [6,7]. **Right**: **Simulated spectral function** obtained from the calculation, showing a replica of the valence band and a camel-backed dispersion of the valence band, which can be interpreted as an exciton-driven Floquet effect [7].*

The results suggest the possibility of driving out-of-equilibrium quantum states in materials using internal bosonic fields that may support longer-lived emergent states.

References

[1] Y.-H. Chan, J. B. Haber, N. Naik, J. Neaton, D. Y, Qiu, F. H. da Jornada, S. G. Louie, *Nano Letters* **23**, 3971 (2023).
[2] Y.-H.Chan†, N. Naik, J. B. Haber, J. Neaton, S. G. Louie, D. Y. Qiu, F. H. da Jornada, *Nano Letter* **26**, 7972 (2024).
[3] M. K. L. Man, J. Madéo, C. Sahoo, K. Xie, M. Campbell, V. Pareek, A. Karmakar, E. L. Wong, A. Al- Mahboob, N. S. Chan, D. R. Bacon, X. Zhu M. M. M. Abdelrasoul, X. Li, T. F. Heinz, F. H. da Jornada, T. Cao, K. M. Dani, *Sciences Advances* **7**, eabg0192 (2021).
[4] O. Karni, E. Barré, V. Pareek, J. D. Georgaras, M. K. L. Man, C. Sahoo, D. R. Bacon, X. Zhu, H. B. Ribeiro, A. L. O'Beirne, J. Hu, A. Al-Mahboob M. M. M. Abdelrasoul, N. S. Chan, A. Karmakar, A. J. Winchester, B. Kim, K. Watanabe, T. Taniguchi, K. Barmak, J. Madéo, F. H. da Jornada T. F. Heinz, K. M. Dani, *Nature* **603**, 247 (2022).
[5] E. Barré, O. Karni, E. Liu, A. L. O'Beirne, X. Chen, H.B.Ribeiro, L.Yu, B.Kim, K.Watanabe, T.Taniguchi, K. Barmak, C. H. Lui, S. Refaely-Abramson F. H. da Jornada, T. F. Heinz, *Science* **376**, 406 (2022).
[6] Y.-H. Chan, D. Y. Qiu, F. H. da Jornada, S. G. Louie, *Proceedings NAS* **118**, e1906938118 (2021).
[7] Y.-H. Chan, D. Y. Qiu, F. H. da Jornada, S. G. Louie, *Proceedings NAS* **120**, e2301957120 (2023).
* Acknowledgement(s): authors acknowledge support from the C2SEPEM at L.B.N.L., funded by the U.S. Department of Energy (DOE) Office of Science under Contract No. DE-AC02-05CH1123, the NPNEQ, funded by the U.S. DOE Office of Science under contract DE-AC52-07NA27344, the U.S. DOE BES Award No. DE-SC0021984, and the National Science Foundation CAREER award through grant no. DMR-2238328.

Revealing unique light-matter interaction of the amplitude mode in Superconductors by terahertz two-dimensional coherent spectroscopy

K. Katsumi[2], J.Fiore[3], M.Udina[3], R. Romero III[1], D. Barbalas[1], J.Jesudasan[4]
P. Raychaudhuri[4], G.Seibold[5], L.Benfatto[3], N. P. Armitage[1]
[1] *The Johns Hopkins University, Baltimore, MD 21218, USA*
[2] *New York University, New York, NY 10003, USA*
[3] *Sapienza University of Rome, 00185 Rome, Italy*
[4] *Tata Institute of Fundamental Research, Colaba, Mumbai 400005, India*
[5] *Brandenburg University of Technology, 03013 Cottbus, Germany*

Light-matter interaction in quantum materials is one of the critical aspects that elucidate their intriguing properties. In particular, the terahertz (THz) frequency range is of great interest as it allows us to access rich low-energy excitations in such materials due to the complex interplay between charge, spin, orbital, and lattice degrees of freedom. Recent advancements in generating an intense THz pulse enabled the investigations of nonlinear light-matter interaction, which can provide information unreachable by the linear light-matter coupling. More recently, THz two-dimensional coherent spectroscopy (THz 2DCS, Fig. 1(a)) has emerged as a new technique to disentangle different nonlinear optical processes of magnons, phonons, and plasmons. Yet, understanding the THz 2DCS spectra is still in its infancy.

In this work, we investigate THz 2DCS in the case of a conventional superconductor NbN to elucidate the light-matter interaction of the amplitude collective excitation of the superconducting order parameter, often referred to as the Higgs mode [1]. Using broad-band THz pulses as light sources, we observed a third-order nonlinear optical response whose power spectrum peaked at twice the superconducting gap energy 2Δ. With narrow-band THz pulses, a THz nonlinear signal was identified at the driving frequency Ω and exhibited a resonant enhancement at temperature when $\Omega = 2\Delta$ (Fig. 1(b)). General theoretical considerations show that such resonance can only arise from a disorder-activated paramagnetic light-matter interaction. Numerical simulations reveal that even for a small amount of disorder, the $\Omega = 2\Delta$ resonance is dominated by the superconducting amplitude mode over the entire investigated disorder range.

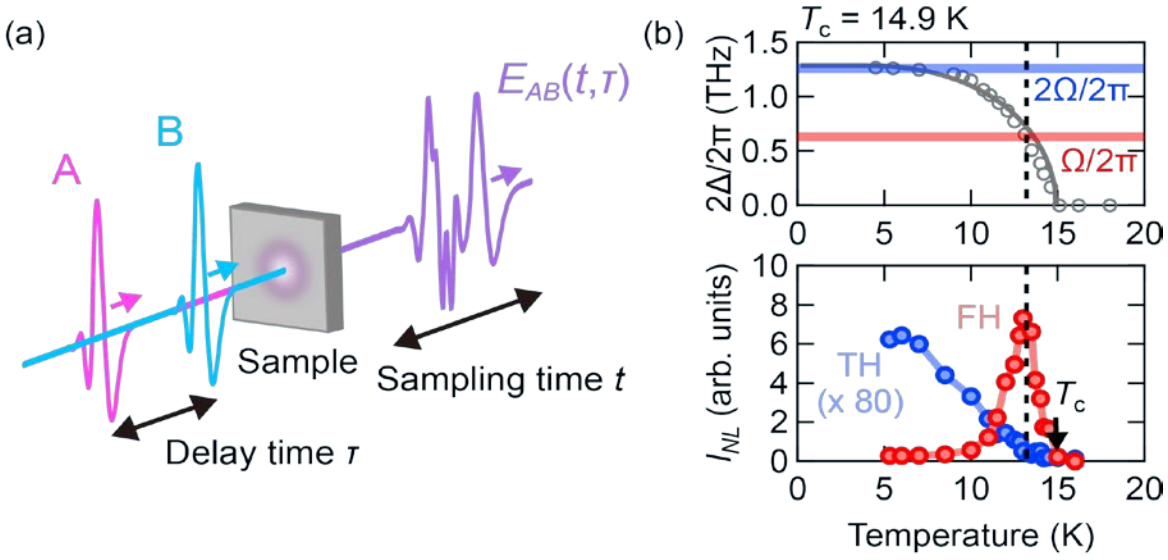

***Fig. 1. (a)**: **Schematic of THz 2DCS. (b)** Temperature dependence of the nonlinear optical responses at τ = 0 ps **(bottom)** and the superconducting gap energy 2Δ **(top)**. FH and TH denote the first-harmonic and third harmonic, respectively.*

This study demonstrated the ability of THz 2DCS to investigate the physics of the amplitude mode in superconductors, which would open a new avenue to study them in other types of superconductors.

References

[1] K. Katsumi, J. Fiore, M. Udina, R. Romero III, D.Barbalas, J. Jesudasan, P. Raychaudhuri, G. Seibold, L. Benfatto, N. P. Armitage, *Physical Review Letters* **132**, 256903 (2024).

Charge-transfer polaritons in van der Waals heterojunctions

B. S. Y. Kim
University of Arizona, Tucson, AZ 85721, USA

The ability to manipulate and probe the emergent behavior in quantum materials with nanoscale precision is at the forefront of condensed matter research and underlies the future progress of new electronic and photonic technologies. Polaritonic platforms utilizing hybrid light-matter excitations with extreme light confinement enable a unique form of experimental inquiry into quantum materials at the nanoscale. Here, we demonstrate a robust strategy to design new polaritonic platforms based on atomically thin van der Waals (vdW) materials using the notion of oxidation-activated charge transfer (OCT) [1]. More specifically, by covering graphene with transition-metal dichalcogenides and subsequently oxidizing the transition-metal dichalcogenides into transition-metal oxides, we activate charge transfer rooted in the dissimilar work functions between transition-metal oxides and graphene. Nano-infrared imaging reveals ambipolar low-loss plasmon polaritons at the transition-metal-oxide/graphene interfaces. Further, by inserting dielectric van der Waals spacers, we can precisely control the electron and hole densities induced by oxidation-activated charge transfer and achieve plasmons with a near-intrinsic quality factor. Using this strategy, we imprint plasmonic cavities with laterally abrupt doping profiles with nanoscale precision and demonstrate plasmonic whispering-gallery resonators based on suspended graphene encapsulated in transition-metal oxides.

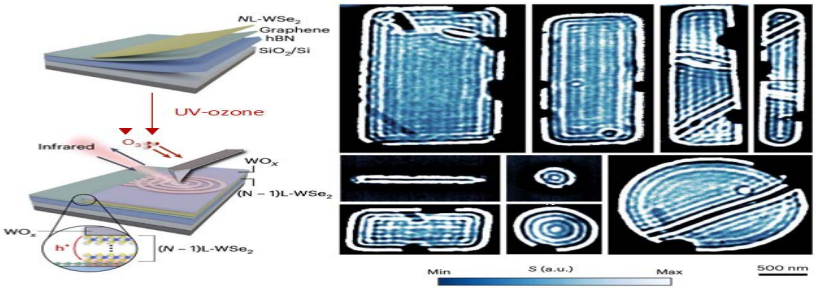

***Fig. 1. Experimental schematics of scanning near-field optical microscopy**, and nano-infrared imaging of graphene plasmonic cavities produced via programmable oxidation- activated charge transfer (OCT) [1].*

Finally, we show the use of OCT to induce a topological transition of polaritons residing at the graphene/α-MoO_3 interface mediated by the coupling between graphene plasmons and α-MoO_3 phonons [2]. These hybrid modes also display an exceptional point in their dispersion, resulting from the direction-dependent plasmon-phonon coupling strengths along the in-plane directions. Our work opens pathways for tailored, strong light-matter coupling in van der Waals materials and for exploring dynamical topological transitions and directional coupling that could inspire new nanophotonic and quantum devices.

References

[1] B. S. Y. Kim, A. J. Sternbach, M. S. Choi, Z. Sun, F. L. Ruta, Y. Shao, A. S. McLeod, L. Xiong, Y. Dong, T. S. Chung, A. Rajendran, S. Liu, A. Nipane S. H. Chae, A. Zangiabadi, X. Xu, A. J. Millis, P. J. Schuck, C. R. Dean, J. C. Hone, D. N. Basov, *Nature Materials* **22,** 838 (2023).
[2] F. L. Ruta, B. S. Y. Kim, Z. Sun, D. J. Rizzo, A. S. McLeod, A. Rajendran, S. Liu, A. J. Millis, J. C. Hone, D. N. Basov, *Nature Communications* **13** 3719, (2022).

Ultrafast spin-exchange interactions in magnetically doped quantum dots for advanced photoconversion

V. I. Klimov
Los Alamos National Laboratory, Los Alamos, NM 87545, USA

Semiconductors have historically played a key role in a variety of energy interconversion schemes. Many useful energy transformations involve processes known as up- and down-conversion. These include, in particular, electron emission from a material due to the Auger up-conversion and carrier multiplication (CM) due to down-conversion via impact ionization. Both of these processes have significant utility in solar photochemistry, photovoltaics, radiation detection, and photocathodes. The fundamental limitation of both the Auger up- and down-conversion arises from competing energy losses due to phonon emission. In particular, for Auger-type energy transfer mediated by direct Coulomb interactions, the rate of energy gain is at least 3 times lower than the rate of energy loss due to phonon emission [1]. As a result, conventional materials do not exhibit appreciable photoemission or carrier multiplication due to the Auger up-/down-conversion. To address this issue, we exploit a new type of ultrafast (subpicosecond) spin-exchange (SE) interactions arising from the embedding of magnetic impurities into zero-dimensional colloidal quantum dots (QDs). In particular, by inserting spin-5/2 manganese ions into CdSe QDs, we achieved a 20-fold increase in the Auger energy transfer rate, making it much faster than phonon emission and allowing direct manipulation of hot nonequilibrium electrons prior to their intraband cooling [1]. We used ultrafast SE interactions to demonstrate highly efficient photoemission induced by visible light pulses. This process was realized as a two-step Auger re-excitation, where a band-edge electron was excited to the vacuum state outside the QD by two successive energy transfers

from excited Mn ions [2]. In undoped QDs, the second step of Auger re-excitation would have been hampered by the relaxation of the hot electrons via phonon emission. However, in Mn-doped structures, due to the extremely high SE energy transfer rates, the hot electron was efficiently excited to the vacuum state before losing any significant energy to phonons Recently, we used Mn-doped CdSe/PbSe core/shell QDs to realize highly efficient CM, a process in which a single absorbed photon generates multiple electron-hole pairs (excitons) [3]. In these structures, CM occurred via two SE steps: (1) SE energy transfer from a hot exciton delocalized throughout the QD to a Mn ion at the core/shell interface, followed by (2) energy- and spin-conserving relaxation of the excited Mn ion to generate two excitons (bright and dark) in the PbSe core. Due to the extremely short SE time scales, both SE steps occurred without significant interference from phonon emission, resulting in high SE-CM efficiency. These works demonstrate the significant utility of the ultrafast CM energy transfer realized with magnetically doped colloidal QDs in practical photoconversion.

References

[1] R. Singh, W. Liu, J. Lim, I. Robel, V.I. Klimov, *Nature Nanotechnology* **14**, 1035 (2019).
[2] C. Livache, H. Jin, O.V. Kozlov, W.D. Kim, I. Fedin, V.I. Klimov, *Nature Photonics.* **16**, 443 (2022).
[3] H. Jin, C. Livache, W.D. Kim, V.I. Klimov, *Nature Materials* **22**, 1013 (2023).

Undressing electron-phonon interactions in FeSe

P. S. Kirchmann[1], S. Gerber[1**], D. Zhu[1], R. G. Moore[1***], W.-S. Lee[1], Z.-X. Shen[2]

[1] *SLAC National Accelerator Laboratory, Menlo Park, CA 94025, USA.*

[2] *Stanford University, Stanford, CA 94305, USA.*

FeSe is an unconventional superconductor with a high ratio of superconducting gap to Fermi energy, and correspondingly small spatial extent of strongly bound Cooper pairs. Our previous work [1] reported strong electron-phonon coupling of the A_{1g} mode, which we explained by cooperative interactions that include spin degrees of freedom. This may help explain how strongly bound Cooper pairs can form despite strong Coulomb repulsion. Here, we present time-resolved X-ray diffraction data of the 5.3THz A_{1g} mode in bulk-like FeSe/STO films as function of temperature and excitation density (fluence). With increasing temperature, the mode softens by 0.9% and damping increases. The mode does not change abruptly at the nematic/structural transition temperature T_S=90K. This is in quality agreement with Raman spectroscopy in thermal equilibrium. In contrast, with increasing fluence, we observe distinct non-thermal signatures: At a critical excitation density, the mode hardens by 3%, the increased damping plateaus, and the amplitude slope decreases. Since the mode always remains a well-defined single harmonic, the projection to the excited state potential energy surface must be completed before the mode starts oscillating, i.e. in less than ¼ mode period of 50fs. This time scale is incompatible with trivial heating that involves the lattice and points to the action of optically excited hot electrons. Non-magnetic DFT calculations consistently predict a harder mode than is observed in experiment and compared to DMFT calculations which include spin fluctuations [2].

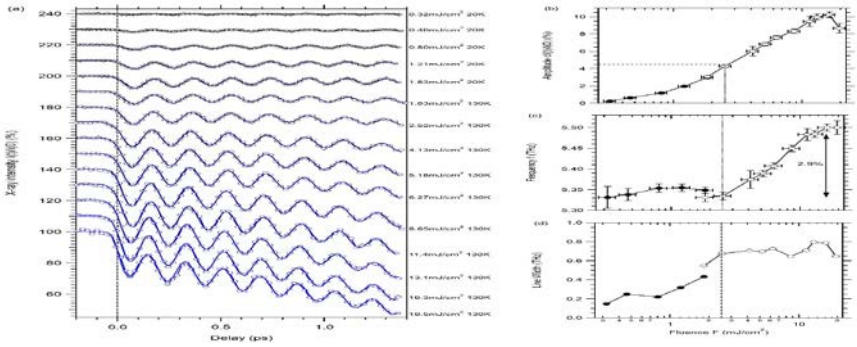

Fig. 1. (a) Time-resolved x-ray diffraction intensity *of the (004) Bragg peak as function of fluence. Amplitude* ***(b)****, frequency* ***(c)*** *and linewidth (d) of A_{1g} mode as function of fluence.*

Our present understanding is that more and hotter electrons create an excited state with reduced spin interactions, which hardens the mode, and is consistent with a reduction of the electron-phonon coupling. In turn, our result further corroborates the notion that cooperative interactions of spin, electron and lattice degrees of freedom govern the low temperature ground state in FeSe. More generally, our approach highlights that excited state methods with non-thermal tuning parameters can isolate microscopic interactions in correlated matter to provide a unique contribution to our understanding of the ground state.

References

[1] S. Gerber, S.-L. Yang, D. Zhu, H. Soifer, J. A. Sobota, S. Rebec, J. J. Lee, T. Jia, B. Moritz, C. Jia, A. Gauthier, Y. Li, D. Leuenberger, Y. Zhang, L. Chaix, W. Li, H. Jang, J.-S. Lee, M. Yi, G. L. Dakovski, S. Song, J. M. Glownia, S. Nelson, K. W. Kim, Y.-D. Chuang, Z. Hussain, R. G. Moore T. P. Devereaux, W.-S. Lee, P. S. Kirchmann, Z.-X. Shen, *Science* **357,** 71(2017).

[2] S. Mandal, R.E. Cohen, K. Haule, *Physical Review* B **89,** 220502(R) (2014).

***** Acknowledgements: Use of the LCLS, SLAC National Accelerator Laboratory, is supported by the U.S. DoE, BES under contract DE-AC02 -76SF00515. S.G., R.G.M., W.-S.L., P.S.K., and Z.-X.S. were supported by the DOE-BES Division of Materials Sciences and Engineering under contract DE-AC02-76SF00515.

** Present: Paul Scherrer Institut, 5232 Villigen, Switzerland. *** Present: Oak Ridge National Laboratory, Oak Ridge, TN 37831, USA.

Full brillouin zone, multi-band reconstruction of the Electronic band-structure from high-harmonic spectra

M. Kolesik
University of Arizona, Tucson, AZ 85721, USA

We demonstrate three-dimensional reconstruction of the electronic structure in both direct-gap (gallium ar-senide) and indirect-gap (silicon) materials, producing multiple energy bands across the entire Brillouin zone. We show that a single pair of well-chosen, properly calibrated high-harmonic spectra is sufficient to obtain a group of energy bands surrounding the electronic gap. The transition dipole moments and Berry connections then can be obtained as by-products of the procedure.All-optical characterization of materials based on the high-harmonic generation (HHG) in off-resonantly ex- cited solids was proposed in a number of modalities. In particular, the principle of the electronic band-structure reconstruction was demonstrated [1] soon after the first measurements of the above-the-gap harmonics from solid targets [2]. However, important issues remain to be understood before the HHG-based all-optical techniques can be fully deployed. For example, it is not yet clear which parts of the band-structure can be reconstructed by purely optical methods. The reconstruction problem is further complicated by the fact that the absolute complex phase is not observable for the transition-dipole moments and Berry connections. Even for gauge-invariant quantities such as Berry curvatures and shift vectors, we do not know how accurately and over what extent of the Brillouin zone they can be mapped. Perhaps the most crucial question is what kind and how many measurements one needs for the reconstruction of band energies.The all-optical reconstruction is an optimization problem in which a set of measurements, dubbed the target in the following, is to be reproduced by a calculation or a simulation which receives the parameterized band- structure as an input. The central assumption is that if one can find a set of parameters for which the simulated material response is close to the target, then the parameterized bands approximate the real ones [3]. Of course, the accuracy of the reconstruction is not only limited by the parameterization, but perhaps mainly by how accurate is the simulation used to produce the material response for each fixed set of parameters.In the previous approaches, the band-structure reconstruction was so far limited to parts of the electronic bands, while using overly simplified material models [4–6]. With a notable exception of [1], the methods relied heavily on the semi-classical model of the HHG process, where the photon energy of the emitted radiation maps onto a local band-gap in the reciprocal space [7]. In most cases, only a sub-set of processes were considered, such as the intra-band currents [8]. Moreover, it has been a common premise that the band energies and the transition dipole moments can be regarded as separate, or independent quantities. In reality, the band energies and the dipole moments are intimately related via the **k**-dependent Hamiltonian. While the bands describe how the energy eigenvalues change throughout the Brillouin zone, the transition dipole moments reflect how the Hamiltonian eigenvectors transform from one point to the other in the reciprocal space. So it is inconsistent to presume known transition dipole moments, when the band energies need reconstruction, which is precisely what some works have done. We put forward a surrogate-model approach. Instead of trying to obtain the band structure directly, one re- constructs a model Hamiltonian instead. Having the optimized model, the energy bands and all other quantities such as dipole moments and Berry connections can be calculated. Our method thus eliminates the inconsistencies in the previous demonstrations when the bands were reconstructed while the dipoles were assumed to be known. An important advantage of the approach is that it respects the material symmetry, and produces multiple bands throughout the whole Brillouin zone. This contribution describes the first proof-of-principle for this novel approach to all-optical reconstruction of the band-structure.For the demonstration of the band structure retrieval, we concentrate on cubic materials with the zinc blende and/or diamond structures. The sp^3s^* tight-binding Hamiltonian $H(\mathbf{k},\{p_i\})$ is given in [9] and [10] lists the parameter sets $\{p_i\}$ for different materials. We refer the reader to Refs. [11–16] for details concerning the design, testing, and for some applications of the sgiSBEs simulator used for the simulations of the target and trial HHG spectra. We used an optimized version of the algorithm given in [11,16] and previously tested against experimental HHG spectra [13]. The method also correctly captures the second-order nonlinearity of the material [12], showing that the absolute scale of the nonlinear response is also correct. This gives us confidence to draw conclusions based on numerical simulations. The target data, and the initial guess are both shown in Fig. 1

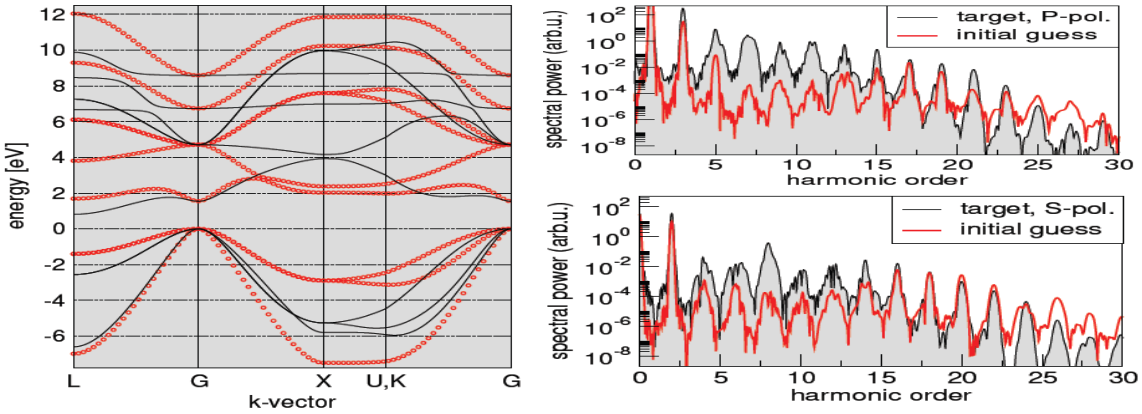

Fig.1. Left: *Target (**open circles**) and the first-guess (**thin black line**) band-structures.* ***Right****: Target and initial-guess S-polarized and P-polarized HHG spectra. The reconstruction aims to minimize the distance between the target and the optimized spectra.*

The target systems is given by the nominal parameters for GaAs and/or Si, and we generated the initial guess by random perturbations of the parameter set.The resulting initial-guess band-structure (black lines, left panel) is distinctly different from that of the target (open circles, left panel). We further assume that the P- and S-polarized HHG spectra (shown as thin black lines) weremeasured for a 110-oriented GaAs sample. The first-guess spectra (thick red lines) are also shown in the figure.

As the fitness function to govern the optimization process, we measure the distance from the target as the average of the absolute value of the difference between the target and simulated spectra in the logarithmic scale. In Fig. 1, it is the vertical average distance between the black and red lines Fig. 2 shows the optimization history together with the nearly perfectly reconstructed band-structure:

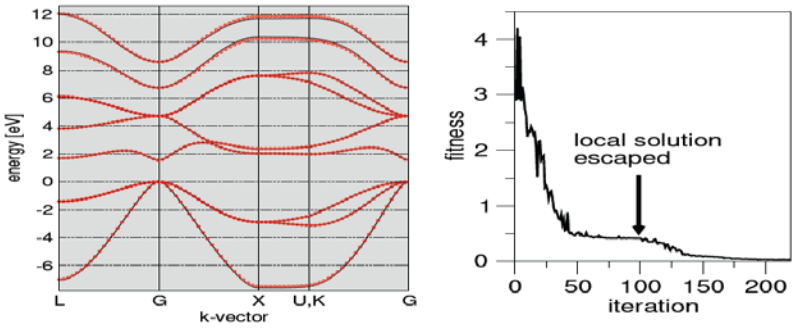

Fig. 2. Left: *Hamiltonian optimization produces a band-structure that agrees accurately with the testing target. Small deviations are only discernible in the bands that contribute little to the HHG spectra.*
Right*: The optimization demands hundreds of full-3D HHG simulations, and moves overa fitness-landscape with numerous false solutions.In the example shown, the optimizer invoked "re-heating" after detection of a stalled solution where indicated by the* ***arrow***

To the best of our knowledge, these results constitute the first simulation-based demonstration of a fully three-dimension, all-optical reconstruction of multiple electronic bands over the entire Brillouin zone utilizing a single pair of high-harmonic spectra excited by a single quasi-monochromatic mid-infrared pulse. The tests presented here utilized idealized targets that guaranteed that an optimal solution existed. In a real-life situation, the target spectra will necessarily contains errors, and could be limited in terms of their bandwidth and in their dynamic range. Accurate spectral calibration is another potential challenge. While comprehensive study of such issues is beyond what we can do in this work, we can present evidence that the reconstruction process based on the surrogate model turns out to be surprisingly robust with respect to experimental errors in the peak excitation amplitude and in the calibration of the target spectrum. This work is thus a significant step toward a practical all-optical material characterization based on the high-harmonic spectroscopy.

Reference

[1] G. Vampa, T. J. Hammond, N. Thire, B. E. Schmidt, F. Legare, C. R. McDonald, T. Brabec, D. D. Klug, P. B. Corkum, *Physical Review Letters* **115** 193603 (2015).
[3] L. Ortmann and A. S. Landsman, *Advances In Atomic, Molecular, and Optical Physics* **70** (2021).
[4] C.-M. Wang, T.-S. Ho, S.-I. Chu, *Journal of Physics* B **49**, 225401 (2016).
[5] S.- Q. Hu, D.-Q. Chen, L.-L. Du, S. Meng, *Proceedings NAS* **121**, e2316775121 (2024).
[6] J. Chen, Q. Xia, L. Fu, *Physical Review* A **104**, 063109 (2021).
[7] G. Vampa, C. R. McDonald, G. Orlando, P. B. Corkum, T. Brabec, *Physical Review* B **91,** 064302 (2015).
[8] L. Li, P. Lan, L. He, W. Cao, Q. Zhang, P. Lu, *Physical Review Letters* **124,** 157403 (2020).
[9] A. D. Carlo, *Semiconductor Science and Technology* **18**, R1 (2002).
[10] P. Vogl, H. P. Hjalmarson, J. D. Dow, *Journal of Physics and Chemistry of Solids* **44**, 365 (1983).
[11] J. Gu,M. Kolesik, *Physical Review* A **106**, 063516 (2022).
[12] M. Kolesik, *Optics Letters* **48**, 3191(2023).
[13] M. Kolesik, J. V. Moloney, *Physical Review* B **108**, 115433 (2023).
[14] M. Kolesik, *Journal of Optical Society of America* B **41**, B7 (2024).
[15] M. Kolesik, *Physical Review* A **109**, 023503 (2024).
[16] M. Kolesik, *to be submitted* (2024).

Non-reciprocal phase transitions

R. Hanai[1], S. Liu[3], C. Weis[3], M. Fruchart[2], V.Vitelli[3], P.B.Littlewood[4]
[1]*University of Kyoto, Kyoto, 606-8501 Japan*
[2] *Ecole Superieure de Physique et de Cimie Industrielles, 75055 Paris, France*
[3]*The University of Chicago, Chicago, IL 60637, USA*
[4]*University of St. Andrews, St Andrews KY16 9AJ, United Kingdom*

Spontaneous synchronization is at the core of many natural phenomena. Your heartbeat is maintained because cells contract in a synchronous wave; some bird species synchronize their motion into flocks; quantum synchronization is responsible for laser action and superconductivity. The transition to synchrony, or between states of different patterns of synchrony, is a dynamical phase transition that has much in common with conventional phase transitions of state – for example solid to liquid, or magnetism – but the striking feature of driven dynamical systems is that the components are "active". Consequently quantum systems with dissipation and decay are described by non-Hermitian Hamiltonians, and active matter can abandon Newton's third law and have non-reciprocal interactions. This substantially changes the character of many-degree-of-freedom dynamical phase transitions between steady states and the critical phenomena in their vicinity, since the critical point is an "exceptional point" where eigenvalues become degenerate and eigenvectors coalesce. We will illustrate this in several different systems – a Bose-Einstein condensate of polaritons, models of multicomponent active matter such as flocks of birds, generalized Kuramoto models, and others. We argue that there is a systematic theory and generalized phase diagram, and corresponding universality behaviors determined by the symmetry of the models. Polariton BEC's are now a well-established phenomenon in semiconductor systems including conventional III-V and II-VI semiconductors, organic semiconductors, transition metal dichalcogenides, and photon condensates. The standard model to describe this phenomenon is the Jaynes-Tavis-Cummings model of two-level systems (excitons) coupled to cavity photons. The system is driven by pumping of the excitons and equilibrated by exciton scattering and decay of the photons. A steady state can be obtained at low density where the excitons and photons coherently combine to form a polariton, and that polariton undergoes BEC. However, there is a potentially different steady state of the same model whereby the photons 'condense' as in a laser, but the excitons are mostly decohered. These solutions are physically different but in terms of an order parameter they both break the same U(1) symmetry so cannot be mathematically distinguished. In analogy to the liquid/gas transition in a thermodynamic system the route between the two phases can be either continuous or via a first order jump. The end point of this first order line is a critical point, and for a dynamical system a critical exceptional point (CEP), where two dynamical solutions merge. This can be modeled by a generalized Gross-Pitaevskii equation with two components (light and matter) and some results are shown in Fig. 1.

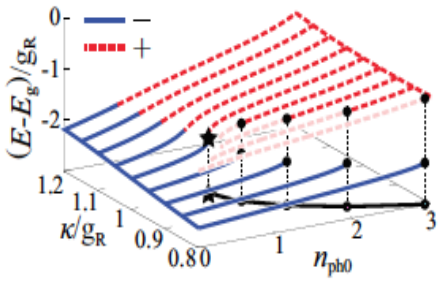

Fig. 1 Stationary solutions of the Gross-Pitaevski equations *for a driven polariton condensate, as a function of loss k and photon number n. g is the Rabi coupling. The CEP is marked by a star (from Ref 1)*

At a conventional critical point a massive mode becomes massless but those soft fluctuations are still orthogonal to the fluctuations of the phase (a Goldstone mode). At a CEP two (acoustic) modes coalesce and the fluctuations are then strongly enhanced. The existence of a scaling theory of such a dynamical phase transition is not yet settled, but it will certainly be different from thermodynamic transitions [3]. The inspiration from non-Hermitian quantum systems suggests that the CEP phenomenon should be more general. Indeed it seems that CEPs are available in many active matter many-body systems provided there are non-reciprocal interactions between different species. A toy model is that of two flocking species which have counter interactions – species A wishes to align with B, but species B wants to antialign with A. Depending on the relative strength of the interactions one would expect to find an

aligned phase (quasi-ferromagnet) or an anti-aligned phase (quasi-antiferromagnet). But in between these limits there is a state unexpected (and unallowed) in a reciprocal model – one where the two species rotate, "chasing" each other. This chiral phase is separated from the other phases by a CEP. At the mean field level (Fig. 2) there is a generalized phase diagram that applies to several different models – including contrarian Kuramoto models, Swift-Hohenberg models of pattern formation, Rosenszweig-MacArthur models of predator-prey interactions, and Wilson-Cowan models of excitatory/inhibitory neurons [2,4].

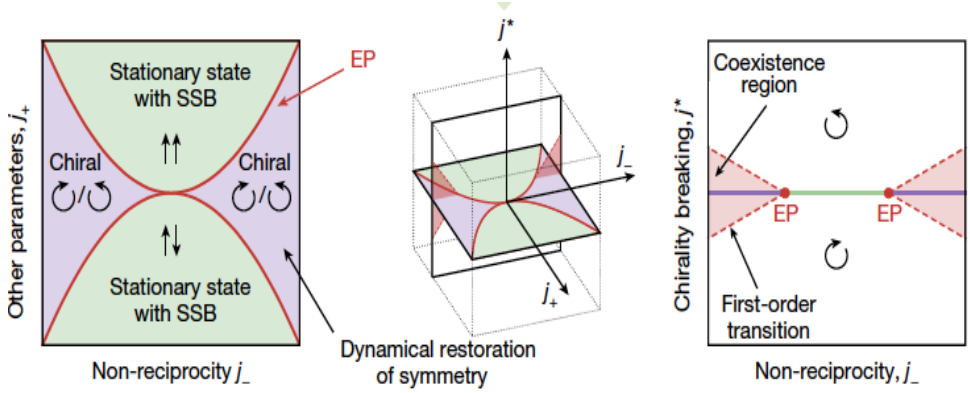

Fig. 2. Mean field phase diagram of non-reciprocal models which have a continuous symmetry*. PT symmetric models are on the left. PT broken models (which includes polariton condensates) are on the right. (From Ref 2).*

Beyond mean field theory it is not expected that long range order will be maintained in low dimensions in the presence of noise, but the scaling of fluctuations in space and time will encode the characteristics of the underlying state, which we expect to be different from the paradigmatic KPZ for example [5]. And these dynamical systems are of course also prone to pattern-forming instabilities [2,5] which are controllable but usually enhanced in the vicinity of CEPs. Polariton systems have intrinsically large coherence lengths, have interaction and decoherence parameters that are readily tuned, and can be characterized both spatially and temporally. We suggest that they may be a productive place to search for novel behavior in non-Hermitian dynamical systems.

References

[1] R. Hanai, A. Edelman, Y. Ohashi, P.B. Littlewood, *Physical Review Letters* **122**, 185301 (2019).
[2] M. Fruchart, R. Hanai, P.B. Littlewood, V. Vitelli, *Nature* **592**, 363 (2021).
[3] R. Hanai, P.B. Littlewood, *Physical Review Research* **2**, 033018 (2020).
[4] C. Weis, M. Fruchart, R. Hanai, K. Kawagoe, P.B. Littlewood, V. Vitelliet, *arXiv:2207.11667* (2022).
[5] S. Liu, R Hanai, X. Huang, P.B Littlewood, *to be submitted*, (2024).

Probing inhomogeneous superconductivity with Terahertz photon echoes

A.Liu[2], D. Pavicevic[1], M. H. Michael[1], A. G. Salvador[3], P. E. Dolgirev[4], M. Fechner[1], P. M. Lozano[5], A. S. Disa[1]
Q. Li[2], G. D. Gu[2], E. Demler[3], A. Cavalleri[1]
[1]*Max Planck Institute for the Structure and Dynamics of Matter, 22761 Hamburg, Germany*
[2]*Brookhaven National Laboratory, Upton, NY 11973, USA*
[3]*ETH Zürich, 8092 Zürich, Switzerland*
[4]*Harvard University, Cambridge, MA 02138, USA*
[5]*SUNY at Stony Brook, Stony Brook, NY 11794, USA*

Disorder is a topic of primary importance for understanding the physics of quantum materials. A well-known example may be found in the family of cuprates, in which hole-doping an insulating parent compound gives rise to the spectacular phenomenon of high-temperature superconductivity. However, the doping concentration which optimizes superconductivity is non-stoichiometric, raising the question of how inevitable doping disorder translates to disorder of the superconducting phase. Conventionally, inhomogeneous superconductivity is probed using scanning tunneling microscopy, which resolves the superconducting gap in space. However, such techniques, in particular Josephson tunneling techniques that isolate the superconducting response, are limited to low temperatures which precludes measurement

of the superconducting phase transition and possible pseudogap physics. Optical-frequency photon echo techniques are also not applicable, due to the large mismatch between optical photon energies and the low energy scales of superconducting order. To overcome these limitations, we translate the technique of multidimensional spectroscopy [1] into the terahertz frequency range to probe superconducting order at its intrinsic energy scales. We apply this technique to the Josephson tunneling resonance in optimally-doped $La_{2-x}Sr_xCuO_4$, which is found at 2 THz.

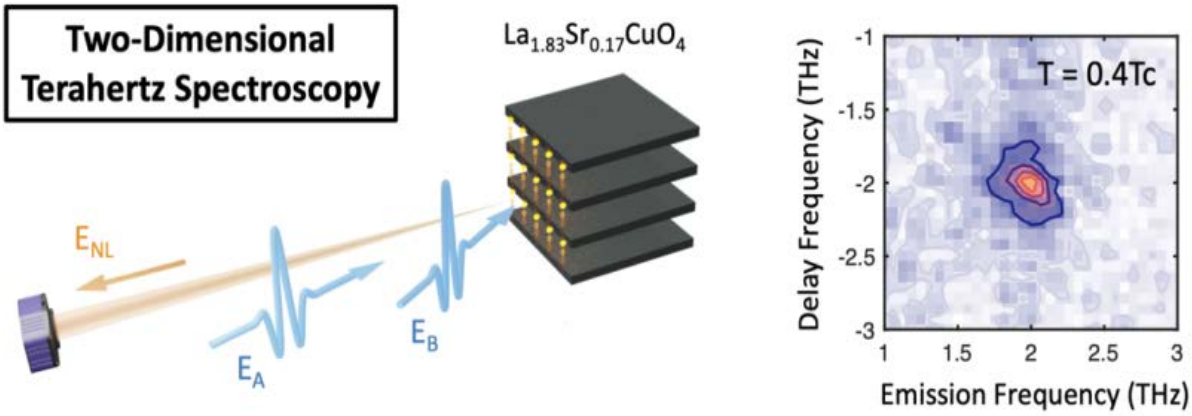

Fig.1. Probing inhomogeneous superconductivity withterahertz photon echoes

The photon echo spectra exhibit clear signatures of disorder, which is observed to remain constant as temperature increases towards the superconducting phase transition [2].

References
[1] S. T. Cundiff, S. Mukamel, *Physics Today* **66**, 44(2013).
[2] A. Liu, D. Pavicevic, M. H. Michael, A. G. Salvador, P. E. Dolgirev, M. Fechner, A. S. Disa, P. M. Lozano, Q. Li, G. D. Gu, E. Demler, A. Cavalleri arXiv preprint arXiv:2308.14849, (2023).

Direct observation of Bose-Einstein condensates of excitons in a bulk Semiconductor at sub-Kelvin temperatures

Y.Morita[1], K. Yoshioka[1], M.Kuwata-Gonokami[2]
[1] The University of Tokyo, Tokyo 113-8654, Japan
[2]RIKEN, Saitama, 351-0198, Japan

Excitons are composite quasiparticles formed in semiconductors when valence electrons are excited to form bound electron-hole pairs with finite lietimes. An unambiguous observation of the Bose-Einstein condensation (BEC) of excitons in a bulk semiconductor and elucidation of its inherent nature have been longstanding problems in condensed matter physics. The 1s paraexcitons with a long lifetime of over several hundred nanoseconds in cuprous oxide have been one of the most promising candidates for exciton BEC. This long lifetime is advantageous for preparing cold paraexcitons via thermal contact with the lattice of cuprous oxide. Active research on paraexciton BEC at liquid helium temperatures around 2 K began since the 1990s [1]. However, it has turned out that the two-body inelastic collisions between paraexcitons is so large at a critical density of 10^{17} cm^{-3} that paraexcitons hardly reach a thermal equilibrium state [2]. In response, the target temperature for paraexciton BEC was set for sub-1 K with reduced BEC transition densities below 10^{17} cm^{-3}. The application of a ^{3}He refrigerator enabled cooling of paraexcitons in a strain-induced trap potential at an exciton temperature of 800 mK. The accumulation of trapped paraexcitons exceeding the BEC critical number led to the observation of a phenomenon called “relaxation explosion,” which suggests the BEC transition [3]. However, two-body inelastic collisions hinder the formation of a stable condensate at a BEC transition density of 10^{16} cm^{-3}. To observe a stable condensate and elucidate its properties, it is necessary to create a dilute condensate at even lower temperatures. We have utilized a cryogen-free dilution refrigerator to cool the lattice of

cuprous oxide at temperatures of sub-100 mK. We found that interactions between trapped paraexcitons and transverse acoustic phonons under the strain field, which functioned as the trap potential, play a crucial role in reducing the exciton temperature well below 1 K. We succeeded in the formation of trapped paraexcitons at a temperature of sub-100 mK [4], which is the lowest temperature of excitons. For the quantitative detection of exciton BEC, we performed mid-infrared induced absorption imaging associated with the dipole-allowed 1s–2p transition of paraexcitons. Absorption measurements of paraexcitons [5, 6] allow us to quantitatively determine the density of paraexcitons, which is an essential parameter for the evaluation of quantum statistical mechanics. To perform absorption imaging, we attached windows to the refrigerator that allowed transmission of a probe light. However, since the wavelength of the probe light is in the mid-infrared region, these windows also transmit thermal flow to the coldest part in the refrigerator, making it difficult to maintain at dilution temperatures. We carefully designed the windows by minimizing the numerical aperture and using a narrow bandpass filter as the window material to reduce incoming thermal radiation. This specialized design for the windows and a high cooling power of the refrigerator allowed us to conduct absorption imaging at a base temperature of 64 mK.

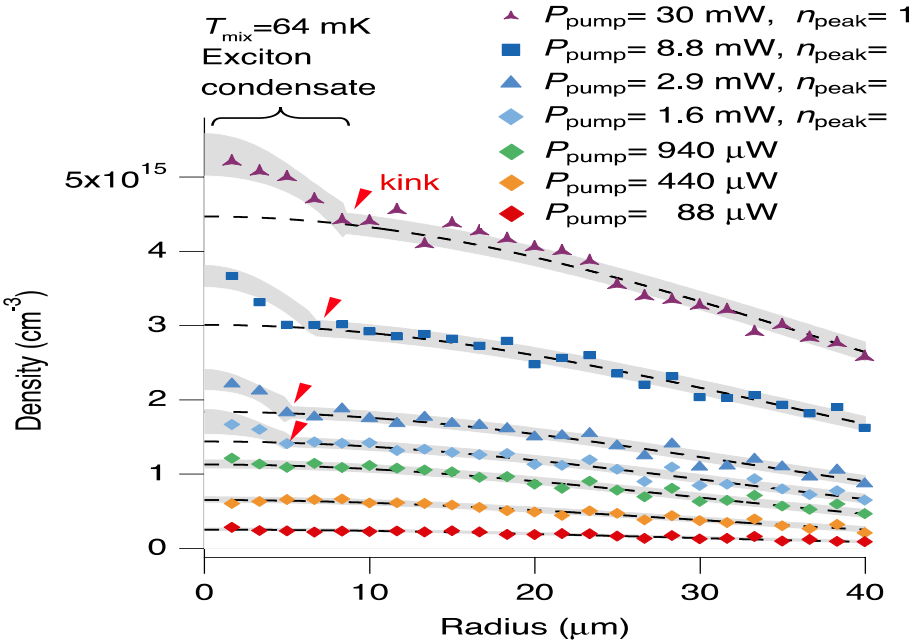

Fig.1 Radial profiles of the paraexciton density measured by induced absorption imaging at various excitation powers at a base temperature of 64 mK. *The* ***black*** *dashed curves show the Gaussian distribution fit to the tail of the radial profiles. The* ***grey*** *shaded curves show the bimodal distribution fit to the radial profile of the density. The localized dense signal around the bottom of the trap potential appears at excitation powers above 1.6 mW.*

The achievement of absorption imaging at dilution temperatures enabled us to extract the spatial density distribution of trapped paraexcitons and to observe the paraexciton condensate [7]. Fig. 1 shows the radial profile of the density distribution at various excitation powers. The radial profile at excitation powers above 1.6 mW distinctly exhibits a non-Gaussian distribution and an appearance of the localized dense signal around the bottom of the trap potential, which corresponds to the paraexciton condensate. The expansion of the paraexciton condensate as a function of the paraexciton density suggests that the exciton-exciton interaction is repulsive. Application of the Gross-Pitaevskii equation allowed us to estimate the scattering length of paraexcitons to be 4 ± 2 nm. While these phenomena are interpreted by conventional theory for BEC, the maximum condensate fraction that we observed is 0.016, which is two orders of magnitude smaller than that expected for an ideal Bose gas. This difference may be a characteristic of the composite boson in a non-equilibrium open system with a balance between generation and decay, such as the finite lifetime of paraexcitons, two-body inelastic collisions between paraexcitons, and suppression of the thermal relaxation processes.

References

[1] D. W. Snoke, J. P. Wolfe, and A. Mysyrowicz, *Physical Review Letters* **64**, 2543 (1990).
[2] K. Yoshioka, T. Ideguchi, A. Mysyrowicz, M. Kuwata-Gonokami, *Physical Review B* **82**, 041201(R) (2010).
[3] K. Yoshioka, E. Chae, and M. Kuwata-Gonokami, *Nature Communications* **2**, 328 (2011).
[4] K. Yoshioka, Y. Morita, K. Fukuoka, and M. Kuwata-Gonokami, *Physical Review* B **88**, 041201 (R) (2013).
[5] M. Kuwata-Gonokami, M. Kubouchi, R. Shimano, A. Mysyrowicz, *Journal of Physical Society of. Japan* **73,** 1065 (2004).
[6] K. Yoshioka, M. Kuwata-Gonokami, *Physical Review* B **91**, 195207 (2015).
[7] Y. Morita, K. Yoshioka, and M. Kuwata-Gonokami, *Nature Communications* **13**, 5388 (2022).

Cavity electrodynamics of van der Waals heterostructures

G. Kipp[1], H.M. Bretscher[1], B. Schulte[1], D. Herrmann[1], K. Kusyak[1], M.W. Day[1], S. Kesavan[1], T. Matsuyama[1]
X. Li[1], S.M. Langner[1], J. Hagelstein[1], F. Sturm[1], A.M. Potts[1], C.J. Eckhardt[1], Y. Huang[2], K. Watanabe[3]
T.Taniguchi[3], A. Rubio[1], D.M. Kennes[4], M.A. Sentef[5], E. Baudin[6], G. Meier[1], M.H Michael[1], J.W. McIver[1]
[1] *Max Planck Institute for the Structure and Dynamics of Matter, 22761 Hamburg, Germany*
[2] *Columbia University, New York, NY 1002, USA*
[3] *National Institute for Materials Science, Tsukuba 305-004, Japan*
[4] *Aachen University, 52062 Aachen, Germany*
[5] *University of Bremen, 28334 Bremen, Germany*
[6] *École Normale Supérieure, 75005 Paris, France*

Van der Waals (vdW) heterostructures host many-body quantum phenomena that can be tuned *in situ* using electrostatic gates [1-3]. These gates are often microstructured graphite flakes that naturally form plasmonic cavities, confining light in discrete standing waves of current density due to their finite size. Their resonances typically lie in the GHz - THz range, corresponding to the same μeV - meV energy scale characteristic of many quantum effects in the materials they electrically control. This raises the possibility that built-in cavity modes could be relevant for shaping the low-energy physics of vdW heterostructures. However, capturing this light-matter interaction remains elusive as devices are significantly smaller than the diffraction limit at these wavelengths, hindering far-field spectroscopic tools. Here, we report on the sub-wavelength cavity electrodynamics of graphene embedded in a vdW heterostructure plasmonic microcavity [4]. Using on-chip THz spectroscopy, we observed spectral weight transfer and an avoided crossing between the graphite cavity and graphene plasmon modes as the graphene carrier density was tuned, revealing their ultrastrong coupling Fig. 1.

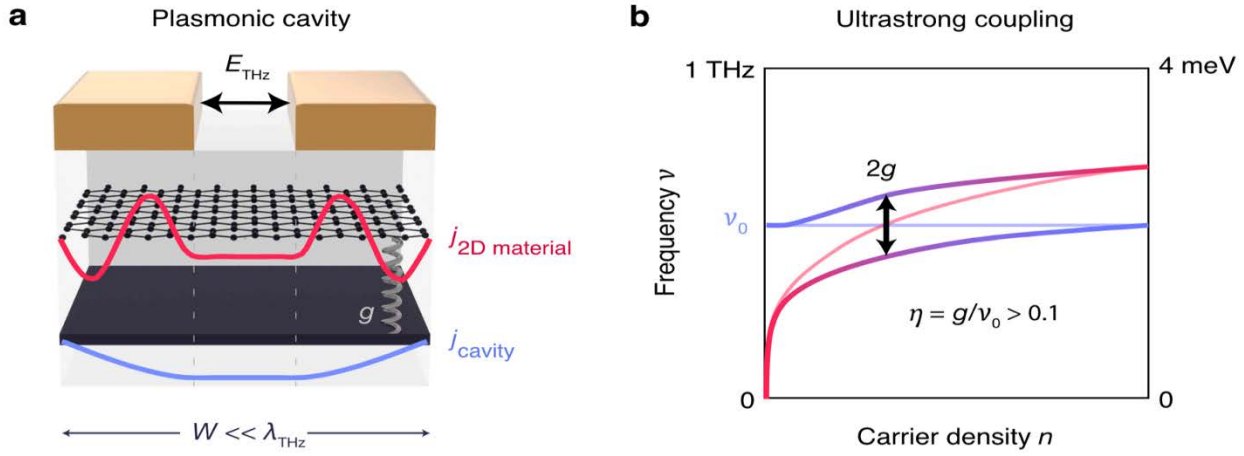

Fig. 1: Plasmonic microcavity setup for ultrastrong coupling of collective modes in 2D materials. ***(a)*** *Schematic of a 2D material embedded in a sub-wavelength ($W \ll \lambda_{THz}$) plasmonic cavity formed by a few-nm graphite flake and surrounding dielectric environment. A collective mode of a 2D material (red), such as a graphene plasmon studied in this work, can hybridize with the plasmonic bare cavity mode (blue).* ***(b)*** *The frequency of the screened plasmonic mode in the 2D material (light magenta line) is tuned with carrier density into resonance with the screened bare cavity mode, v_0 (light blue line). The cavity and plasmon modes hybridize due to coupling mediated by unscreened currents between the metal traces and an avoided crossing appears, with an energy splitting of twice the coupling strength, g. When η, the ratio of g/v_0, exceeds the value of 0.1, the system is in the ultrastrong interaction regime.*

Our findings show that intrinsic cavity modes of metallic gates can sense and manipulate the low-energy electrodynamics of vdW heterostructures. This opens a pathway for deeper understanding of emergent phases in these materials and new functionality through cavity control [5].

References

[1] E. Y. Andrei, A.H. MacDonald, *Nature Materials* **19**, 1265 (2020).
[2] L. Balents, C. R. Dean, D. K. Efetov, A.F. Young, *Nature Physics* 16, 725 (2020).
[3] K. F. Mak, J. Shan, *Nature Nanotechnology* **17**, 686 (2022).
[4] G. Kipp, H.M. Bretscher, B. Schulte, D. Herrmann, K. Kusyak, M. W Day, S. Kesavan, T . Matsuyama, X. Li, S. M. Lagner, J Hagelstein F. Strum, A. M. Potts, C. J. Erckhardt, Y. Huang, K. Watanabe, T. Taniguchi, A. Rubio, D. M. Kennes, M. A. Sentef, E. Baudin, G. Meier M. H. Michael, J. W. McIver, *arXiv:2403.19745* (2024).
[5] F. Schlawin, D. Kennes, M. A. Sentef, *Applied Physics Reviews* **9**, (2022)

Ultrafast time-reversal symmetry breaking without magnetic fields in 2D heterostructures

B. Arnoldi,[1] S. Zachritz,[2] S. Hedwig,[1] M. Aeschlimann,[1] B. Stadtmüller,[3] O.L.A. Monti[2]
[1]*Rheinland-Pfälzische Technische Universität Kaiserslautern-Landau, 67653 Kaiserslautern, Germany*
[2] *The University of Arizona, Tucson, AZ 85721. USA*
[3] *Universität Augsburg, 86159 Augsburg, Germany*

The ability to store and manipulate information encoded onto the spin angular momentum is of central interest in spintronics, quantum information science and novel spin-based low-energy electronics modalities [1]. Ferromagnetic materials have been at the center of focus for this purpose, but exhibit severe limitations. Alternatively, one may rely on materials with broken inversion symmetry and strong spin-orbit coupling. Such Rashba systems permit however only the manipulation of spin texture and not of spin polarization, limiting the modalities available for spintronic device implementations. In this regard, the ability to generate spin polarization and spin current on femtosecond time-scales has been even more challenging: Current approaches relying on superdiffusive spin-transport in ferromagnetic structures are limiting due to the need for external magnetic fields. Here we show that it is possible to create spin polarization on ultrafast timescales by transient symmetry breaking in an otherwise inversion symmetric material. We combine time-, spin- and angle-resolved photoemission (ARPES) to drive interfacial charge-transfer in the 2D heterostructure of C_{60} on the diamagnetic and inversion symmetric [2H] polymorph of WSe_2. Optical excitation of C_{60} drives electrons to WSe_2 on a time-scale of a few hundred fs, and the charge-separation is accompanied by the build-up of a layer-dependent electric field across the heterointerface. This electric field induces a layer-dependent Stark shift.

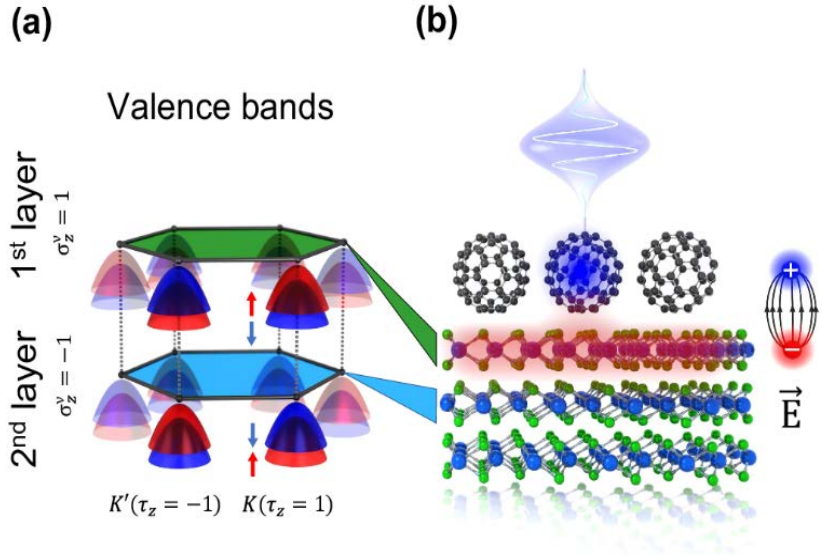

Fig. 1 Ultrafast time-reversal symmetry breaking without magnetic fields in 2D heterostructures.. a) *First Brillouin zone of WSe2 showing the two different layers of the unit cell (green and red) and the large spin-orbit splitting at the K and -K points (blue and green).* ***b)*** *Heterostructure of one monolayer of C_{60} on [2H] WSe_2, and the symmetry-breaking electric field induced by interfacial charge transfer.*

Since the unit cell consists of two layers of WSe_2, this breaks the inversion symmetry of [2H] WSe_2 in the near-surface region. Consequently, the layer degeneracy is lifted, and the ensuing transient layer polarization couples to the valley degree of freedom. Because of the presence of strong spin-valley-layer locking in materials such as WSe_2, the layer- and thus valley-polarization creates a transient layer-dependent spin polarization. We track the evolution of all relevant excited and charge-separated states as well as the band edges at high symmetry points of the Brillouin zone by time- and spin-resolved ARPES, demonstrating unambiguously that time-reversal symmetry can be broken in heterostructures of diamagnetic materials, without the need for an external magnetic field or ferromagnetic structures [2]. Our work constitutes a new path for ultrafast spin manipulation without the need for external magnetic fields and in diamagnetic heterostructures, and may pave the way to ultrafast generation of spin currents.

References

[1] A. Hirohata, K. Yamada, Y. Nakatani, I. - L. Prejbeanu, B. DIeny, B. Pirro, B. Hillebrands, *Journal of Magnetism and Magnetic Materials* **509** 166711 (2020)
[2] B. Arnoldi, S.L. Zachritz, S. Hedwig, M. Aeschlimann, O.L. Monti, B. Stadtmüller, *Nature Communications* **15**, 3573 (2024).
[3] X. Zhang, Q. Liu, J.W. Luo, A.J. Freeman, A. Zunger, *Nature Physics* **10**, 387 (2014).

* We acknowledge support by the Deutsche Forschungsgemeinschaft (DFG, German Research Foundation)—TRR 173 —268565370 Spin+X: spin in its collective environment (Project A02) and by the Air Force Office of Scientific Research under award FA9550-21-1-0219. B. Stadtmüller acknowledges financial support from the Dynamics and Topology Center funded by the State of Rhineland Palatinate.

Revealing unconventional quantum echoes and pseudo-spin soliton states in Superconductors via terahertz 2D coherent spectroscopy

M. Mootz[2], C. Huang[1], L. Luo[2], I. E. Perakis[3], J. Wang[1]
[1]*Iowa State University, Ames, IA 50011, USA*
[2]*Ames National Laboratory, Ames, IA 50011, USA*
[3] *University of Alabama at Birmingham, Birmingham, AL 35294, USA*

Terahertz (THz) two-dimensional coherent spectroscopy (2DCS) has emerged as a powerful technique for probing the complex dynamics of quantum materials. This method enables the direct observation of coherent quantum phenomena by tracking the interactions and temporal evolution of quantum states at THz frequencies. In superconductors THz 2DCS provides unique insights into the collective excitations and non-equilibrium dynamics of the order parameter, which are crucial for understanding the fundamental physics governing superconductivity and exploring novel quantum states that could be harnessed for future quantum technologies [1-5]. In this talk, we will discuss the discovery of two unconventional phenomena in superconductors revealed through THz 2DCS. The first example is the observation of an unconventional quantum echo in a niobium superconductor, emerging at the Higgs mode frequency in THz 2DCS [6]. This echo results from the interference between multiple Higgs and quasi-particle coherences. Specifically, a pair of nearly single-cycle THz pulses modulates the superconducting gap, generating a Higgs dynamical grating, which scatters echo signals. These echoes are markedly different from conventional echoes observed in atomic and semiconductor systems. The key features of this unconventional echo include: (1) previously inaccessible rephasing spectral peaks at the Higgs mode frequency (Fig. 1(a)), (2) pronounced negative-time signals arising from the anharmonic coupling between Higgs mode and quasiparticle excitations (Figs. 1(b) and 1(c)), and (3) an asymmetric delay in echo formation that extends beyond the limits set by inhomogeneously broadened oscillators (Fig. 1(d)). These findings shed light on the unique nonlinear dynamics of superconductors and highlight the potential of Higgs echo spectroscopy in probing quantum coherence in these systems.

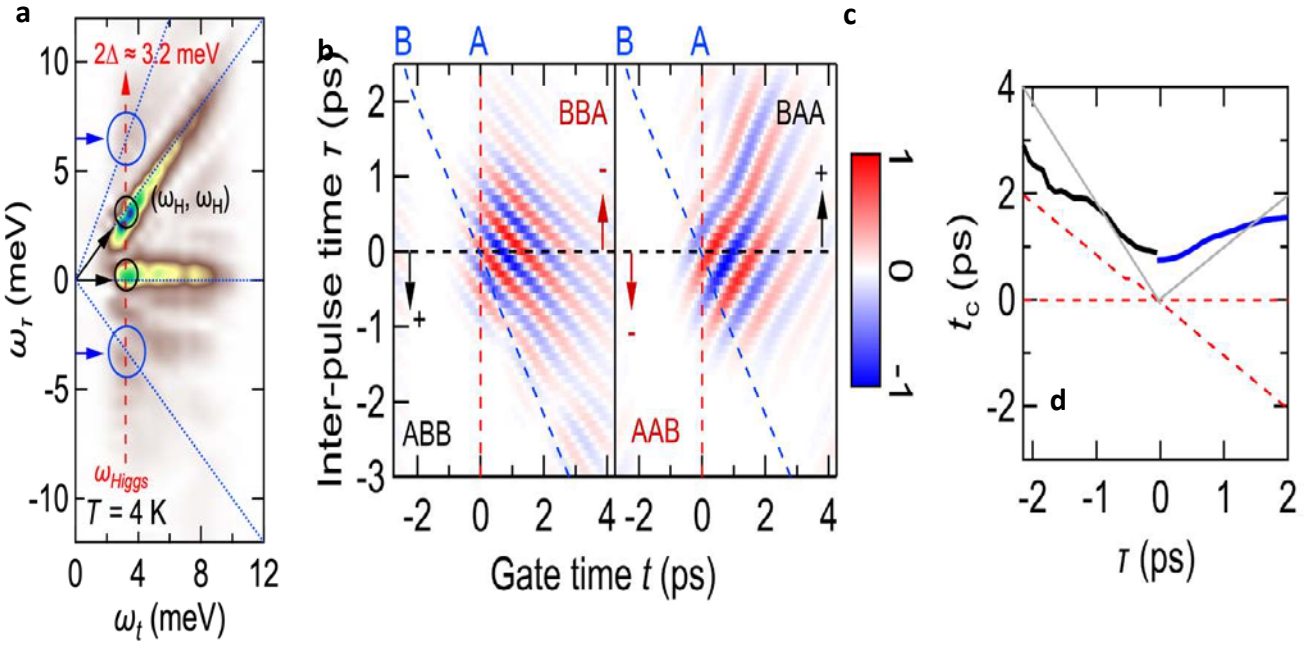

Fig. 1 Higgs echo spectroscopy of a Niobium superconductor. *(**a**) Two-dimensional Fourier transform of the measured nonlinear differential transmission $E_{NL}(t, \tau)$, created by THz pump electric fields of $E_{A,B} \sim 50$ kV cm−1 at 4 K, showing Higgs echo signals (blue circles) in addition to Higgs signals (black circles). (**b**), (**c**) Higgs-echo signals ABB and BAA in time domain resulting from the inverse Fourier transformation of the signals indicated by blue circles in (**a**). The ABB (BAA) pulse sequences show a negative time signal (red arrows) when pulse B (A) arrives before pulse A (B). (**d**) Temporal positions of the ABB and BAA echoes, t_c (blue and black lines), are time-delayed compared to both driving pulses (dashed red lines). Remarkably, the echo formation time exhibits a pronounced deviation from symmetric temporal positions relative to the pulse-pair excitations (depicted by gray lines), deviating notably from conventional photon echoes.*

Building on these observations, we further explored the impact of intense THz pulses on superconducting condensates, leading to the discovery of a pseudo-spin soliton state. In this second example, we demonstrate that intense, multi-cycle THz laser pulses can induce a transition to this pseudo-spin soliton state in an iron-based superconductor. This soliton state arises from the synchronization of individual Cooper-pair states, leading to undamped oscillations of the order parameter. The transition to the soliton state is characterized by the emergence of Floquet-like spectral sidebands (Fig. 2(c)-(e)), which display highly nonlinear dependencies on temperature and the THz field strength.

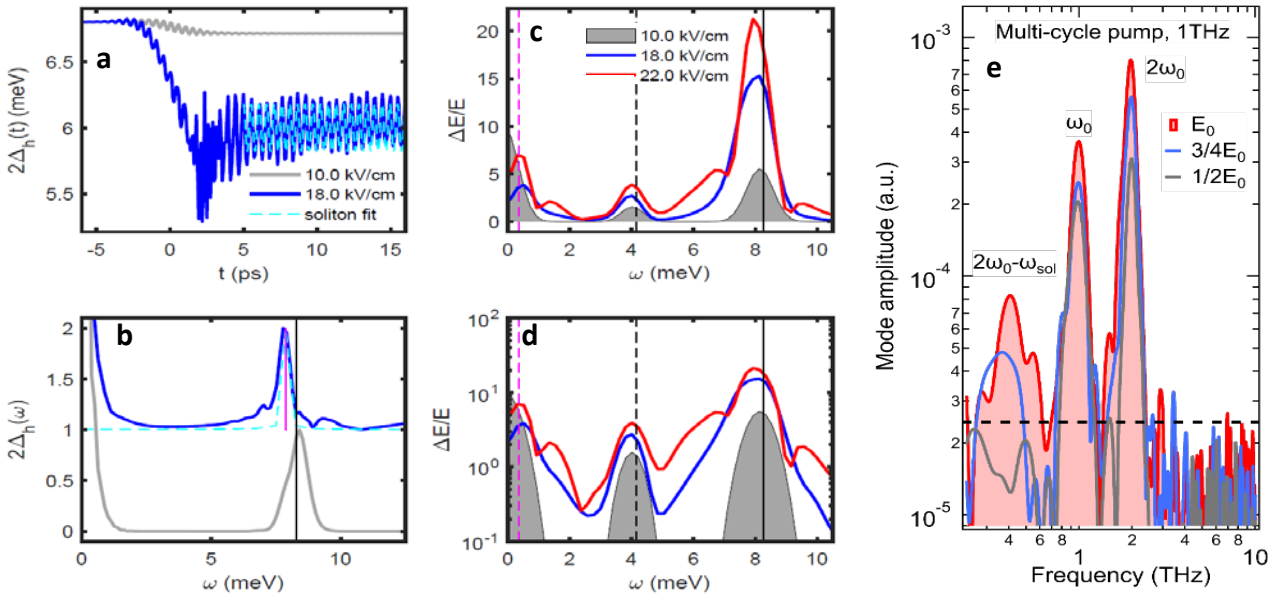

Fig. 2 Discovery of pseudo-spin solitons in a FeAs superconductor. *(**a**), (**b**) Simulated order parameter dynamics in a multiband superconductor driven by a multi-cycle ω_0 = 1 THz pump pulse for a weak (gray line) and a strong THz electric field (blue line) (**a**) and the corresponding spectra (**b**). Traces are offset for clarity. The order parameter dynamics exhibits second-harmonic oscillations during the excitation process for weak THz field excitation (gray line), resulting in a second-harmonic generation peak at $\omega = 2\omega_0$ in the spectrum ((**b**), vertical black line). Above a critical driving field (blue line), the order parameter dynamics is characterized by undamped oscillation which persist after the pulse. The corresponding order parameter spectrum shows a strong signal at ω_{sol} = 7.5 meV ((**c**), vertical magenta line), which we identify as a pseudo-spin soliton (dashed cyan lines in (**a**) and (**b**)). (**c**), (**d**)Simulated pump-probe spectra for three different pump electric field strengths in linear and semi-logarithmic scales. A soliton sideband peak develops at $\omega = 2\omega_0 - \omega_{sol}$ (dashed magenta line) above critical driving field. Dashed (solid) black lines indicate fundamental (second harmonic) generation peak. (**e**) Measured pump-probe spectra show the emergence of soliton sideband with increasing pump field strength.*

We propose that these sidebands result from difference-frequency nonlinear processes between the THz excitation and solitons in the non-equilibrium superconducting state. This interpretation is supported by quantum kinetic simulations of the Anderson pseudo-spin model driven by multi-cycle THz pulses (Fig. 2(a)-2(d)), which reveal the synchronization of a continuum of pseudo-spin oscillators, analogous to Dicke superradiance. The emergence of this synchronization during the latter part of the multi-cycle THz pulse underscores the complex interplay between the order parameter and the pseudo-spin dynamics in superconductors. The observation of pseudo-spin soliton states not only underscores the potential of THz 2DCS to unlock new quantum phenomena but also holds promise for advancing quantum technologies, such as above-GHz speed quantum gates, quantum memory, and sensing applications that exploit enhanced coherence.

References

[1] L. Luo, M. Mootz, J. H. Kang, C. Huang, K. Eom, J. W. Lee, C. Vaswani, Y. G. Collantes, E. E. Hellstrom, I. E. Perakis, C. B. Eom, J. Wang *Nature Physics* **19**, 201(2023).

[2] M. Mootz, L. Luo, J. Wang, l. E. Perakis, *Communications Physics* **5**, 47(2022).

[3] M. Mootz, L. Luo, C. Huang, J. Wang, l. E. Perakis, *Physical. Review* B **109**, 014515 (2024).

[4] B. Cheng, D.Cheng, K.Lee, M.Mootz, C.Huang, L.Luo, Z.Chen, Y.Lee, B.Y.Wang, I. E.Perakis, Z-X.Shen, H.Y.Hwang, J.Wang, arXiv2310.02589v1(2023)

[5] B. Cheng, D. Cheng, K. Lee, M. Mootz, C. Huang, L. Luo, Z. Chen, Y. Lee, B. Y. Wang, I. E. Perakis, Z.-X. Shen, H. Y. Hwang, J. Wang, *Nature Materials* **23**, 775 (2024).

[6] C. Huang, M. Mootz, L. Luo, D. Cheng, J. M. Park, R. H. J. Kim, Y. Qiang, V. L. Quito, Y. Yao, P. P.Orth, I. E. Perakis, J.Wang ,arXiv:2312.10912v1(2023)

* The research was supported by the U.S. Department of Energy, Office of Basic Energy Science, Division of Materials Sciences and Engineering (Ames National Laboratory is operated for the U.S. Department of Energy by Iowa State University under Contract No. DE-AC02-07CH11358).

Nonlinear light-matter interactions: fundamentals and applications

Z. Zhang, K. A. Nelson
Massachusetts Institute of Technology, Cambridge, MA, 02139 USA

Nonlinear light-matter interactions continue to entice us with new prospects for fundamental understanding and spectroscopic applications. Strong tailored light pulses at terahertz (THz) and mid-infrared frequencies offer particularly fertile ground for new discoveries involving collective excitation mechanisms and the study of quasiparticles and their couplings. Here, we present two examples that illustrate these possibilities. In the first example, we find that strong THz fields can achieve nonlinear control of magnon modes based on their nonlinear couplings, which manifest as magnon upconversion [1], magnon-magnon mixing that generates coherent photon emission at magnon sum and difference frequencies [2], and magnon parametric amplification. Our observations have been conducted using a *2D THz polarimetry* technique (see Fig. 1a), which is made possible by single-shot detection of coherent THz signals [3,4]

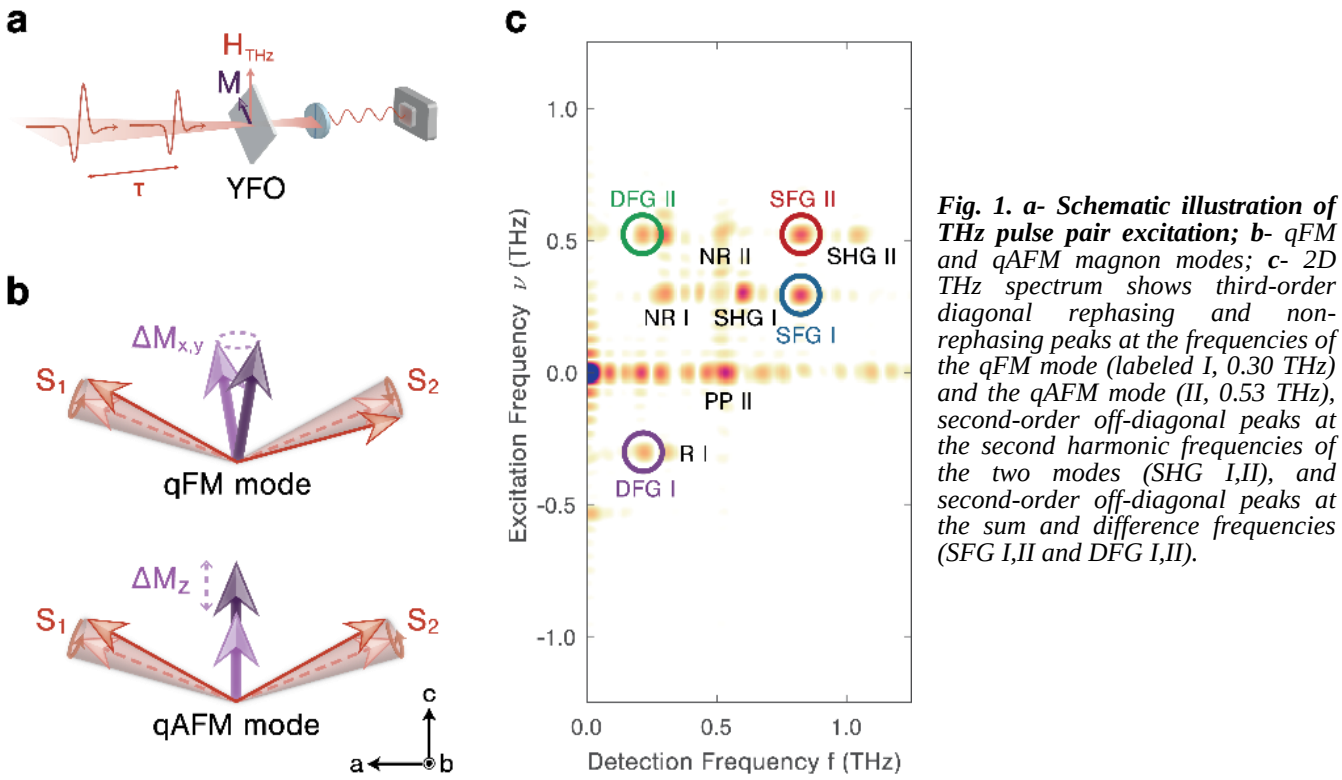

Fig. 1. a- Schematic illustration of THz pulse pair excitation; b- *qFM and qAFM magnon modes;* ***c-*** *2D THz spectrum shows third-order diagonal rephasing and non-rephasing peaks at the frequencies of the qFM mode (labeled I, 0.30 THz) and the qAFM mode (II, 0.53 THz), second-order off-diagonal peaks at the second harmonic frequencies of the two modes (SHG I,II), and second-order off-diagonal peaks at the sum and difference frequencies (SFG I,II and DFG I,II).*

This method allows us to rapidly collect over a hundred 2D THz spectra with various crystalline orientations relative to the incident THz field polarization, enabling us to reveal the underlying symmetries of unique nonlinear excitation pathways. We focus on the prototypical antiferromagnetic insulators $YFeO_3$ and $ErFeO_3$, in which the two adjacent spins in the unit cell are antiferromagnetically ordered but slightly canted, giving rise to a small net magnetization. This unique magnetic structure allows for two distinct magnon modes, known as the quasi-ferromagnetic (qFM, involving precession of the magnetization about its initial direction) and quasi-antiferromagnetic (qAFM, involving modulation of the magnetization amplitude) modes, as shown in Fig. 1b. The modes are driven by orthogonal THz magnetic field polarizations. We drive a crystalline sample with a pair of variably time-delayed THz pulses, and we measure the full time-dependent THz signal field that emerges from the sample on each laser shot. 2D Fourier transformation of the nonlinear signal with respect to the inter-pulse delay time and the signal field measurement time yields a 2D spectrum, which reveals a surprising set of four emergent peaks that appear only when both magnon modes are driven out of equilibrium by THz fields that are polarized between crystallographic axes (see Fig. 1a) [2]. Two of these signals (SFG I and SFG II) are detected at the sum frequency of the two magnon modes, while the other signals (DFG I and DFG II) are detected at

the difference frequency. The presence of these peaks indicates that second-order nonlinear sum and difference frequency generation occur as a result of interactions between distinct magnons. The two excitation frequencies (I and II) reveal the time-ordering of the two THz field interactions that first generate one magnon coherence and then generate the sum or difference-frequency signal. In other measurements, we find that nonlinear driving of the qFM mode only (with THz fields polarized perpendicular to the initial magnetization direction) results in a coherent response of the qAFM mode, revealed by coherent signal polarized along the initial magnetization direction [1]. This occurs because precession of the magnetization decreases its component along its initial direction, which corresponds to excursion of the qAFM mode. This is a unidirectional nonlinear coupling mechanism that should be ubiquitous in this material class. The second example explores the nonlinear excitation of carriers by sub-bandgap laser pulses to induce photoluminescence (PL) in the unconventional semiconductor $CrPbBr_3$ [5]. In our experiments, we generate an infrared laser pulse with photon energy below the bandgap and focus it on the sample at room temperature (Fig. 2a). We then resolve the resulting PL spectrally and measure it as a function of the driving electric field amplitude. Figures 2b and 2c display the field-dependent PL spectra for two selected pump photon energies (0.62 and 0.25 eV), both significantly below the 2.34-eV bandgap. The data clearly show that substantial PL signals can be detected for both photon energies when the pump electric fields are sufficiently strong. By varying the frequency and amplitude of the driving AC fields, we address the fundamental question of when the light acts quantum mechanically, as quantized units of energy that undergo multiphoton absorption, and when it acts as a classical field that pulls on charged electrons and may exceed a threshold for ionization.

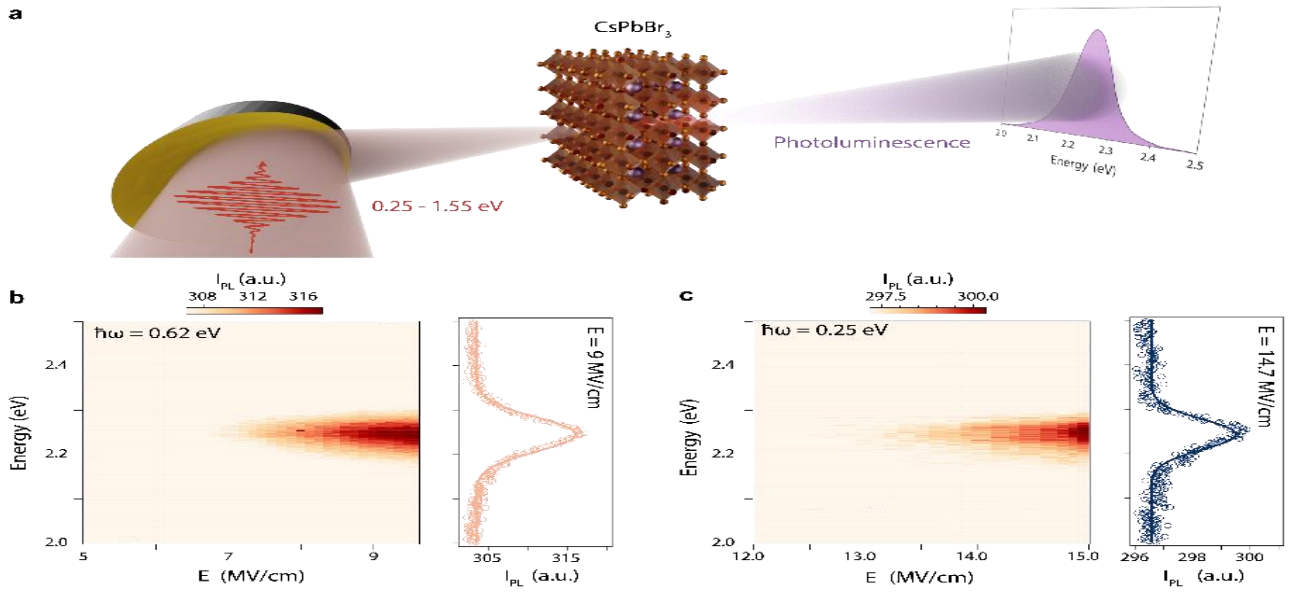

***Fig. 2. a- Schematic illustration of the experimental setup for photoluminescence (PL) measurement**; **b**- E-field-dependent PL spectra pumped at 0.62 eV and a characteristic spectrum at E = 9 MV/cm; **c**- E-dependent PL spectra pumped at 0.25 eV and a characteristic spectrum at E = 14.7 MV/cm.*

Our results align with Keldysh's 1964 treatment of the transition from multiphoton absorption to field-induced electron tunneling under intense AC driving forces [6]. We are able to fully span the transition region and the regimes far from it.

References

[1] Z. Zhang, F. Y. Gao, Y.-C. Chien, Z.-J. Liu, J. B. Curtis, E. R. Sung, X. Ma, W. Ren, S. Cao, P. Narang, A. von Hoegen, E. Baldini, K. A. Nelson *Nature Physics* **20,** 788 (2024).

[2] Z. Zhang, F. Y. Gao, J. B. Curtis, Z.-J. Liu, Y.-C. Chien, A. von Hoegen, M.T. Wong, T. Kurihara, T. Suemoto, P. Narang, E. Baldini, K, A. Nelson *Nature Physics* **20,** 801 (2024).

[3] F. Y. Gao, Z. Zhang, Z.-J. Liu, K. A. Nelson, *Optics Letters* **47**, 3479 (2022).

[4] B. S. Dastrup, P. R. Miedaner, Z. Zhang, K. A. Nelson, *Review of Scientific Instruments* **95**, 033005 (2024).

[5] Z. Zhang, H. Ning, Z.-J. Liu, J. Hou, A. D. Mohite, E. Baldini, N. Gedik, K. A. Nelson, arXiv:2407.15253 (2024).

[6] L. V. Keldysh, *Ionization in the field of a strong electrmagnetic wave* (1964)

* Acknowledgement: ZZ and KAN acknowledge support from the U.S. Department of Energy, Office of Basic Energy Sciences, under Award No. DE-SC0019126.

Terahertz control of magno-phononics in van der Waals antiferromagnets

H. Ning[1], T. Luo[1], B. Ilyas[1], E. Viñas Boström[3], A. von Hoegen[1]
J. Park[4], J. Kim[4], J.-G. Park[4], D. M. Juraschek[5], A. Rubio[6], N. Gedik[1]
[1] *Massachusetts Institute of Technology, Cambridge, MA 02139, USA*
[2] *Max Planck Institute for the Structure and Dynamics of Matter, 227618 Hamburg, Germany*
[3] *Universidad del Pais Vasco, 20018 San Sebastian, Spain*
[4] *Seoul National University, Seoul 08826, Republic of Korea*
[5] *Tel Aviv University, Tel Aviv 6997801, Israel*
[6] *The Flatiron Institute, New York, NY 10010, USA*

Coherent manipulation of magnetism via lattice provides unprecedented opportunities for controlling spintronic functionalities on the ultrafast timescale [1,2]. By coherently driving magnons and phonons in the THz spectral range, a vast array of phenomena can emerge from their intricate coupling. Here, I will present two demonstrations that leverage the strong coupling between magnons and Raman-active phonons in van der Waals antiferromagnets. First, I will discuss how this interaction facilitates both linear and quadratic excitation of magnon-polarons — magnon-phonon hybrid quasiparticles — using intense THz pulses. This approach provides an innovative method to control quasiparticle dynamical symmetry by tuning the THz field strength and polarization. The polarimetry of the resulting coherent oscillation amplitude reveals a breaking of the crystallographic C_2 symmetry, driven by strong interference between the two excitation channels. Second, I will demonstrate how nondegenerate chiral phonons can be induced by coupling to chiral magnons. Such nondegeneracy enables their coherent excitation with linearly polarized terahertz pulses. By tuning the terahertz drive polarization and measuring phase-resolved polarimetry of the resulting coherent oscillations, we determine the ellipticity and map the trajectory of these hybrid quasiparticles.

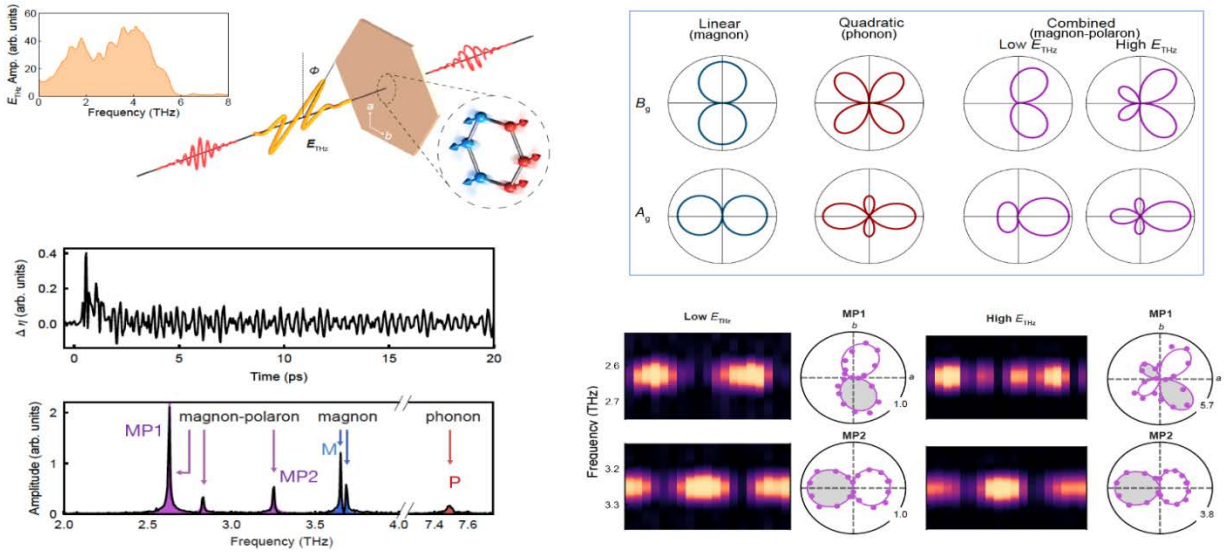

***Fig. 1. Left**: Schematic of the broadband THz pump and 800 nm polarization ellipticity probe setup with a characteristic time trace and its Fourier transform with magnons (blue), phonons (red), and hybrid magnon-polarons (purple) highlighted. **Right**: Expected and experimentally measured polarimetry of different modes.*

Our findings outline a novel roadmap towards phonon-controlled spintronic functionalities and unlock a wide range of possibilities to manipulate material properties, ranging from generation of metastable magnetic states via displacive phonon excitation to the modulation of exchange interactions by phonon-Floquet engineering [3].

References

[1] A. Kirilyuk, A. V. Kimel, T. Rasing, *Review of Modern Physics* **82**, 2731 (2010).
[2] P. Nemec, M. Fiebig, T. Kampfrath, A. V. Kimel, *Nature Physics* **14**, 229 (2018).
[3] H. Hubener, U. De Giovannini, A. Rubio, *Nano Letters* **18**, 1535 (2018).

* The work at MIT was support by the US DoE (BES DMSE), Gordon and Betty Moore Foundation's EPiQS Initiative grant GBMF9459, and the MIT-Israel Zuckerman STEM Fund. E.V.B. acknowledges funding from the EU's Horizon Europe research and innovation programme under the Marie Sklodowska - Curie grant agreement No. 101106809. A.R. was supported by the Cluster of Excellence Advanced Imaging of Matter (AIM), Grupos Consolidados (IT1249-19), SFB925, and the Max Planck Institute New York City Center for Non-Equilibrium Quantum Phenomena. A. v. H. gratefully acknowledges funding by the Humboldt Foundation. D.M.J. is supported by Tel Aviv University. The work at SNU was supported by the Korea's National Research Foundation (Grant No. 2020R1A3B2079375).

Many-body interactions on linear and non-linear optical properties of Low-dimensional materials

V. Perebeinos
SUNY University at Buffalo, Buffalo, NY 14260, USA

Atomically thin two-dimensional materials are direct bandgap semiconductors with a rich interplay of the valley and spin degrees of freedom, which offer the potential for electronics and optoelectronics. A strong Coulomb interaction leads to tightly bound electron-hole pairs or excitons and two-electron one-hole quasiparticles or trions. We solve the two-particle and three-particle problems for the wavefunctions for excitons and trions in the basis set of the model- Hamiltonian for single particles. The calculated linear and nonlinear absorptions, photoluminescence spectra, and polariton spectra as a function of doping and temperature explain the experimental data in 2D monolayers and predict novel spectroscopic features due to the many-body Coulomb interactions [1-5].

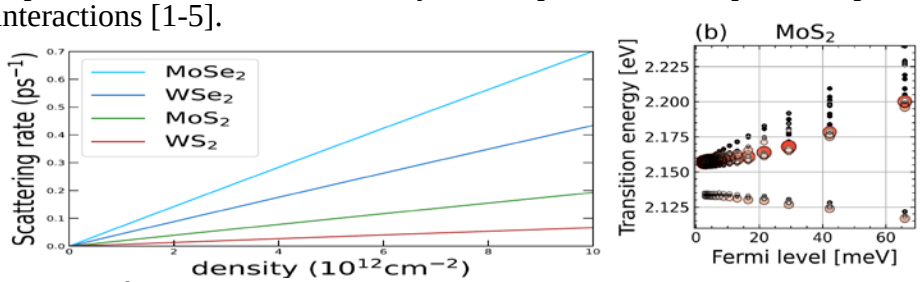

***Fig. 1. Left**: Phonon-assisted Auger decay of excitons in doped transition metal dichalcogenide monolayers as a function of carrier concentration [6].*
***Right:** Doping dependence of the transition energies in MoS2. The size of the circles are proportional to the oscillator strengths of the excited states [4].*

Exciton lifetime plays a crucial role in optoelectronic applications. I will also discuss the phonon-assisted Auger non-radiative decay mechanism of excitons in doped 2D materials [6]. Finally, I will discuss the role of many-body interactions on second harmonic generation in carbon nanotubes [7].

References

[1] Y. V. Zhumagulov, A. Vagov, N.Y. Senkevich, D.R. Gulevich, V. Perebeinos, *Physical Review* B **101**, 245433 (2020).
[2] Y. V. Zhumagulov, A. Vagov, P.F. Junior, D.R. Gulevich, V. Perebeinos, *Journal of Physical Chemstry* **153**, 044132 (2020).
[3] Y. V. Zhumagulov, S. Chiavazzo, D. R. Gulevich, V. Perebeinos, I. A. Shelykh, O. Kyriienko, *npj Computational Materials* **8**, 92 (2022)
[4] Y. V. Zhumagulov, A. Vagov, D. R. Gulevich, V. Perebeinos, *Nanomaterials* **12**, 3728 (2022)
[5] V. D. Neverov, A. E. Lukyanov, Y. V. Zhumagulov, D. R. Gulevich, A. V. Krasavin, A. Vagov, V. Perebeinos, *Physical Review* B **105**, 239902 (2022)
[6] B. Scharf, V. Perebeinos, *arXiv:2408.00097* (2024).
[7] R. Xu, J. Doumani, V. Labuntsov, N. Hong, A.C. Samaha, W. Tu, F. Tay, E. Blackert, J. Luo, M. El Tahchi, W. Gao, J. Lou, Y. Yomogida, K. Yanagi R. Saito V. Perebeinos, A. Baydin, J. Kono, H. Zhu, *arXiv:2407.04514* (2024).

Imaging valence-electron motion in solids

D. A. Reis
Stanford PULSE Institute, Menlo Park, CA 94025, USA

X-ray free-electron lasers have emerged as powerful probes of the structure and dynamics of matter on the relevant length and time scales of atomic motion in chemistry and materials. Yet much of chemistry and the functional properties of materials depend on the valence electron density that is only a small fraction of the electron density. Here we will describe recent results on x-ray scattering from optically-driven crystals, where phase-matched nonlinear sum frequency generation is particularly sensitive to the valence electron motion within a unit cell. In this case the scattered x rays appear as sidebands in energy and momentum about the ordinary elastically scattered Bragg peaks and their amplitude is proportional to the magnitude square of the spatial and temporal Fourier components of the driven charge density [1-4]. We present measurements of the first and second order sidebands in single crystal silicon excited below the band gap [5]. We find that the polarization dependence of the second order sideband from a single Bragg peak already reveals important information about the local symmetry of the interstitial electrons, even without knowing the phase of the nonlinear structure factors. Extension of this method to imperfect crystals will allow us to probe the microscopic origins of the strong-field and far-from equilibrium response in a variety of materials. We will thus also describe the first x-ray an optical mixing measurements on MgO using a purpose-built monochromator and analyzer on the PAL-XFEL[5]. Finally, we expect to report results of experiments on LCLS which will be conducted a few weeks before the conference.

References

[1] P. M. Eisenberger, S. L. McCall, *Physical Review* A **3**, 1145 (1971).
[2] I. Freund, B. F. Levine, Physical Review Letters **25**, 1241(1970).
[3] T. E. Glover, D. M. Fritz, M. Cammarata, T. K. Allison, S. Coh, J. M. Feldkamp, H. Lemke, D. Zhu, Y. Feng, R. N. Coffee, M. Fuchs, S. Ghimire, J. Chen S. Shwartz, D. A. Reis, S. E. Harris, J. B. Hastings, *Nature* **488,** 603 (2012)..
[4] D. Popova-Gorelova, D. A. Reis, R. Santra, Physical Review B **98**, 224302 (2018).
[5] C. Orenelis-Skarin, *to be submitted* (2024).
* Acknowledgments: This work was supported by the AMOS program within the Chemical Sciences, Geosciences, and Biosciences: Division, US DOE the support of the LCLS and PAL - XFEL, and past support from SACLA and SwissFEL.

Layered transient structures induced by pulsed energy in semiconductors

M.K. Rafailov
University of Alberta, Edmonton T6G 1H9, Canada

High peak power low energy pulse, inducing nonequlibrium state and may create curious transient structures in a bulk semiconductor. Negative Photoresponse - NPR [1] was observed as a result of such interaction and has been broadly discussed with the purpose to find potential applications as well to understand its counter-intuitive nature. Fig.1 show such a response in specific types of photodetectors where instead of predicted unipolar response [2], very long lasted voltage with changed polarity has been observed. NPR that is lasting up to ms and depends only on pump intensity and pulse dwell time, is a combination of two factors-electronic responses to excitation and transient structure dimensionality (depth) defined by excitation-resulted material bleaching-Fig.1

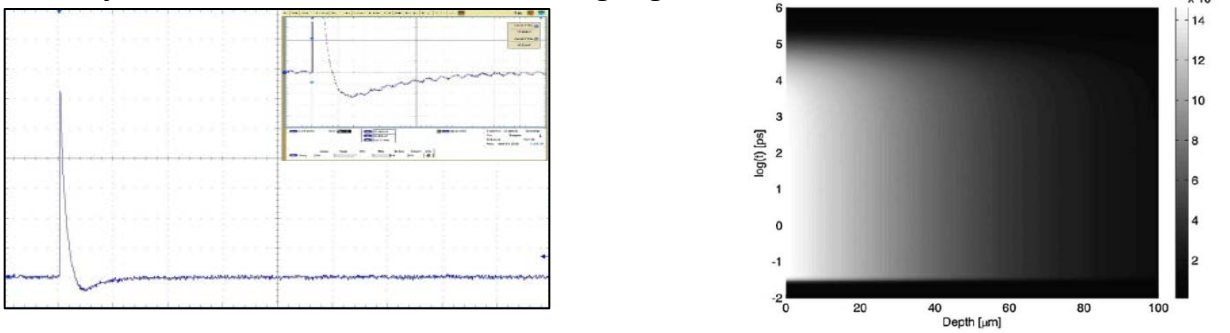

Fig.1. Left. NPR-excitation by short pulse Irradiation: *NPR lasting up to μs experimentally observed in Ge & Si-p-i-n diodes;* ***inset*** *-modulated low intensity signal structure is fully preserved with the NPR;* ***Right:*** *Simulated bleaching in Si - after [2].*

With respect to pulse "time of flight" a transient bleached structure exists for up to μs [2]. That opens a new opportunity for extending of nonequlibrium lifetime in semiconductor structures-specifically ones with p-n junctions, under periodic excitation with below MHz pulse rate. From one side it opens new opportunities in remote sensing, while, since bleaching depends on pulse flight time -which is for 10fs in Ge is~750nm, a layered combination of electrically isolated 2D p-n or p-i-n structures may be used as an effective power-generating device even for cw-sources. Few plausible mechanisms for explanation of the NPR have been discussed, most recently in [3]. The same principle also can be used while train of electric pulses is used as a pumping source. Speed difference in 6-orders leads to considering ns-dwell time electric pulses as "ultrafast" for such excitation, while the dwell time defined by dimensions of a material. In such a case the only limitations for pulse width and, thereto pumping power will be the capacitance-C which is directly depends on layer thickness. And in such a case we may need a potential or bias to move pulses across a layer. While results of positive response is strongly depending on R-C parameters it will be plausible in low dimentionals semiconductor structures to see above mentioned enveloping of nonequlibrium with carrier velocity. Farther considering electronic pumping of such low dimensional structures, it has been once tested in organic light emitting diodes [4] electronic pumping strongly depends on capacitance-size of the structure demonstrated high efficiency in maintain nonequlibrium even in relatively thick materials-Fig.2.

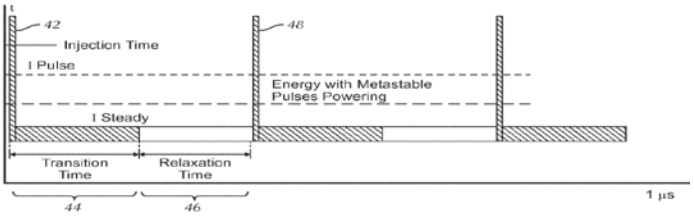

Fig.2. Schematic of thina layered heterostructure electrically pumped by train of electric pulses. *From [4]*

Using transient layered structures as well as switching to electronic pumping, is a plausible way for proliferating nonequlibrium-related phenomena in multiple applications: from above-THz electronics to remote sensing, and photovoltaics in general.

References

[1] I. K. Zak. M.K. Rafailov. *Proceedinas SPIE* **9467**. 946726-1 (2015).
[2] X- A. Dou, X. Sun, X. Li, X. Chen, *Optik* **126,** 3267 (2015).
[3] M. Yuan, M. K. Rafailov, R. Binder, *Journal of Applied Physics* 134, 174503 (2023).
[4] M. K. Rafailov, US Patent 10242618, *US Patent ad Trademark Office* (2019).

Ultrafast pump-probe nano-imaging of coupled polaron-cation dynamics in triple cation perovskites

M. B. Raschke
University of Colorado, Boulder, CO 80309, USA

Ultrafast infrared spectroscopy in its extension to nano-imaging provides access to vibrational and low energy carrier dynamics in molecular, semiconductor, quantum, or polaritonic materials. In addition, to simultaneously probe both ground and excited state dynamics we have developed ultrafast heterodyne pump-probe nano-imaging with far-from-equilibrium excitation. In ultrafast movies with simultaneous spatial, spectral, and temporal resolution we can image heterogeneities in electron-phonon, cation-lattice, and coupled polaron dynamics on their elementary time and length scales (Fig. 1) [1,2].

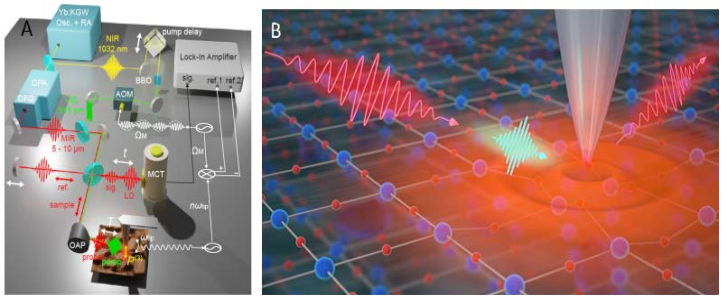

Fig. 1. (A) Development of ultrafast nano-imaging in heterodyne fs s-SNOM resolving excited state dynamics *with fs-nm spatio-spectral-temporal resolution.* ***(B)****. In ultrafast movies with electronic pump and low-energy IR probe spectroscopy heterogeneities in electron-phonon, cation-lattice, and coupled polaron dynamics can be resolved on the elementary time and length scales.*

As exemplary application we use this approach of ultrafast pump-probe nanoimaging to provide a real-space and real-time view of the coupled electron-lattice dynamics underlying the photophysical response of hybrid organic-inorganic perovskites. Their photovoltaic performance and other photonic functions are still poorly understood in part because of the multi-scale chemical and structural heterogeneities. While polaron formation following the photoexcitation is believed to relate to the effective carrier transport observed, the elementary physical processes underlying electron-phonon coupling to both the perovskite lattice and molecular cations constituents have not yet been resolved.

First, in ultrafast visible-pump infrared-probe nano-imaging we resolve the photoinduced carrier dynamics in triple cation perovskite films, with a ~20 % variation in sub-ns relaxation dynamics with spatial disorder on tens to hundreds of nanometer which we attribute to the heterogeneous evolution of polaron delocalization and increasing lifetime (Fig. 2) [3].

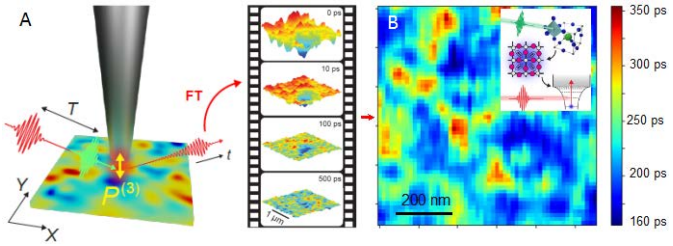

Fig. 2. (A) Ultrafast nano-imaging of photoinduced polaron dynamics *in triple cation perovskites.* ***(B)*** *Ultrafast movie resolving heterogeneity in carrier dynamics and polaron radius underlying the performance of perovskite-based photophysical devices of solar cells, lasers, and light emitting diodes.*

We then apply a combination of ground and excited state spectroscopic nanoimaging of the formamidinium (FA) cation vibration where we use vibrational solvatochromism as a probe of the static and dynamic evolution of the local molecular environment. A transient vibrational blueshift we model as signature of nano-scale spatial variations in the polaron-cation coupling based on a combination of vibrational Stark shift, FA orientation, and lattice-field effects [4].

The high degree of local variation in polaron-cation coupling dynamics points towards the missing link between the optoelectronic heterogeneity and associated carrier dynamics. The results suggest that there is a lot of room for improved synthesis and device engineering and that perovskite photonics performance is far from any fundamental limits.

References

[1] J. Nishida, A.H. Alfaifi, T.P. Gray, S.E. Shaheen, M.B. Raschke, *ACS Energy Letters* **5**, 1636 (2020).
[2] J. Nishida P.T.S. Chang, J.Y. Ye, P. Sharma, D.M. Wharton, S.C. Johnson, S.E. Shaheen, *Nature Communi*cations **13**, 6582 (2022).
[3] J. Nishida, S.C. Johnson, P.T.S. Chang, D.M. Wharton, S.A. Dönges, O. Khatib, M.B. Raschke, *Nature Communications* **13**, 1083 (2022).
[4] E. Wilcken, B. Esses, M. B. Raschke, *submitted* (2024).

* Acknowledgement: project supported by National Science Foundation (NSF) Science and Technology Center on Real - Time Functional Imaging (STROBE) under Grant DMR 1548924.

Quest to reveal the Higgs excitation in superconductors by NEARS

M. Rübhausen
Universität Hamburg, 22761 Hamburg, Germany

The U(1) gauge invariant version of the superconducting BCS state as formulated by P.W. Anderson is characterized by the Higgs mode as the elementary excitation of the superconductor in the two particle channel [1]. This mechanism inspired Y. Nambu and in particular P. Higgs to formulate the Higgs mechanism for elementary particle physics leading subsequentially to the discovery of the Higgs particle [2-3]. Varma pointed out early that the Higgs particle is a Raman active excitation. [4] Indeed experiments by Sooryakumar and Klein showed the first measurement of the Higgs mode in superconductors already in 1980 – a finding later confirmed in 2014. [5,6] Due to its weak coupling to light the Higgs mode remained quite elusive to experiments, despite the case in $NbSe_2$ where it gained strength in the Raman cross section by coupling to a CDW. However, over the past 20 years there was a continuous build up of experimental evidence for the Higgs mode in Raman scattering of HTCs. Already in 2005 Budelmann et al. noticed by using resonance Raman spectroscopy a distinct in-gap quasiparticle excitation as part of the overall gap feature seen in HTCs.[7] In 2009 Saichu et al. obseverd and in gap feature reacting on a pump on a different time scale as compared to the expected pair breaking peak suggesting the presence of a distinct in-gap excitation.[8] Since then many studies by different techniques in particular THz measurements have provided a growing body of evidence for the presence of the Higgs mode.[9]

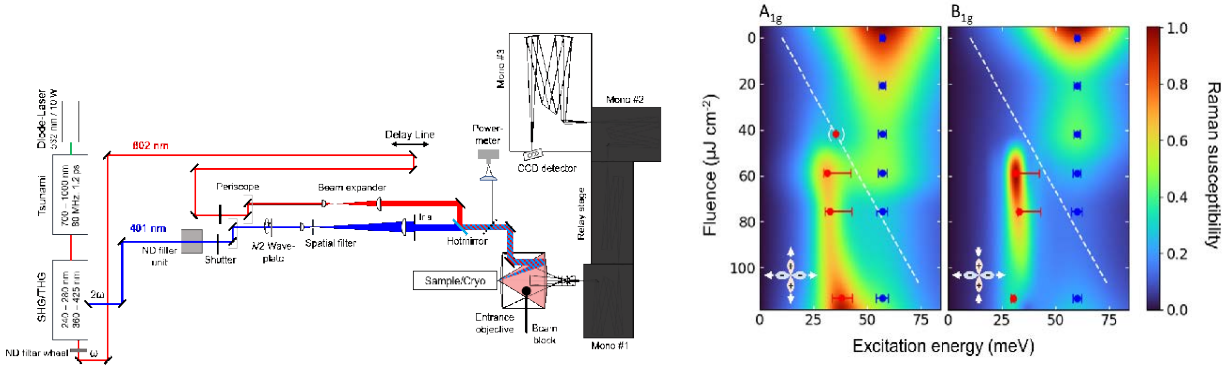

***Fig. 1. Left** :**Nonequilibrium Raman instrument** for the simultaneous measurement of energy gain and energy loss data. At infinite temperatures the energy gain and energy loss data would be equal. The NEARS measurements show a stronger Anti-Stokes (energy gain) contribution compared to the Stokes contribution which is only possible when pumping a novel state in the superconductor leading to population inversion. We assign this state tentatively to the Higgs mode and derive the excitation landscape of a superconductor in the single particle and two-particle channel (see panel on the **Right**). Figures are taken from Ref. [10].*

However, Raman scattering is susceptible to a combination of pair breaking excitations and superconducting quasiparticle excitations. The development of non-equilibrium Raman scattering (NEARS) allows to discriminate the different contributions by comparing the Anti-Stokes and Stokes (energy gain / energy loss) spectra in order to identify modes that get populated in a superconductor after a quench of the Mexican hat potential (see Fig. 1 – left) . We will discuss the detailed measurement procedure and will outline the presence of a new in-gap mode in the superconducting state. Its symmetry dependent behavior is consistent with the Higgs mode in the superconductor and incompatible with other excitations. From the fits it is then possible to determine the excitations landscape of a superconductor (see Fig.1, *right*). We will also outline future plans to further support our assignment and what needs to be done to systematically evaluate the presence of the Higgs mode in HTCs.

References

[1] Y. Nambu, *Physical Review* **117**, 648 (1960).
[2] P. Anderson, *Physical Review* **110**, 827 (1958).
[3] P. Higgs, *Comptes Rendus Physique* **8**, 970 (2007).
[4] C. M. Varma, *Journal of Low Temperature Physics* **126**, 901 (2002).
[5] R. Soorvakumar. M. V. Klein. Phvsical Review Letters **45**. 660 (1980).
[6] M-A. Méasson, Y. Gallais, **M.** Cazayous, **B.** Clair, P. Rodiere, L. Cario, A. SacutoM. *Physical Review* B **89**, 060503 (2014).
[7] D. Budelmann, B. Schulz, M. Rübhausen, M.V. Klein, M.S. Williamsen, P. Guptasarma,*Physical Review Letters* **95**, 057003 (2005).
[8] R. P. Saichu, I. Mahns, A. Goos, S.Binder, P.May, S. G.Singer, B.Schulz, A.Rusydi, J.Unterhinninghofen, D. Manske, P. Guptasarma, M. S. Williamsen M. Rübhausen, *Physical Review Letters* **102**, 177004 (2009).
[9] R. Shimano.N. Tsuii. *The Annual Review of Condensed Matter Phvsics* **11.** 103 (2020).
[10]T. E. Glier. M. Rerrer, L.Westphal, G.Lüllau, L.Feng, S.Tian, J.Dolgner, R.Haenel, M.Zonno, H.Eisaki, M.Greven, A. Damascelli, S. Kaiser, D. Manske M. Rübhausen**,** *arXiv 2310.08162*, (2024).

* Acknowledgements: We acknowledge many scientific discussions with Tomke Glier, Dirk Manske, Stefan Kaiser, Mika Rerrer, Lea Westphal, Garret Lüllau, Liwen Feng, Sida Tian, Jakob Dolgner, Rafael Haenel, Marta Zonno, Hiroshi Eisaki, Martin Greven, and Andrea Damascelli.

Controlling excitons in 2D semiconductor heterostructures

J. R. Schaibley
University of Arizona, Tucson, Arizona 85721, USA

Two dimensional (2D) semiconductors, such as $MoSe_2$ and WSe_2, host tightly bound excitons (electron-hole pairs) that interact strongly with light. These monolayer semiconductors can be stacked together to realize heterostructures that exhibit new excitonic effects. In this presentation, I will discuss the optical response of two different 2D semiconductor heterostructures. First, I will review the progress towards understanding interlayer excitons (IXs) in $MoSe_2$ -WSe_2 heterobilayers. These IXs host a rich moiré physics associated with the spatially modulated interactions between layers. I will discuss our recent discoveries related to exciton transport in structures that have a hBN separator between the $MoSe_2$ and WSe_2 layers. IXs also possess a large permanent dipole moment that allows for their energy to be tuned with an out-of-plane electric field. By nano-patterning a gate on top of the $MoSe_2$-WSe_2 heterostructure, we have demonstrated quantum dot-like potentials (Fig.1. a-b), which have potential applications toward realizing deterministic single photon emitters [1, 2].

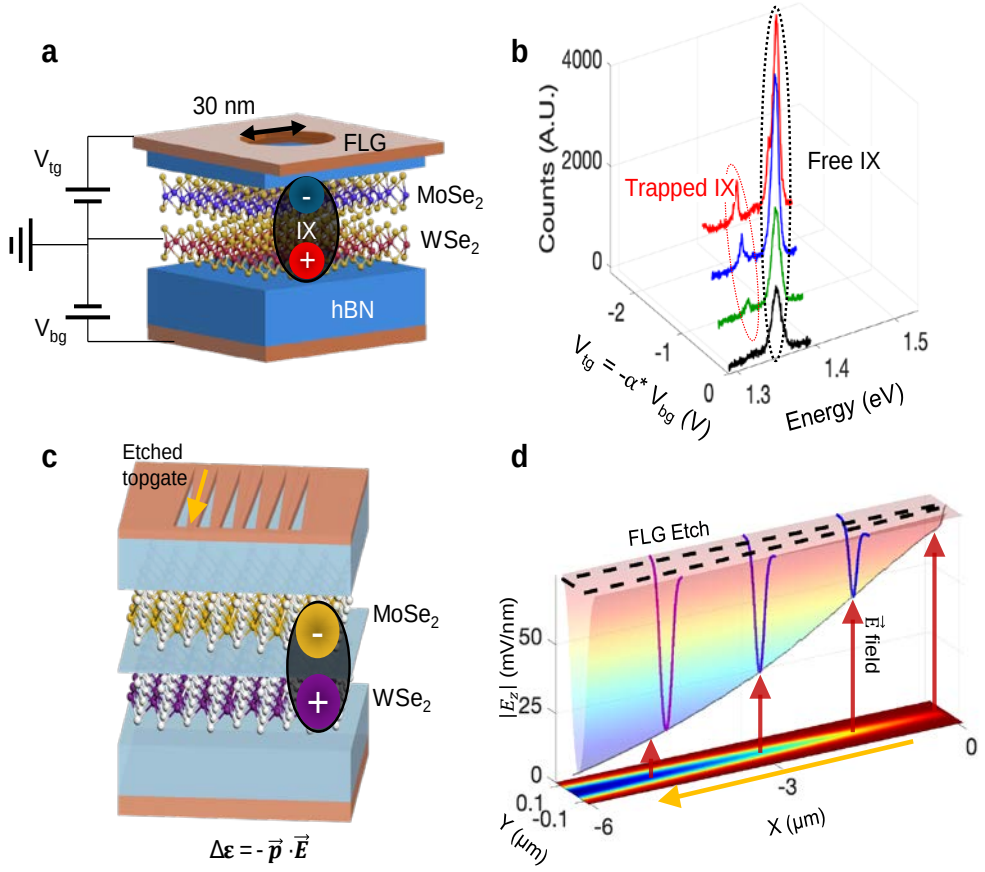

Fig. 1. ***(a) Depiction of a $MoSe_2$-WSe_2 heterostructure with a nanopatterned top gate.*** *(**b**) Photoluminescence spectra as a function of applied top and bottom gate voltage (Vtg, Vbg). The spatial modulation of the out-of-plane electric field (due to the hole) results in a trapped IXs under the nanopatterned hole shown in b. (**c**) Depiction of the IX ramp device consisting of nanopatterned long, skinny isosceles triangles in the top bilayer graphene gate. (**d**) A COMSOL simulation of the out-of-plane electric field shows a ramp/slide energy potential for IXs that is used for high speed IX transport.*

Using the same architecture, we have demonstrated high speed IX currents based on "slide" like quasi-one dimensional channels (Fig.1, c-d), which have applications to excitonic circuitry [3].

References

[1] D. N. Shanks, F. Mahdikhanysarvejahany, T. G.Stanfill, M.R. Koehler, D. G. Mandrus, T. Taniguchi, K. Watanabe, B. J. LeRoy, J. R. Schaibley, *Nano Letters* **21,** 13 (2021)

[2] D. N. Shanks, F. Mahdikhanysarvejahany, M. R. Koehler, D. G. Mandrus, T. Taniguchi, K. Watanabe, B. J. LeRoy, J. R. Schaibley, *Physical Review* B **106,** 16 (2022).

[3] D. N. Shanks , F. Mahdikhanysarvejahany, T. G. Stanfill, M. R. Koehler, D. G. Mandrus, T.Taniguchi, K Watanabe, B. J. LeRoy, J.R. Schaibley, *Nano Letters* **22,** 16 (2022).

* Acknowledgement(s): J.S. acknowledges support from National Science Foundation grants DMR-200358, ECCS-2054572; and Air Force Office of Scientific Research grants FA9550-20-1-0217, FA9550-21-1-0219, FA9550-22-1-0312.

Carrier dynamics in models of charge density wave materials and Excitonic insulators: a density-matrix approach

S. Michael, H. C. Schneider
Rheinland-Pfälzische Technische Universität Kaiserslautern-Landau, 67653 Kaiserslautern, Germany

Progress in time- and angle-resolved photoemission spectroscopy (trARPES) has made it possible to investigate the ultrafast non-equilibrium material response after optical excitation [1]. For complex materials, the "symmetry" can be changed via optically induced phase transitions [2], which offer new ways to manipulate material properties on ultrafast timescales. We theoretically study models of materials that exhibit a charge-density wave with Peierls and/or excitonic insulator character and study the quenching of their ordered phase in a microscopic density-matrix approach. For a model system of a quasi-twodimensional material, which includes both electron-hole and electron-phonon interactions leading, respectively, to excitonic and coherent-phonon contributions, we discuss how interaction processes affect microscopic anomalous expectation values and present a dynamical picture of the quenching of the phase. We use projection techniques to switch between a unit-cell and supercell representation, which allows us to illustrate the time-dependent appearance of additional bands and anomalous expectation values. We introduce a model composed of a tight-binding band structure where the quasiparticle band dynamics is determined by an excitonic and a lattice contribution, leading to the band structure shown in Fig. 1 (a), (b). The excitonic contributions are included at a quasiparticle level based on anomalous expectation values and the lattice distortion is modeled by a coherent phonon. Based on this quasiparticle ground state, we set up the equations of motion for the non-equilibrium carrier dynamics including the optical excitation, the carrier-carrier as well as the carrier-phonon scattering contributions.

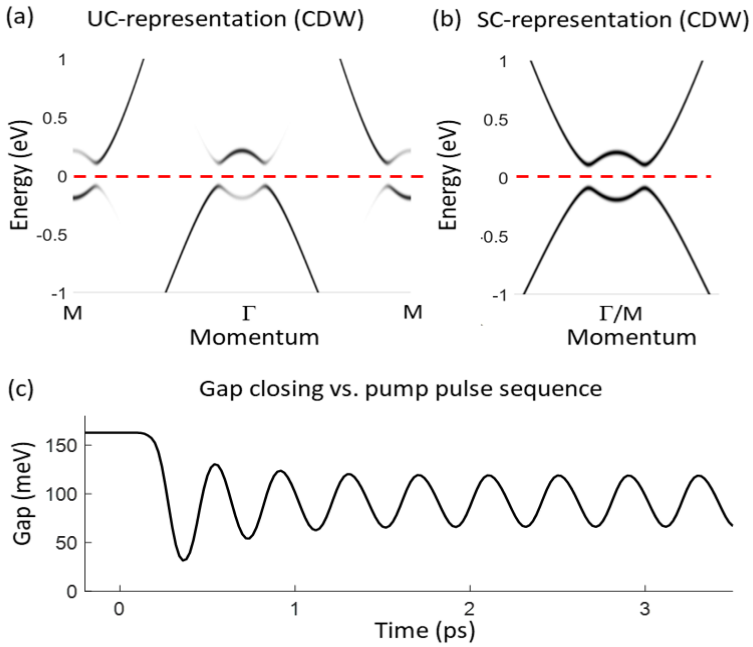

Fig. 1. Band-structure of the charge-density wave phase *in the unit-cell representation* ***(a)*** *and in the supercell representation* ***(b)****. Gap dynamics for a modulated optical pump field* ***(c).***

Numerical results are presented for the build-up of the equilibrium CDW phase from the normal phase, the non-equilibrium dynamics during a quenching of the phase due to an optical excitation and the potential of the setup for optical amplification. The gap dynamics that results in an optical amplification setup with a high modulation frequency in the midinfrared regime is shown in Fig. 1(c).

References

[1] T. Rohwer , S. Hellmann, M.Wiesenmayer, C.Sohrt, A. Stange, B.Slomski, A.Carr, Y.Liu, L. M.Avila, M.Kalla¨ne , S. Mathias, L. Kipp, K .Rossnagel M. Bauer, *Nature* **471,** 490 (2011).
[2] S. Mathias,S. Eich, J. Urbancic, S. Michael, A. V. Carr, S. Emmerich, A. Stange, T. Popmintchev, T. Rohwer, M. Wiesenmayer, A. Ruffing, S. Jacobs S. Hellmann, P. Matyba, C. Chen, L. Kipp, M. Bauer, H. C. Kapteyn, H. C. Schneider, K. Rossnagel, M. M. Murnane, M. Aeschlimann, *Nature Communications* **7**, 12902 (2016)
[2] S. Michael, H. C. Schneider, *Physical Review B* **105**, 235108 (2022).

Nonlinear polariton physics: controlling light with light in Semiconductor microcavities

S. Schumacher
Paderborn University, 33098 Paderborn, Germany

Polaritons in planar semiconductor microcavities are composite particles formed from photons and excitons. They inherit long-lived coherences from their photonic part while polariton-polariton interaction gives rise to strong nonlinearities. In recent years, polariton systems have proven a fruitful playground for nonlinear photonics, with a broad spectrum of fundamental physics and concepts for novel functional photonic elements to explore. Nowadays, polariton condensation is quite routinely observed up to room temperature using for example perovskite semiconductors as the optically active material [1], increasing the potential technological relevance of our studies. We will introduce the subject and give an overview of some of our recent work, time permitting including examples covering polariton vortex formation and control [2], quantum properties of polaritons [3,4], and the interplay of non-Hermitian physics and nonlinearity [5]. We will discuss in detail how spatially shaping the intensity profile of an off-resonant excitation laser can be used to create optically induced and re-configurable potential energy landscapes. This allows to control the flow of polaritons in the two-dimensional plane or to create, stabilize, and trap fundamental topological excitations such as solitons and vortices. For example in an annular trap, a polariton vortex can be created and subsequently controlled, such that its rotation direction (or vortex charge) can be switched with an ultrashort light pulse, cf. Fig.1. This switching of vorticity in turn can be detected in the finite orbital angular momentum of the light emitted from the system [2].

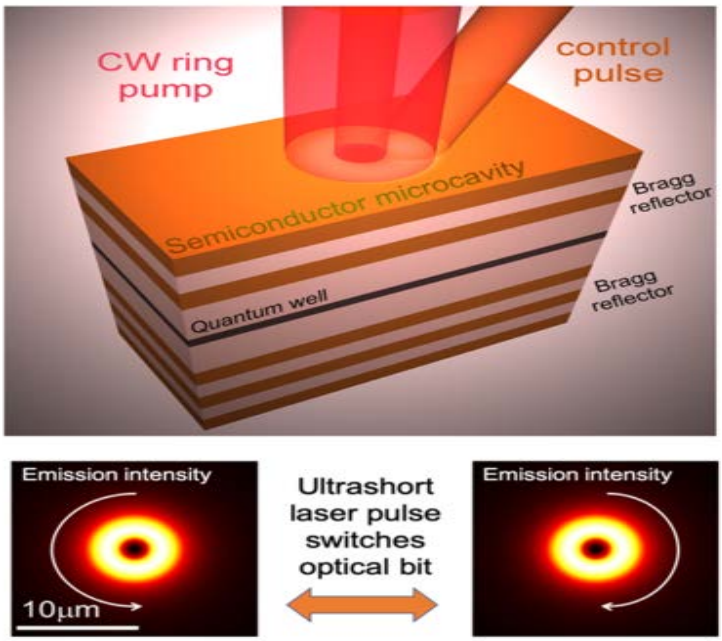

Fig. 1 Polariton vortex formation and control in an optically induced annular trap. *After [2].*

Furthermore, we may touch upon some of our other recent activities in the field. This includes the extension of our semi-classical analysis of the polariton condensate dynamics to the tomography of polariton quantum states, for example leading us to investigate the polariton quantum coherence and allowing the re-construction of the system density matrix [3], proposals for the realization of macroscopic analogues of qubits in polariton systems [4], and the interplay of non-Hermitian physics and nonlinearity [5].

References

[1] Y. Li, X. Ma, X. Zhai, M. Gao, H. Dai, S. Schumacher, T. Gao, *Nature Communications* **13**, 3785 (2022).
[2] X. Ma, B. Berger, M. Assmann, R. Driben, T. Meier, C. Schneider, S. Höfling, S. Schumacher, *Nature Communications* **11**, 897 (2020).
[3] C. Lüders, M. Pukrop, F. Barkhausen, E. Rozas, C. Schneider, S. Höfling, J. Sperling, S. Schumacher, M. Assmann, *Physical Review Letters* **130** 113601 (2023).
[4] Y. Xue, I. Chestnov, E. Sedov, E. Kiktenko, A. K. Fedorov, S. Schumacher, X. Ma, A. Kavokin, *Physical Review Research* **3**, 013099 (2021).
[5] J. Wingenbach, S. Schumacher, X. Ma, *Physical Review Research* **6**, 013148 (2024).

Fast light-driven antiferromagnetic domain walls

K L. Seyler[1], H. Zhang[3], D. van Beveren[2], C. R. Rotundu[4], Y. S. Lee[5], Ran Cheng[3], D. Hsieh[2]
[1] *University of Arizona, Tucson, AZ 85721, USA*
[2] *California Institute of Technology, Pasadena, CA 91125, USA*
[3] *University of California Riverside, Riverside, CA 92521, USA*
[4] *SLAC National Accelerator Laboratory, Menlo Park, CA 94025, USA*
[5] *Stanford University, Stanford, CA 94305, USA*

The ability to quickly and precisely manipulate domain walls in magnetic materials is critical for novel high-speed spintronic memory and computing devices [1-5]. Antiferromagnetic (AFM) materials are promising for such devices because their fast spin dynamics can enable high domain wall velocities [6]. However, we are still at the dawn of understanding how to drive and detect fast AFM domain wall motion. Recent studies have mostly focused on current-induced domain wall dynamics via spin-transfer or spin-orbit torques in ferrimagnets and synthetic antiferromagnets [3, 5], leaving a wide variety of AFM material platforms and driving mechanisms unexplored. In this talk, we describe a different approach to driving fast AFM domain walls using light-induced coherent spin waves. Using the room-temperature easy-plane AFM insulator $Sr_2Cu_3O_4Cl_2$, we demonstrate direct spatiotemporal imaging of AFM domain walls using time-resolved second-harmonic generation (Fig. 1a), allowing us to study the effect of ultrafast laser excitation on domain wall dynamics. We observe fast coherent AFM domain wall motion with velocities of ~50 km/s (Fig. 1b, c). The motion direction is controllable through both the helicity of the pump laser pulse and the winding number of the domain wall. These observations are explainable by the presence of large-amplitude AFM spin waves that coherently drive the domain wall spins, a picture supported by simulations. Our work reveals new opportunities for light-driven coherent AFM domain wall manipulation.

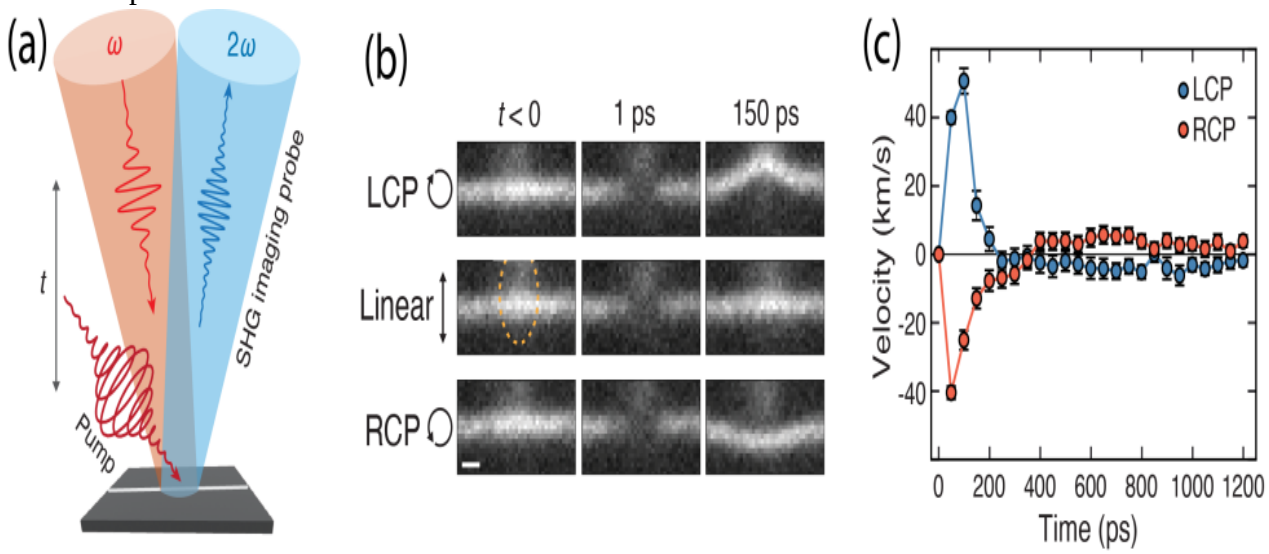

Fig. 1. ***(a)*** *Schematic of pump-probe SHG imaging experiment.* ***(b)*** *SHG images of an antiphase domain wall at selected pump-probe time delays for linear, left circular, and right circular pump polarizations. The dashed oval indicates the pump excitation spot. The vertical scale of each image is 20 μm.* ***(c)*** *Velocity of the domain wall center (at the location of maximum movement) over time for different pump polarizations.*

Our work reveals new opportunities for light-driven coherent AFM domain wall manipulation.

References

[1] D. A. Allwood, G. Xiong, C. C. Faulkner, D. Atkinson, D. Petit, R. P. Cowburn, *Science* **309**, 1688 (2005).
[2] S. S. P. Parkin, M. Hayashi, L. Thomas, *Science* **320**, 190 (2008).
[3] D. Kumar, T.Jin, R.Sbiaa, M.Kläui, S.Bedanta, S.Fukami, D.Ravelosona, S.-H.Yang, X.Liu, S.N.Piramanayagam, *Journal of Applied Physics* **958**, 1(2022)
[4] Z. Luo, A. Hrabec, T. P. Dao, G. Sala, S. Finizio, J. Feng, S. Mayr, J. Raabe, P. Gambardella, L. J. Heyderman, *Nature* **579**, 214 (2020).
[5] L. Caretta, C. O. Avci, *APL Materials* **12**, 011106 (2024).
[6] O. Gomonay, T. Jungwirth, J. Sinova, *Nature Physics* **14**, 213(2018).

* Acknowledgement(s): SHG experiments were supported by the Institute for Quantum Information and Matter (IQIM), an NSF Physics Frontiers Center (PHY-1733907), and the Brown Science Foundation. KLS acknowledges a Caltech Prize Postdoctoral Fellowship. The work at Stanford and SLAC (crystal growth and sample characterization) was supported by the U.S. Department of Energy (DOE), Office of Science, Basic Energy Sciences, Materials Sciences and Engineering Division, under contract DE-AC02-76SF00515.

Revealing the magnetization dynamics and spin polarization in Compensated magnets on ultrafast timescales

B. Stadtmüller
Augsburg University, 86159 Augsburg, Germany

Fundamental to the advancement of spintronics and quantum technology in solids is the ability to encode, manipulate and store information about the spin angular momentum of electrons on ever faster timescales. To date, ferromagnets have been the natural driving target for these efforts, leading to optical manipulation schemes that can change the spin order on the timescale of optical excitation. However, intrinsic limitations of ferromagnets in terms of miniaturization and efficiency have prompted the search for compensated spin systems that can still support (ultrafast) spin functionalities.Therefore, in this contribution, we shed light on the ultrafast magnetic response of the two known classes of compensated magnets, namely antiferromagnets (AFMs) and the recently discovered class of altermagnets. This class of compensated magnets is characterized by the broken time-reversal symmetry and the momentum-split band structure [1], which distinguishes them from the more conventional AFMs with their spin-degenerate band structure as shown in Fig. 1.

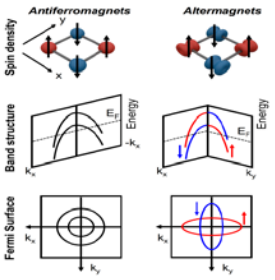

Fig. 1 Illustration of the two classes of compensated magnets. (a) *Collinear spin arrangement and spin density on the crystal structure. Sketch of the band structure* ***(b)*** *and Fermi surface* ***(c)*** *of both types of collinear compensated magnets. (Adapted from [1])*

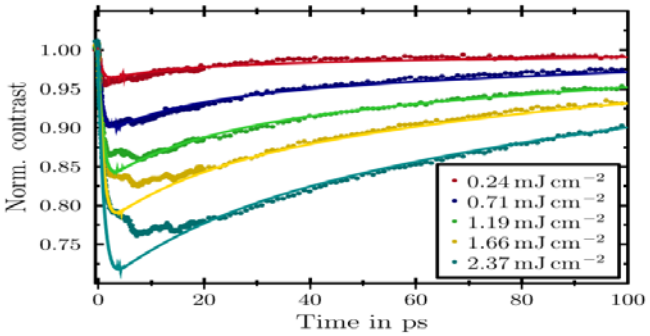

Fig. 2 Temporal evolution of the MOBF signal of a Pt(2nm)/NiO bilayer structure after optical excitation with fs IR pulses. *The data points are shown as colored dots, while the solid lines represent simulated traces obtained by a temperature-based model.*

First, we focus on the ultrafast magnetization dynamics of collinear antiferromagnets (AFMs). For such compensated magnets, recent experiments have demonstrated the possibility of optically exciting (THz) magnon modes, opening up new possibilities for manipulating AFMs [2] on picosecond timescales. Here we show that these timescales can be further reduced by exploiting the strong non-equilibrium excitation of AFMs using fs laser pulses. For the insulating antiferromagnet NiO, we demonstrate a substantial reduction of magnetic order on the sub-picosecond timescale. This non-coherent manipulation of the NiO magnetic order can be achieved either by direct optical excitation of the electron system with UV pulses or by indirect energy and angular momentum transfer from an adjacent ultrathin metal film that was optically excited with ultrashort IR pulses. We monitor the transient changes in the magnetic order of NiO by following the magneto-optical birefringence (MOBF) signal in an all-optical pump-probe setup [3]. An example data set for a Pt/NiO bilayer structure after excitation with fs IR pulses is shown in Fig. 2 for different fluences of the pump pulses.Despite the ultrafast changes in magnetic order of AFMs upon optical excitation, the Kramers degeneracy of the electronic bands of AFMs prevents the direct optical generation of spin polarization in these compensated systems. This will be substantially different for the compensated magnets with altermagentic spin order.

In the second part of this contribution, we therefore investigate the ultrafast optical response of altermagnets with d-wave spin splitting. As an example, we consider ultrathin films of RuO_2, for which signatures of an altermagentic phase have been reported [4]. By combining theoretical calculations with ultrafast magneto-optics experiments, we demonstrate the generation of a macroscopic spin polarization in the otherwise fully compensated altermagnet RuO_2 [5]. Crucially, the sign and magnitude of the excited spin polarization can be fully controlled by the orientation of the linear polarization of the pump pulses. This optically generated spin polarization persists for at least 300 fs after the optical (see Fig. 3) which we attribute to the intrinsic timescale of the spin-flip scattering processes in RuO_2.

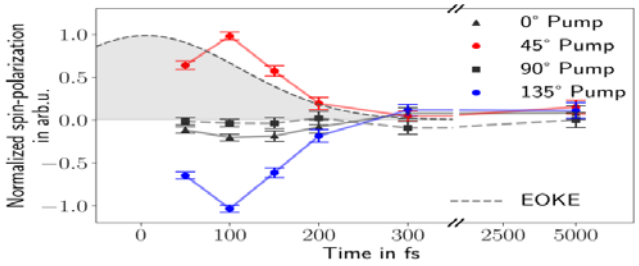

Fig. 3 Temporal evolution of the optically excited spin polarization *for different orientations of the linearly polarized pump pulses (1.5 eV photons) with respect to the crystallographic [100] direction of the lattice. The cross-correlation of the pump and probe pulses can be estimated from the electro-optical Kerr trace (EOKE), which is included as a* ***gray*** *shaded area [5].*

Our results thus reveal the fast non-equilibrium magnetic dynamics in d-wave altermagnets and demonstrate the equivalent of a spin-splitter in the optical domain on ultrafast timescales.

References

[1] L. Šmejkal, J Sinova, T Jungwirth, *Physical Review* X 12, 031042 (2022)
[2] D. Bossini, M. Pancaldi, L.Soumah, M. Basini, F. Mertens, M. Cinchetti, T. Satoh, O. Gomonay, S. Bonetti, *Physical Review Letters* **127,** 077202(2021)
[3] S. Wust C.Seibel, H.Meer, P.Herrgen, C. Schmitt, L. Baldrati, R. Ramos, T.Kikkawa, E.Saitoh, O. Gomonay, J. Sinova, Y. Mokrousov, H. C. Schneider M. Klaui, B.Rethfeld, B. Stadtmuller, M. Aeschlimann. arXiv:2205.02686 (2022).
[4] O. Fedchenko, J. Minár, A. Akashdeep, S. W. D'Souza, D. Vasilyev, O. Tkach, L. Odenbreit , Q. Nguyen, D. Kutnyakhov, N. Wind, L. Wenthaus M. Scholz, K.Rossnagel, M.Hoesch, M. Aeschlimann, B. Stadtmüller, M. Kläui , G. Schönhense, T. Jungwirth, A. B. Hellenes , G. Jakob , L. Šmejkal J. Sinova, H.-J. Elmers, *Science Advances* **10**, eadj4883 (2024)
[5] M. Weber, S. Wust, L.Haag, A. Akashdeep, K. Leckron, C. Schmitt, R.Ramos, T. Kikkawa, E.Saitoh, M. Klaui, L. Smejkal, J. Sinova, M. Aeschlimann G. Jakob, B. Stadtmuller, H. C. Schneider, arXiv: 2408.05187 (2024).

Nonresonant Raman control of material phases

J. (Tristan) Shi, A. M. Lindenberg
Stanford University, Stanford CA 94305, USA

Important advances have recently been made in the search for materials with complex multi-phase landscapes that host photoinduced metastable collective states with exotic functionalities, such as high-temperature superconductivity, ferroelectricity, or topological properties. In almost all cases so far, the desired phases are accessed by exploiting light-matter interactions via the imaginary part of the dielectric function through above-bandgap or resonant mode excitation. Nonresonant Raman excitation of coherent modes has been observed experimentally and proposed as a means of dynamically controlling material functions [1-3]. However, the atomic excursion driven by this approach has been perturbative, and these prospects have been hindered by the concomitant excitation of carriers and subsequent heating-induced sample damage. Here, we demonstrate that it is possible to overcome this challenge by employing nonresonant ultrashort pulses with low photon energies significantly below the bandgap [4]. We first achieve this in a prototypical ferroelectric, lithium niobate, using mid-infrared (MIR) pulse excitation and concurrently monitoring the lattice dynamics using femtosecond stimulated Raman scattering (FSRS) and second harmonic generation. Large-amplitude ferroelectric soft mode displacements driven by nonresonant Raman excitation can reverse the Raman polarizability sign (see Fig. 1A) and the second harmonic phase, indicating a ferroelectric reversal. We extend this to tin selenide, a material with complex energy landscapes requiring simultaneous excitation of multiple modes to trigger phase transformation. Using time-domain Raman scattering and time-resolved X-ray diffraction to monitor MIR-excited tin selenide, we observe the suppression of A_g Raman modes beyond a critical MIR field strength (see Fig. 1B), indicating a new phase formation. Reconstructed atomic displacements from structural factor changes show distinct lattice dynamics compared to heat or carrier excitation.

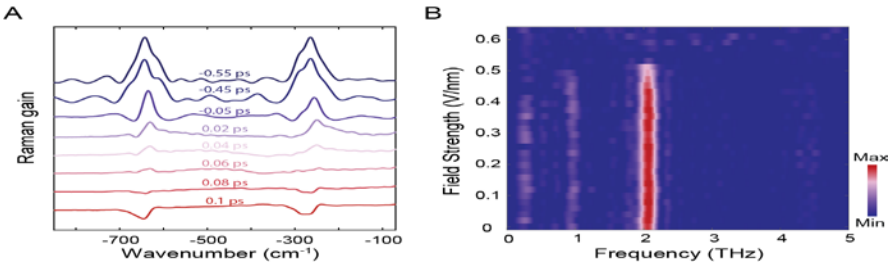

Fig. 1. (A) The FSRS spectrum *of $LiNbO_3$ at varying MIR-FSRS delays shows a reversal in the Raman gain sign.* ***(B)*** *Time-domain Raman scattering of SnSe, measured 12 ps after the MIR arrival, displays abrupt mode suppression beyond a critical MIR field strength.*

Further corroborated with first-principle calculations, this discovery introduces a novel phase control method that goes beyond the conventional resonant excitation approach and unlocks exciting possibilities for facile manipulation of phases and chemical reactivity with complex energy landscapes at reduced energy consumption and ultrafast operation speeds.

References

[1] Y. Yan, J. Gamble, B. Edward, K. Nelson. *Journal of Chemical Physics* **83**, 5391 (1985).
[2] A. Weiner, D. Leaird, G. Wiederrecht, K. Nelson, *Science* **247**, 1317 (1990).
[3] S. Fahy, R. Merlin, *Physical Review Letters* **73**, 1122 (1994).
[4] J. Shi, C. Heide, H. Xu, Y. Huang, Y. Shen,*(to be submitted)* (2024).

Inhomogeneous photosusceptibility of VO_2 films at the nanoscale

A. J. Sternbach
University of Maryland at College Park, College Park, MD 20742, USA

We investigated an inhomogeneous light induced phase transition in vanadium dioxide (VO_2) with around 250 fs temporal resolution and 20 nm spatial resolution. Following homogeneous free-carrier injection, we observe inhomogeneous optical contrast that is interpreted as a signature of transient metallicity. A detailed assessment of the thin film varying the sample temperature, infrared frequencies, pump-probe time delays, fluences and real-space locations are used to assess the origins of the contrast. The energetic cost of producing a metallic state is, notably, found to be inhomogeneous. Our results indicate that the energetic barrier for metallic nucleation is inhomogeneous [1]. Our analysis of the growth rate indicates that the nucleation is likely to be mediated by pre-existing boundaries within our film [2].

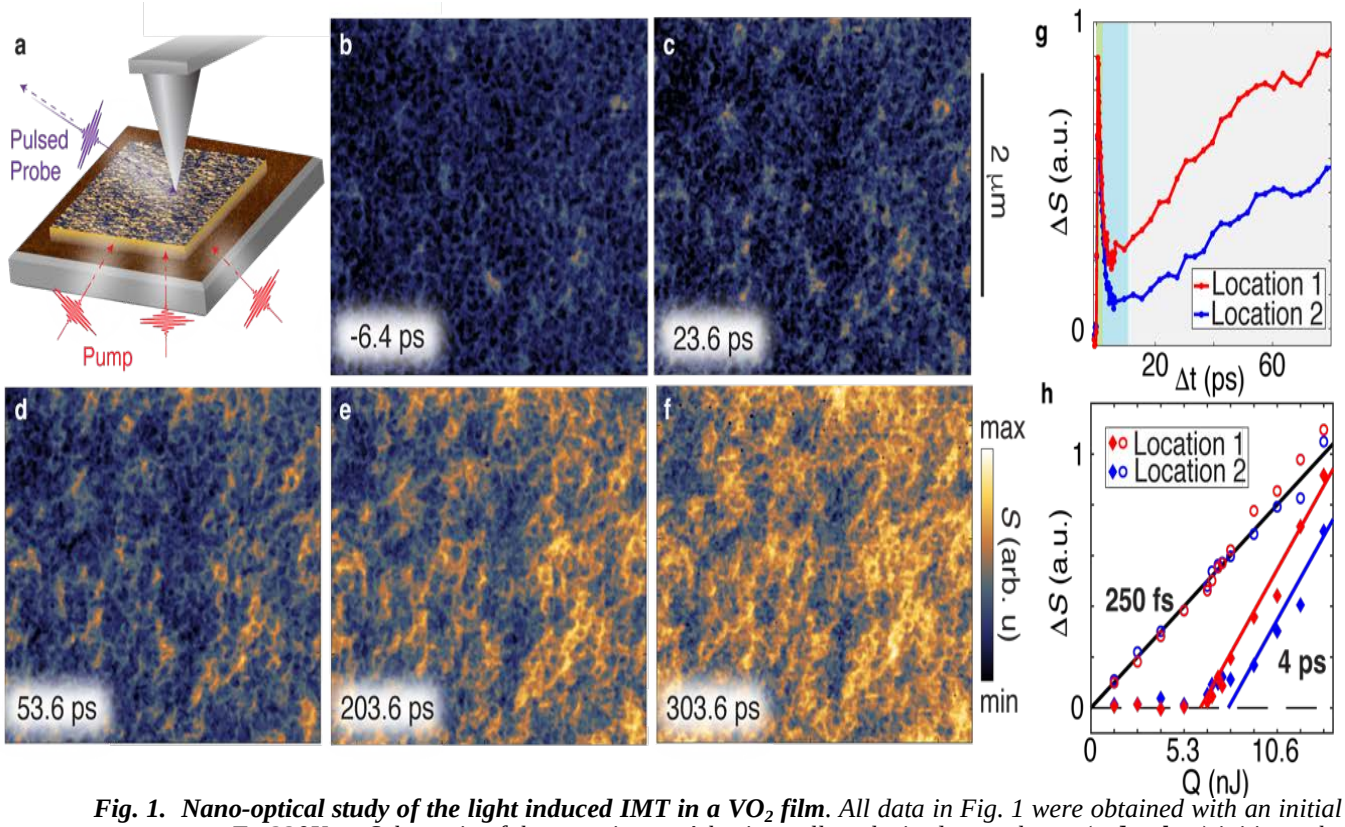

Fig. 1. Nano-optical study of the light induced IMT in a VO_2 film. *All data in Fig. 1 were obtained with an initial temperature T_i=330K.* ***a****, Schematic of the experiment. A horizontally polarized pump beam (**red pulses**) initiates the insulator-to-metal transition. We use a vertically polarized 8 μm wavelength pulsed probe (**purple pulse**) focused on an AFM tip to monitor the local near-field amplitude, S, at a variable time delay, Δt, after photoexcitation. In our experiments, temperature dependent data is obtained by changing the initial (equilibrium) temperature of the sample, T_i, with a heat stage.* ***b-f****, Images of S, using 5.3 nJ of photo-excitation power, obtained* ***b****, before photoexcitation: Δt = -6.4 ps, and* ***c-f****, after photoexcitation:* ***c****, Δt=23.6 ps,* ***d****, Δt=53.6 ps,* ***e****, Δt=203.6 ps,* ***f****, Δt=303.6 ps.* ***g****, Dynamics of the pump induced change of the near-field amplitude ΔS obtained at two representative locations, Location 1 and Location 2 where values of S are near the extremes of high and low contrast observed in panel* ***f****, respectively. The* ***green****,* ***blue****, and* ***gray*** *shaded regions mark the first, second and third stages, respectively, of the three-step response to photoexcitation as described in the main text.* ***h****, Data of ΔS are shown against the photo-excitation energy at the same two locations investigated in panel (**g**). Data collected at Δt=250 fs are shown with open circles, while data obtained at Δt=4 ps are shown with filled diamonds. Note that systematic inhomogeneity observed at Δt=250 fs and above Q_c likely derives from carriers that have abruptly transitioned to the metallic state.*

Our analysis of the growth rate indicates that the nucleation is likely to be mediated by pre-existing boundaries within our film [2].

References

[1] A. J. Sternbach, T. Slusar, F. L. Ruta, S. Moore, X. Chen, M. K. Liu, H. T. Kim, A. J. Millis, R. D. Averitt, D. N. Basov, *Physical Review Letters* **132**, 186903 (2024).
[2] A. J. Sternbach, F. L. Ruta, Y. Shi, T. Slusar, J. Schalch, G. Duan, A. S. McLeod, X. Zhang, M. Liu, M. Liu, A.J. Millis, H.-T. Kim, L.-Q. Chen R. D. Averitt, D. N. Basov, *Nano Letters* **21**, 9052 (2021).

Superoscillatory terahertz waveform shaping for high contrast Sensing and imaging

P. Peng, D.R. Lindberg, G. McCaul, D.I. Bondar, D. Talbayev
Tulane University, New Orleans, LA 70118, USA

Given an optical pulse of a limited bandwidth, can we change its capacity to distinguish between two samples in the linear optical regime by pulse shaping? This general question carries fundamental importance in optical sensing and imaging and is illustrated in Fig. 1a. The same incident pulse $E_0(t)$ passes through the samples 1 and 2 and the transmitted fields $E_1(t)$ and $E_2(t)$ are compared in the time domain. Our task is to maximize a measure of contrast between the fields $E_1(t)$ and $E_2(t)$ by changing the relative amplitudes and phases of the constituent Fourier components of the input pulse $E_0(t)$. We find that there exists a class of waveforms that maximize the time-domain contrast between the pair of samples – the superoscillation waveform, where a band-limited signal oscillates faster than its fastest Fourier component within a limited temporal window. Superoscillations appear in the windows of destructive interference between the constituent harmonics of the waveform, Fig. 1b. Our results indicate that superoscillations enable a new functionality in linear optical sensing – the 100-fold enhancement in the optical contrast of the terahertz wave passing through two similar samples. We observe the 100-fold contrast enhancement both in our numerical simulations with Gaussian time-domain harmonics and in our experimental realization with narrow-band quasi-sinusoidal terahertz harmonics. The current experimental results have been made possible by our group's recent synthesis of time-domain terahertz superoscillations [1].

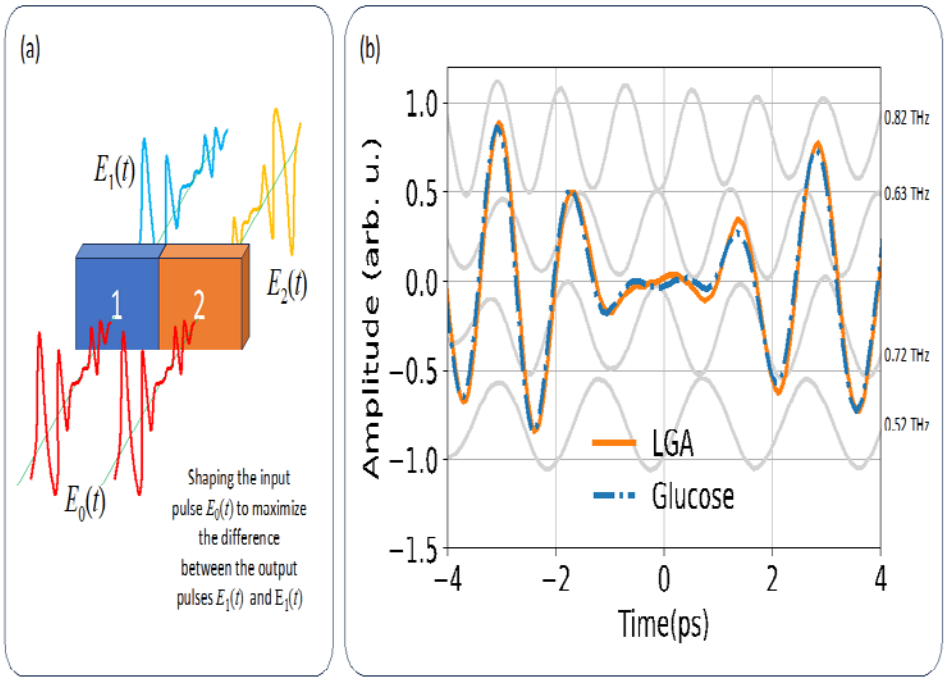

***Fig. 1. (a)**: **Illustration of the main question:** can we shape the input optical field $E_0(t)$ to maximize the contrast in the time domain between the output fields $E_1(t)$ and $E_2(t)$ that pass through the optically similar samples 1 and 2? The output fields are determined by the linear optical properties of the two samples.*
***(b)**: Transmitted superoscillatory waveforms for two samples of molecular crystalline materials, L-Glutamic acid (LGA) and anhydrous a-D-Glucose (glucose). The superoscillations appear in the 1.2-ps interval centered on the time axis origin. The gray quasi-sinusoidal waves shown in the background display the four constituent fundamental harmonics of the transmitted waveforms. Superoscillations maximize the contrast between the full transmitted waveforms within the 1.2-ps window of destructive interference.*

Out findings carry potentially profound implications for the imaging applications of THz technology – the improved contrast would be highly beneficial for tumor diagnostics and visualization using THz light in the medical field, among others. In addition, the significant increase in contrast happens in a very short observation window. This means that we can drastically shorten the time needed to construct an image with good level of contrast, which is advantageous for in-vivo imaging because it can minimize problems caused by extended imaging time, such as occlusion effects.

Reference

[1] G. McCaul, P. Peng, M. Ortiz Martinez, D. R. Lindberg, D. Talbayev, D. I. Bondar, *Physical Review Letters* **131,** 153803, (2023).

* Acknowledgement: authors acknowledge the generous support from the W.M. Keck Foundation.

Commissioning results from the ASU compact X-ray source

S.W Teitelbaum[1], S.Tilton[1], L.Malin[1], E. Adamo[1], G.Babic[1], T. Brown[1], R. DeMott[1], A.Dupre[1], K. Eckrosh[1]
D.Smith[1], J.Houkal[1], J.Vela[1], R.Jaswal[1], A.Seemaan[1], S.R, Rendour[1], S Jachim[1], E Ros[1], A Martinez[1]
R.Larsen[1], H.Loos[2], H.S. Lee[1], A.Gardeck[1], S.G.E.Tantawi[2], R.Kaindl[1], P.Fromme[1], A.Sandhu[3], M.R. Holl[1]
W.S. Graves[1]

[1]*Arizona State University, Tempe AZ 75287, USA*
[2] *SLAC National Accelerator Laboratory, Menlo Park, CA 94025, USA*
[3]*University of Arizona, Tucson AZ 85721, USA*

Bright sources of sub-picosecond hard x-rays such as x-ray free electron lasers (XFELs) have revealed new details of atomic structure, and materials dynamics [1,2]. However, the cost and scale of these facilities is prohibitive for routine use at research institutes such as universities, and limits the scope and impact of these sources, and to date, there are only five hard x-ray free electron lasers (XFELs) worldwide. Inverse Compton Scattering (ICS) is a promising approach to developing scalable ultrafast x-ray sources at a much lower cost per facility than full-scale x-ray free electron lasers (XFELs), filling a key parameter area of light sources between single-user rotating anode x-ray sources and large user facilities like synchrotrons and FELs. ICS-based x-ray sources use the oscillating electromagnetic field of a laser to replace the magnetic undulators at synchrotrons and XFELs. Optical wavelengths are four orders of magnitude shorter than a typical magnetic undulator period (microns vs cm) which reduces the electron beam energy (and concomitant accelerator cost), by orders of magnitude. ICS sources are flexible depending on the desires of the end user, accommodating ultrashort pulses[3], synchrotron-like quasi-CW radiation [4], or high energy x-rays[5].The ASU Compact x-ray light source (CXLS) is an inverse Compton scattering (ICS) source focused on producing ultrafast x-ray pulses for applications in structural biology, biomedical imaging and materials science research. The source is based on an X-band linac that accelerates to electrons to 30 MeV electrons. These electrons collide with a 200 mJ, 1 kHz thin-disk laser to produce hard x-rays rays in the 4-19 keV energy range via ICS. Here, we present the laser systems design, commissioning results, and first application areas from the CXLS. In this presentation, we present the latest results and diagnostic tools developed for the production of first light, and designs for a future light source based on a similar concept. At present, the CXLS produces $>10^9$ photons/second over its full bandwidth, with full-scale operation expected to exceed 10^{10} photons/second at the source point. The average flux of this source is comparable to a bend magnet beamline flux at a synchrotron, or ~1% of the on-target average flux of a monochromatized, copper-linac based XFEL (e.g. LCLS, SACLA, SwissFEL) [6.7]. The source is compact, with an accelerator approximately ten meters long. The entire facility, including laser systems, microwave power supplies, accelerator, endstations, and support labs, fits in a 1,000 m^2 university laboratory space.The CXLS uses two Yb-based laser amplifier systems, both seeded by the same 72 MHz oscillator (light conversion Flint). The first amplifier is a Light Conversion Pharos system, producing 1.03 mJ at 1 kHz, with a central wavelength of 1030 nm. The unit has a built in fourth harmonic module that produces >100 uJ of 257 nm radiation for use in a photocathode. The laser system used for ICS is a 200 mJ, 1 kHz, 1.5 ps thin-disk Yb regenerative amplifier (Trumpf DIRA 200-1). The amplifier is seeded by a 10.27 MHz fiber preamplifier that is in turn seeded by the excess output of the Pharos built-in oscillator, after bending down-counted to the 7th subharmonic from 72 MHz to 10.27 MHz, chirped to 100 ns, and transported to the laser room via an armored fiber cable. A regenerative amplifier amplifies the chirped pulses to up to 208 mJ, before they are compressed to 1.5 ps pulses, with >145 mJ transported to the interaction point. The pulse is transported via a vacuum pipe to the accelerator vault, where it is focused to a 10 micron waist and collides with the focused electron beam to produce x-rays. The x-rays are then collimated by a multilayer Montel mirror with a 10 mrad acceptance aperture and a 3% relative energy bandwidth. Both amplifiers are synchronized against thermal drift via a cross-correlation system with feedback to a delay within the regenerative amplifier cavity. Beam steering fluctuations during transport for the ICS laser are corrected using a dual-camera feedback system. We discuss further developments for long-term beam stabilization, diagnostics and feedback.X-rays generated by the collision are observed with a Ce:YAG scintillator screen located just after the electron-laser collision point (Fig.2(b)). The x-ray beam has an RMS divergence of 10 mrad, and a source size of 3-5 μm RMS, primarily determined by the focused laser spot size.In conclusion, we demonstrate an ICS-based hard x-ray source with a compact (~10-meter) form factor that produces sufficient flux for time-resolved hard x-ray experiments. This source also serves as a prototype for a fully spatiotemporally coherent XFEL under construction.

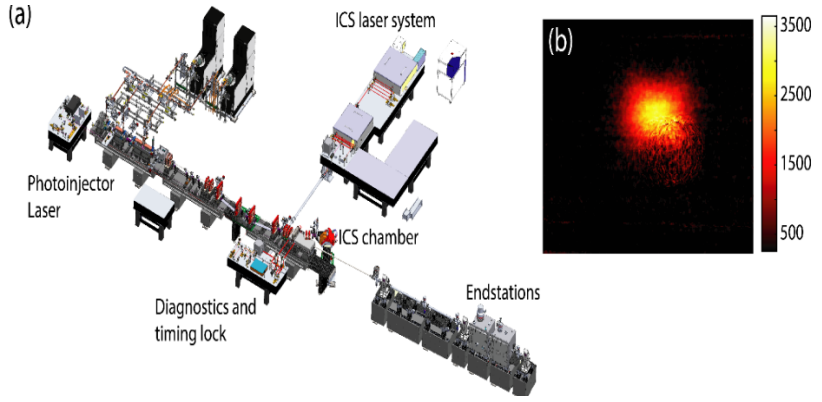

Fig. 1: (a) Layout of the key components of the ASU CXLS*. The accelerator (center) is powered by two 6 MW modulators (**top left**) and sourced with the 4th harmonic of a 1030 nm Yb laser (**left**). The electron beam collides with an ICS laser (**top**) to produce x-rays that are transported through a shield wall to the end stations (right). (b) Image of the x-ray beam on a scintillator screen approximately 300 mm from the source point.*

The next-generation compact XFEL(CXFEL) will use emittance exchange combined with nanopatterned silicon gratings to produce microbunched electron beams. Inverse Compton scattering from the microbunched beam enables a fully spatiotemporally coherent, few-meter-scale XFEL lasing in the soft x-ray regime (250 eV - 2.5 keV).

References
[1] C. Pellegrini, *Physica Scripta* **T169**, 014004 (2016).
[2] A. Ishchenko, C. Gati, V. Cherezov, *Current Opinion in Structural Biology* **51**, 44 (2018).
[3] W.S. Graves, W. Brown, F.X. Kaertner, D. E. Moncton, *Nuclear Instruments and Methods in Physics Research Section A: Accelerators, Spectrometers Detectors and Associated Equipment* **608**(1), S103 (2009).
[4] B. Hornberger, J. Kasahara, M. Gifford, R. Ruth, R. Loewen, *Proceedings of SPIE* **11110**, 11110-03(2019).
[5] S. Chen, N. D. Powers, I. Ghebregziabher, C. M. Maharjan, C. Liu, G. Golovin, S. Banerjee, J. Zhang, N. Cunningham, A. Moorti, S. Clarke, S. Pozzi D. P. Umstadter, *Physical Review Letters* **110**, 155003 (2013).
[6] D. Zhu, A. Robert, T. Henighan, H.T. Lemke, M. Chollet, J.M. Glownia, D. A. Reis, M. Trigo, *Physical Review* B **92**, 054303 (2015).
[7] D. Zhu, Y. Feng, S. Stoupin, S.A. Terentyev, H.T. Lemke, D.M. Fritz, M. Chollet, J.M. Glownia, R. Alonso-Mori, M. Sikorski, S. Song, T.B. van Driel, G. J. Williams, M. Messerschmidt, S. Boutet, V.D. Blank, Y.V. Shvyd'ko, A. Robert, *Review of Scientific Instruments* **85**, 063106 (2014).
* Acknowledgements: The authors acknowledge support from NSF grants No. 2153503 and 1935994.

All-optical discovery of ferro-rotational density wave in RTe3

Y. Wang[1], B. Singh[2], K. Burch[2]
1 Columbia University, New York, NY 10025
2 Boston College, Chestnut Hill, MA 02467

Detecting unconventional density waves and identifying their underlying mechanisms has been a significant challenge. In this talk, I will present the discovery of a rare ferro-rotational charge density wave (CDW) order arising from orbital modulation, which involves a nontrivial order parameter. Utilizing Raman spectroscopy and quantum interference, we have revealed the first Axial Higgs mode from CDW GdTe3[1]. Further experiments with Raman and Second Harmonic Generation (SHG) of Rare-Earth Tritellurides series materials demonstrate that the axial Higgs mode breaks all vertical mirror symmetries while retaining inversion symmetry. Additionally, SHG and Muon Spin Rotation (Mu-SR) experiments confirm the absence of time-reversal symmetry breaking. This phenomenon can be explained by an uncommon combination of orbital and charge order, attributed to the unique quantum geometry of Rare-Earth Tritellurides.

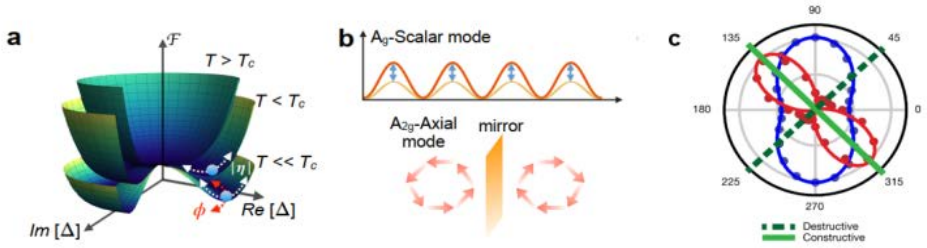

Fig. 1. a Free energy versus CDW order parameter components. b *Diagram of the conventional- (scalar) and unconventional- (axial) CDW amplitude mode.* ***c*** *Angular dependence of the CDW amplitude mode of the Raman modes extracted from Voigt fits of thespectra in parallel (**blue dots**) and cross (**red dots**) linear polarization.*

I will also discuss how this discovery establishes Higgs spectroscopy as a powerful tool to reveal unconventional orders and the potential for controlling experiments to both probe and unlock new states in these materials.

References
[1] Y. Wang, I. Petrides, G.McNamara, Y. Wang, I. Petrides, G. McNamara, M. M. Hosen, S. Lei, Y.-C. Wu, J. L. Hart , H. Lv, J. Yan, D. Xiao, J. J. Cha P. Narang, L. M. Schoop, K.S. Burch,. *Nature* **606**, 896 (2022).
* Acknowledgement(s): This work was primarily supported by the AFOSR under Grant No. FA9550-20-1-0282. Some Raman experiments were enabled by equipment provided through AFOSR DURIP award FA9550-20-1-0246. Work by GM and MG was supported by the NSF, Award No. DMR-200334 and DMR-2310895. PS and VP are grateful for the support of the DoE, Office of Basic Energy Sciences under award number DE-SC0018675.

THz optoelectronics and ultrafast dynamics of layered Topological semimetals

J. Xiao
University of Wisconsin-Madison, Madison, WI 53706, USA

The emergent atomically thin layered materials enable the unique control of new phases of matter for high-performance electronics and optoelectronics. One remarkable example is the recent discovered nonlinear Hall effect (NLHE) in topological semimetals, which is mediated by their diverging quantum geometrical properties [1-3]. In this talk, I will report how we leverage this new notion for high-performance THz optoelectronics and ultrafast electronics. Firstly, I will show our recent demonstration on high-performance THz sensing devices based on those new discovered effects [4]. In particular, we investigate the NLHE response in THz regime on a layered type-II Weyl semimetal in both noninteracting state and correlated state.

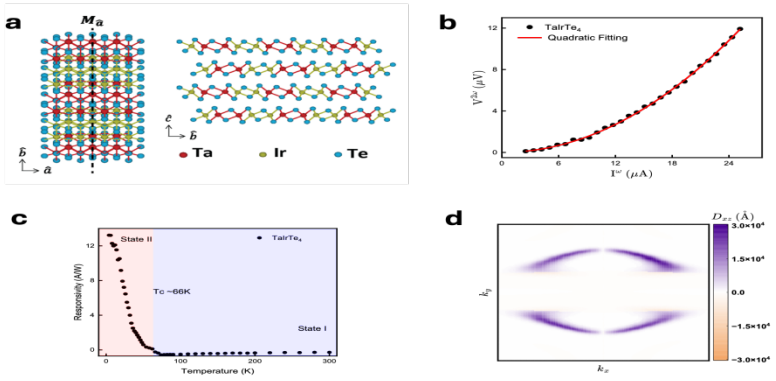

Fig. 1. (a) *Top and side views for crystal structure of few-layer $TaIrTe_4$. The lack of the screw-axis and glide-plane symmetries at few-layer limit allows an in-plane polar axis along the mirror line for nontrivial in-plane nonlinear Hall effect.* ***(b)*** *Large nonlinear hall effect of a bilayer $TaIrTe_4$ at 300K.****(c)*** *Temperature dependent large THz photoresponsivity of a bilayer $TaIrTe_4$ device.* ***(d)*** *Calculated local Berry curvature dipole distribution for the proposed correlated charge ordering.*

Leveraging a custom-designed and in-house fabricated plasmonic photosensing device, we attained ultra-large and tunable photoresponsivity in this atomically thin topological semimetal. Moreover, the intrinsic response time is down to picosecond level.

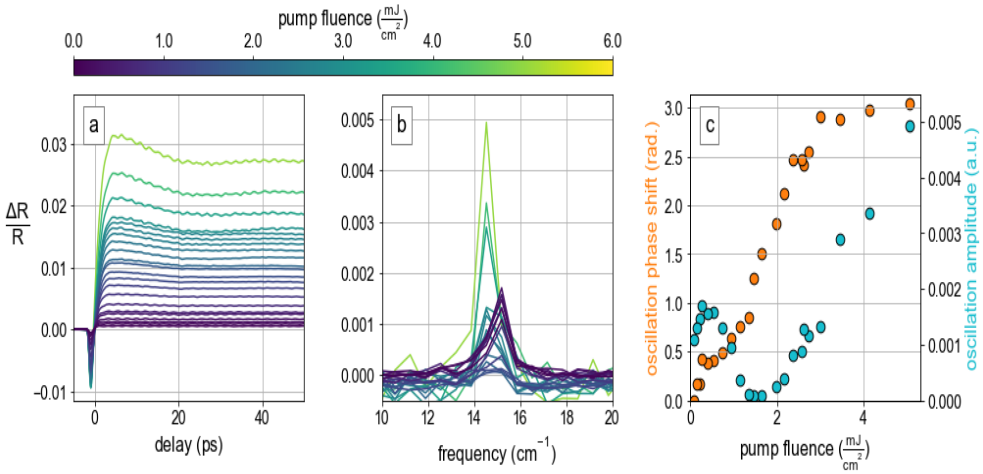

Fig. 2. Ultrafast structural dynamics of $TaIrTe_4$ at room temperature. *Fluence dependence of* ***(a)*** *and* ***(b)*** *obeys shared colorbar.* ***a)*** *800nm transient reflectance following 1300nm pump.* ***b)*** *Fluence dependence of low frequency shear mode extracted by Fourier transforming the oscillatory component of* ***(a)****.* ***c)*** *phase (orange) and amplitude (cyan) fluence dependence of the shear mode.*

Our findings illuminate a new mechanism for low-energy photon harvesting and transduction via quantum properties. Along this line, I will report the ultrafast structural and electronic ordering dynamics of those topological semimetals to show their potential for ultrafast electronics [5, 6].

References

[1] Q. Ma, S.-Y. Xu, H. Shen, D. Macneill, V. Fatemi, T.-R. Chang, A. M. M. Valdivia, S. Wu, Z. Du, C.- H. Hsu, S. Fang, Q. D. Gibson, K. Watanabe T. Taniguchi, R.J. Cava, E.Kaxiras, H.-Z. Lu, H. Lin, L. Fu, N. Gedik, P. Jarillo-Herrero, *Nature* **565**, 337 (2019).
[2] K Kang, T. Li, E. Sohn, J Shan, K. F Mak, *Nature Materials* **18**, 324 (2019).
[3] J. Xiao, Y. Wang, H. Wang, C. D. Pemmaraju, S. Wang, P. Muscher, E. J. Sie, C. M. Nyby, T. P. Devereaux, X. Qian, X. Zhang, A. M. Lindenberg *Nature Physics* **16**, 1028 (2020).
[4] T. Xi, H. Jiang, J. Li, Y. He, Y. Gu, C. Fox, Y. Mao, J. Rollins, T. Taniguchi, K. Watanabe, D. van der Weide, D. Rhodes, Y. Zhang, Y. Wang, J. Xiao *submitted*, (2024).
[5] D.Lafayette, *submitted,(* 2024).
[6] F. Fan, T. Xi, J. Li, C. Fox, Y. He, J. Rollins, T. Taniguchi, K. Watanabe, D. Rhodes, Y. Zhang, J. Xiao (to be submitted, 2024).
* Acknowledgement(s): J. X. acknowledge support the ONR through Grant N00014-24-1-2068. J.X. acknowledge the additional support from the NSF under Grant No. DMR-2237761 and under Grant No. DMR-2309000.

Quantifying transient structure and phonon evolution in Photoinduced transitions by MeV ultrafast electron diffraction

C. Xu[1], P. Liu[1], D. Xiang[2], D.Qian[2], A. Zong[1]
[1]Stanford University, Stanford, CA 94305, USA
[2]Shanghai Jiao Tong University, Shanghai 200240, China

Photoinduced phase transitions in quantum materials, especially those at high photoexcitation densities, often involve a transient modification of the lattice structure and phonon population [1–5]. A precise determination of the lattice and phonon dynamics is hence instrumental in understanding the nature of the transient state and in unraveling the intricate couplings between different degrees of freedom that lead to the equilibrium ground state. Such is the case of the photoinduced insulator-to-metal transition in VO_2 [1,3,5–7]. In equilibrium, the change in its electrical conductivity upon heating coincides with a monoclinic (where V atoms are dimerized) to tetragonal lattice change [8]. After photoexcitation, distinct evolutions of electronic and lattice structure were observed, motivating a plethora of experimental works in mapping out the transient state [1,7,9–13], where a metastable monoclinic metastable state may be present [7].

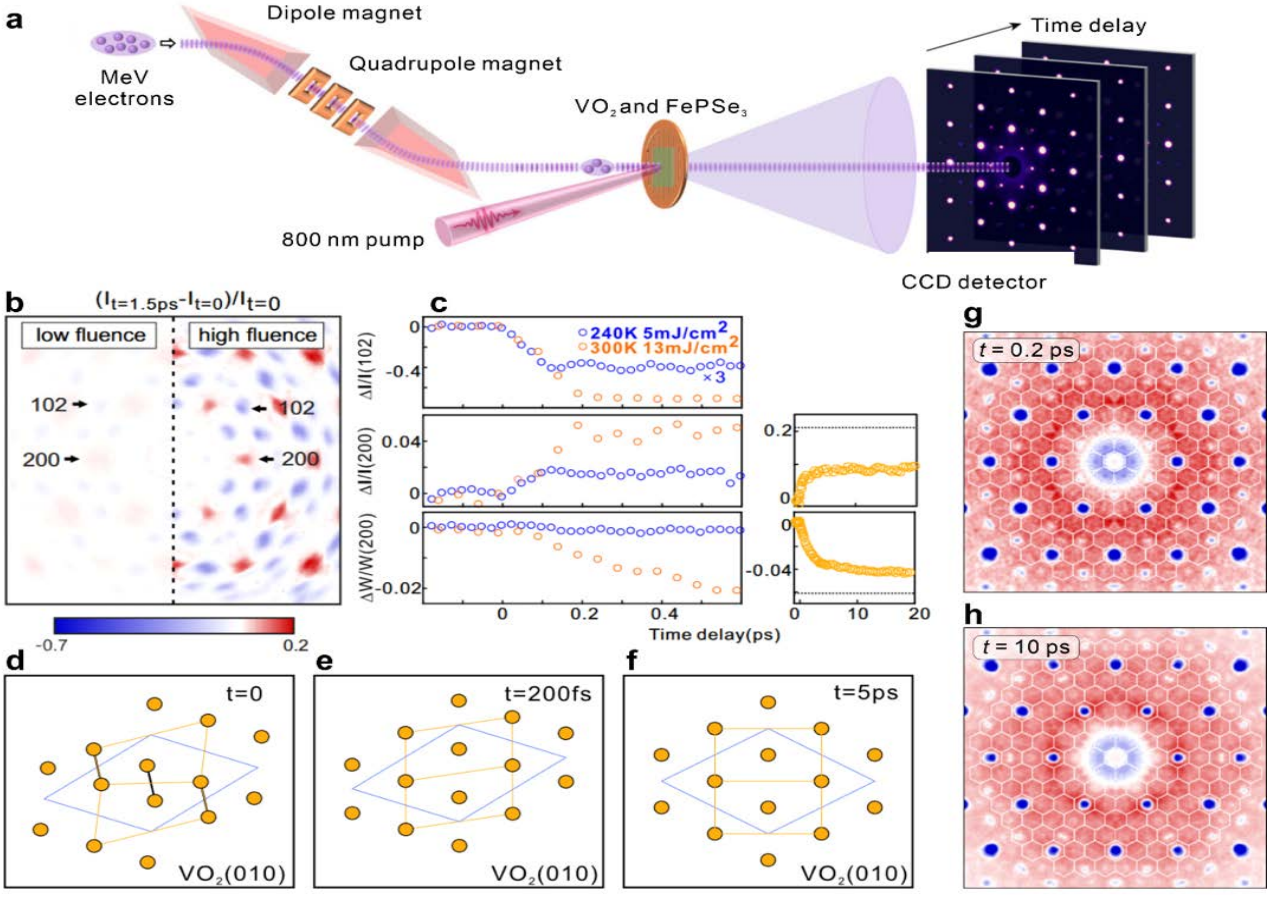

Fig. 1. a. Schematic of the MeV ultrafast electron diffraction setup*, where a double-bend achromatic lens consisting of a pair of dipole magnets and three quadrupole magnets are used to compress the electron pulse and to reduce the timing jitter* [19]*.* ***b****. Differential electron diffraction intensity at t = 1.5 ps after photoexcitation under a low fluence (5 mJ/cm^2 at 240 K) and a high fluence (13 mJ/cm^2 at 300 K).* ***c****.* ***Left:*** *Time evolution of the intensity for (102) peak (top), (200) peak (middle), and width of (200) peak (bottom).* ***Right:*** *Data up to 20 ps for the intensity of 200 peak and the width of 200 peak under a high fluence. The black dashed line marks the level of relative change when a 100% M_1-R transition occurs based on the thermal transition data.* ***d–f****. Schematic of the monoclinic M_1 phase with V–V dimers and zigzag chains at t = 0 (**d**), transient monoclinic structure without V–V dimers and zigzag chains at t = 200 fs (**e**), and the R phase at t = 5 ps (**f**). Orange dots represent the projected positions of V atoms on the (010) plane. Black lines represent the V–V dimers. Orange lines are a guide for the eyes. Blue quadrilateral indicates the unit cell using M_1-phase's representation* [6]*.* ***g, h****. Nonequilibrium electron diffuse scattering of $FePSe_3$ at 0.2 ps (**g**) and 10 ps (**h**).*

However, despite intense efforts, the atomic pathway during the phase transition remains hotly debated, where issues such as transition timescale [1,5,7,10,12,14] and complications caused by polycrystallinity [7,10] and transient heating [15] present additional challenges in nailing down the lattice evolution during the electronic transformation. In the first part of the talk, I will discuss our recent efforts in synthesizing freestanding quasi-single-crystal VO_2 films, whose photoinduced structural dynamics was investigated via MeV ultrafast electron diffraction [6] (Fig. 1a-b).By focusing on a large number of Bragg peaks in the MeV electron diffraction pattern, we observed that the disappearance of vanadium dimers and zigzag chains does not coincide with the transformation of crystal symmetry. After photoexcitation, the initial structure (Fig. 1c) is strongly modified within 200 fs, resulting in a transient monoclinic structure without vanadium dimers and zigzag chains (Fig. 1d). Then, it continues to evolve to the final tetragonal structure in approximately 5 ps (Fig. 1f). In addition, only one laser fluence threshold for different Bragg peaks was observed instead of two thresholds suggested in polycrystalline samples previously [7], demonstrating the absence of the monoclinic metallic state in our quasi-single crystalline samples.

In the second part of my talk, I will shift focus from Bragg peaks to diffuse scattering signals in between the Bragg peaks, which offer a momentum-resolved view of nonthermally populated phonons induced by photoexcitation. Here, we examined $FePSe_3$, a van der Waals antiferromagnet that demonstrates strong spin-lattice coupling, which, in equilibrium, manifests as chiral phonons that couple selectively to magnons of the same chirality [16], a strain-tunable symmetry-breaking zigzag antiferromagnetic order [17], and the concomitance of lattice collapse, spin quenching, and superconductivity under pressure [18]. Thus, investigating the photoinduced phonon dynamics in $FePSe_3$ via diffuse scattering offers an opportunity to disentangle the spin and lattice degrees of freedom, clarifying the microscopic mechanism behind spin-lattice interactions. By leveraging the high signal-to-noise ratio and high temporal resolution in MeV electron diffraction, a clear change in the diffuse pattern was observed from 0.2 ps to 10 ps (Fig. 1f-g), giving us an atomistic view of the phononic response and helping us understand the out-of-equilibrium coupling between spin and phonon when antiferromagnetism is transiently suppressed.Our experiments illustrate the need for a quantitative description of lattice and phonon responses in describing photoinduced phase transitions of correlated systems, highlighting the exciting opportunities offered by high-energy electron diffraction in investigating phonon-related interactions in a broad range of quantum materials.

References

[1] P. Baum, D.-S.Yang, A.H. Zewail, *Science* **318,** 788 (2007).
[2] A. Zong, A.Kogar, Y.-Q. Bie, T. Rohwer, C. Lee, E. Baldini, E. Ergecen, M. B. Yilmaz, B. Freelon, E. J. Sie, H. Zhou, J. Straquadine, P.Walmsley P. E. Dolgirev,A.V. Rozhkov,I.R. Fisher,P.Jarillo-Herrero,B. V. Fine, N.Gedik, *Nature Physics* **15,** 27 (2019).
[3] S. Wall, S. Yang, L. Vidas, M. Chollet, M. Glownia, M. Kozina, T. Katayama, T. Henighan, M. Jiang, T.A. Miller, D.A. Reis, L.A. Boatner, O. Delaire M. Trigo, *Science* **362**, 572 (2018).
[4] Y. Cheng, A. Zong, L. Wu, Q. Meng, W. Xia, F. Qi, P. Zhu, X. Zou, T. Jiang, Y. Guo, J.van Wezel, A.Kogar, M.W. Zuerch, J.Zhang, Y. Zhu, D,Xiang *Nature Physics* **20, 54 (2024).**
[5] J. Li. L.Wu.S.Yang, X.Jin.W.Wang, J.Tao, L.Boatner.M.Babzien.M.Fedurin.M.Palmer. W.Yin. O.Delaire.Y.Zhu.*Phvsical Review* X **12**.021032 (2022)
[6] C. Xu, C Jin, Z Chen, Q Lu, Y Cheng, B Zhang, F Qi, J Chen, X Yin, G Wang, D Xiang, D Qian, *Nature Communications* **14,** 1265 (2023).
[7] V. R Morrison, RP Chatelain, KL Tiwari, A Hendaoui, A Bruhács, M Chaker, BJ Siwick, *Science* **346,** 445 (2014).
[8] F. J. Morin, *Physical Review Letters* **3**, 34 (1959).
[9] A. S. Johnson, D. Perez-Salinas, K.M. Siddiqui, S. Kim, S. Choi, K. Volckaert, P.E. Majchrzak, S. Ulstrup, N. Agarwal, K. Hallman, R.F. Haglund Jr. C. M. Günther, B. Pfau, S. Eisebitt, D. Backes, F. Maccherozzi, A. Fitzpatrick, S. S. Dhesi, P. Gargiani, M. Valvidares, N. Artrith, F.de Groot, H. Choi D. Jang, A. Katoch, S. Kwon, S.H. Park, H. Kim, S.E. Wall, *Nature Physics* **19,** 215 (2023).
[10] A. Sood, X.Shen,Y.Shi,S.Kumar,S. J. Park, M. Zajac,Y.Sun, L.-Q.Chen, S.Ramanathan,X.Wang,W.C.Chueh,A.M.Lindenberg, *Science***373**, 352(2021)
[11] D. Wegkamp, M. Herzog, L.Xian, M.Gatti, P. Cudazzo, C.L. McGahan, R.E. Marvel, R. F.Haglund,Jr. ,A. Rubio, M. Wolf, J.Stahler, *Physical Review Letters* **113**. 216401 (2014).
[12] A. Cavalleri, T. Dekorsy, H.H.W. Chong, J.C. Kieffer, R.W. Schoenlein, *Physical Review* B **70,** 161102 (2004).
[13] M. F. Jager, C. Ott, P. M. Kraus, C. J. Kaplan, W. Pouse, R. E. Marvel, R. F. Haglund, D. M. Neumark,S. R. Leone, *Proceedings of the National Academy of Sciences* **114**, 9558 (2017).
[14] M. R.Otto, L. P. R. de Cotret, D. A. Valverde-Chavez, K. L. Tiwari, N. Émond, M.Chaker, D. G. Cooke, B. J. Siwick, *Proceedings of the National Academy of Sciences* **116**, 450 (2019).
[15] L. Vidas, D. Schick, E. Martínez, D. Perez-Salinas, A. Ramos- Álvarez, S. Cichy, S. Batlle-Porro, A. S. Johnson, K. A. Hallman, R. F. Haglund, Jr. S. Wall, *Physical Review* X **10**. 031047 (2020).
[16] J. Cui, E. V. Boström, M. Ozerov, F. Wu, Q.Jiang, J.H. Chu, C. Li, F. Liu, X. Xu, A. Rubio, O. Zhang, *Nature Communications* **14**, 3396 (2023).
[17] K. Hwangbo, E. Rosenberg, J. Cenker, Q. Jiang, H. Wen, D. Xiao, J.H. Chu, X. Xu, arXiv:2308.08734,(2023).
[18] Y. Wang, J. Ying, Z. Zhou, J. Sun, T. Wen, Y. Zhou, N. Li, Q. Zhang, F. Han, Y.Xiao, P.Chow, W. Yang, V.V. Struzhkin, Y.Zhao,H-K.Mao, *Nature Communications* **9**, 1914 (2018).
[19] Y. Cheng, A. Zong, J. Li, W.Xia, S. Duan, W. Zhao, Y.Li, F. Qi,J.Wu,L.Zhao, P.Zhu, X.Zou, T. Jiang, Y. Guo, L.Yang, D. Qian, W.Zhang, A.Kogar M. W. Zuerch, D. Xiang, J. Zhang, *Nature Communications* **13**, 963 (2022).

Ab initio description for propagation and dephasing in Ultrafast and nonlinear photonics

K. Yabana
University of Tsukuba, Tsukuba 305-8577, Japan

Theoretical and computational description of light-matter interactions fall into two main approaches. One is numerical electromagnetics, which solves the macroscopic Maxwell equations where properties of matters are considered in terms of dielectric functions. The other is first-principles quantum mechanical methods for calculating dielectric functions. The separation of electromagnetism (EM) and quantum mechanics (QM) is justified by the two conditions: The electromagnetic field of light is sufficiently weak that the perturbation theory of quantum mechanics can be used to interaction between electrons and electromagnetic fields. The material through which the light propagates is sufficiently large to allow a coarse-grained approximation. However, in current frontiers of optical science, numerous developments have occurred in those areas where EM and QM cannot be separated. For example, interaction of strong laser pulse with matter causes extremely nonlinear phenomena such as high harmonic generations. In the interaction of nanostructures and pulsed light, nonlocal responses caused by quantum effects in nanostructures are often significant. We have been developing a theoretical and computational method in which EM and QM are combined directly. Employing first-principles time-dependent density functional theory (TDDFT) for electronic dynamics, we have succeeded to describe light propagation of extremely strong pulsed light and/or in nanostructures [1,2]. The method has been implemented in an open-source software SALMON that has been developed by the authors' group [3]. Fig,1(a) summarizes our theoretical and numerical method [4].

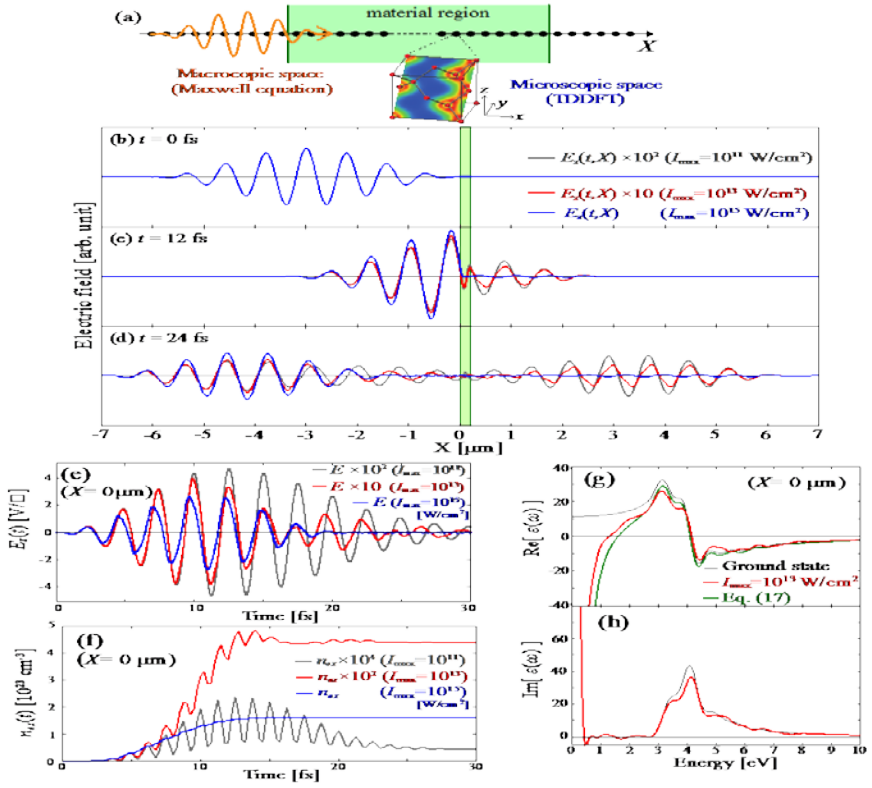

Fig. 1. Overview of multiscale Maxwell-TDDFT calculation*. A pulsed light irradiates normally on Si thin film of 200nm thickness.*
(a) *Grid system for light propagation.*
(b-d) *Snapshots of light propagation.*
(e) *Electric field and* ***(f)*** *number of excited electrons at the front surface of the thin film.* ***(g-h)*** *Dielectric function at the front surface after the pulsed light exited. Taken from [4]*

We describe one-dimensional light propagation through a thin film of dielectrics by solving Maxwell equation (one-dimensional wave equation) for the vector potential $A(X,t)$, employing a uniform grid for X-coordinate. At each grid point of X, we consider electronic motion and describe it employing time-dependent Bloch orbitals, $u_{nkX}(r,t)$. We note that this Bloch orbital depends on the grid index X. The time-evolution of the Bloch orbitals is described by the time-dependent Kohn-Sham equation, the basic equation of TDDFT.

Electronic motion is caused by the vector potential $A(X,t)$, and the macroscopic current at X is calculated from the Bloch orbitals $u_{nkX}(r,t)$. In this way, we can describe light propagation and electronic dynamics simultaneously by solving the coupled equations of Maxwell and TDDFT. Since two grid systems of different resolutions are used, we call it multiscale method. Figure 1(b-d) describe typical calculations for the light propagation of a pulsed light of several intensities through a silicon (Si) thin film of 200nm thickness. In Fig. 1(b), the electric field of the initial pulse that locates in front of the film is shown where the film is exhibited as a thin green area. The pulse is set as the average frequency of $\hbar\omega$ = 1.55eV, below the direct bandgap of Si. In Fig. 1(d), a snapshot of the electric field at t = 24 fs is shown. It is observed that the nonlinear effects appear more significantly in the transmitted pulse than in the reflected pulse. Fig. 1(e-h) show typical physical quantities that are obtained from this calculation. Fig. 1(f) shows the excited carrier density and Fig. 1(g) and (h) show the real and the imaginary parts of the dielectric function at the front surface of the thin film after the pulse exited.

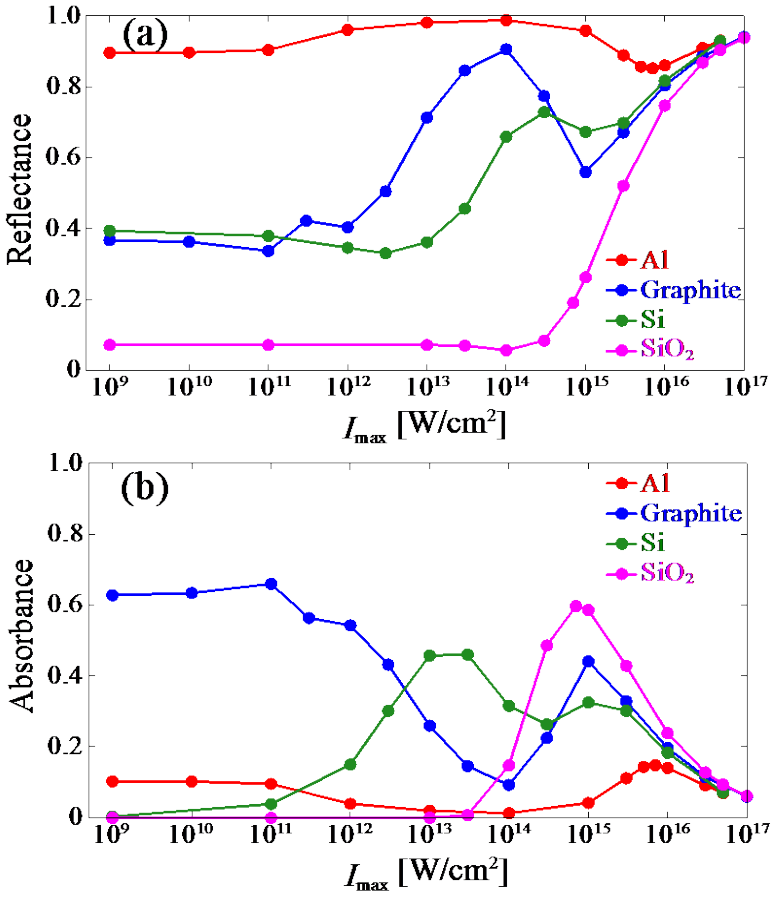

Fig. 2. *(a) Reflectance and (b) absorption for a pulse irradiation of thin films of Al, graphite, Si and SiO_2. Taken from [4]*

Fig, 2 shows a typical result of multiscale Maxwell-TDDFT calculation [4]. In ordinary optics, optical response of materials varies widely from material to material, reflecting their band structure. However, in the response to extremely intense pulsed light, it has been well recognized that all materials show total reflection by the plasma. We have systematically investigated how the optical response of various materials changes when the maximum intensity of the pulsed light increases. Fig. 2(a) and (b) show the reflectance and absorbance of a 50-200 nm-thick thin films irradiated normally with a linearly-polarized pulsed light of 1.55eV frequency, with the maximum intensity of the pulses on the horizontal axis. At sufficiently low intensities, the optical response is linear and is described by a dielectric function, as expected. As the intensity increases, multiphoton or saturable absorption takes place. At around 10^{15} W/cm^2, all materials show strong absorption and plasma reflections follow at further strong intensities.

I will discuss nonlinear behavior in the propagation of intense pulsed light, in particular, for high harmonic generations from semiconductor solids [5] in addition to the systematic behavior described above. I also pay attention to the ab initio description of dephasing effect. Thermal and zero-point motion of ions is considered to be responsible for the dephasing effects that has the typical time scale of 10 fs. It can be described by ab initio calculations using large supercell [6]. We examine such effects in linear and nonlinear regimes.

References

[1] K. Yabana, T. Sugiyama, Y. Shinohara, T. Otobe, G.F. Bertsch, *Physical Review* B **85**, 045134 (2012).
[2] S. Yamada, M. Noda, K. Nobusada, K. Yabana, *Physical Review* B **98**, 245147 (2018).
[3] M. Noda, S.A. Sato, Y. Hirokawa, M. Uemoto, T. Takeuchi, S. Yamada, A.Yamada, Y.Shinohara, M. Yamaguchi, K. Iida, I. Floss, T. Otobe K.-M. Lee K. Ishimura, T. Boku, G.F. Bertsch, K. Nobusada, K. Yabana, *Computer Physics Communications* **235**, 356 (2019).
[4] A. Yamada, K. Yabana, *Physical Review* B**109**, 245130 (2024).
[5] S. Yamada, T. Otobe, D. Freeman, A. Kheifets, K. Yabana, *Physical Review* B**107**, 035132 (2023).
[6] D. Freeman, A. Kheifets, S. Yamada, A. Yamada, K. Yabana, *Physical Review* B**106**, 075202 (2022).

Tracking ultrafast non-local charge dynamics in graphene using on-chip terahertz spectroscopy

K.Yoshioka
NTT Corporation, 243-0198 Atsugi, Japan

The development of ultrafast laser spectroscopies has revolutionized our ability to observe and manipulate electronic states within solids at the femtosecond timescale. However, current high-frequency electronics are still confined to the nanosecond or gigahertz regimes. We aim to bridge this gap by developing ultrafast devices and/or signal processing techniques that operate at the intrinsic timescales of the materials themselves. To this end, we have developed terahertz (THz) electronics [1] capable of measuring sub-picosecond responses of electrical currents on a chip using laser-triggered photo-conductive switches. Specifically, we have achieved ultrahigh-speed optical-to-electrical (O-E) conversion using a graphene photodetector with operational speeds reaching 220 GHz, and have gained a comprehensive understanding of the O-E conversion mechanisms [2]. Furthermore, we have successfully demonstrated the electrical generation, propagation control, and detection of 1.2-picosecond plasmon wavepackets in graphene, thereby enhancing our understanding of ultrafast transport properties [3].

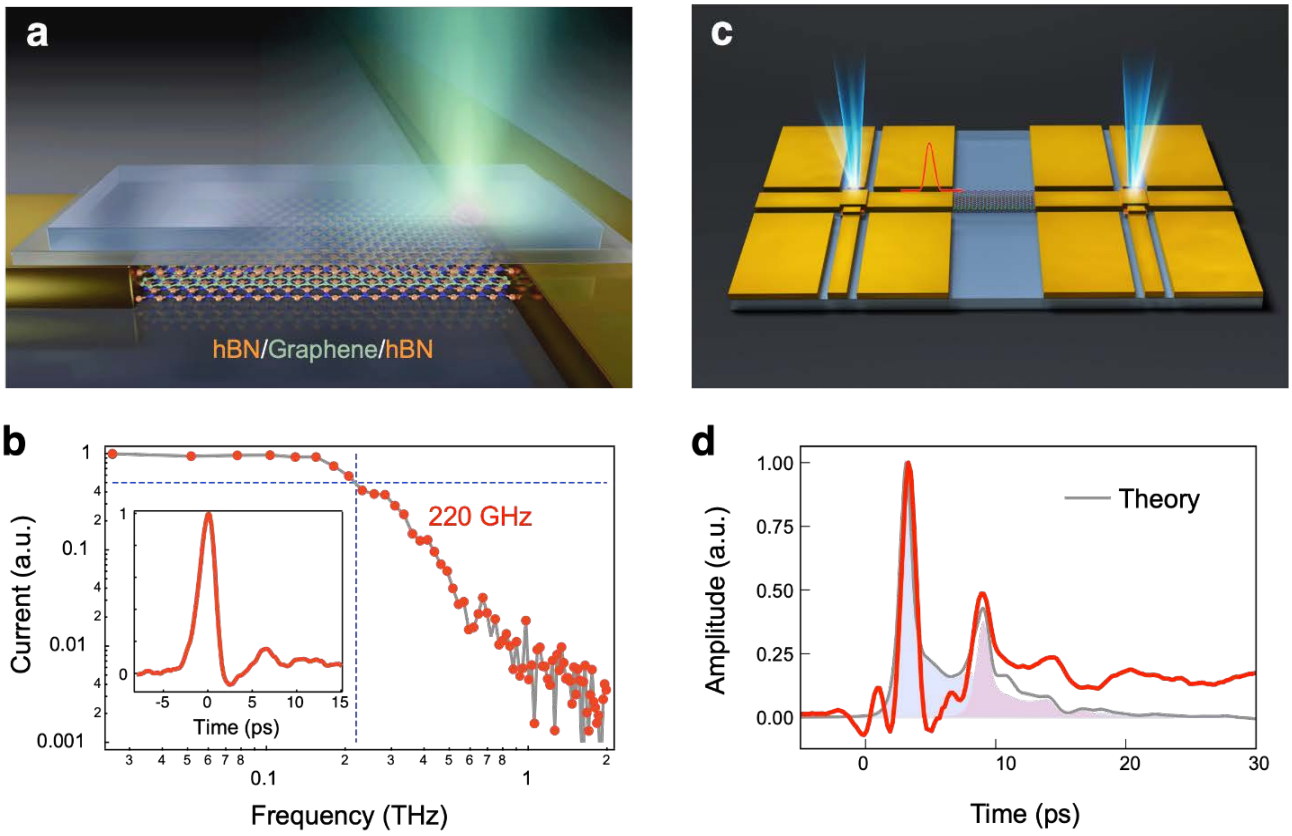

***Fig. 1. a**: **Schematic illustration of the graphene photodetector measurement**. **b**: **Frequency response** of the ultrafast O-E conversion with the 3dB bandwidth of 220 GHz. The inset shows te time domain waveform. **c**: Schematic illustration of the graphene plasmon measurement. **d**: **Time-domain waveform of the plasmon wavepackets**, showcasing a pulse duration of 1.2 ps. The waveform is reproduced using a plasmon theory that accounts for the first echo pulse due to an impedance mismatch in the circuit.*

We envision that our THz electronics approach will bridge the gap between ultrafast optical science and device engineering through a detailed understanding of ultrafast non-local charge dynamics in various van der Waals heterostructures beyond graphene.

References

[1] K. Yoshioka, N. Kumada, K. Muraki, M. Hashisaka, *Applied Physics Letters* **117**, 161103 (2020).
[2] K. Yoshioka, T. Wakamura, M. Hashisaka, K. Watanabe, T. Taniguchi, N. Kumada, *Nature Photonics* **16**, 718 (2022).
[3] K. Yoshioka, G. Bernard, T. Wakamura, M. Hashisaka, K. Sasaki, S. Sasaki, K. Watanabe, T. Taniguchi, N. Kumada, *Nature Electronics* **7**, 537 (2024)

Interplay of valley polarized dark trion and dark Exciton-polaron in monolayer WSe_2

X. Cong[1], P. A. Mohammadi[1], M. Zheng[1], K. Watanabe[2], T. Taniguchi[2], D. Rhodes[3], X.-X. Zhang [1]
[1]*University of Florida, Gainesville*, FL 32611, *USA*
[2]*National Institute for Materials Science*, Tsukuba, Ibaraki 305-0044, Japan
[3]*University of Wisconsin Madison, Madison, WI 53706, USA*

The interactions between charges and excitons involve complex many-body interactions at high densities. The exciton-polaron model has been adopted to understand the Fermi sea screening of charged excitons in monolayer transition metal dichalcogenides (TMD). The results provide good agreement with absorption measurements, which are dominated by dilute bright exciton responses. The Fermi-polaron model treats the quasiparticle responses of a single mobile impurity in a surrounding Fermi sea. In comparison, the exciton density in monolayer TMD can be tuned by laser fluence and be comparable to or exceed the charge density, where the analogy to a single mobile impurity no longer applies. The modification to Fermi sea screening at high exciton densities, however, is still not well understood. Apart from the bright excitons previously studied in reflection contrast measurements, different spin and momentum dark exciton species have been established, which are also expected to have many-body interactions with charges. The coupling between these different species of exciton-polarons has not yet been experimentally investigated.Here we investigate the Fermi sea dressing of spin-forbidden dark excitons in monolayer WSe_2 [1]. With a Zeeman field, the valley-polarized dark excitons show distinct p-doping dependence in photoluminescence when the carriers reach a critical density (see Fig. 1). This density can be interpreted as the onset of strongly modified Fermi sea interactions and shifts with increasing exciton density. Through valley-selective excitation and dynamics measurements, we also infer an intervalley coupling between the dark trions and exciton-polarons mediated by the many-body interactions.

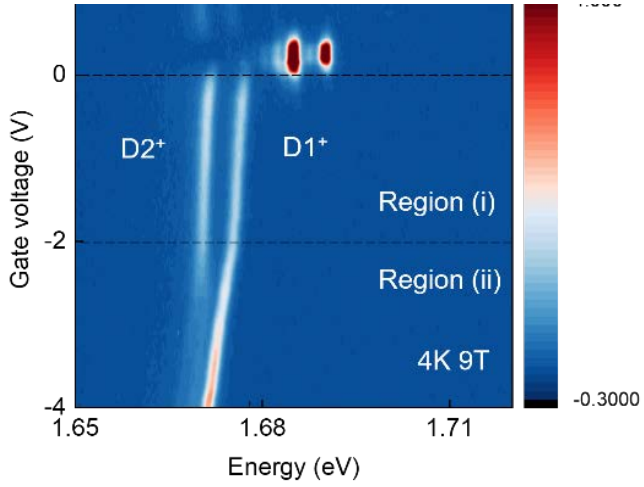

Fig. 1. Dark exciton emission from a monolayer WSe_2 *device at 4K, 9T out-of-plane magnetic field. D1+ and D2+ and the Zeeman-split dark trions. The dashed line at ~ -2V marks the crossover between region (i) and region (ii), which is also assigned to be the dark trion to dark exciton-polaron crossover for D1+. At the crossover, D2+ broadens and quenches in amplitude.*

Our results reveal the evolution of Fermi sea screening with increasing exciton density and the impacts of polaron-polaron interactions, which lay the foundation for understanding electronic correlations and many-body interactions in 2D systems.

References

[1] X. Cong, P.A. Mohammadi, M. Zheng, K.Watanabe, T. Taniguchi, D. Rhodes, X.X. Zhang, *Nature Communications* **14**, 5657 (2023).

* Acknowledgment: X-X. Zhang acknowledges the support from NSF DMR -2142703.

Transient absorption microscopy of photocarrier transport in solids

H. Zhao
The University of Kansas, Lawrence, KS 66045, USA

Transient absorption microscopy is a noninvasive and nondestructive technique used to study the transport properties of solid materials. In these measurements, a tightly focused laser pulse injects photocarriers into the sample, creating a localized carrier density distribution. A time-delayed, tightly focused, and spatially scanned probe pulse is then used to monitor the spatiotemporal evolution of these injected carriers. This is achieved by recording the transient absorption of the probe, which reflects the carrier-induced change in the sample's absorption coefficient. In practice, transient absorption can be measured through pump-induced changes in either transmittance or reflectance. Recent studies utilizing transient absorption microscopy to investigate photocarrier transport in solid materials will be presented. Two graphene-based heterostructures will be discussed. In the first, a graphene monolayer is stacked with a transition metal dichalcogenide few-layer and an organic semiconductor film. This design enables unipolar doping of graphene with one type of carrier [1], and fast diffusion of these carriers in graphene was observed. In the second case, two graphene layers are separated by a type-II transition metal dichalcogenide hetero-bilayer. It was shown that the two graphene layers are photodoped with electrons and holes, respectively.

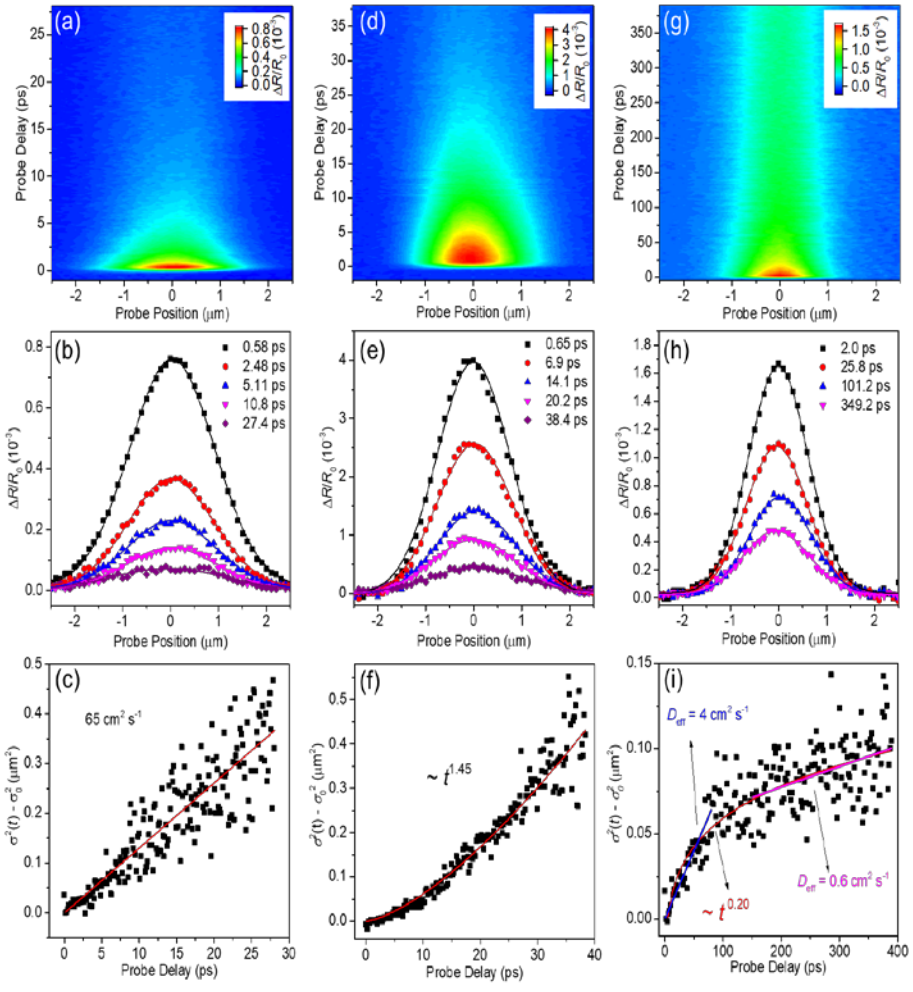

Fig. 1. In-plane transport of photocarriers in a graphene/MoS_2 /$MoSe_2$/graphene 4-layer heterostructure.
(a) *Spatiotemporally resolved differential reflectance with a 3.10 eV pump and a 1.55 eV probe, monitoring holes in the top graphene layer.*
(b) *Examples of the spatial profiles shown in* ***(a)*** *at various probe delays and the corresponding Gaussian fits (curves).* ***(c)*** *The variance of the profiles shown in (a) as a function of probe delay. The red line is a linear fit.*
(d–f) *Same as* ***(a)–(c)*** *but measured with a 3.10 eV pump and a 1.88 eV probe, monitoring electrons in the bottom graphene layer.*
(g–i) *Same as* ***(d)–(f)*** *but measured on a MoS_2/$MoSe_2$ heterostructure, monitoring interlayer exciton transport.*

Remarkably, electrons exhibit quasi-ballistic transport behavior at room temperature for about 20 ps, as illustrated in Fig. 1 [2]. Additionally, the latest results on other materials will be briefly reported.

References

[1] P. Valencia-Acuna, F. Rudayni, K. Rijal, W.-L. Chan, H. Zhao, *ACS Nano* **17**, 3939, (2023).
[2] R. J. Scott, P. Valencia-Acuna, H. Zhao, *ACS Nano* **17**, 25368, (2023).

* Acknowledgement(s): Research supported by the U.S. Department of Energy, Office of Basic Energy Sciences, Division of Materials Sciences and Engineering under Award No. DE-SC0020995.

Magnetism and magnetic phase transitions in CrSBr

L. Zhao
University of Michigan, Ann Arbor, MI 48109, USA

CrSBr is a layered antiferromagnet that has attracted great interest recently, because of its anisotropic orthorhombic crystal lattice, robust magnetism with a high transition temperature, linearly polarized excitons with a large binding energy, coupling between magnetism, magnons and excitons, etc. Yet, when looking into the magnetism of CrSBr more carefully, we noticed an unexpected and counterintuitive, increasing trend of the magnetic onset temperature as the thickness of CrSBr decreases, albeit the large uncertainty of the critical temperature for monolayer CrSBr [1].In the antiferromagnetic phase of CrSBr, the spins are aligned ferromagnetically along the in-plane b-axis direction within the layer and antiferromagnetically between adjacent layers. This in-plane spin orientation and the vanishing magnetization pose challenges in directly detecting the magnetic order parameter, especially in the thin layer limit. Here, we use polarization dependent second harmonic generation (Fig. 1a) to probe the magnetic order and magnetic phase transitions in bulk CrSBr (Fig. 1b), bilayer CrSBr, and monolayer CrSBr. For bulk CrSBr, we have identified two magnetic phase transitions, a surface layered antiferromagnetic phase transition at 140K and then a bulk phase transition at 132K [2] (Fig. 1c). The fact that the surface orders at a higher temperature than the bulk does is counterintuitive, which reminds us of the unexpected enhancement of transition temperature in thinner layers. Meanwhile, this enhanced surface onset temperature and the split between surface and bulk phase transitions have been predicted in the model of "extraordinary phase transition" for semi-infinite systems with stronger interactions at the surface than inside the bulk [3]. For bilayer CrSBr, we have captured a single magnetic phase transition at 140K [5] which is consistent with the literature report [1]. We have further identified the broken symmetries across this phase transition and shown its consistency with the layered antiferromagnetic order.

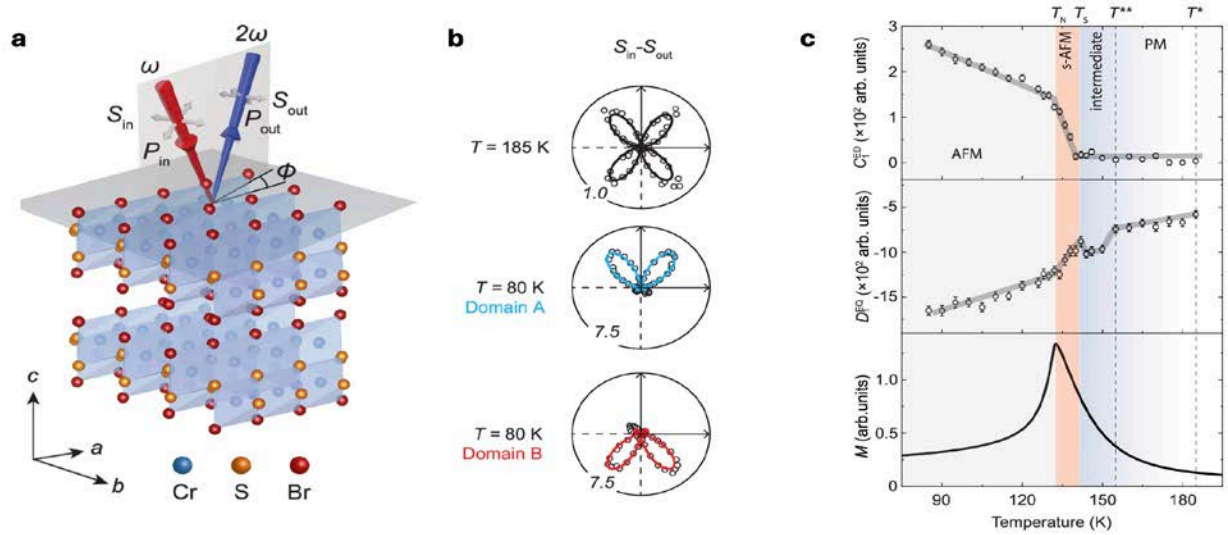

***Fig. 1.a:Sketch of the experimental geometry of our second harmonic generation measurements. b**: The polarization dependence of second harmonic generation data above and below the magnetic critical temperature. **c:** Temperature dependence of the surface, bulk magnetic order, and the bulk magnetization.*

For monolayer CrSBr, we have detected a transition temperature as high as 155K [5] which is even higher than the bilayer case by ~10% and higher than the reported 146K in literature [1]. We note that this 155K transition temperature in the monolayer CrSBr coincides with the characteristic temperature scale of the short-range ordering in bulk CrSBr [2,4] (T^{**} in Fig. 1c).

References

[1] K. Lee,A.H. Dismukes, E. J. Telford, R.A. Wiscons, X. Xu, C. Nuckolls,C. R. Dean,X.Roy,X.Zhu, *Nano Letters* **21**, 3511 (2021).
[2] X. Guo, W.Liu, J.Schwartz, S. H.Sung, D.Zhang, M.Shimizu, A. L. N. Kondusamy, L. Li, K. Sun, H. Deng, H.O. Jeschke, I. I. Mazin, R. Hovden, B. Lv L. Zhao, *Nature Communications* **15**, 6472 (2024)
[3] T. C. Lubensky, M.H. Rubin, *Physical Review* B **12**, 3885 (1975)
[4] W. Liu, X. Guo, J. Schwartz, H. Xie, N. Dhale, S. H. Sung, A. L. N. Kondusamy, X. Wang, H. Zhao, D. Berman, R. Hovden , L. Zhao, B. Lv, *ACS Nano* **16**, 15917 (2022)
[5] X. Guo, C. Wang, W. Liu, Q. Li, H. Deng, K. Sun, B. Lv, L. Zhao, *to be submitted* (2024).

Time domain views of quantum matter at 2D semiconductor interfaces

E. Arsenault, Y. Li, X. Zhu
Columbia University, New York, NY 10027, USA

Two-dimensional moiré interfaces of two dimensional (2D) van der Waals (vdW) crystals constitute the most versatile material platforms for the exploration of new physical phenomena, particularly emergent quantum phases. Here, we explore the stability origins of correlated states in WSe_2/WS_2 moiré superlattices using pump-probe exciton sensing, Fig. 1a & 1b. We find that ultrafast electronic excitation leads to partial melting of the Mott states on time scales five times longer than predictions from the charge hopping integrals and that the melting rates are thermally activated, with activation energies of 18±3 and 13±2 meV for the one- and two-hole Mott states, Fig. 1c and 1d. respectively, suggesting significant electron-phonon coupling. DFT calculation of the one-hole Mott state confirms polaron formation and yields a hole-polaron binding energy of 16 meV. These findings reveal a close interplay of electron-electron and electron-phonon interactions in stabilizing the polaronic electron crystal [1]. We also show distinct time-domain signatures of correlated insulators at fillings of one (ν = -1) and two (ν = -2) holes per moiré unit cell in the angle-aligned WSe_2/WS_2 system. Following photo-doping, we find that the disordering time of the ν = -1 state is independent of excitation density (n_{ex}), Fig. 1e, as expected from the characteristic phonon response time associated with a polaronic state. In contrast, the disordering time of the ν = -2 state scales with $1/\sqrt{n_{ex}}$, Fig. 1f, in agreement with plasmonic screening from free holons and doublons. These states display disparate reordering behavior dominated either by first order (ν = -1) or second order (ν = -2) recombination, suggesting the presence of Hubbard excitons and free carrier-like holons/doublons, respectively.

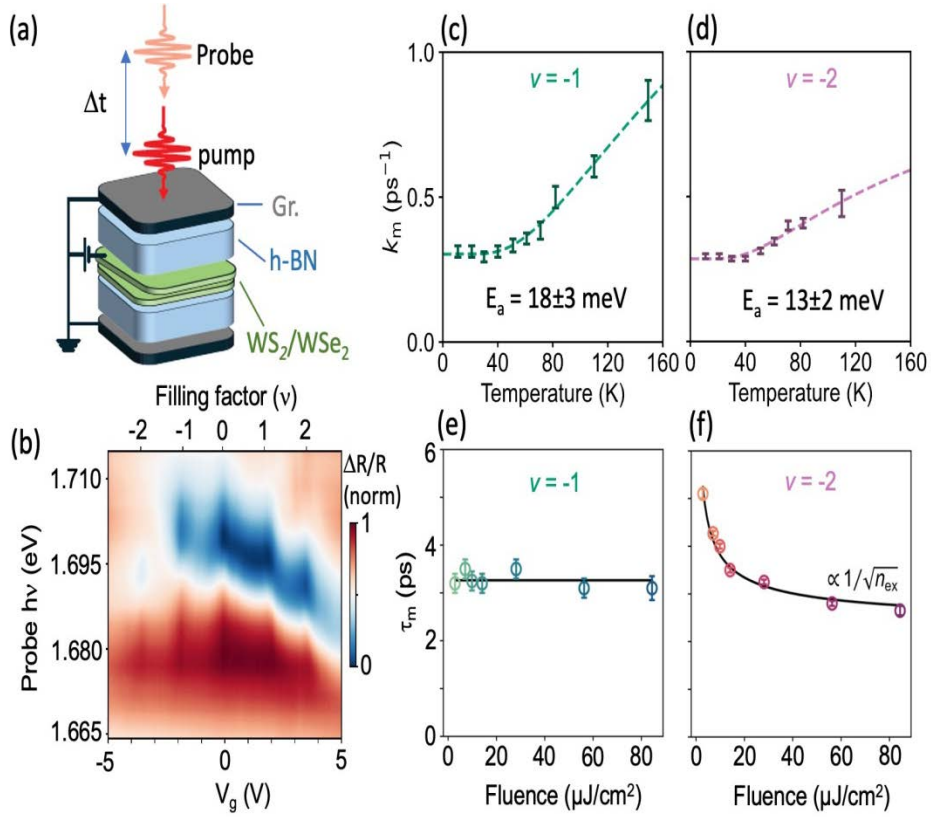

Fig. 1. Pump-probe spectroscopy reveals polaronic and screening effects in Mott states in hole-doped WS_2/WSe_2 bilayers.
(a) *Schematic illustration of a WS_2/WSe_2 moire heterobilayer with twist angle $\theta = 60^o$.*
(b) *Exciton sensing of correlated Mott insulator states from reflectance spectroscopy. Enhancement exciton oscillator strength is seen at with one (ν = 1) and two (ν = 2) electrons or one (ν = -1) and two (ν = -2) holes per moiré unit cell.* ***(c)*** *and* ***(d)*** *Pump-probe spectroscopy gives melting time constants as a function of temperature for the ν = -1* ***(c)*** *and ν = -2* ***(d)*** *states. The temperature dependences give thermal activation energies of E_a.* ***(e)*** *and* ***(f)*** *Fluence-dependent melting time constants reveal distinct Mott states at the ν = -1* ***(e)*** *and ν = -2* ***(f)****, respectively. From [1] & [2]*

Our work delineates the roles of electron-phonon (e-ph) versus electron-electron (e-e) interactions in correlated insulators on the moiré landscape and establishes non-equilibrium responses as mechanistic signatures for distinguishing and discovering quantum phases [2].

References

[1] E. Arsenault, Y.Li1, B.Yang, X.Wang, H.Park, E.Mosconi, E.Ronca, T.Taniguchi, K.Watanabe, D. Gamelin, A. Millis, C.R. Dean, F. de Angelis, X. Xu X-Y. Zhuet.Physical Review Letters **132**. 126501(2024).
[2] E. A, Arsenault, Y. Li, B. Yang, T. Taniguchi, K. Watanabe, J.C.Hone, C.R. Dean, X. Xu, X.Y. Zhu, *arXiv:2406.15067*, (2024).

Ultrafast imaging of domain wall motion in Ferroelectric superlattices

A. Zong[1], J. Chen[2], S.-C. Lin[1], S. Das[1], E. Berger[1], X. Shen[3], P. Kramer[3], X. Cheng[3], F. Ji[3], D. Luo[3]
J. England[3], A. Reid[3], M. Minitti[3], R. Ramesh[1], S. Griffin[4], D. Flannigan[2], M. Zuerch[1]
[1]*University of California – Berkeley, CA 94720 Berkeley, USA*
[2]*University of Minnesota, MN 55455 Minneapolis, USA*
[3]*SLAC National Accelerator Laboratory, CA 94025 Menlo Park, USA*

Domain wall propagation in conventional ferroelectric materials under an electric field is often hindered by disorder and hence its velocity is orders-of-magnitude lower than the speed of sound [1-2]. The recent discovery of quasi-long-ranged topological polar textures in oxide superlattices-such as polar vortices and skyrmions [3-7] offers an alternative platform to investigate domain wall motion in ferroelectrics, where atomic-scale disorder plays a minor role in nanotextures with characteristic size on the order of 10 nm. Here, we study the domain dynamics of polar textures in a $PbTiO_3/SrTiO_3$ superlattice using time-resolved electron diffraction and microscopy extending our earlier works on studying charge and topological ordering in a putative excitonic insulator [8-10]. Following photoexcitation, we observed a rapid suppression of the polar texture within 1 ps, where textures within one domain are preferentially melted.

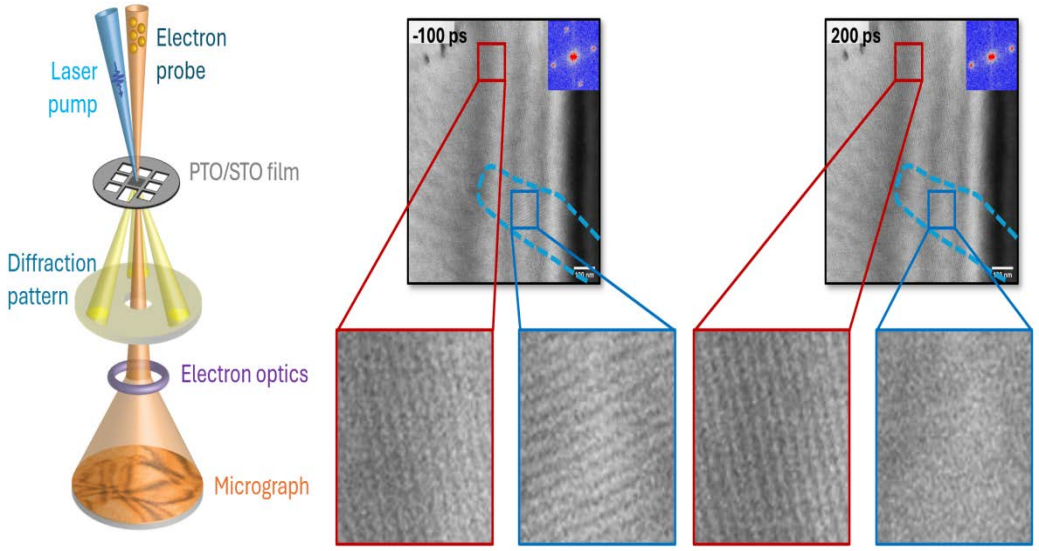

Fig. 1 Left: *Sketch of ultrafast electron microscopy experiment.* ***Center****: Ferroelectric superlattice domains forming stripe domain of two orientations here shown before photoexcitation.* ***Right****: Following photoexcitation preferential melting of order in one domain orientation is observed.*

The selective melting leads to a fast expansion of the other domain, whose boundary propagates near the sound speed characteristic of the collective motion of nanotextures. The spatiotemporal visualization of this ultrafast domain wall motion not only yields insights into the fundamental limit of its velocity in ferroelectric systems but also introduces new possibilities of memory devices based on topological polar textures.

References

[1] P. Gao, C.T. Nelson, J. R. Jokisaari, S.-H.Baek, C. W.Bark, Y Zhang, E Wang, D. G.Schlom, C.-B.Eom, X.Pan, *Nature Communications* **2**, 591 (2011)
[2] G. Catalan, J. Seidel, R. Ramesh, J. F. Scott, *Review of Modern Physics* **84**, 119 (2012).
[3] R. Ramesh, D. G. Schlom, *Nature Reviews Materials* **4**, 257 (2019).
[4] S. Das, Z. Hong, V. A. Stoica, M. A. P. Gonçalves, Y. T. Shao, E. Parsonnet, E. J. Marksz, S. Saremi, M. R. McCarter, A. Reynoso , C. J. Long A. M. Hagerstrom, D. Meyers, V.Ravi, B.Prasad, H. Zhou, Z. Zhang, H. Wen, F. Gómez-Ortiz, P. García-Fernández, J. Bokor, J. Íñiguez, J. W. Freeland N. D. Orloff , J. Junquera, L. Q. Chen , S. Salahuddin, D. A. Muller, L. W. Martin, R. Ramesh, *Nature Materials* **20**, 194 (2021).
[5] S. Das, Z. Hong, V. A. Stoica, M. A. P. Gonçalves, Y. T. Shao, E. Parsonnet , E. J. Marksz, S. Saremi, M. R. McCarter, A. Reynoso, C. J. Long A.M. Hagerstrom, D. Meyers, V. Ravi , B. Prasad, H. Zhou, Z. Zhang, H. Wen, F. Gómez-Ortiz, P. García-Fernández, J. Bokor, J. Íñiguez, J. W. Freeland, N. D. Orloff, J. Junquera, L. Q. Chen , S. Salahuddin, D. A. Muller, L. W. Martin, R. Ramesh, *Nature* **568**, 7752 (2019),
[6] V. A. Stoica, N. Laanait, C. Dai, Z. Hong, Y. Yuan, Z. Zhang, S. Lei, M. R. McCarter, A. Yadav, A. R. Damodaran, S. Das, G. A. Stone J. Karapetrova, D. A. Walko, X. Zhang, L. W. Martin, R. Ramesh, L.-Q. Chen, H. Wen, V. Gopalan J. W. Freeland, *Nature Materials* **18**, 373 (2019).
[7] A. K. Yadav, K. X. Nguyen, Z. Hong, P. García-Fernández, P. Aguado-Puente, C. T. Nelson, S. Das , B. Prasad, D. Kwon, S. Cheema , A. I.Khan, C. Hu J. Íñiguez, J. Junquera, L.-Q. Chen, D.A. Muller, R. Ramesh S. Salahuddin, *Nature* **565**, 7740 (2019),
[8] Y. Cheng, A. Zong, J. Li, W. Xia, S. Duan, W. Zhao, Y. Li, F. Qi, J. Wu, L. Zhao, P. Zhu, X. Zou, T. Jiang, Y. Guo, L. Yang, D. Qian, W. Zhang A. Kogar, M. W. Zuerch, D. Xiang, J, Zhang, *Nature Communications* **13**, 963 (2022).
[9] A. Zong, S.-C. Lin, S. A. Sato, E. Berger, B. R. Nebgen, M. Hui, B. Q. Lv, Y. Cheng, W. Xia, Y. Guo, D. Xiang,M. W. Zuerch, *arXiv*::*2407.00772*,(2024)
[10] Y.Cheng, A. Zong, L.Wu, Q.Meng, W.Xia, F.Qi, P. Zhu, X.Zou, T.Jiang, Y.Guo, J. van Wezel, A. Kogar, M.W. Zuerch, J. Zhang, Y. Zhu, D.Xiang, *Nature Physics* **20**, 54 (2024).

AUTHOR INDEX

AUTHOR INDEX

MILESTONES 2016-2025

Ultrafast Dynamics and Metastability
Ultrafast Bandgap Photonics

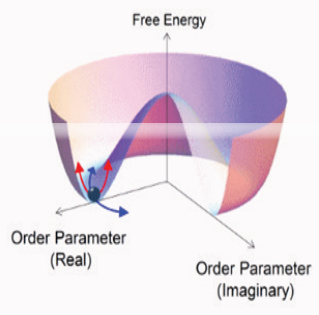

Physica Scripta – 2017
Focus: Ultrafast Bandgap Photonics

Guest Editors: Michael K. Rafailov and Luca Perfetti, 2017
http://iopscience.iop.org/journal/1402-4896/page/Focus-issue-on-Ultrafast-Bandgap-Photonics

Ultrafast Bandgap Photonics
Baltimore, 2016
http://spie.org/Publications/Proceedings/Volume/9835
Anaheim, 2017
http://spie.org/Publications/Proceedings/Volume/10193
Orlando, 2018
https://spie.org/Publications/Proceedings/Volume/10638

Ultrafast Dynamics and Metastability 2017 Workshop
Washington, DC, 2018
https://sites.google.com/a/georgetown.edu/ultrafast-dynamics-and-metastability-archive-2017/

Ultrafast Dynamics and Metastability & Ultrafast Bandgap Photonics 2019
V International Workshop Washington, DC, April 2019

Ultrafast Bandgap Photonics: Dynamics and Metastability of Transient States 2019
VI International Conference St. Petersburg, 2019

Ultrafast Bandgap Photonics: Dynamics and Metastability of Transient States 2020
VII International Symposium Hersonissos, Crete, Greece June 2022

Ultrafast Dynamics and Metastability & Ultrafast Bandgap Photonics 2021
VIII International Workshop Washington, DC, November 2021

Ultrafast Dynamics and Metastability & Ultrafast Bandgap Photonics 2022
IX International Workshop Washington, DC, November 2022

Ultrafast Bandgap Photonics: Dynamics and Metastability of Transient States 2023
X International Symposium Hersonissos-Crete, Greece June 2023

Ultrafast Dynamics and Ultrafast Bandgap Photonics 2024
XI International Symposium 2023 Hersonissos-Crete, Greece June 2024

Ultrafast Dynamics & Metastability : Ultrafast Bandgap Photonics 2024
XII International Conference Tucson, AZ, September 25-28, 2024

Ultrafast Dynamics and Ultrafast Bandgap Photonics 2025
XIII International Symposium and Summer School
Aldemar Knossos Conference Cente
Hersonissos-Crete, Greece June 11-20 2025